THE UNIVERSITY
of EDINBURGH

Characterisation and diagnostic potential of extracellular small RNAs in filarial nematodes

Juan Fernando Quintana Alcala

Doctor of Philosophy The University of Edinburgh 2017

DECLARATION

I, the undersigned, hereby declare that the content of this thesis has been composed by myself, that the work described herein is my own unless acknowledge otherwise, and that the work has not been submitted for any degree or professional qualification. I, the undersigned, confirm that the work submitted is my own, except where work which has formed part of jointly-authored publications has been included. The contribution of the other authors to this work has been explicitly indicated below. I confirm that the appropriate credit has been given within the thesis where reference has been made to the work of others.

Juan Fernando Quintana Alcala Date: 16/10/2017

Abstract

Filarial infections (lymphatic filariasis and onchocerciasis) are amongst the major neglected tropical diseases, and together account for more than 120 million infections in tropical and subtropical regions. The gold-standard technique for the diagnosis of filariases relies on the detection of microfilariae (mf) either in blood smears (lymphatic filariasis) or in skin biopsies (onchocerciasis). The secretion of extracellular RNAs (exRNAs) by parasitic nematodes has opened new avenues for the development of novel biomarkers for helminthiases, including filariasis. However, rather little is known about the origin and regulation of these RNAs inside the nematodes. One outstanding question is whether the secretion of small RNAs is distinct across the developmental stages of parasitic nematodes. Similarly, it is not clear whether the secretion of miRNAs is affected by treatment with anthelminthic chemotherapy or their potential as biomarkers for infection.

Litomosoides sigmodontis is a murine filarial nematode closely related to filarial nematodes of medical and veterinary importance, including *Onchocerca spp.* and *Brugia spp*. *L. sigmodontis* has been extensively used to decipher multiple aspects of filarial biology, including parasite development, vaccine, and host-pathogen interactions. Therefore, we decided to use this model to address fundamental questions regarding the secretion of small RNAs and their biomarker potential. Our *in vitro* studies demonstrate that some extracellular miRNAs are enriched in a sex- and stage-specific manner in the Excretion/Secretion (ES) products from early larval and adult stages from the rodent filarial nematode *Litomosoides sigmodontis*. Moreover, our data demonstrates that the gravid adult female worms secrete a plethora of miRNAs enriched in the secretome of this developmental stage when compared to adult males or mf. Further characterization studies show that the miRNAs are likely to be secreted in association with extracellular vesicles (EVs), as previously reported for other parasitic nematodes, including the human pathogen *Brugia malayi*. Interestingly, Ivermectin, which is typically used to treat filarial infections, does not have consistent effects on the secretion of miRNAs by gravid adult female worms *in vitro*, requiring further *in vivo* experiments to determine the effect of IVM on detection of extracellular parasite-derived miRNAs. *In vivo* experiments, using murine models of infection with *L. sigmodontis* (gerbils and

BALB/c mice), as well as human samples from patients infected with *Onchocerca volvulus* and cattle infected with *Onchocerca ochengi*, demonstrated the presence of filarial-derived miRNAs, including female-specific miRNA markers, in biofluids from infected hosts. Further statistical analysis showed that two parasite-derived miRNAs, miR-71 and miR-100d, can significantly discriminate infected animals from naïve controls with high sensitivity/specificity (>80%/100%). The results presented in this PhD thesis provide an initial framework to understand the secretion of small RNAs throughout nematode development, the potential interactions between anthelminthic chemotherapy and small RNA trafficking and secretion, as well as the use of parasite-derived miRNAs for the development of a new generation of biomarkers for filarial infections.

Lay Abstract

Filarial infections are chronic diseases caused by several parasitic worms, and infect more than 150 million people in tropical and sub-tropical regions of the globe. The highest incidence occurs in sub-Saharan Africa, where these diseases have a massive economic impact and are often associated with social stigma. Infection with different species of these worms produce lymphatic filariasis, or "elephantiasis", due to the enlargement of the lower limbs found in chronically infected patients. Similarly, infection with another parasitic worm, called *Onchocerca volvulus,* produces a disease known as onchocerciasis or "River blindness", which severely reduces pigmentation in the skin and, in the worst cases, causes visual impairment and blindness.

In this PhD thesis, we studied a class of very short RNAs, called microRNAs, which control gene expression inside cells in many organisms, including parasitic worms. We have found that these molecules not only act within the cell, but are also released by these parasites both *in vitro* and *in vivo*. Furthermore, we investigated the potential use of these parasite microRNAs for diagnostics of filarial infections.

We demonstrated that adult female worms secrete several microRNAs which can be viewed as sex- and/or stage-specific signature for this lifecycle stage. Excitingly, we found several of these female-derived microRNAs in multiple biofluids, including serum and plasma from infected African patients. To further investigate this, we used a mouse model of infection, and determined that at least two of these parasite-derived microRNAs can robustly discriminate between uninfected and infected animals. This thesis provides an important framework to further understand the role of female-derived microRNAs as diagnostic tools for filarial infections, and provides a strong rational for further technological developments of a microRNA-based diagnostic platform for filarial infections.

PUBLICATIONS & CONTRIBUTIONS

Publication 1	**Quintana JF**, Makepeace BL, Babayan S, Ivens A, Pfarr KM, Blaxter M, Debrah A, Wanji S, Ngangyung HF, Bah GS, Tanya VT, Taylor DW, Hoerauf A, Buck AH (2015) Extracellular Onchocerca-derived small RNAs in host nodules and blood, Parasites & Vectors 8(1):58.
Authors contributions – General	**JFQ** performed experiments, co-designed studies and co-wrote the manuscript with AHB; BM, SAB, DWT, KMP and AH coordinated accessibility of material, edited manuscript and co-conceived project with AHB; AI, **JFQ** and AHB analysed the data, MB provided genome data, advice and edited manuscript, AD, SW, HFN, GSB, VNT provided crucial sample material. AHB wrote paper with **JFQ** and supervised the work. All authors read and approved the final version of the manuscript.
Candidate's contributions - specific	1) Collection of mouse serum, human serum & plasma, nodule fluids - SAB, BM, DWT, KMP and AH. 2) RNA extractions, RNA QC, small RNA library preparation – **JQF**, AHB. 3) Illumina sequencing analysis – AI, MB, AHB, **JFQ**.
Confirmation	Date: 04/07/2017 Signature:  Print Full Name: Amy H. Buck
Publication 2	**Quintana JF**, Babayan SA, Buck AH (2016). Small RNAs and extracellular vesicles in filarial nematodes: from nematode development to diagnostics. Parasite Immunology doi: 10.1111/pim.12395; PMID: 27748953.
Authors contributions – General	Literature review: **JFQ** conceived and wrote manuscript with AHB; **JQF** created figures; SAB and provided advice and edited the manuscript. All authors read and approved the final version of the manuscript.
Confirmation	Date: 04/07/2017 Signature:  Print Full Name: Amy H. Buck

The bioinformatics analysis detailed in chapter 3 to 5 of this thesis was conducted mainly by Dr. Alasdair Ivens, whereas I performed most of the DESeq2 analysis in these chapters. I would personally like to thank Al for his invaluable assistance and support through this learning process.

I would also like to thank Dr. Matthew Taylor and Ms Alison Fulton for their contribution and help in setting up *L. sigmodontis* infections. Similarly, I would like to acknowledge the help of Dr. Coralie Martin and Dr. Nathaly Vallarino Lhermitte, for their support and time spent teaching how to collect ES products from multiple developmental stages, and for assistance in setting up *in vitro* experiments to test the effect of Ivermectin on protein and miRNA secretion by gravid adult female worms. The time spend in Paris was invaluable and I am deeply grateful.

The experimental data with human samples provided in chapter 5 is a result of collaborative work with Dr. Paul Dickinson and Dr. Amy H Buck. I would like to also acknowledge the contribution of Dr. Benjamin Makepeace, Dr. Kenneth Pfarr and Dr. Achim Hoerauf for providing invaluable human and bovine material, which is also described in chapter 5.

I would like particularly acknowledge the extremely helpful discussions and support with experimental design I have had from Dr. Simon A. Babayan. Thanks for always having the time to talk about science, experiments, and politics over lunch.

Prof. Mark Blaxter was involved in helpful discussions that helped me to define a conceptual framework for this PhD thesis.

Dr. Amy H. Buck was involved in the planning and comprehension of all the chapters included in this PhD thesis.

The University of Edinburgh, through its School of Biological Sciences Scholarships, funded this PhD thesis. The Wellcome Trust UK, the Bill & Melinda Gates Foundation, and the Human Frontier Science Program funded the laboratory of Dr. Amy H. Buck.

Acknowledgements

I left home almost 9 years ago, in the middle of one of the darkest times in the history of my country, Venezuela. 9 years ago, I also left behind many people who are not physically here today, including my grandparents, to whom I never had the chance to hug again or say goodbye. You taught me how to be strong, resilient, honest, but most importantly, how to truly connect with those you love. Your spirits wandered with me during the last few months of my PhD, and I felt you at every step of the way. Today, I want to dedicate these pages to you, Alejandro, Nina, and Leyland. There is not a single day that I don't miss you.

I could not have made it through this long journey without the continuous love and support from my best friends, my mum and dad. You faced vicissitudes, and still you never gave up. You are strong and brave, and I admire you for what you truly are. I'm honoured to be a little piece of you both. These pages are also dedicated to you. I also want to thank my wonderful siblings, who are an important part of my life; Maria, Andrea, Darling, and Fernando Jose. Together with mum and dad, you are one of the most valuable gifts I have in life.

Matthew, we found each other just when I thought I didn't have the strength to keep going. You are one of the kindest souls I have ever connected with. You see everything, you see every part, you saw all my light, and you loved all my dark. I have no words to describe how grateful I am to you.

I have been lucky enough to have found incredible friends in this lifetime. Karen, Carlos, Douglas, Massiel, Lisette, Adriana, Virginia, Indira, Shinny, I hold you dearly and very close to my heart every single day. I will be forever grateful for your honest, deep, and meaningful friendships. I don't need anything else if I have you around. Igor, the best dog in the world, you came into my life just a few days after leaving home. You have been my companion and best friend for a long time now, and even thought you don't understand human language, I honour your friendship with this lines.

My professional life has been guided by wonderful people. Pimali and Emilia taught me the beauty of biology, and the excitement of doing experiments, right from the first day of my undergraduate studies. Maria Pilar showed me how fascinating parasites are, and Amy taught me how to ask questions, how to be excited about science but critical at the same time, how to be thorough, and how to answer my own questions. With you, Amy, I also found my voice as a scientist, and I explored many facets of my "scientific persona" I didn't know I had. Amy, thank you for all the lessons, all the guidance, and all the support. It will all be with me forever. I also want to thank Simon Babayan for always having the time to meet me, discuss my project, and for sharing laughs and very insightful discussions over lunch. Most of the work here would not have been possible without you and Amy.

I also want to thank all the past and current members of the Buck lab for all the advice, help, and guidance whenever I needed them. I especially want to thank you, Franklin, for your invaluable friendship, and Dr. Paul Dickinson for technical support. Similarly, I want to thank the members of the Macias Ribela lab (Specially Sara!), the Zamoyska lab (David, Sonja, Mate, Cara, Celine, and the rest of you), Zaiss lab (Rucha and Carlos), the Taylor lab (Alison, you are a rock star!), and the members of the Blaxter lab (Dominik and Sujai) for all your help and discussions. Al, a big thank you for your bioinformatic expertise, and for always having the time and the energy to teach me something new.

Finally, I would like to thank everyone at IIIR for all your help and support during these fantastic 5 years. You will always be remembered with gratitude.

Abbreviations

~	Approximately
18S rRNA	18S ribosomal ribonucleic acid
µ	Micro
µL	Microliter
µg	Microgram
µM	Micromolar
AAMϕ	Alternatively-activated macrophages
ABZ	Albendazole
Ag	Antigen
AGO	Argonaute
AM	Adult males
APC	Antigen Presenting Cells
bp	Base pairs
CD	Cluster of differentiation
CCL	Chemokine CC Ligand
CDS	Coding sequence
CXC	Chemokine receptor
^{o}C	Degrees Celsius
DC	Dendritic cells
DOX	Doxycycline
DGCR8	DiGeroge Syndrome Critical Region 8 Protein
dH_2O	Distilled water
DNA	Deoxyribonucleic acid
ELISA	Enzyme-Linked Immunosorbent Assay
FACS	Fluorescence Activated Cell Sorting
FBZ	Flubendazole
FCS	Foetal Calf Serum
FSC	Forward Scatter
g	Gravitational force or grams
gAF	Gravid adult females
h	Hours
HSP	Heat-Shock Protein
IFN	Interferon
Ig	Immunoglobulin
iL3s	Infective 3rd Larval stage
IL	Interleukin
i.p.	Intraperitoneal injection
IVM	Ivermectin
jAM	Juvenile Adult males
kb	Kilobase
kDa	Kilodalton
L4	4th larval stage
LAMP	Loop-mediated Isothermal Amplification

LNA	Locked Nucleic Acid
M	Molar
m^7G	7-methylguanosine cap
mf	Microfilariae
MHC	Major Histocompatibility Complex
min	Minute
miRNA	microRNA
mL	Millilitre
mM	Millimolar
mRNA	Messenger ribonucleic acid
MVB	Mutivesicular bodies
MW	Molecular weight
ncRNA	Non-coding ribonucleic acid
nM	Nanomolar
nt	Nucleotide
ORF	Open reading frame
P	Probability value
PBMC	Peripheral-blood mononuclear cells
PBS	Phosphate Buffered Saline
PCR	Polymerase Chain Reaction
PFA	Paraformaldehyde
pgAF	Pre-gravid adult females
pH	Measure for the hydrogen ion concentration
p.i.	Post infection
piRNA	PIWI-associated ribonucleic acid
PIWI	P-element Induced Wimpy Testis
pM	Picomolar
Pol	Polymerase
PolyA	Poly-Adenosine tail
Pre-miRNA	Precursor microRNA
Pri-miRNA	Primary microRNA
qRT-PCR	Quantitative reverse transcription polymerase chain reaction
RBC	Red blood cells
RISC	RNA-induced silencing complex
RNA	Ribonucleic acid
RNases	Ribonucleases
RPMI	Roswell Park Memorial Institute
rRNA	Ribosomal ribonucleic acid
RT	Reverse Transcription
s.c.	Subcutaneous injection
SDS	Sodium Dodecyl sulphate
SD	Standard deviation
Sec	Second
siRNA	Short interfering ribonucleic acid
snoRNA	Small nucleolar ribonucleic acid
snRNA	Small nuclear ribonucleic acid

SSC	Side Scatter
TCR	T cell receptor
TGF-β	Transforming growth factor-beta
T_h	T helper cell
TRBP	Transactivation-response RNA-Binding protein
Treg	Regulatory T cell
tRNA	Transfer ribonucleic acid
TNF-α	Tumour Necrosis factor alpha
UTR	Untranslated region of mRNA
VEGF	Vascular endothelial growth factor
WHO	World Health Organisation
XPO-5	Exportin 5
XRN1	5'-3' Exoribonuclease 1

Table of contents

List of figures

List of tables

Caminante, son tus huellas el camino y nada mas;
Caminante, no hay camino se hace camino al andar.
Al andar se hace camino, y al volver la vista atras
se ve la senda que nunca se ha de volver a pisar.
Caminante no hay camino sino estelas en el mar.

Wanderer, your footsteps are the path, and nothing else;
Wanderer, there is no path, the path is made by walking.
Walking makes the path, and on glancing back
one sees the path that will never trod again.
Wanderer, there is no path, just waves in the sea.

Antonio Machado, "Campos de Castilla" (1912)

Chapter 1: **Introduction**

1.1 Filarial Nematodes

1.1.1 Classification and lifecycle

The phylum Nematoda includes several species of medical and veterinary importance (De Ley, 2006). Perhaps one of the most fascinating traits of the members of this phylum is their highly heterogeneous lifestyles, including free-living and parasitic species. In this regard, the transition from a free-living to a parasitic lifestyle in nematodes is not fully understood but has been shown to arise multiple times independently during their evolution (Blaxter, & Koutsovoulos, 2014). The members of this phylum are classified according to a clade system, based on ribosomal small subunit genes (Blaxter, De Ley, et al., 1998). Filarial nematodes belong to the clade III nematodes (Superfamily *Filarioidea)*, together with other parasitic species with different lifestyles, such as the gastrointestinal parasites of the *Ascaris* genus (Blaxter, De Ley, et al., 1998; Bouchery, Lefoulon, et al., 2013; Lefoulon, Bain, et al., 2015).

The members of the *Filarioidea* superfamily parasitize a great variety of animals, ranging from amphibians to mammals (Lefoulon, Bain, et al., 2015;2016). Insect vectors are required for development of the immature larvae (L1, also called microfilariae) into the infective third stage larvae (iL3) and for transmission into the final vertebrate hosts (Bain, & Babayan, 2013; Hoffmann, Petit, et al., 2000). Importantly, at least eight filarial species infect humans, and of these, at least three are responsible for most of the morbidity due to filariasis: *Wuchereria bancrofti* and *Brugia malayi* cause lymphatic filariasis (also known as elephantiasis), and *Onchocerca volvulus* causes onchocerciasis (also known as river blindness). The other five species are *Loa loa*, *Mansonella perstans*, *Mansonella streptocerca*, *Mansonella ozzardi* and *Brugia timori* (Hise, & Pearlman, 2004; Lefoulon, Bain, et al., 2015; Taylor, Hoerauf, et al., 2010).

Morphologically, filarial nematodes are unsegmented, cylindrical roundworms (Bain, & Babayan, 2013). They have four main longitudinal chords, a tri-radiated oesophagus and an oesophageal nerve ring (Bain, & Babayan, 2013). These organisms display sexual dimorphism, and in general the adult males are much smaller than adult females (Bain, & Babayan, 2013). The adult nematodes are long and slender, and reside in the lymphatic tissue (*W. bancrofti*, *B. malayi*), subcutaneous

nodules (*O. volvulus*) or connective tissue (*M. ozzardi, M. perstans*) (Utzinger, Becker, et al., 2012). Their cuticle is complex and composed of multiple layers of collagen which is covered by a lipid epicuticle, as well as a negatively charged glycocalyx (Page, Hamilton, et al., 1992). Other structures, such as digestive tubes, the nervous system and reproductive organs are easily identified in these worms, particularly in the adult stages (Morris, Bennuru, et al., 2015).

A simplified overview of the lifecycles of filarial nematodes of medical and veterinary importance is depicted in **Figure 1.1**. The cycle begins when the insect vector takes up the microfilariae (L1 stage) during a blood meal from an infected individual. Within the insect, the larvae migrate through the gut wall to the thoracic muscles, and undergo two moulting steps (L1 to L2, and L2 to L3) into the infective L3 usually within 7 to 21 days (Bouchery, Lefoulon, et al., 2013; Tamarozzi, Halliday, et al., 2011). Then, these developmentally-arrested L3 larvae migrate to the mouthparts of the insect, and are deposited with the saliva on the skin of the host during subsequent blood meals (Bouchery, Lefoulon, et al., 2013). During this process, the larvae enter through the lesion made by the insect into the vertebrate host. The infective larvae then migrate through the tissues and undergoes two moulting steps into sexually mature adult worms in the final tissue of residence (e.g. subcutaneous tissue or lymphatics), in a process that normally requires several months, depending on the species (Bain, & Babayan, 2013; Brattig, 2004; Hoffmann, Petit, et al., 2000; Taylor, Hoerauf, et al., 2010). Upon completion of the developmental schedule, the adult filarial nematodes can survive for more than a decade within the vertebrate host and can produce thousands of microfilariae per day (Brattig, 2004; Tamarozzi, Halliday, et al., 2011)

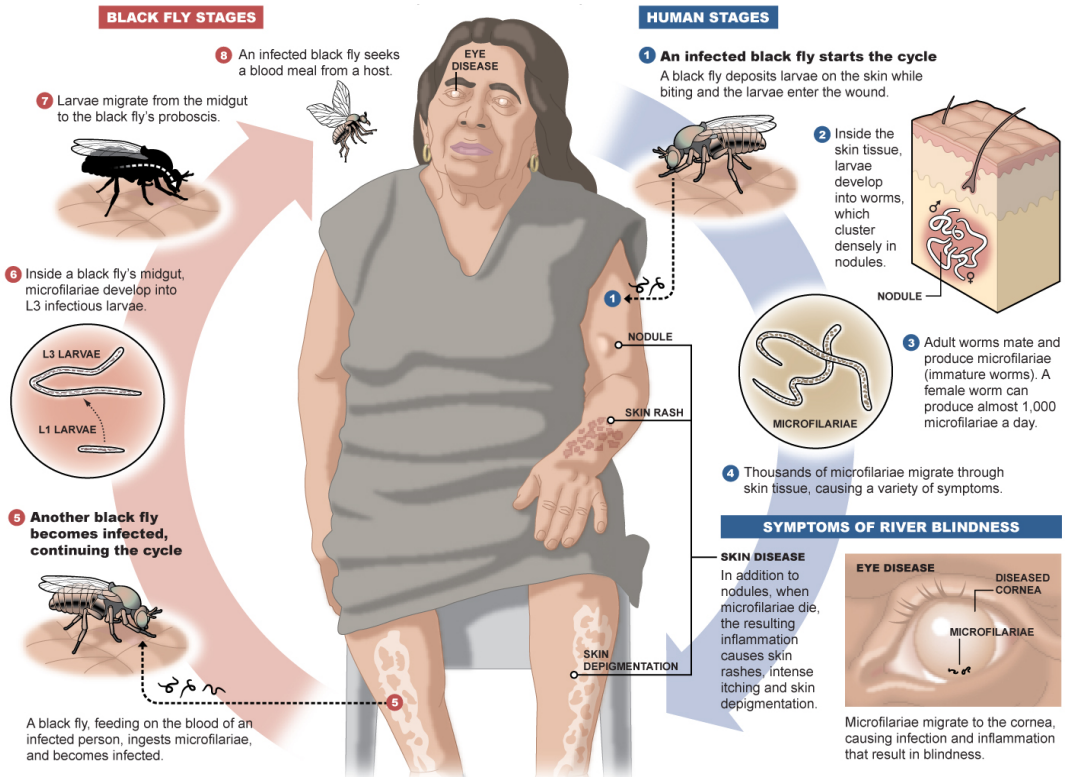

Figure 1.1 Lifecycle of the human pathogen *Onchocerca volvulus*. Two stages are depicted in the figure, an insect (black fly) stage and a human stage. The maturation of the infective L3 stages takes place in the insect vector, which inoculates the human host during a blood meal. Adulthood (males and female worms) is reached after two moulting steps. The adult worms then mate and the adult female worms release microfilariae (mf) that are normally found in the skin, producing the typical skin rash and depigmentation observed during chronic onchocerciasis. Similarly, a population of mf can also travel to the eye, where an exacerbated immune reaction against them eventually leads to damage of the ocular tissue, inducing visual impairment and blindness (*Taken from https://www.cartercenter.org/news/publications/health/river_blindness_multimedia.html*)

Filarial nematodes are normally found in tropical and sub-tropical regions of the planet, including Africa, South America and Asia, and are endemic in more than 80 countries located these regions (**Figure 1.2**) (Rebollo, & Bockarie, 2017). The geographic distribution of filarial nematodes is closely linked to the availability of the specific insect vectors (Taylor, Hoerauf, et al., 2010), and latest estimations showed that in these regions more than 100 million individuals are thought to be infected and more than a billion to be at risk of infection (Ballesteros, Tritten, ONeill, et al., 2016; Taylor, Hoerauf, et al., 2010). Almost 90% of the reported cases of lymphatic filariasis are caused by *W. bancrofti*, with the remaining 10% being attributed to *B. malayi*, whereas all the reported cases of onchocerciasis are exclusively attributed to *O. volvulus* (Taylor, Hoerauf, et al., 2010). Other filarial species such as *L. loa* (African eye worm) and *Mansonella spp.* are found in the rain forests of West and Central Africa, as well as in the Amazonas (Debrah, Nausch, et al., 2017; Fischer, Bamuhiiga, et al., 1997; Nutman, Miller, et al., 1986; Simonsen, Onapa, et al., 2011; Wanji, Amazigo, et al., 2011)

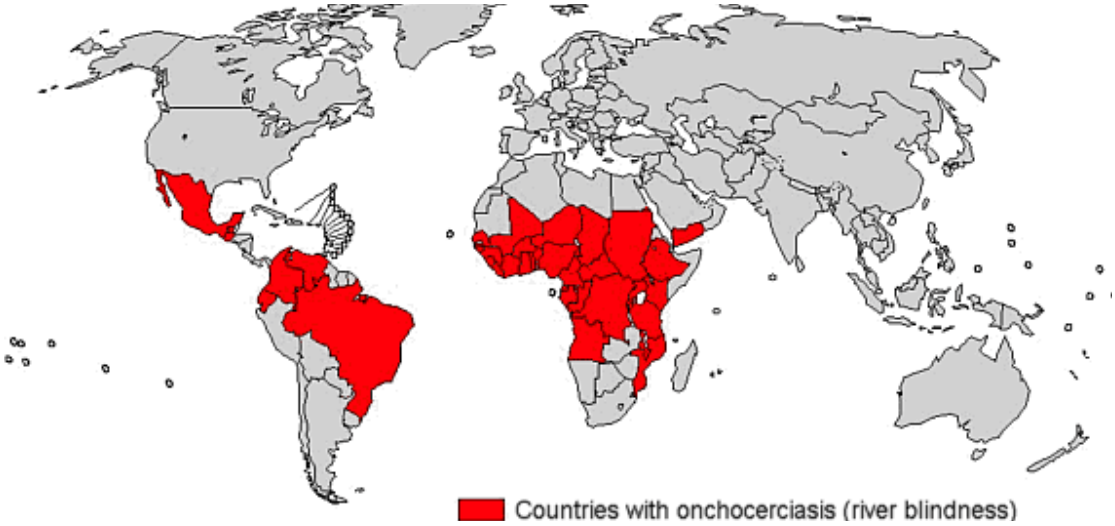

Figure 1.2 Geographical distribution of onchocerciasis. Onchocerciasis is normally found in tropical and subtropical regions, and it is widely distributed in the sub-Saharan Africa, as well as in several foci in central and south America (*Taken from* http://www.who.int/blindness/partnerships/onchocerciasis_disease_information/en/)

1.1.2 *Wolbachia* endosymbiont

One interesting aspect of the biology of filarial nematodes is the presence of the endosymbiont *Wolbachia pipiens* (Taylor, Voronin, et al., 2012). This bacterium is an obligate endosymbiotic, gram-negative α-proteobacteria, commonly found not only in nematodes but also in insects (Fenn, Conlon, et al., 2006). *Wolbachia* is broadly classified into several supergroups; supergroups A, B, E, H, I and K are found in insects and arthropods, whereas supergroups C, D and J are limited to filarial nematodes (Fenn, Conlon, et al., 2006; Lefoulon, Bain, et al., 2015;2016). Interestingly, the supergroup F is found in both arthropods and filarial hosts (Bouchery, Lefoulon, et al., 2013; Lefoulon, Bain, et al., 2016). Indeed, most of the filarial nematodes of medical and veterinary importance harbour *Wolbachia*, except for *L. loa*, *Achanthocheilonema vitae* and *O. flexuosa* (Taylor, Voronin, et al., 2012). In this regard, recent evidence has demonstrated the presence of ancestral *Wolbachia* DNA in the nuclear genome of *A. vitae*, *L. loa* and *O. flexuosa*, thus arguing in favour of a hypothesis that proposes that an ancestral *Wolbachia* infection was followed by a secondary loss of the endosymbiont, and providing evidence for multiple infections during the evolution of the filarial nematodes (Scot, Gheding, et al., 2012). *Wolbachia* is found in all the lifecycle stages of filarial nematodes, although the magnitude of the infection varies considerably during the development of the nematode host (Fischer, Beatty, et al., 2011; Taylor, Voronin, et al., 2012). At a tissue level, this bacterium is commonly detected in the cells of the lateral chord, although it is strongly detected in the reproductive tissue of female worms, such as the ovarian tissue, morulae, oocytes and developing embryos (Landmann, Foster, et al., 2010). Therefore, it has been demonstrated *Wolbachia* is maternally inherited and asymmetrically distributed in developing embryos following on egg fertilization (Fischer, Beatty, et al., 2011; Landmann, Bain, et al., 2012; Landmann, Foster, et al., 2010).

The basis of the mutualistic relationship between the *Wolbachia* endosymbiont and the filarial nematode hosts are extremely complex and are not fully elucidated. Perhaps the most notorious evidence of this rich and complex interaction is derived from observation where depletion of *Wolbachia* by antibiotic treatment leads to stunning, sterilisation and death of adult parasitic nematodes (Allen, Adjei, et al., 2008; Kon, Pattison, et al., 1998). At the genomic level, the sequencing of both filarial and *Wolbachia* genomes have provided solid arguments for the existence of a

mutualistic relationship between these two organisms (Choi, Tyagi, et al., 2016; Fonslow, Stein, et al., 2013; Lefoulon, Bain, et al., 2016). *Wolbachia* possess a 1.08Mb circular genome predicted to encode for 806 protein-coding genes, including important metabolic genes (e.g. biosynthesis of riboflavin, Flavin adenine dinucleotide (FAD), and Haem group) which are not encoded in the *Brugia malayi* genome, characterised for being ~95 Mb in size and expected to express >11,000 protein coding genes (Fenn & Blaxter, 2006;Scot et al., 2012). Similarly, *Wolbachia* seems to rely on the nematode amino acid synthesis pathways for its growth within its host (Darby, Armstrong, et al., 2012; Scot, Ghending, et al., 2012). At a transcriptional level, *Wolbachia* expresses a great proportion of genes involved in protein metabolism, RNA metabolism and stress responses, as well as ligands of the mammalian Toll-like receptors (TLRs) (Darby, Armstrong, et al., 2012; Luck, Anderson, et al., 2015), and thus it is thought to play a metabolic role that is advantageous for the nematode host (Darby, Armstrong, et al., 2012; Fenn, & Blaxter, 2006). Moreover, the transcriptional profile of *Wolbachia* seems to vary extensively across the lifecycle of the parasite, displaying a strong bias for transcripts critical for Haem, nucleotide, riboflavin, folate metabolism in mf compared to other developmental stages (Luck, Evans, et al., 2014). It is important to note that *Wolbachia* has lost most of the cell wall structures commonly associated with Gram-negative bacteria (Taylor, Voronin, et al., 2012), with no clear evidence of a canonical extracellular peptidoglycan structure, and is unable to grow outside the nematode host (Taylor, Voronin, et al., 2012). Therefore, it is thought that the nematode also confers with protection and provides nutrients essential for its growth (Taylor, Voronin, et al., 2012).

1.1.3 *Litomosoides sigmodontis* as a model organism to study filarial biology

A challenge in the study of fundamental aspects of filarial biology is the difficulty of maintaining the lifecycle of human pathogens in genetically tractable hosts, such as rodents (Attout, Martin, et al., 2000). This has, in turn, limited both access to some lifecycle stages and the ability to address fundamental questions under relevant physiological conditions. Nonetheless, these issues have been traditionally circumvented by the study of alternative parasite species that are closely related to filariae of medical and veterinary importance. One of such organisms is *Litomosoides*

sigmodontis, whose lifecycle can be maintained in fully permissive rodents (Hoffmann, Petit, et al., 2000) (**Figure 1.3**). Phylogenetic analysis based on 5S ribosomal DNA spacers profiling have placed *L. sigmodontis* as part of the family *Onchocercideae* (Lefoulon, Bain, et al., 2015). *L. sigmodontis* completes its lifecycle from the infective L3 to the release of microfilariae by adult females in gerbils (*Meriones unguiculatus*) and BALB/c mice, and therefore allows the study and modulation of distinct states of infection (Attout, Martin, et al., 2000). This rodent parasite can be found naturally in the cotton rat (*Sigmodon hispidus*), which can survive rather high blood microfilariae levels (up to 10.000Mf/μL blood). As described earlier, during the blood meal from an infected rat, the arthropod intermediate host (*Ornithonyssus bacoti* mite) ingests the microfilariae, which then migrate to the thorax and reach the infective L3 stage within 10-14 days. The L3 then migrate from the thorax to the mouthparts of the insect, and are transmitted to the vertebrate host during the next blood meal. Once in the vertebrate host, the L3s make their way through the skin via the lymphatic vessels to the heart, the blood circulation and finally the lungs, from which they penetrate into the thoracic cavity (Babayan, Read, et al., 2010; Hoffmann, Petit, et al., 2000). Ten to twenty days post-infection, up to 90% of the L3s have moulted to L4 stage and are often detected in the thoracic and peritoneal cavities, and >99% of these reach the thoracic cavity 28 days post infection (Babayan, Read, et al., 2010; Hoffmann, Petit, et al., 2000) (**Figure 1.3**). The male and female adult worms then mature within 25-33 days post-infection when they become sexually active. At this point, the viviparous females release microfilariae into the thoracic cavity (**Figure 1.3**). These microfilariae penetrate the heart and eventually reach the blood circulation. Microfilariae are detectable in the blood between 60-130 days post infection (**Figure 1.3**). The infection of BALB/c mice ends with the encapsulation of adult worms by host inflammatory cells and the eventual absorption of dead parasites by the host, normally observed at 180 days post-infection (Babayan, Read, et al., 2010; Babayan, Ungeheuer, et al., 2003; Bain, & Babayan, 2013; Hoffmann, Petit, et al., 2000).

1.1.3.1 Immunity against *L. sigmodontis*

Early studies of the immune response against *L. sigmodontis* infection demonstrated that the depletion of CD4+ T cells results in a higher *L. sigmodontis* worm burden and an increased and prolonged microfilaremia, thus indicating the important role of

adaptive immunity to control the infection caused by *L. sigmodontis* (Al-Qaoud, Taubert, et al., 1997). Further studies indicated that IL-5 deficient mice can have up to a 200-fold higher parasitic load and prolonged patency when compared to wild type mice. This suggests that IL-5, or IL-5-producing cells, are involved in the control of adult worm development and microfilaremia during primary infections (Al-Qaoud, Pearlman, et al., 2000; Babayan, Read, et al., 2010; Volkmann, Bain, et al., 2003; Volkmann, Saeftel, et al., 2001). These studies demonstrate the involvement of humoral factors (such as IL-5), as well as innate and adaptive immunity for the control and clearance of filarial nematodes. Interestingly, BALB/c mice have been demonstrated to be susceptible to the infection by *L. sigmodontis,* whereas C57BL/6 mice are naturally resistant to the infection caused by *L. sigmodontis* (Babayan, Ungeheuer, et al., 2003), providing a framework to understand, at a cellular and molecular level, the susceptibility to filarial infections observed in human populations (described in next sections) (Le Goff, Lamb, et al., 2002). Using these two mouse strains, it has been demonstrated that the infective larvae migrate and settle in the pleural spaces at the same rate regardless of the host genetic background (Babayan, Ungeheuer, et al., 2003). However, both T_h1 (pro-inflammatory) and T_h2 (anti-inflammatory) immune responses were observed in C57BL/6 mice, and were accompanied by an expansion of infiltrating leukocytes to the pleural cavity, which resulted in retardation of worm growth, moulting and killing (Babayan, Ungeheuer, et al., 2003). Intriguingly, both IL-6 and IL-5 were strongly produced only when stimulating cells from the lymph nodes draining the site of infection with infective larvae antigen preparations, thus indicating that host-derived factors might constitute potent environmental cues that filarial parasites use to coordinate their development and reproduction (Babayan, Ungeheuer, et al., 2003). This was further demonstrated in IL-5 knockout mice on a C57BL/6 background, where it was concluded that filarial parasites accelerate their development and reproductive schedule in response to IL-5 driven eosinophilia, which is "sensed" by the parasite as a predicting factor future life expectancy (Babayan, Read, et al., 2010). These studies in *L. sigmodontis* have provided important insights into the way in which the immune system counteracts filarial infections, but has also provided strong evidence to understand how filarial nematodes actively respond to the immune response mounted against them, with important implications for vaccination strategies (Babayan, Allen, et al., 2012).

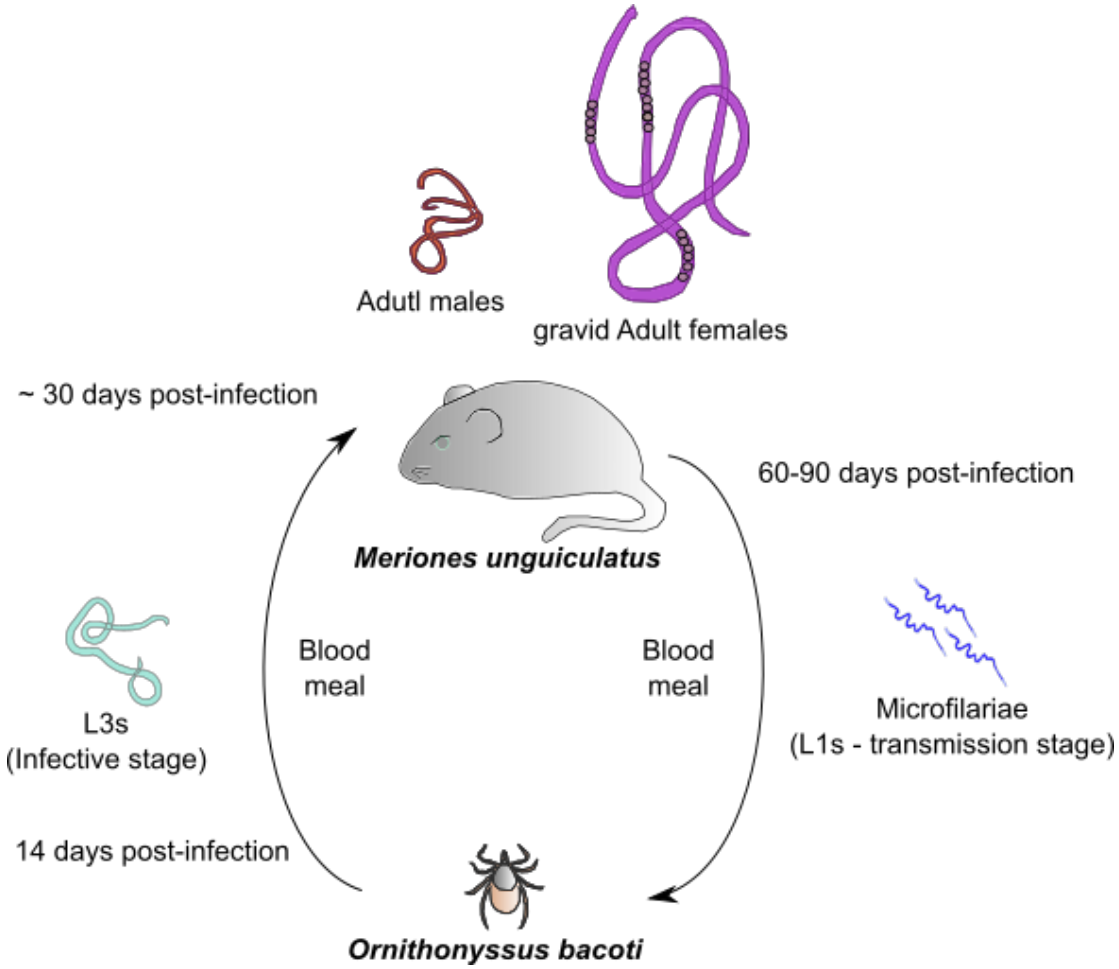

Figure 1.3 *Litomosoides sigmodontis* lifecycle. As shown for the lifecycle of *O. volvulus* and other filarial nematodes, the lifecycle involves a vector stage (*O. bacoti*) and a host stage (*M. unguiculatus*). When the vector takes a blood meal from an infected rodent, it ingests microfilariae (transmission stage), which then undergoes two moulting steps within 14 days post-infection to reach the L3 (infective) stage. This larval stage is quiescent and only resumes development when the mite inoculates the vertebrate host during a blood meal. Within the vertebrate host, the infective stage moults to L4s (not depicted here) within 20 days post-infection, and to adult males and females within ~30 days post-infection. These two stages normally reside in the pleural space, where they mate, releasing tens of microfilariae per day. The microfilariae can be detected in circulation between day 60-90 post-infection.

1.2 Regulation of the immune system by filarial nematodes

Parasitic nematodes have evolved sophisticated mechanisms to withstand the host immune response, rendering them able to reside and reproduce within the vertebrate host for prolonged periods of time, without causing severe pathology (Taylor, Hoerauf, et al., 2010). One of such mechanisms involve adjusting the parasite's developmental schedule and the brood size in response to immune factors that are predictors of the life expectancy of the parasite of the host (e.g. IL-5-driven eosinophilia) (Babayan, Read, et al., 2010; Kochin, Bull, et al., 2010). Similarly, other mechanisms involve the release of factors, broadly termed Excretory/Secretory (ES) products, which have immunomodulatory properties (Maizels, & Yazdanbakhsh, 2003).

1.2.1 Parasite Excretion/Secretion (ES) products in the host-parasite interface

Several functions have been associated with the release of extracellular factors, including modulation of the host immune response, and therefore constitutes an active and intricate form of communication with the vector and/or vertebrate host (Hewitson, Grainger, et al., 2009). The ES products have been characterised using both functional analyses (e.g. enzymatic activity) and proteomic approaches (Hewitson, Grainger, et al., 2009), and are often composed of proteinases, inhibitors of proteases, antioxidant enzymes, and immunomodulatory components (Hewitson, Grainger, et al., 2009; Maizels, & McSorley, 2016; Maizels, & Yazdanbakhsh, 2003). However, the complexity of ES products seems ever growing, and it is now accepted that they also contain parasite-derived nucleic acids (Buck, Coakley, Simbari, Mcsorley, et al., 2014; Coakley, Maizels, et al., 2015; Marcilla, Trelis, et al., 2012; Tritten, Clarke, et al., 2016; Tritten, & Geary, 2016). This will be discussed in more detail in section 1.6.

1.2.1.1 Origin of nematode ES products

In nematodes, the sources of ES products include specialised excretory and secretory tissues and organs such as the gut, the excretory-secretory system, the reproductive tissue and uterine fluids, the cuticle, amongst others (**Figure 1.4**) (Morris, Bennuru, et al., 2015). In *C. elegans*, the excretory-secretory system is composed of 4 cells: the

pore cell, duct cell, excretory canal cell (H cell) and the excretory gland cell (Buechner, 2002). The excretory canal is filled with fluids, has the appearance of a letter "H" and is the largest cell in *C. elegans* as it extends almost the entire length of the worm (Buechner, 2002). The excretory gland cell presumably collects fluids and then empties them outside via the excretory duct and the pore cells to which it is connected by gap junctions, thus acting as a form of renal system (Buechner, 2002). Similarly, the gut in nematodes has specialised secretory functions, with the release of molecules involved in enzymatic digestion of food, or protection of the parasites' gut epithelium from attack by its intestinal digestive enzymes, and material resulting from turnover would be shed from the gut of actively feeding adult nematodes (McGhee, 2007). Another likely source of ES product is constituted by the uterine fluids released during egg shedding and/or release of larvae from gravid female worms (Chehayeb, Robertson, et al., 2014; Moreno, & Geary, 2008). In fact, comparison of the uterine fluids with other tissues from *A. suum* revealed the high complexity of this fraction, with some of its components being recognized by sera from naturally infected pigs (Chehayeb, Robertson, et al., 2014). Similarly, molecules derived from the cuticle of nematodes make a substantial contribution of the contents of ES products of parasites maintained *in vitro* and are probably also shed *in vivo* (Morris, Bennuru, et al., 2015). The active shedding of such surface molecules may have profound implications for the development of host-protective immune responses to parasitic nematodes since they may provide antigen suitable for stimulation of anti-surface immune responses (Gregory, & Selkirk, 1989; Guiliano, Hong, et al., 2004; Kwan-Lim, Gregory, et al., 1989), as demonstrated in *Trichinella spiralis* (Hewitson, Harcus, et al., 2008), *Toxocara canis* (Grieve, 1990), *Dirofilaria immitis* (Grieve, 1990), and *B. malayi* (Bennuru, Semnani, et al., 2009).

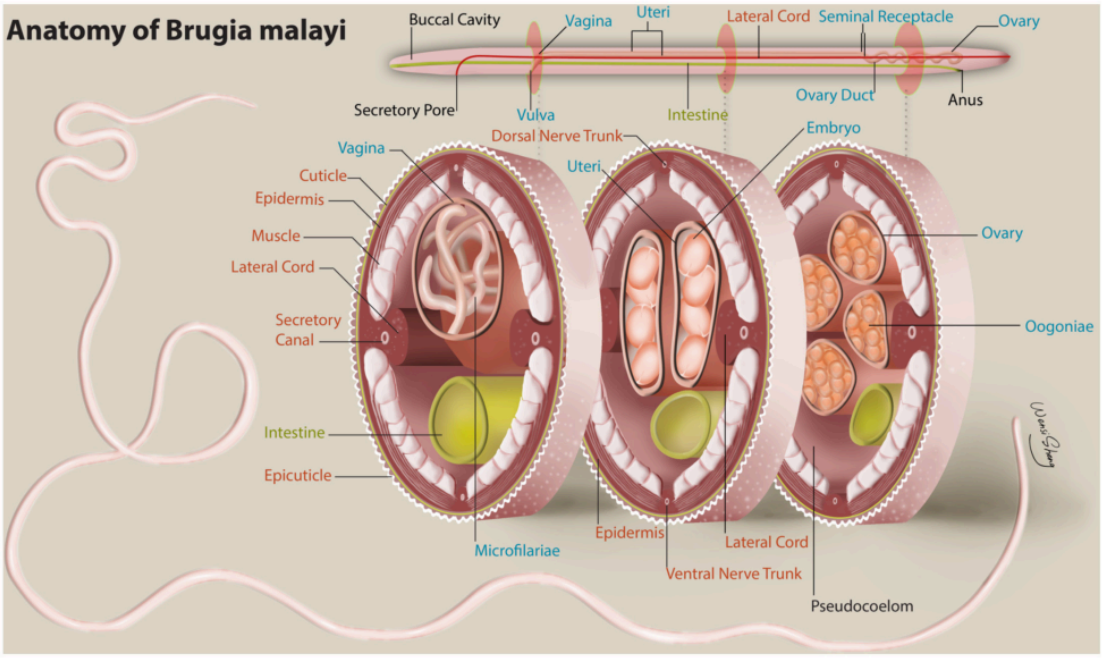

Figure 1.4 Anatomical structure of the gravid adult female of *B. malayi*. The cartoon depicts the major structures and organs identified in adult filarial female worms, such as the cuticle, the secretory canals, the reproductive organs and the digestive tube (Taken from Morris, Bennuru, et al., 2015).

1.2.1.2 Effector function of ES products

A wide variety of direct immunomodulatory effects of ES products from different parasitic nematodes have been extensively reported and may at least partially explain how their mechanisms of immune evasion are orchestrated (Hewitson, Grainger, et al., 2009). The effector functions of the ES products are involved in establishing a permissive, hypo-responsive status in the host that allow for the parasite to successfully establish an infection (Maizels, & Yazdanbakhsh, 2003). Broadly, the immunological properties of the helminth ES products involve the induction of suppressive alternatively-activated macrophages (AAMϕ) (Kreider, Anthony, et al., 2007), induction and regulation of regulatory T (Treg) cell activity (Allen, & Macdonald, 1998; Grainger, Smith, et al., 2010), as well as the impairment of antigen presentation by antigen presenting cells (APCs) such as dendritic cells (DCs) (Segura, Su, et al., 2007; White, & Artavanis-Tsakonas, 2012) (**Figure 1.5**). Interestingly, many ES products from nematodes are modified post-translationally forming antigenic glycoconjugates, thought to confer them with stability in the extracellular milieu (Ditgen, Anandarajah, et al., 2014; Hewitson, Grainger, et al., 2009). An example of these post-translationally modified secreted protein is the ES-62, which has been demonstrated to be modified with an N-type glycan containing phosphoryl-choline (PC-glycan) (Houston, & Harnett, 2004). ES-62 exerts an immunomodulatory effect on a variety of mechanisms that involve impairment of lymphocyte function including T and B lymphocytes (Marshall, Grierson, et al., 2005; Wilson, Deehan, et al., 2003), as well as APCs such as DCs and macrophages (Eason, Bell, et al., 2016; Goodridge, Wilson, et al., 2001). Rather than acting in an immunosuppressive manner, ES-62 induces a T_h2 anti-inflammatory phenotype, characterised by the production of IL-10, reduced levels of IL-12, IFN-γ and pro-inflammatory cytokines, and IgG1 rather IgG2 antibodies (Harnett, & Harnett, 2006; Harnett, McInnes, et al., 2004). The immunomodulatory properties of the helminth ES products has begun to be explored for its potential in the therapeutic treatment during inflammatory and allergic diseases (Harnett, Melendez, et al., 2010; Harnett, McInnes, et al., 2004; Maizels, & McSorley, 2016; McInnes, Leung, et al., 2003)

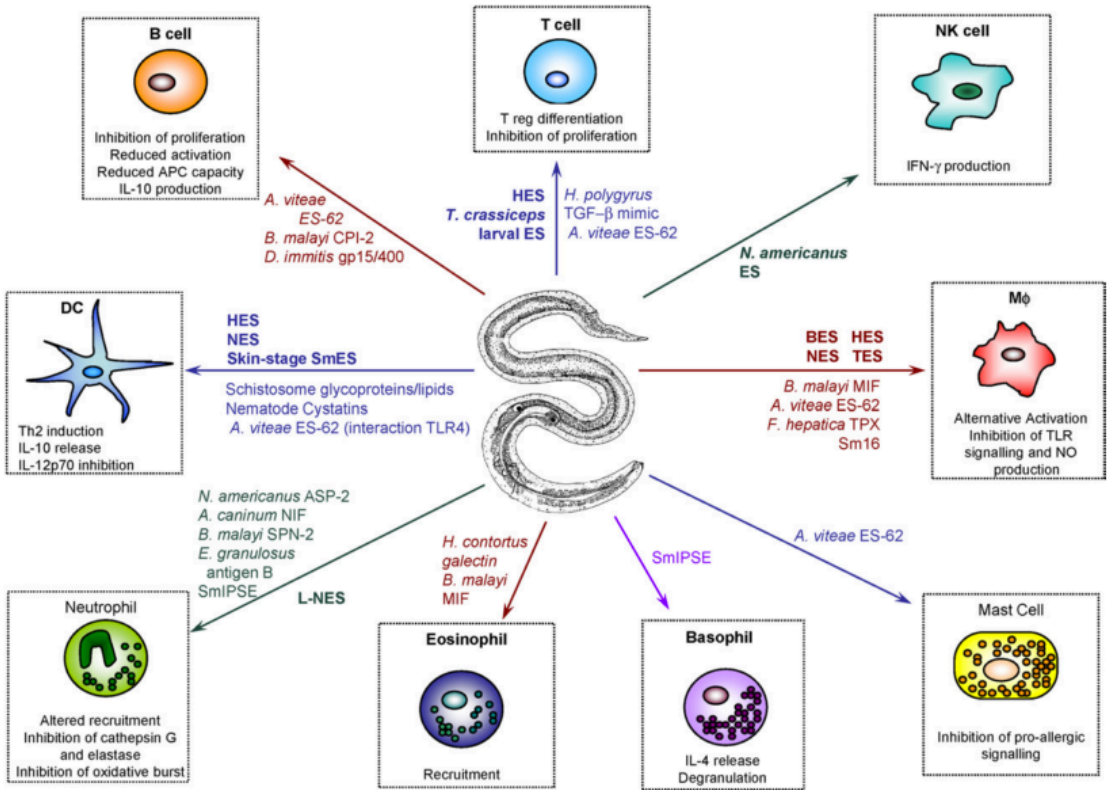

Figure 1.5 Mechanisms of immune evasion mediated by helminth Excretory/Secretory (ES) products. The image summarises some of the described immunomodulatory properties of ES products from multiple helminth pathogens of medical and veterinary importance, including *B. malayi*, *T. canis*, and the trematode *S. mansoni*. Abbreviations: APC; Antigen presenting cells; ASP, *Ancylostoma* secreted protein; BES, *B. malayi* ES; CPI, cysteine proteinase inhibitor (cystatin); HES, *H. polygyrus* ES; IPSE, IL-4 inducing principle of schistosome eggs; L-NES, Larval *N. brasiliensis* ES; MIF, Macrophage migration inhibitory factor; NES, Adult *N. brasiliensis*; NIF, Neutrophil inhibitory factor; Sm, *Schistosoma mansoni*; SPN, Serine Proteinase Inhibitor (serpin); TLR, Toll-like receptor; TGF-β, transforming growth factor beta; TES, *T. canis* ES (Taken from Hewitson, Grainger, et al., 2009)

1.3 Immunopathology of filarial infections

1.3.1 Lymphatic filariasis

In the majority of the clinical cases of onchocerciasis and lymphatic filariasis, an immunological hallmark of infection is a heavy parasite burden and a reduced antigen-specific T cell response (hypo-responsive status), characterised by low productions of IFN-γ and IL-5 (Hoerauf, Satoguina, et al., 2005). These puzzling observations (high infection load vs. low immune response), together with the spectrum of clinical symptoms observed in these patients, were soon demonstrated to be intricately orchestrated by a multitude of immunological signals leading to a "permissive" response to the infection in the host, which serves to limit severe pathology (Maizels, & Yazdanbakhsh, 2003; Taylor, Hoerauf, et al., 2010). It is important to note that the host immune responses initiated upon filarial infection involve two different pathogens, the filarial nematode and the *Wolbachia* endosymbiont (Hise, & Pearlman, 2004; Tamarozzi, Halliday, et al., 2011). In general, patients suffering from lymphatic filariasis exhibit a wide range of clinical manifestations, which are often associated with the frequency and intensity of the host inflammatory response to dying or dead worms (Taylor, 2003; Taylor, Hoerauf, et al., 2010; Taylor, Voronin, et al., 2012). Dead worms are normally encapsulated within granulomas in the lymphatic system, and it is thought that the *Wolbachia* released upon worm death induce the activation of immune effectors and evoke a cellular and humoral response associated with T-cell helper (T_h)-1 and T_h17 phenotypes (Taylor, Hoerauf, et al., 2010). The release of *Wolbachia* components are concomitantly recognised by Toll-like Receptor (TLR) 2 and TLR6 expressed in several cell types, including DCs, resting macrophages, neutrophils and stromal cells (Bouchery, Lefoulon, et al., 2013; Brattig, Bazzocchi, et al., 2016). The engagement of *Wolbachia* antigens to the TLR receptor activates both innate and adaptive immune responses (Taylor, Hoerauf, et al., 2010), leading to a multitude of effects, including neutrophil degranulation, macrophage polarisation, induction of T_h1-mediated pro-inflammatory responses, among others (Babu, Anuradha, et al., 2011; Bouchery, Lefoulon, et al., 2013; Taylor, 2003; Taylor, Voronin, et al., 2012). In lymphatic filariasis, an exacerbated production of vascular endothelial growth factor (VEGF)-A and VEGF-C promotes lymphangiogenesis, lymphatic endothelial proliferation and dilation of the lymphatic vessels, eventually inducing the formation of hydrocele and

lymphedema in lower limbs (Pfarr, Debrah, et al., 2009) (**Figure 1.6**). Interestingly, it has been demonstrated that treatment of infected patients with Doxycycline (DOX) not only reduces the levels of *Wolbachia* in the filarial parasite, but also induces a reduction on the plasma levels of VEGF-C/VEGF-3, thus ameliorating the dilation of lymphatic vessels and improving the pathology of lymphedema patients (Panic, Duthaler, et al., 2014; Pfarr, Debrah, et al., 2009).

Figure 1.6 Typical limb malformation associated with lymphatic filariasis. During the chronic stage of the infection, lymphatic filariasis is characterised by malformation of the lower limbs, often accompanied by limited mobility (*Taken from* http://globalhealth.org/the-morbidity-management-and-disability-prevention-for-blinding-trachoma-and-lymphatic-filariasis-mmdp-project/)

1.3.2 Onchocerciasis

In onchocerciasis, the prevalence of the infection and disease in a community is related to the proximity to rivers, normally inhabited by the black fly vector (Taylor, Hoerauf, et al., 2010). Due to social and economic activities around the rivers in these regions, the disease is most frequently diagnosed in male patients around 20-30 years of age with infection intensity varying geographically (Taylor, Hoerauf, et al., 2010). In hyper-endemic regions, about 60% of the population present mf in skin snips, often with > 50 worms per mg of skin. The pathology induced by onchocerciasis is associated with mf death, which results in itching, acute and chronic papular dermatitis and lichenified onchodermatitis (Taylor, Hoerauf, et al., 2010). Ocular lesions, leading to severe visual impairment and blindness, result from the migration of mf to the eye tissue and the subsequent inflammatory response induced by their death (Allen, Adjei, et al., 2008; Babalola, 2011; Taylor, 2003; Utzinger, Becker, et al., 2012) (**Figure 1.1)**. In these cases, the mf-associated inflammation causes punctate keratitis, sclerosing keratitis, iridocylitis, permanent visual impairment and complete blindness (**Figure 1.1 and 1.7**) (Allen, Adjei, et al., 2008; Babalola, 2011; Taylor, 2003; Utzinger, Becker, et al., 2012). Further studies in a mouse model of corneal keratitis have shown that *Wolbachia* induces a TLR2- and TLR6-dependent production of the T_h1 cytokines IFN-γ and IL-1β, as well as chemokine production, leading to the recruitment and activation of neutrophils and eosinophils (Brattig, 2004; Hoerauf, Satoguina, et al., 2005; Tamarozzi, Halliday, et al., 2011). These innate immune cells release pro-inflammatory mediators that ultimately induce tissue damage to form corneal haze and opacity (Babalola, 2011).

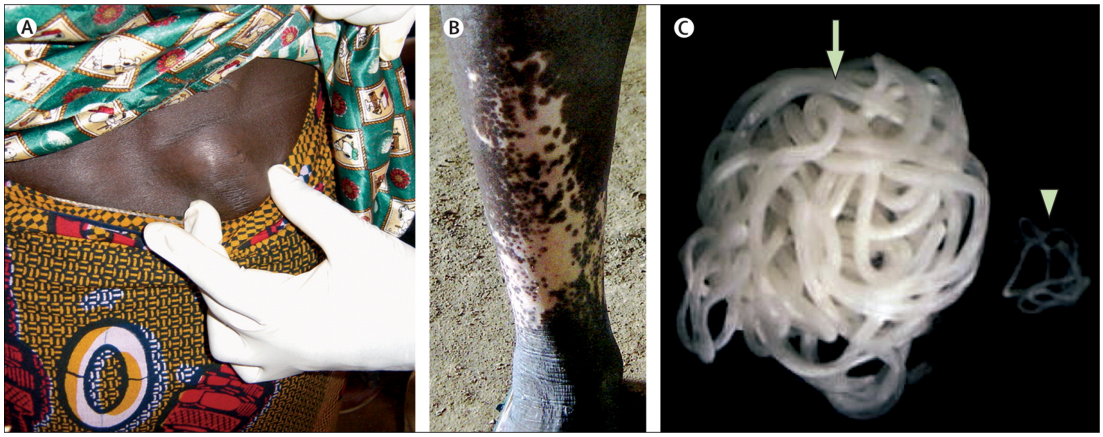

Figure 1.7 Infection caused by *O. volvulus*. A) picture of a subcutaneous nodule (onchocercoma) at the level of the hip, B) Skin depigmentation (also known as "leopard skin"), C) Picture of an adult female (left) and an adult male (right) *O. volvulus* worm (Taken from Taylor, Hoerauf, et al., 2010).

Analysis of human populations infected with *O. volvulus* have revealed that the clinical spectrum is broad, and the onchocerciasis patients are traditionally classified into three main groups:

1. Patients with generalised onchocerciasis (GEO), characterised by a generalised hypo-responsiveness to filarial antigens with an overall suppression of both T_h1 and T_h2 responses, which permits high parasite loads and reduced immune-related damage to the host (Arndts, Specht, et al., 2014; Katawa, Layland, et al., 2015; Kurniawan, Yazdanbakhsh, et al., 1993; Sartono, Kruize, et al., 1995; Utzinger, Becker, et al., 2012). This group encompasses the majority of the clinical cases of onchocerciasis and is characterised by a weak proliferative response to filarial antigens by T cells (Kurniawan, Yazdanbakhsh, et al., 1993; Sartono, Kruize, et al., 1995). Also, these patients normally exhibit high serum levels of parasite-specific IgG4 and IgE (Kurniawan, Yazdanbakhsh, et al., 1993; Sartono, Kruize, et al., 1995). This generalised immune hypo-reactivity is associated with the production of the anti-inflammatory cytokines TGF-β and IL-10 by Treg cells (Arndts, Specht, et al., 2014; Maizels, & Yazdanbakhsh, 2003; Metenou, & Nutman, 2013; Taylor, van der Werf, et al., 2009). Tregs, together with the expansion of AAMϕ, exert a strong suppression of inflammatory responses, leading to high parasitic burdens without an exacerbated and detrimental immune response against the parasites (Metenou, & Nutman, 2013) (**Figure 1.8**).

2. Hyper-reactive onchocerciasis or "Sowda", characterised by a strong T_h2 cytokine response, together with high levels of anti-*O. volvulus* IgG1 and IgG3, as well as pronounced eosinophilia, and hypersensitivity (Katawa, Layland, et al., 2015; Korten, Hoerauf, et al., 2011; Kurniawan, Yazdanbakhsh, et al., 1993). These patients exhibit very low parasitic burden, reflected by low number of cutaneous onchocercoma, adult filariae worms and mf (Arndts, Specht, et al., 2014). Additionally, these patients show higher levels of IFN-γ and equivalent levels of filarial-specific IL-4 secreting lymphocytes when compared to GEO patients, indicative of bias towards a T_h1-type of response (Katawa, Layland, et al., 2015) (**Figure 1.8**). Other histopathological features of Sowda include extensive follicular hyperplasia and activation of the lymph germ centres, an increase in the number of plasma cells producing IgE and IgG class antibodies, and high number of eosinophils surrounding degenerated mf (Kurniawan, Yazdanbakhsh, et al., 1993) (**Figure 1.8)**. In this regard, eosinophils are thought to

damage filarial worms by releasing cytotoxic cationic proteins as well as newly formed mediators such as oxygen radicals, and are the most like effector cells inducing mf killing in Sowda (Arndts, Specht, et al., 2014; Hoerauf, Satoguina, et al., 2005; Nfon, Makepeace, et al., 2006)

3. Endemic normal (EN) or "Putatively immune" (PI) patients, represented by a small population, these are individuals living in close contact to the vector and residing in endemic areas, and yet do not acquire detectable patent infection despite exposure (Elson, Guderian, et al., 1994; Tamarozzi, Halliday, et al., 2011; Turaga, Tierney, et al., 2000; Ward, Nutman, et al., 1988). The immune response in these patients is characterised by mixed T_h1/T_h2 response, likely to be triggered by both nematode and *Wolbachia* components (Turaga, Tierney, et al., 2000), although other factors, such as the presence of IgG3, are also associated with the resistance to infection observed in patients within this category (Tamarozzi, Halliday, et al., 2011).

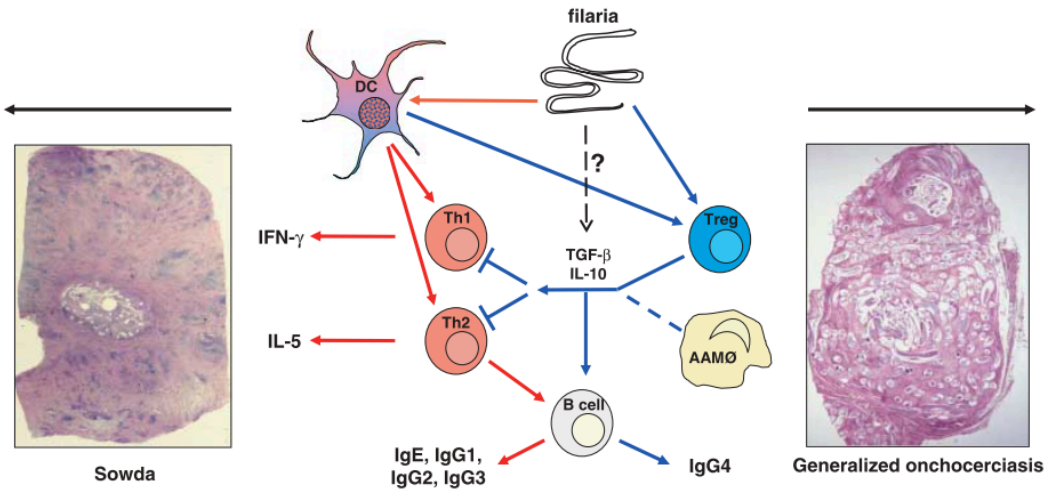

Figure 1.8 Polarised host reactivity and immunomodulation in human onchocerciasis, exemplified by generalised onchocerciasis (GEO) vs Hyper-reactive onchocerciasis or "Sowda" The clinical spectrum of onchocerciasis is depicted. In one extreme, pro-inflammatory immune responses (red network) are mediated by T_h1 and T_h2 reactions, with a concomitant production of IFN-γ, IL-5, respectively, as well as IgG1-3 and IgE by B cells. If these reactions are not down-regulated, further effector cells such as eosinophils, neutrophils and pro-inflammatory macrophages are recruited and attack the adult worms and microfilariae, resulting in a low parasitic burden but a high amount of tissue damage and cell infiltration (as shown in the tissue section), which are typically found in Sowda patients. On the other extreme, most the clinical cases are characterised by an overall down-regulatory mechanism mediated by regulatory T cells (Tregs) and alternatively activated macrophages (AAM), aided by dendritic cells. Upon encountering filarial antigens, these cells secrete IL-10 and TGF-b, which together hamper the activation of both T_h1 and T_h2 T cell subsets, but also stimulates the secretion of IgG4 by B cells. This results in a high parasite burden and low cell infiltrations, inflammation and tissue damage. These are all events found in GEO patients (Taken from Hoerauf, Satoguina, et al., 2005)

1.4 Treatment and prevention

Filarial infections are challenging to control as their lifecycles are complex, involving a stage in the vector and a stage in the vertebrate host. Therefore, several efforts aim to understand and control the vector population but perhaps not surprisingly, one of the most successful strategy thus far rely on administration of anthelminthic chemotherapy, mostly through community-based mass drug administration (MDA) (Arndts, Specht, et al., 2014). The overall goal of the MDA is to reduce the likelihood of transmission and/or the transmission rate in endemic regions, while also providing relief to infected patients (Arndts, Specht, et al., 2014). Current control and elimination programmes launched by the World Health Organisation (WHO), such as the Global Programme to Eliminate Lymphatic Filariasis (GPELF), the African Programme for Onchocerciasis Control (APOC), and the Onchocerciasis Elimination Programme of the Americas (OEPA) have ambitiously established an international agenda which seeks to control and eliminate transmission in multiple foci in sub-Saharan countries as well as in Latin America (Boatin, Basáñez, et al., 2012; Crump, Morel, et al., 2012). These programmes coordinate and provide MDA to several communities in endemic regions in the Sub-Saharan Africa as well as in Latin America (Panic, Duthaler, et al., 2014; Taylor, Hoerauf, et al., 2010). Since 1989, Ivermectin (IVM) has been the main anthelminthic chemotherapy provided as part of MDA programmes to control onchocerciasis in Africa and Latin America (Panic, Duthaler, et al., 2014; Wolstenholme, Maclean, et al., 2016). Traditionally, IVM has been has been administered alone in MDA programmes, although a combination with other anthelminthic compounds, such as Albendazole (ABZ) and/or the anti-*Wolbachia* Doxycycline (DOX), has been shown to be far more effective at suppressing circulating mf than DOX, IVM or ABZ alone, achieving complete mf clearance in ~40% of the treated patients (Fischer, King, et al., 2017; Panic, Duthaler, et al., 2014). Following the success of the OEPA programme, which has used MDA of IVM alone to abrogate transmission in most endemic foci (Hotez, Bottazzi, et al., 2008), the goal of the African Programme for Onchocerciasis Control (which covers a vastly greater area) has shifted from control to eradication (Crump, Morel, et al., 2012). However, major challenges to this endeavour remain, such as the potential emergence of resistance to IVM (Osei-Atweneboana, Eng, et al., 2007), the risk of severe adverse reactions to IVM in loiasis-endemic areas (Gardon, Gardon-Wendel, et

al., 1997), and significant limitations in the accurate and rapid diagnosis of infection (Boatin, Toé, et al., 2002; Eberhard, Cupp, et al., 2017).

1.5 Diagnosis of filarial infections

As discussed previously, the major focus of the anti-filarial agenda, currently managed by the WHO, aims to control and eliminate filarial infections in several endemic foci. To achieve these challenging goals, the control and elimination programmes require the demarcation and prioritisation of endemic areas for intervention via community-directed MDA, as well as the establishment of ways in which the success of the MDA can be monitored, when to halt the intervention, and how to maintain a successful surveillance on these foci during post-MDA (Boatin, Basáñez, et al., 2012; Crump, Morel, et al., 2012). Therefore, these programmes are broadly classified into four main phases, as proposed by Weil & Ramzy (Weil, & Ramzy, 2007). The first two phases involve mapping endemic areas, planning the MDA strategies, and monitoring the MDA, whereas the last two phases aim to decide when to stop MDA and how to maintain an effective surveillance post-MDA to control for an increase in the transmission rates (Weil, & Ramzy, 2007).

1.5.1 Parasitological and antigenic diagnostics

Despite the enormous effort towards the implementation of these programmes and the specific requirements that need to be met in each phase of the control and elimination programmes, the gold standard diagnostic technique for filariasis involves the detection of circulating mf in blood smears (LF) or skin biopsies (onchocerciasis) (Rebollo, & Bockarie, 2017; Weil, & Ramzy, 2007). Some of the limitations of this diagnostic method are associated with the discomfort they often cause, it is labour-intensive, and its efficacy has recently been revisited as it might not be a reliable diagnostic method in post-MDA surveillance (Eberhard, Cupp, et al., 2017; Guzmán, Awadzi, et al., 2002). An alternative diagnostic method, rarely used in the field nowadays, involves the application of diethylcarbamazine (DEC) patches directly to the skin (Boatin, Toé, et al., 2002). DEC induces extensive mf death in the site of application, leading to the appearance of pruritus and rash in infected patients but not in uninfected patients, and is indicative of a positive results (also known as the Mazzotti test) (Taylor, Hoerauf, et al., 2010). Nevertheless, this method has shown to

be less sensitive than skin biopsies, and its use has decreased over time (Alhassan, Li, et al., 2015; Boatin, Toé, et al., 2002).

Antigen testing is comparatively more sensitive than mf detection in biopsies, it is quick, inexpensive and easy to perform (Rebollo, & Bockarie, 2017; Weil, & Ramzy, 2007). The availability of immunoassays such as the Ov16 serological test for onchocerciasis (Park, Dickerson, et al., 2008), has greatly enhanced the ability to detect residual transmission or the re-emergence of infection by using young children as "sentinels", or via spot checks (Weil, Steel, et al., 2000). Other antigen testing methods, such as the commercially-available test kits to detect the *Brugia* antigen BmR1 or Bm14 (Rahmah, Taniawati, et al., 2001), are currently being deployed in *Brugia*-endemic countries where both *B. malayi* and *B. timori* are normally found (Weil, & Ramzy, 2007). The potential of other antigens as biomarkers to define and prioritise areas for intervention, such as the detection of the N-acetyltyramine-O,β-glucuronide (NATOG) in urine, is attractive but has not been fully addressed yet (Lagatie, Ediage, et al., 2016). In this regard, preliminary studies have shown that NATOG has limited potential for diagnosis of *O. volvulus*-infected, amicrofilaremic patients (Lagatie, Ediage, et al., 2016). However, one of the main hurdles of diagnostic tools based on the detection of parasite antigens is that too often these methods cannot discriminate between past and ongoing infections, thus limiting its diagnostic potential for monitoring MDA success (Weil, & Ramzy, 2007). Similarly, some of these parasite antigens exhibit long half-lives in biofluids, which makes it difficult to be used for post-MDA surveillance purposes (Weil, & Ramzy, 2007).

1.5.2 Molecular diagnostics

Alternatively, molecular diagnostics tools have been demonstrated to provide sensitive methods to diagnose helminthic infections (Alhassan, Li, et al., 2015; Fink, Fahle, et al., 2011). One of such methods involves the detection of parasite DNA in a wide variety of bodily fluids by either polymerase chain reaction (PCR) or high-throughput deep sequencing, which has proven to be successful in the diagnosis of infections caused by *S. mansoni* (Srivastava, Mehrotra, et al., 2011), gastrointestinal parasitic nematodes (Taniuchi, Verweij, et al., 2011) and *Leishmania* (Srivastava, Mehrotra, et al., 2011), and filarial nematodes (Boatin, Toé, et al., 2002; Favia, Cancrini, et al., 2000; Poole, Tanner, et al., 2012). Similarly, molecular

xenomonitoring techniques, which involve the detection of parasite nucleic acids in insect vectors collected in endemic regions, are also important for monitoring the progress of the implemented control programmes, as well as for the estimation of the likelihood of transmission in populations subjected to MDA (Weil, & Ramzy, 2007). In this regard, the detection of the DNA biomarker *O. volvulus* glutathione S-transferase 1a (*OvGST1a*) in black flies by loop-mediated isothermal amplification (LAMP) has proven to be a sensitive and rapid method that can be directly applied to monitor populations of vectors in the field (Alhassan, Makepeace, Lacourse, et al., 2014). Another DNA-based method involves the detection of the *Brugia* repetitive element *HhaI* by LAMP in blood, and has been demonstrated to be a rapid method that is highly sensitive and specific to *B. malayi* and *B. timori*, but not to other filarial nematodes, including *W. bancrofti*, *O. volvulus*, or *D. immitis* (Poole, Tanner, et al., 2012). This *Brugia* DNA-based method could potentially be adopted in places where it is urgent to develop new ways of mapping areas with *Brugian* filariasis (Weil, & Ramzy, 2007). Some of the diagnostic methods discussed thus far are summarised in **Table 1.1**. Apart from DNA-based tests, the detection of other nucleic acids, such as small non-coding RNAs have also become popular as attractive biomarkers for filarial infections (Quintana, Babayan, et al., 2016; Tritten, Burkman, et al., 2014; Tritten, & Geary, 2016; Tritten, Neill, et al., 2014). This will be discussed in more detail in the next section.

Table 1.1 Summary of parasitological and molecular diagnostic methods for filariasis

Diagnostic test	Filarial parasite	Method	Reference
Parasitological & Antigen diagnostics			
Skin biopsies ("Skin snips")[1,4]	*O. volvulus*	Skin biopsy followed by microscopic examination	(Boatin, Toé, et al., 2002; Eberhard, Cupp, et al., 2017[4]; Taylor, Keyvan-Larijani, et al., 1987)
Blood smears[1]	*Brugia spp., W. bancrofti, L. loa, D. immitis*	Blood sampling and microscopic examination	(Gardon, Gardon-Wendel, et al., 1997; Weil, & Ramzy, 2007)
DEC patch test[1]	*O. volvulus*	Direct application on the skin	(Boatin, Toé, et al., 2002)
Palpation of nodules[1]	*O. volvulus*	Direct clinical examination	(Arndts, Specht, et al., 2014; Zouré, Noma, et al., 2014)
IgG4 against Ov16[2]	*O. volvulus*	ELISA, antibody card test	(Oguttu, Byamukama, et al., 2014; Weil, Steel, et al., 2000)
IgG4 against BmR1 & BmR14[1]	*B. malayi, B. timori*	Dipstick	(Fischer, Bonow, et al., 2005)
Molecular diagnostics			
1. Repetitive elements			
O-150 repeat[1,3]	*O. volvulus*	PCR	(Alhassan, Li, et al., 2015; Boatin, Toé, et al., 2002; Fink, Fahle, et al., 2011)
HhaI repeat[1]	*B. malayi*	PCR, LAMP, HAD	(Alhassan, Li, et al., 2015; Fink, Fahle, et al., 2011)
SspI repeat[1,3]	*W. bancrofti*	PCR and PCR-based protocols	(Alhassan, Li, et al., 2015; Fink, Fahle, et al., 2011)
2. Other genes/sequences			
Glutathione S-transferase 1a (OvGST1a)[3]	*O. volvulus*	PCR, LAMP	(Alhassan, Li, et al., 2015; Alhassan, Makepeace, LaCourse, et al., 2014)
Collagen (TC8100)[3]	*B. malayi L3s*	RT-PCR	(Alhassan, Li, et al., 2015; Laney, Buttaro, et al., 2008)

These methods have been reported in [1]Clinical diagnostics, [2]Surveillance of communities, or [3]Xenomonitoring (detection of filarial load in insects).
[4]Although traditionally used for the diagnosis of onchocerciasis, it is still controversial whether skin snip test is a suitable tool for programmatic evaluation, monitoring of onchocerciasis elimination, and surveillance post-MDA (Eberhard, Cupp, et al., 2017).

1.6 Extracellular small RNAs in filarial nematodes

It is now recognized that small RNA molecules not only exert their function within, but can also operate beyond the limits of the cell. One key feature of these extracellular RNAs (exRNAs) is their remarkable stability in hostile environments such as human biofluids (Hoy, & Buck, 2012). Several studies have demonstrated that the stabilization of exRNA can occur through direct association with lipid and RNA-binding proteins, such as low-density lipoprotein (LDL) particles or Argonautes (AGO) complexes, or encapsulation within extracellular vesicles (EVs) (reviewed by Hoy, & Buck, 2012; Mittelbrunn, & Sánchez-Madrid, 2012; Turchinovich, Samatov, et al., 2013). Interestingly, EVs and exRNAs have also been found in ES products from a diverse range of parasites, from microbes to nematodes (reviewed by Coakley, Maizels, et al., 2015).

Most of the literature detailing exRNA in helminths focuses on their encapsulation within EVs although the origins of these are not all well documented. EVs that pellet upon ultracentrifugation could derive from the endocytic pathway (termed exosomes) or from budding of the plasma membrane (often termed microvesicles) and these can be difficult to distinguish by their sizes: exosomes are generally 40-100 nm and microvesicles can range from 100-1000nm (Quintana, Babayan, et al., 2016). It seems likely that such heterogeneity exists in parasite EVs, an area that remains largely unexplored, which could be key to understanding the diversity of their functions (Coakley, Maizels, et al., 2015). Initial reports in the trematodes *Echinostoma caproni* and *Fasciola hepatica* suggested that EVs (30-100 nm) could derive from tegumental structures and could be a mechanism for transferring material to host cells (Cwiklinski, de la Torre-Escudero, et al., 2015; Marcilla, Trelis, et al., 2012). EVs with similar sizes have also been characterized in the human pathogenic trematodes *Schistosoma mansoni* (Nowacki, Martin T. Swain, et al., 2015) and *Schistosoma japonicum* (Wang, Li, et al., 2015), the carcinogenic liver fluke *Opisthorchis viverrini* (Chaiyadet, Sotillo, et al., 2015), the clade V gastrointestinal nematode *Teladorsagia circumcincta* (Tzelos, Matthews, et al., 2016), and the clade I whipworm *Trichuris suis* (Hansen, Kringel, et al., 2015). In our own work, we showed that the clade V gastrointestinal parasitic nematode *H. polygyrus* secretes EVs that are enriched in proteins known to be abundant in the intestinal tissue of the parasite as well proteins associated with exosome biogenesis (e.g. ALIX) (Buck, Coakley, Simbari, Mcsorley,

et al., 2014). In the context of filarial infections, a recent report focusing on *B. malayi* showed that both iL3s and gravid adult females secreted EVs *in vitro* (Zamanian, Fraser, Agbedanu, Harischandra, et al., 2015). The EVs detected in the *in vitro* ES products from iL3s were described as homogeneous, based on size, ranging between 50 -120 nm. Proteomic analysis of the iL3s revealed an enrichment for several proteins previously termed exosome markers, including HSP70 and Rab-1 (Zamanian, Fraser, Agbedanu, Harischandra, et al., 2015).

1.6.1 Biogenesis of microRNAs

Three primary RNAi pathways have been characterized in animals: the microRNA (miRNA) pathway, the endo/exo-small interfering RNA (endo/exo-siRNA) pathway and the P-element Induced Wimpy testis (PIWI)-interacting RNA (piRNA) pathway (Hoogstrate, Volkers, et al., 2014; Weick, & Miska, 2014). These pathways are distinguished by the origin and identity of the small RNA guide and target, as well as the properties of the AGO protein to which they bind. In general AGOs have two main functions: 1) recognizing and binding small RNA and 2) mediating the interaction with other proteins required for small RNA loading, association with targeted RNAs, gene silencing activity, and/or subcellular localization (Buck, & Blaxter, 2013; Youngman, & Claycomb, 2014). From a structural standpoint, they are generally ~90-100 kDa monomeric proteins containing at least two domains: a PAZ domain (involved in 3'-end recognition and binding of the small RNA) and a PIWI domain, which binds to the 5' end of the small RNA and in some cases includes an RNaseH-like activity that can carry out endonucleolytic cleavage ("slicing") of the targets (Buck, & Blaxter, 2013; Hutvagner, & Simard, 2008).

The microRNA pathway is one of the best characterized RNAi pathways in nematodes (Bartel, 2009). These molecules, first described in *C. elegans* over two decades ago, are encoded within the genome as stem-loop structures that undergo a series of maturation events to produce the short RNA guide. In nematodes, as in other animals, miRNAs can either derive from within intragenic sequences (generally within the introns) or from independent, intergenic transcriptional units (Grishok, 2005). These transcripts, termed the primary miRNAs (pri-miRNAs), are mostly derived from the activity of RNA polymerase II (**Figure 1.9**). Some miRNAs are clustered together in discrete genomic regions suggesting coordinated expression

(Kim, Han, et al., 2009). Once transcribed, miRNA biogenesis involves a series of maturation events starting with cleavage by the microprocessor complex in the nucleus (Kim, Han, et al., 2009; Winter, Jung, et al., 2009). The microprocessor is composed of the RNase III endonuclease DROSHA, and DCRG8, among other scaffold proteins, and cleaves the pri-miRNA to produce a shorter hairpin (pre-miRNA) with a 5' monophosphate and a ~2 nt overhang at the 3' end (**Figure 1.9**). The pre-miRNA is then actively transported to the cytoplasm by Ran-GTP protein and members of the Exportin family (predominantly EXP-5). Once in the cytoplasm, the pre-miRNA is recognized by a second RNase III endonuclease called DICER that catalyses cleavage of the hairpin to produce a double stranded duplex approximately 22 nt in length, where both 3'ends display a ~2 nt overhang (Kim, Han, et al., 2009; Winter, Jung, et al., 2009). One strand of this miRNA duplex is then incorporated into RISC through association with the AGO protein (**Figure 1.9**). The miRNA then guides RISC to target messenger RNAs to elicit inhibition of translation, accelerated mRNA de-adenylation and/or endonucleolytic cleavage of the mRNA, depending on the degree of complementarity between the miRNA and its target (Kim, Han, et al., 2009; Winter, Jung, et al., 2009) (**Figure 1.10**). In animals, miRNAs are generally not perfectly complementary to their targets and recognition is dominated by the "seed" site defined as nucleotides 2-7 in the 5' end of the miRNA (**Figure 1.10**) (Kim, Han, et al., 2009).

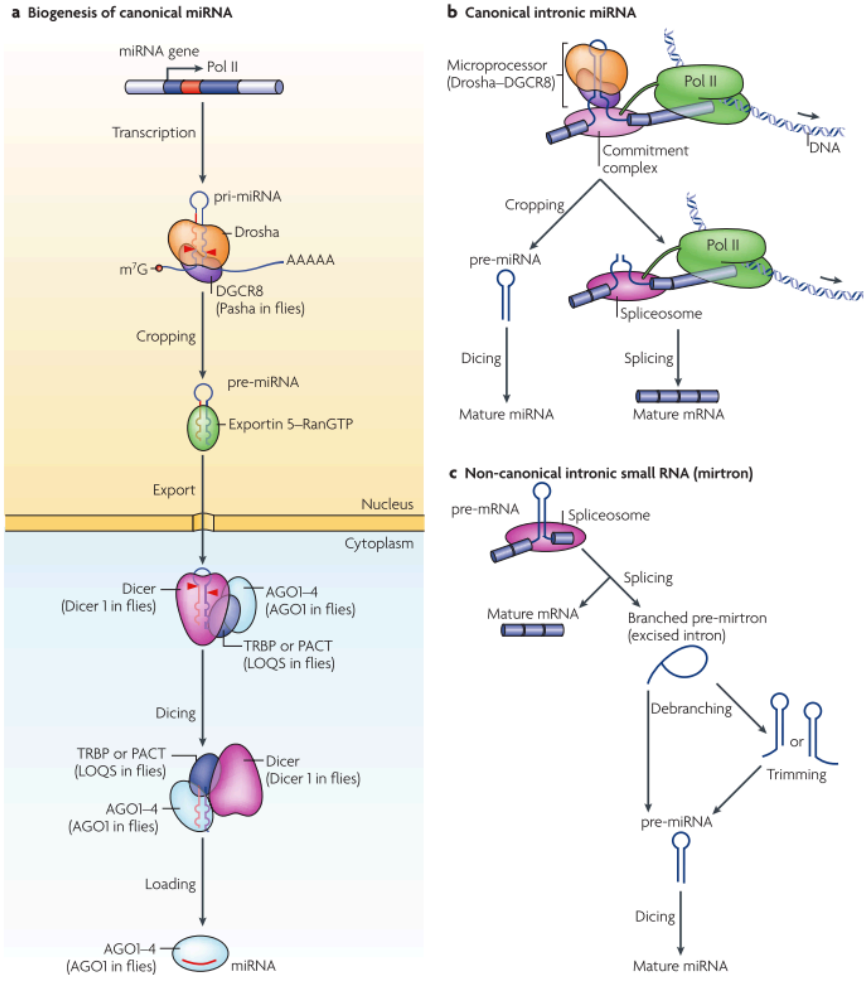

Figure 1.9 miRNA biogenesis pathways. A) Canonical miRNA genes are transcribed by RNA polymerase II (Pol II) to generate the primary transcripts (pri-miRNAs), which are often capped with m7G at the 5' end and polyadenylated at the 3' end. The initiation step ("cropping") is mediated by the microprocessor complex, formed by Drosha and DiGeorge syndrome critical region gene 8 (DGCR8). The enzymatic processing of the pri-mRNA leads to the formation of a ~65 nucleotide hairpin called pre-miRNA. Pre-miRNAs have a short stem plus ~2 nt 3' overhang, which facilitates its transport to the cytoplasm mediated by Exportin 5 (EXP5). Once in the cytoplasm, the RNase III Dicer catalyses the second processing ("dicing") step to produce miRNA duplexes. Dicer, together with other binding partners such as TBRP, PACT and Argonaute (AGO)1-4 mediate the processing of pre-miRNAs as well as the assembly of the RNA-Induced Silencing Complex or "RISC". One strand of the mature duplex remains on the AGO protein as the mature miRNA, whereas the other strand is degraded. AGO is thought to be associated with Dicer in the dicing step as well as in the RISC assembly step. B) Canonical intronic miRNAs are processed co-transcriptionally before mRNA splicing. The splicing commitment complex is thought to tether the introns while Drosha cleaves the miRNA hairpin. The pre-miRNA enters the miRNA pathway, whereas the rest of the transcript undergoes pre-mRNA splicing and produces mature mRNA for protein synthesis. C) Non-canonical intronic small RNAs are produced from spliced introns and debranching. Because such small RNAs (called "mirtrons") can derived from small introns that resemble pre-miRNAs, they bypass the Drosha processing step. Some introns have tails at either the 5' end or 3' end, so they need to be trimmed before pre-miRNA export. (Taken from Kim, Han, et al., 2009)

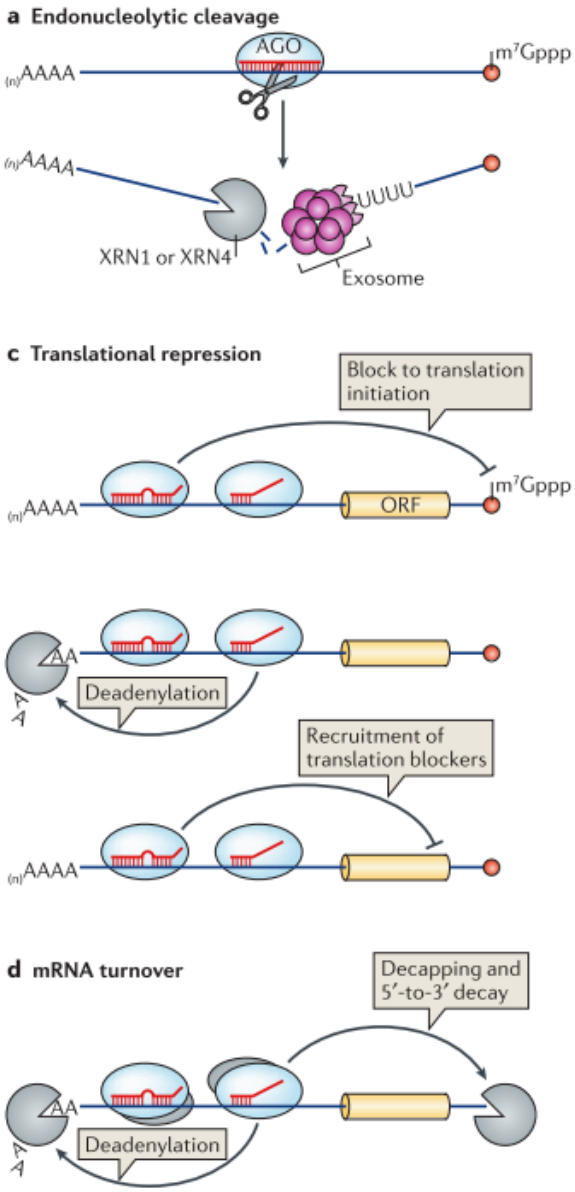

Figure 1.10 miRNA function. A) Some miRNAs direct endonucleolytic cleavage (slicing) of their mRNA targets. The 5′-to-3′ exoribonuclease XRN1 in animals, together with the major cellular 3′-to-5′ exonucleolytic complex, the exosome, subsequently degrade the sliced mRNA fragments. The 3′ end of the 5′ cleavage product is frequently uridylated, perhaps to mark these fragments for decay. B) Biochemical studies have suggested that miRNAs have a role in blocking translational initiation, in poly(A) tail shortening or in the recruitment of protein cofactors that can interfere with translation. C) In many cells and tissues, miRNA-directed translational repression is indistinguishable from mRNA destruction via decapping and 5′-to-3′ decay. This has led to the suggestion that miRNAs directly target mRNAs for decay. Another possibility is that the inhibition of translation by miRNAs (as shown in B) triggers subsequent mRNA decay, and the temporal delay between these two effects can vary depending on the surveillance mechanisms in place in cellular contexts. (Taken from Ameres, & Zamore, 2013)

1.6.2 Extracellular miRNAs as diagnostics for helminthiases

Parasitic nematodes release a myriad of RNAs, including small non-coding RNAs such as miRNAs, likely to be released either in association with protein complexes and EVs (Buck, Coakley, Simbari, McSorley, et al., 2014; Manzano-Román, & Siles-Lucas, 2012; Marcilla, Martin-jaular, et al., 2014). In both *H. polygyrus* and *B. malayi*, it has been demonstrated that EVs contain several miRNA families, including miR-71 and members of the let-7 and miR-100 families (Buck, Coakley, Simbari, McSorley, et al., 2014; Zamanian, Fraser, Agbedanu, & Harischandra, 2015). Moreover, these studies in *H. polygyrus* and *B. malayi* showed that the secreted RNA population is distinct from the RNA isolated from the total worm (Buck, Coakley, Simbari, Mcsorley, et al., 2014; Zamanian, Fraser, Agbedanu, Harischandra, et al., 2015). While these observations suggest that a subset of the total miRNA population expressed within the worm is secreted, it does not provide information on whether this subset is selectively exported from the cell from which it derives. Recent studies in mammalian cells suggest that that the selective sorting of miRNAs into EVs involves specific RNA binding proteins such as HuR hnRNPA2B1 (Mukherjee, Ghoshal, et al., 2016; Villarroya-Beltri, Gutiérrez-Vázquez, et al., 2013). The presence of ribosomal proteins in the EVs secreted by *B. malayi* iL3s was also noted (Zamanian, Fraser, Agbedanu, Harischandra, et al., 2015), though it is not known whether these proteins were bound to the rRNA fragments also found in such products. It is important to mention that it is still unclear whether or how different RNA processing pathways converge with EV biogenesis and secretion. In some systems, components of the RNA Induced Silencing Complex (RISC) have been detected in EVs or shown to co-migrate with endosomal MVB fractions in density gradients (Gibbings, Ciaudo, et al., 2009). Interestingly, one AGO protein was also identified in both vesicle and vesicle-depleted fractions from *H. polygyrus in vitro* (Buck, Coakley, Simbari, Mcsorley, et al., 2014), although the mechanistic aspects associated with secretion of AGO proteins in nematodes or others parasites are still unknown.

Beyond their potential roles in parasite-to-host, and in parasite-to-parasite communication, one interesting finding is that, similar to host-derived exRNAs, the parasite-derived exRNAs are highly stable in circulation (Cai, Gobert, et al., 2016; Quintana, Babayan, et al., 2016). As proposed for host-derived exRNAs, their

stability is thought to be mediated by their inclusion within EVs (Cai, Gobert, et al., 2016; Quintana, Babayan, et al., 2016). It is therefore not surprising that these molecules can be readily detected in serum from infected hosts, including humans, and have been proposed as novel biomarkers for helminthiases (Cai, Gobert, et al., 2016; Hoy, & Buck, 2012; Hoy, Lundie, et al., 2014; Quintana, Babayan, et al., 2016; Tritten, & Geary, 2016). In this regard, three miRNAs derived from the human parasitic trematode *Schistosoma mansoni* can significantly discriminate egg-positive patients from egg-negative patients with high sensitivity and specificity, highlighting the potential application of circulating, parasite-derived miRNAs as biomarkers for infection (Hoy, Lundie, et al., 2014).

Whilst it might be expected that all nematode parasites can or do release exRNA and EVs, there are several factors that will influence the ability to detect these molecules in different host fluids. For example, it is logical that the localization of the parasite within the host dictates the presence of parasite-derived exRNAs in different biofluids. The close contact between some filarial nematodes and the lymphatic system (*Wuchereria bancrofti*, *L. loa*, *Brugia spp.*) could account for a widespread distribution mechanism of any secreted parasite products into the bloodstream, such that they are readily detectable in serum and plasma (and perhaps urine) (**Figure 1.11**). Conversely, the presence of a nodular structure in onchocerciasis may impose a physical barrier for the trafficking of locally secreted parasite products to the bloodstream. However, the presence of a vascularized system surrounding the onchocercomata nodule may be seen as a "window" for dissemination of such products (Attout, Hoerauf, et al., 2009) (**Figure 1.12**). The mechanisms by which parasite EVs and exRNAs can bypass physical barriers (for example, those imposed by the nodular structure in *Onchocerca spp.*) and reach the bloodstream are not well understood yet but could help inform to what extent these molecules can be effectively used as biomarkers for different filarial infections. Lastly, the potential species-specificity of some miRNAs (e.g. miRNAs poorly or not conserved between parasitic species or even between parasites and hosts) makes them attractive candidates as diagnostics. A pan-filarial small RNA-based biomarker, or a female-specific miRNA biomarker, could be useful as a point-of-care diagnostic test aiming to monitor populations subjected to mass drug administration (MDA) or for surveillance purposes. Similarly, it is expected that several technological approaches must be considered in order to improve not only the platforms currently available for

exRNA detection (reviewed in Alhassan, Li, et al., 2015; Pritchard, Cheng, et al., 2012) but also the way in which these technologies can be transferred in a field-friendly manner. However, several aspects need to be first addressed for the development of a miRNA-based diagnostic application for human filariasis. In this regard, it is important to understand whether the secretion of miRNAs by filarial nematodes is developmentally regulated, whether the anthelminthic chemotherapy used as part of the MDA programmes influence miRNA secretion, and if these molecules can be used as biomarkers for filarial infections.

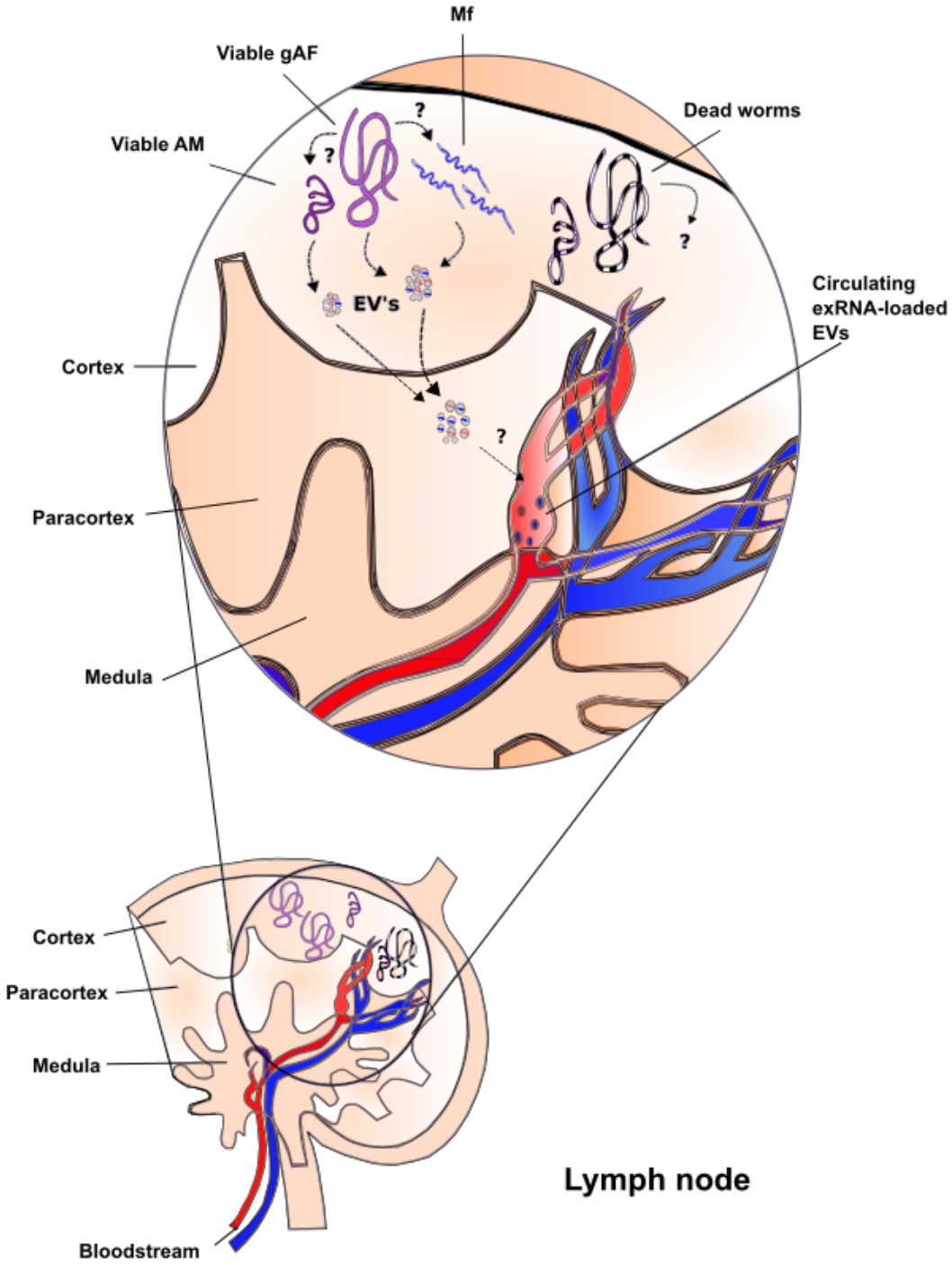

Figure 1.11 Proposed routes of EV secretion *in vivo* in lymphatic filariasis. Depiction of filarial nematodes (for example *Brugia* spp.) residing within a lymph node. A hypothesis is that the lack of a nodular structure (as observed in infection from *Onchocerca spp*) might facilitate the accessibility of EVs into the circulation. It is also unclear whether the detection of EVs and small RNAs is exclusively associated with viable worms or can be also derived from moribund or dead worms (Quintana, Babayan, et al., 2016).

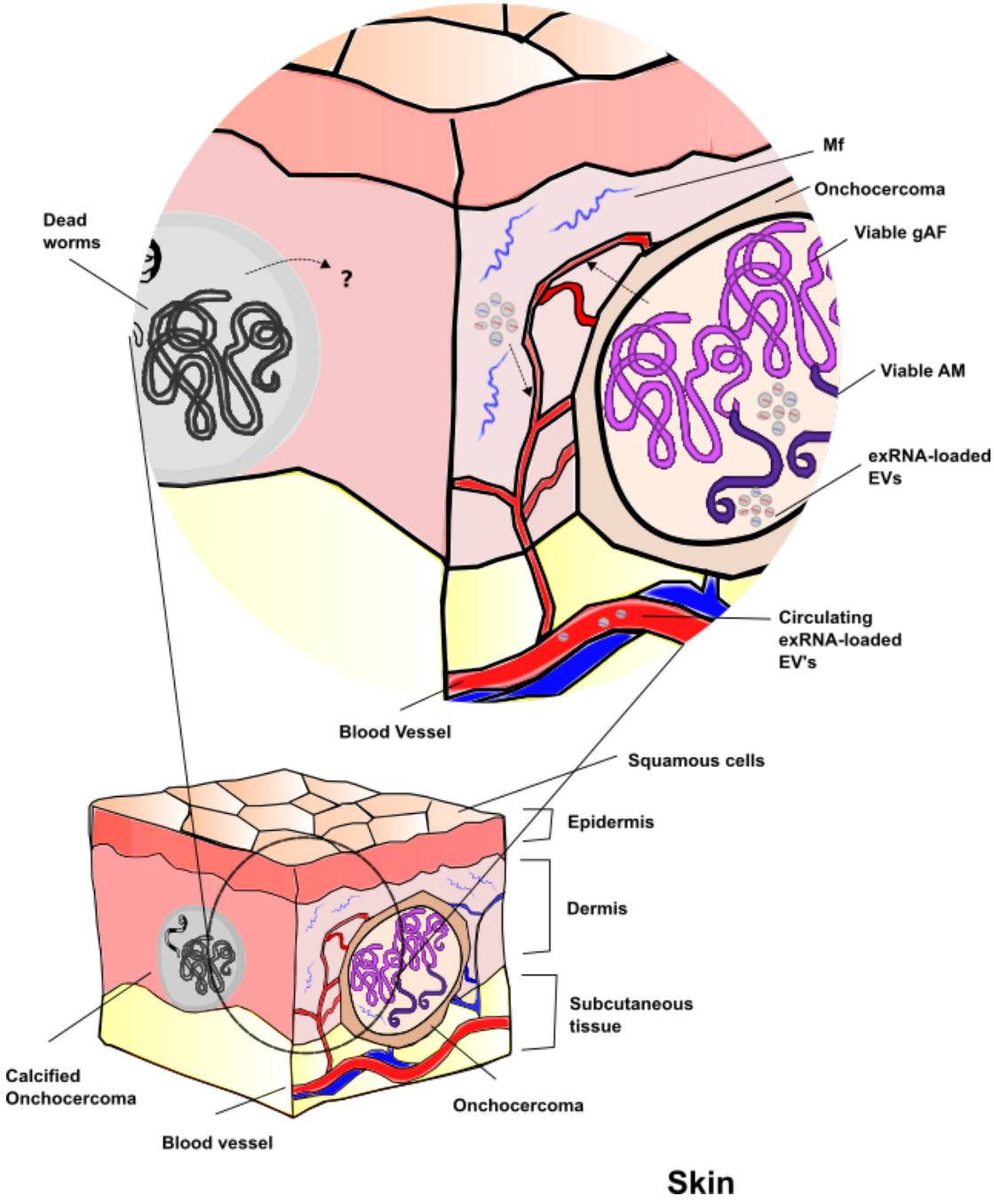

Figure 1.12 Proposed routes of EV secretion *in vivo* in onchocerciasis. Depiction of a nodule-forming species member of the *Onchocerca* genus (for example, *O. volvulus* or *O. ochengi*) residing within a nodular structure termed an onchocercoma. It is not yet clear whether or how the nodular structure imposes a physical barrier for dissemination of small RNA-loaded EVs into the bloodstream. Similarly, it is unclear whether the detection of EVs and small RNAs is exclusively associated with viable worms or can be also derived from moribund or dead worms (Quintana, Babayan, et al., 2016).

1.7 Hypotheses and objectives of this thesis

Based on the information presented thus far and considering recent studies into the role of parasite-derived microRNAs as biomarkers for helminthiases, we hypothesise that filarial-derived extracellular miRNAs:

1. Could exhibit stage- and sex-specific patterns of secretion throughout nematode development
2. May be detectable in biofluids from infected hosts compared to naïve or uninfected controls
3. May be useful as potential biomarkers for filarial infections

This PhD thesis aims to:

1. Determine the small RNA profile of the secretome from several lifecycle stages of the filarial parasite *L. sigmodontis in vitro*
2. Determine the effect of anthelminthic chemotherapy on miRNA secretion
3. Determine whether filarial-derived miRNAs can be used as biomarkers for infection

Chapter 2: **Material and Methods**

2.1 Ethics statement for human and animal works

Human samples kindly provided by Dr. K. Pfarr and Prof. A. Hoerauf, from the University of Bonn

Archived human plasma from *O. volvulus* infected and uninfected volunteers was collected as part of a European Union Seventh Framework Programme for Research grant, contract 131242 "Enhanced Protective Immunity Against Filariasis (EPIAF)", (http://www.filaria.eu/projects/projects/epiaf.html). Infected individuals were those with palpable nodules and microfilaridermia by skin snip. Uninfected individuals were defined as persons with no palpable nodules and microfilariae negative skin snips. Serum or EDTA plasma was collected as previously described (Arndts, Specht, et al., 2014). The Committee on Human Research Publication and Ethics at the University of Science and Technology in Kumasi, Ghana, and the Ethics Committee at the University of Bonn, Germany approved the use of archived plasma samples. Collection of sera from onchocerciasis patients in Cameroon was approved by the Cameroon Ethics Committee and the Ministry of Public Health as part of the EU FP7 contract 131242 (EPIAF) and in compliance with the Helsinki declaration on the use of humans in biomedical research. Prior to recruitment, the nature and objectives of the study were explained to potential participants and those who agreed to take part in the study signed a consent form while an assent was obtained from parents or guardians of children who were enrolled in the study. Participation was voluntary. All the parasite stages were harvested from animals maintained at the University of Edinburgh in compliance with the UK Home Office Animals (Scientific Procedures Act) 1986 project license and the recommendations of the local ethical review committee.

2.2 Animals

All the animals used in this PhD thesis were maintained under specific pathogen free (SPF) conditions at the University of Edinburgh Animal Facilities. Animal experiments were conducted under Project Licenses granted by the Home Office (United Kingdom), references 70/8548 and 70/8896, in accordance with local guidelines and approved by the Ethical Review Committee of the University of Edinburgh and described in section 2.1.

2.3 Buffers and culture media

2.3.1 Culture media

2.3.1.1 Cell culture medium

For *ex vivo* macrophage culture, we used RPMI-1640 medium (Sigma; R0883-500ML), supplemented with Heat-inactivated Foetal Bovine Serum (FBS) (Gibco; 10500), Penicillin-Streptomycin mix (10,000U/mL Stock - ThermoFisher Scientific; 15140122), D-(+)-glucose (45% Stock - Sigma; G8769-100ML), and Gentamycin 10 mg/mL (Life Technologies; 15710-049).

2.3.1.2 Worm culture medium

For worm culture, the supplemented medium was as described in 2.3.1.1 but did not contain FBS. Additionally, the HEPES buffer pH 7.4 - 7.6 (1M stock - Sigma; H3537-100ML) was used to control the pH. Details on final concentrations are provided in each individual experiment.

2.3.2 Buffers for Flow Cytometry

2.3.2.1 FACS buffer

To prepare the FACS buffer, PBS 1X (Sigma; D8537-500ML) was mixed with BSA Fisher Scientific; BP9700-100) to a final concentration of 2%, and 0.05% Sodium Azide (Sigma; S2002). FACS buffer was kept ice-chilled or at 4^{o}C.

2.3.2.2 Fixation buffer

The Flow Cytometry Fixation buffer was made of 2% Paraformaldehyde (PFA – 37% Stock. ACROS Organics; 119690025) in PBS 1X (Sigma; D8537-500ML). Fixation buffer was kept ice-chilled or at 4^{o}C.

2.4 Parasitology

2.4.1 *Litomosoides sigmodontis* lifecycle and harvest of larval and adult stages

The parasite *L. sigmodontis* was maintained by passage through 12-week-old male gerbils (*Meriones unguiculatus*), and the arthropod intermediate host mite (*Ornithonyssus bacoti*). The infections were conducted as follows: 10 days prior to infection, the mites, which had been kept in glass containers filled with ~5 cm bedding material and a removable cover, ~27^{0}C and atmospheric humidity of 70%, were allowed to have a blood meal on an infected gerbil (mf counts >500 mf/µl blood from infected gerbils). The infective stage larvae (vector-derived L3s; vL3s) were dissected directly from the mite vector 14 days after the blood meal, and left to crawl out of the mite carcase for about 1h at room temperature in RPMI-1640 media containing 5% Horse serum. For infection of gerbils, doses of ~100 vL3s were picked using glass Pasteur pipettes, and placed onto Syracuse dishes. A final volume of ~150-200 µl, containing ~100 vL3s, were then aspirated to 1 mL syringes with a 21-gauge needle. Gerbils were inoculated intraperitoneally and kept in specific pathogen free (SPF) conditions. Mock doses were prepared using supplemented RPMI-1640 media alone and inoculated into control (uninfected gerbils). The worms normally undergo two moulting steps within the vertebrate host at 2-3 days post infection (L3s to L4s), and 25-30 days post-infection (L4s to adult stages) (Bain, & Babayan, 2013). Mating and production of circulating microfilariae in gerbils occurs around day 90 post-infection (Bain, & Babayan, 2013) (**Figure 1.3**).

2.4.2 *In vitro* culture of *L. sigmodontis* and preparation of Excretory/Secretory (ES) products

A total of 500 vL3s (n = 2), from the pool of vL3s used for gerbil infection, were used to generate ES products from infective larvae. Based on the reported developmental timing of *L. sigmodontis* in gerbils, we also harvested host-derived L3s (hL3s; n = 2) and L4s (n = 2) from infected gerbils 3 and 20 days post-infection, respectively. Similarly, juvenile adult males (jAM; n= 2) and pre-gravid adult females (pgAF; n = 2) were recovered from the pleural/peritoneal cavity of gerbils at 32 days post-infection (**Figure 2.1**). It is important to mention that the presence of a primordial vulva in the anterior end was the morphological feature that we chose for

discriminating between pgAF and jAM (Attout, Babayan, et al., 2005). Fully developed and sexually mature adult worms (adult males – AM, *n* = 10; gravid adult females – gAF, *n* = 12) were harvested 90 days post-infection, from the pleural and peritoneal cavities. The microfilariae (mf) were also harvested but this included some challenges. It has been shown that the blood-derived mf contain a high proportion of mouse-derived proteins, thus limiting the confidence in the secretome factors being unambiguously derived from the parasite (Armstrong, Babayan, et al., 2014). To try to circumvent this issue we obtained mf released by gAF *in vitro* during the first 24 hours of culture (*n* = 8). The gAF culture medium after 24h was centrifuged at 1500x*g* for 15 min and 4°C, and the pellet resuspended in 25 mL of worm culture medium supplemented with 100 U/mL penicillin, 100 µg/mL streptomycin, 1 % D-(+)-glucose and 0.1 mg/mL gentamycin and 30 mM HEPES. Given their small size, at the time of harvest, the vL3s, hL3s, L4s, jAM and pgAF were picked with glass Pasteur pipettes, placed onto Syracuse dishes, and washed 5 times with worm culture medium supplemented with 100 U/mL penicillin, 100 µg/mL streptomycin, 1 % D-(+)-glucose and 0.1 mg/mL gentamycin and 30 mM HEPES pH 7.4. Worms were then placed in supplemented culture medium at a density of 1-2 worms/mL, except for vL3s, that were kept at a density of 250 worms/mL. The worms were incubated at 37^{o}C / 5% CO_2 in a HERA cell 150 incubator (Thermo Scientific) (**Figure 2.1**). Given that these developmental stages are small and fragile, we decided to harvest the spent media as a single time point, after 72h in culture. We monitored the motility of the worms as an indication of health and viability; stretched and immotile worms were considered dead and excluded from experiments, whereas contracting and motile worms were considered healthy and fully viable, and were kept for further assays. The harvested media was then centrifuged at 1,500xg for 20 min on an Eppendorf Benchtop centrifuge (Eppendorf; 5415R) to remove any cell debris, filtered through a 0.22 µm filter (Millex; SLGP033RS), and the filtered media was kept at -20^{o}C until further analysis (**Figure 2.1**).

For generating ES products from adult worms, we first placed the worms into 50 mL flacon tubes containing 45 mL of warm supplemented worm culture medium (same media used for washes of larval stages). They were then washed 5 times with warm supplemented worm culture medium by decanting the content of the falcon tube and immediately replacing it with fresh media. The worms were then placed onto glass

petri dishes in 5 mL 1X PBS (Sigma; D8537-500ML), and incubated for 1h at 4^{o}C. This treatment allows the worms to disentangle, thereby facilitating the sexing; gAF worms are ~ 8cm in length, whereas AM are significantly smaller (~1-2 cm in length). After sexing, the worms were placed in supplemented worm culture medium at a worm density of 1-2 worms/mL and, as described for larval stages, incubated at 37^{o}C/5% CO_2 in a HERA cell 150 incubator (Thermo Scientific). For these stages, we harvested the spent media every 24h for a total of 72h, replacing with fresh supplemented worm culture medium every time. The health status of adult worms was assessed by determining the head-to-tail movement over a period of 1 minute in three independent measurements. The spent media was then centrifuged at 300xg for 20 min on a HERAEUS Multifuge centrifuge 3SR+ (Thermo Scientific) to remove any cell debris and released mf from ES products from gAF. The mf-free supernatant was filtered through a 0.22 μm filter (Millex; SLGP033RS), and the clear media was kept at -20^{o}C until further analysis. In the case of the spent media from gAF worms, the pellet containing mf was resuspended in 1 mL of media and the number of released mf, quantified using a Neubauer chamber and 10 μL of Trypan Blue (Sigma; 93595-50ML), was used as an indicative of viability and health.

Pooled ES products from AM and gAF were prepared by mixing equivalent volumes of ESP harvested at 24h, 48h and 72h for a total of 13.5 ml. For time course secretion of small RNAs *in vitro* by gAF worms (detailed in chapter 4), we used up a similar volume of 0-24h and 48-72h ES products (~15 mL for each time point). These samples were 10X concentrated using a 15 ml Vivaspin 6 5 kDa MWCO (Sartorius; VS0621) down to 1.5 ml, similar to the volume used to culture the larval stages (**Figure 2.1**).

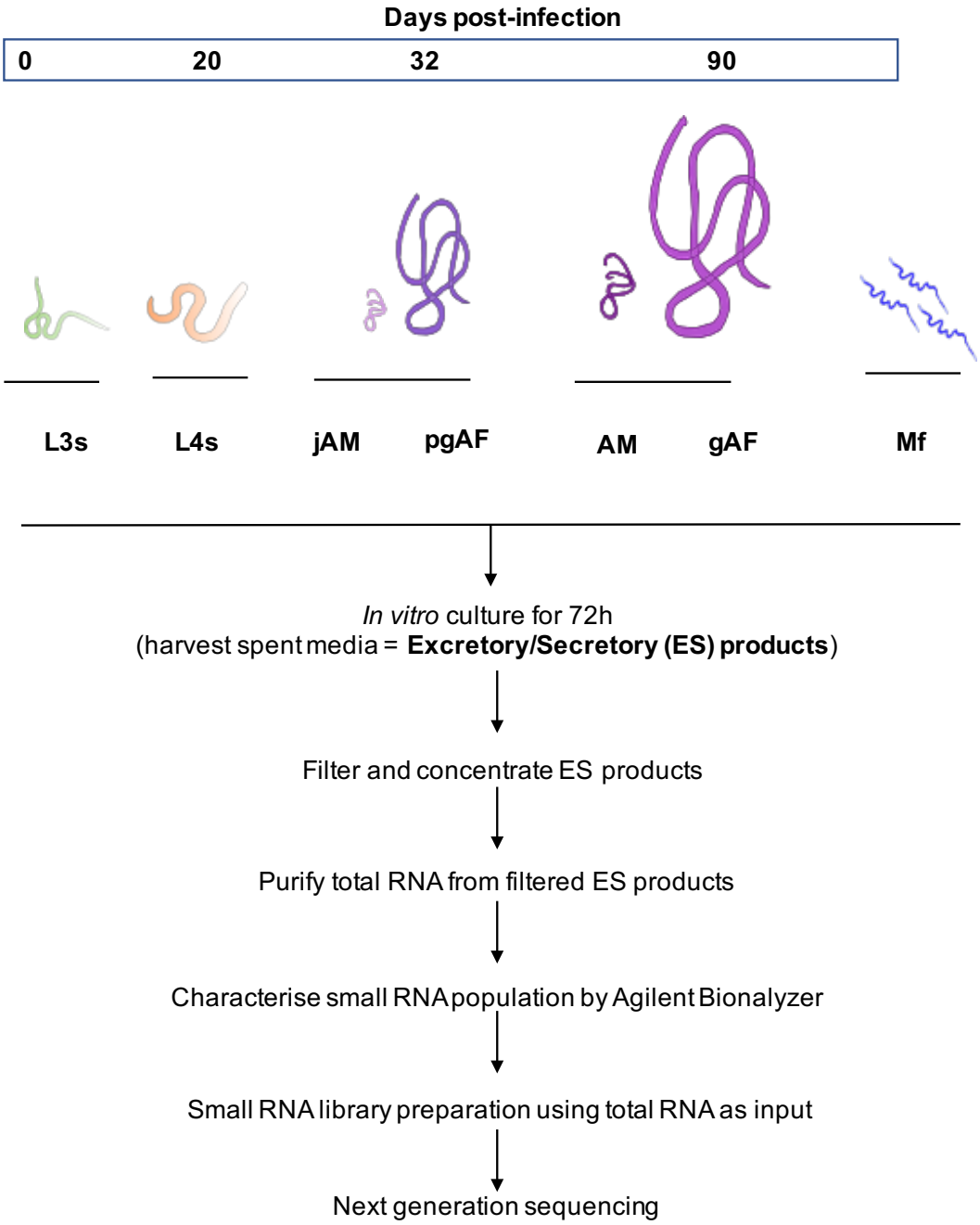

Figure 2.1 Protocol for obtaining Excretory/Secretory (ES) products from larval and adult stages of *L. sigmodontis*. Adult ES products were concentrated down to 1.5 mL (same volume obtained from larval ES products). All ES products were filtered through 0.22 µm filters to remove cell debris prior RNA extraction.

2.4.3 *In vitro* viability assay of gravid adult female worms (MTT assay)

Adult worms were separated by sex as described in 2.4.2, and female worms were placed in 24-well plates at a density of 1 worm/well in 2 mL of supplemented worm culture medium, and incubated at 37°C. Viability was assessed by MTT at time 0h (worms freshly retrieved from the gerbils), 24h, 48h and 72h as follows: 1 mL of medium was replaced with 1 mL of 1 mg/ml of 3-(4,5-Dimethylthiazol-2-yl)-2,5-Diphenyltetrazolium Bromide (MTT) (Life technologies; M6494) to a final concentration of 0.5 mg/mL. Worms were then incubated at 37°C for 1h in a HERA cell 150 incubator (Thermo Scientific). After the MTT incubation, medium was replaced with 0.5 mL of 100% Dimethyl sulphoxide (DMSO – Sigma; D2650) and incubated for 30 min at room temperature covered in foil. An aliquot of 200 μL was taken from each well and absorbance at 492nm on a Multiskan Ascent plate reader (Labsystems). A purple colour is indicative of mitochondrial activity, and therefore of fully viable worms. 100% DMSO was used as blank, and in preliminary experiments we also included hot EtOH-fixed gAF as "dead worm" controls. MTT readouts obtained from dead worms displayed similar optical density as 100% DMSO alone (data not shown), and thus we decided to use DMSO as control in subsequent experiments.

2.4.4 *In vitro* motility assay of gravid adult female worms

Motility of gravid adult female worms was assessed by counting the number of anterior-to-posterior end (head-to-tail) movements that occurred in one minute using lenses and a magnification of 20X. The measurements were conducted in triplicate per animal. An arbitrary scoring system was employed as follow: 1) Non-motile, relaxed or random and spastic movements, 2) Partially motile, with some indication of head-to-tail movement and/or worms partially coiled, 3) Worms fully motile, well-defined sinusoidal and head-to-tail movement, and/or fully coiled.

2.4.5 Adult female worm fertility assay and embryograms

Qualitative and semi-quantitative assays were used to monitor the health status of the adult female worms *in vitro*. To do this, the spent media was recovered at indicated time points and the mf were pelleted by centrifugation at 300xg for 10 min at room temperature. The pellet was resuspended in 100 μL of PBS 1X (Sigma; D8537-

500ML), and a 10 μL drop was placed on a glass slide. The specific embryonic stages reported in here was classified as Oocytes (Oo), Dividing eggs (DE), Pretzel-like stage (Pmf) and stretched mf (mf), as previously described (Ziewer, Hübner, et al., 2012). A total of 5 fields/drop were examined under the microscope (400X) to determine the relative proportion of each of the embryonic stages in each experimental group. An arbitrary scoring system was employed, were "+" equals to 1-10 embryonic stage/well, "++" equals to 11-20 embryonic stage/well, and "+++" equals to >20 embryonic stage/well. This was then plotted and represented as the relative proportion of each of the embryonic stages/sample/experimental group.

2.4.6 *In vitro* treatment of gravid adult females with Ivermectin

24-well plates containing a single gravid female worm per well were prepared as described in 2.4.3. Culture plates were split into worms treated with either 10% or 1% DMSO (vehicle) (Sigma; D2650), or worms treated with either 10μM or 1μM of Ivermectin (Sigma; I8898-250MG). Ivermectin solution was prepared by dissolving the powder to a concentration of 20 μM in 100% DMSO. After the first 24h incubation ("0h"), spent media was harvested, spun down at 300g x 10 min on a benchtop microcentrifuge (Eppendorf; 5415R) to pellet mf. The supernatant was filtered through a 0.22 μm filter (Millex; SLGP033RS), and the cleared supernatants were kept at -20^{o}C. The pellets were resuspended in 100 μL of PBS 1X (Sigma; D8537-500ML) for mf quantification using a Neubauer chamber and Trypan Blue, as described in 2.4.2. Adult female worms were washed twice with PBS 1X (Sigma; D8537-500ML) and medium was replaced with supplemented worm culture medium containing 10 μM or 1 μM of Ivermectin, or DMSO alone as "vehicle" (10% and 1%, equivalent to the corresponding concentrations of DMSO in each drug dilution), in a final volume of 2 mL/worm/well. Similarly, viability was monitored by MTT as described in 2.4.3. Other parameters, such as fertility (defined as number of mf released *in vitro*) and motility (defined as heat-to-tail movement) were also assessed at every time point, as described in 2.4.4 and 2.4.5, respectively.

2.4.7 Extracellular vesicle purification, quantification and visualisation

Isolation of extracellular vesicles (EVs) by solvent-based precipitation was performed as previously described (Gallart-Palau, Serra, et al., 2015), with some modifications. Briefly, 500 μL of pooled ES products from gravid adult female worms were incubated with 4 volumes (2 mL) of cold acetone (-20^{o}C). 500 μL of pooled ES products were kept aside as a "Total" fraction. The mixture of ES products and cold acetone was then vortexed for 15 seconds, incubated for 5 min at -20^{o}C, followed by centrifugation at 3,000xg for 5 min. After centrifugation, the protein pellet was resuspended in 500 μL, whereas the EV-containing supernatant was placed onto a new tube, and the acetone was evaporated at room temperature using a DNA SpeedVac DNA110 system (Savant). The final volume of the EV-containing supernatant was brought down to 500 μL. The fraction containing the EVs was quantified by Tunnable Resistive Pulse Sensing (TRPS) method on an Izon qNano Instrument (Izon). Data acquisition and analysis were performed using the Izon Control Suite software version V3.1. EV samples were analysed using NP150 nanopore at 7 mbar pressure. Calibration runs were performed before and after each sample run using 114 nm diameter carboxylated polystyrene (standard) beads. Serial dilutions of the standard beads were used to determine the quantitative range within each run (data not shown). Each EV sample was measured in triplicates and results are reported as average of the three technical replicates. For visualisation of the vesicles, the purified ultracentrifuge pellets from *L. sigmodontis* ES products (Protein concentration ranging from 0.02 to 0.4 μg/μL) were fixed in 2% PFA, deposited on Formvar-carbon coated TEM grids and treated with glutaraldehyde prior to treatment with uranyl oxalate and methyl cellulose as described before (Simbari, Mccaskill, et al., 2016). Images were taken on a Philips CM120 Transmission Electron Microscope using a Gatan Orius CCD camera.

2.4.8 Protein quantification

For all the experiments conducted here, the protein concentration of samples was measured using the Qubit Protein quantification kit (Invitrogen; Q33211). 10 μL of samples were added to 190 μL of Qubit Buffer (1:20) containing 1 μL of Qubit Dye (1:200), both provided with the kit. Three standard samples provided with the kit

(concentrations ranging from 0 μg/μL to 0.4 μg/μL) were included to create a standard curve. The samples, including the standards, were incubated for 15 min at room temperature covered in tin foil. The fluorescence intensity was then measured using a Qubit 2.0 Fluorimeter (Invitrogen; Q32866), according to the manufacturer's protocol.

2.5 Animal models of infection

2.5.1 Collection of blood, serum, and pleural/peritoneal (PLEC/PEC) exudates from gerbils

2.5.1.1 From gerbils

Infected gerbils or naïve controls were culled by CO_2 asphyxiation in accordance with the UK Home Office regulation. Animals were exsanguinated by cardiac bleed and blood was incubated for 1h at room temperature, centrifuged at 400xg for 10 min at room temperature to retract the clog and the supernatant was further cleared by centrifugation at 16,000xg for 5 min. The cleared serum was kept at -20°C. The pleural and peritoneal (PEC/PLEC) washes were recovered by carefully irrigating both cavities with 2 ml of cell culture medium supplemented with 100 U/ml penicillin, 100 μg/ml streptomycin, 30 mM HEPES and 1 % D-(+)-glucose. The washes were placed in 15 ml falcon tubes, centrifuged at 1500 rpm for 15 min at 4°C and the supernatants were filtered through 0.22 μm filters to remove any cell debris of mf released *in vivo*. The cleared PEC/PLEC washes were kept at -20°C.

2.5.1.2 From mice

Whole blood was drawn from naïve or infected BALB/c mice by brachial bleeding (~1 mL final volume). The blood harvested directly into a 1.5 mL Eppendorf tube and allowed to sit for 1h at RT to form a clot. For serum collection, the clot was separated from the serum by centrifugation at 2500g for 15 min at 4^{o}C, the supernatants were collected into new 1.5 mL Eppendorf tubes and spun down at 10,000g for 1 min to remove remaining cells. The resultant supernatants were transferred into new 1.5 mL Eppendorf tubes and stored at -80^{o}C until further experiments.

2.5.1.3 Quantification of circulating mf in blood

For quantification of circulation mf, a total of 30 μL of blood harvested by cardiac puncture was added to 300 μL of BD FACS Lysing Buffer (BD; 349202), vortexed for 15 seconds, and centrifuged at 300xg for 10 min at room temperature. The

supernatant was discarded and the pellet was resuspended in 100 µL of PBS 1X (Sigma; D8537-500ML), placed onto a glass slide, and the number of stretched microfilariae was quantified by microscopic examination of the slide at a magnification of 400X.

2.5.2 Purification of adherent macrophages and flow cytometry

2.5.2.1 Purification of adherent macrophages

To harvest Pleural/Peritoneal (PLEC/PEC) macrophages, we first culled gerbils or mice by CO_2 asphyxiation. After removing the skin from the abdomen, a small incision was made in the peritoneum, through which 5 mL of warm (37^{o}C) supplemented cell culture medium was flushed into the cavity. The incision was then clamped, and the animals were shaken to allow all the cells from the cavity to come into suspension. The media was carefully recovered from the peritoneal cavity using a plastic Pasteur pipette and placed into a 15-mL falcon tube kept on ice. After washing the peritoneal cavity, an incision was made into the diaphragm, and 5 mL of warm media were flushed into the pleural cavity. The cavity was then washed several times using a plastic Pasteur pipette. The Pleural wash was then pooled together with the peritoneal washes. The PLEC/PEC washes were then centrifuged for 10 min at 400xg and 4^{o}C. The cell pellet was resuspended in 1 mL of supplemented media and the concentration of viable cells was determined by staining with Trypan Blue (Sigma; 93595-50ML) and counted on a Neubauer chamber. To obtain purify PLEC/PEC macrophages, the cell concentration was adjusted to 1.5x10^{6} cells/ml in supplemented RPMI-1640 medium and the cells were allowed to adhere to the surface of either flat-bottomed polystyrene 96-well plates (Grenier Bio-One) (for flow cytometry) or polystyrene 6-well plates (Grenier Bio-One) (for RNA extraction). Cells were cultured for 45 min (96-well plate) and 1 hr (6-well plate) at 37^{o}C. Non-adherent cells and microfilariae were removed by gentle and extensive washes five times with warm (37^{o}C) 1X PBS (Sigma; D8537-500ML).

2.5.2.2 Flow cytometry

The expression of cell surface markers from adherent macrophages was assessed by flow cytometry. Cells adhered to flat-bottom polystyrene 96-well plate (Grenier Bio-One, Germany) (as described in 2.13.1) were washed extensively with warm (37^{o}C) 1X PBS (Sigma; D8537-500ML), and the absence of microfilariae was verified by

observation with a microscope. After the washes, the adherent cells were incubated with a 1:750 dilution of Live/Dead Aqua Stain (Life Technologies; L23105) in FACS buffer. The cells were then stained by incubating for 10 min at room temperature in the dark. The excess stain was washed off by addition of 100 μL FACS buffer followed by centrifugation at 300xg for 5 min at room temperature. The samples were subsequently incubated with Fluorescence-conjugated antibodies (**Table 2.1**) diluted 1:200 in FACS buffer for 30 min on ice (covered in tin foil) in 50 μL of FACS buffer-antibody mix followed by a wash step. Lastly, the samples were then washed 2 times in FACS buffer, and incubated for 10 min with 100 μL of 2% Paraformaldehyde covered in tin foil, to allow adherent cells to detach from the plate. The detached cells were then recovered by pipetting up and down multiple times, centrifuged at 300xg for 10 min, washed twice with 300 μL FACS buffer, and the final pellet was resuspended in 300 μL of FACS buffer. The acquisition of fluorescent signals was conducted on a LSR II (BD, Bioscience, USA) Flow cytometer. Single stains were conducted to adjust the voltage intensity in the flow cytometer. Our gating strategy consisted on viable cells that displayed the expression of the hematopoietic lineage CD45.2. We then excluded non-macrophage cells (termed "lineage-specific" cells) by using an antibody cocktail against the following surface antigens: CD3 (T cells), CD19 (B cells), Ly6G (Neutrophils), and SiglecF (Eosinophils). Once the non-monocytes/macrophage populations were excluded, we determined the expression of Ly6C (Pro-inflammatory monocytes) and CD11C to define a population consisting of pro-inflammatory monocytes ($Ly6C^+$ $CD11c^-$ cells), dendritic cells (Ly6C- CD11c+ cells), and macrophages, which were further confirmed by the co-expression of the surface markers CD11b and F480.

Table 2.1 List of antibodies used for flow cytometry

Antibody	fluorescent dye	Cell population	Provider/Catalogue number
CD45.2	PerCP	Haematopoietic cells	BioLegend /109827
CD3	BV421	T cells	BD Biosciences/564008
CD19	BV421	B cells	BD Biosciences/562701
Ly6G	BV421	Neutrophils	BD Biosciences/562737
SiglecF	BV421	Eosinophils	BD Biosciences/562681
Ly6C	AF700	Pro-inflammatory monocytes	BioLegend / 128023
CD11c	BV605	Dendritic cells	BD Biosciences/563057
CD11b	BV711	Myeloid/Macrophages	BD Biosciences/563168
F480	PECy7	Macrophages	BioLegend/123113

2.5.3 *O. ochengi* nodule fluids

Sample kindly provided by Dr. B. Makepeace from the University of Liverpool and Dr. S Wanji from the University of Buea (Cameroon)

Bovine skins containing numerous *O. ochengi* onchocercomata were obtained from Ngaoundéré abattoir, Adamawa Region, Cameroon (Wahl, G, Achu-Kwi, MD, Mbah, D, Dawa, O, Renz, 1994). Freshly excised nodules were screened visually, and discarded if hard or discoloured, which are signs of calcification. Nodules were rinsed in PBS, dried thoroughly, and pricked with a 21G hypodermic needle. The nodules were gently squeezed, and the expressed fluid (~0.5 µl) collected with a micropipette, pooling from >10 nodules per biological replicate. The fluid was spun at 500 g for 5 min to pellet any cellular material or Mf, and the supernatant was stored at -80°C. The samples were shipped to the UK on dry ice and remained frozen prior to analysis.

2.6 RNA extraction

2.6.1 RNA extraction from gravid adult female worms

Adult female worms obtained from infected gerbils 90 days post-infection were washed three times in PBS 1X (Sigma; D8537-500ML), examined under the lenses to exclude broken worms or microgranulomas, and kept in 1 mL of Trizol (Ambion; 15596026) in 2.0 mL Eppendorf tubes. Worms were lysed using stainless steel beads (Qiagen) in a TissueLyser II (Qiagen) at a frequency of 30/sec for 2 min repeated twice. After lysis, samples were spun down at 10,000xg for 5 min to pellet any debris and 0.7 mL of the supernatant was used for total RNA extraction using miRNeasy mini kit (Qiagen; 217004), per manufacturer's instructions. After washes, total RNA was eluted in 50 μl of nuclease-free distilled water, quantified by Qubit 2.0 Fluorimeter (Invitrogen; Q32866) and the Qubit High Sensitivity RNA kit (Invitrogen; Q32855) according to manufacturer's recommendations. Integrity of the RNA was then determined using the Bioanalyzer Total RNA pico kit (Agilent; 5067-1514), and kept at -80^{o}C.

2.6.2 RNA extraction from ES products

Total RNA from lifecycle stages ES products (described above) was purified from 1.5 mL of ES products added to 5.25 mL of Trizol LS Reagent (ThermoFisher; 10296028), using the miRNAeasy mini kit (Qiagen; 217004) and following manufacturer's recommendations. Final elution was carried out in 25 μl of nuclease-free distilled water. The relative small RNA content from these samples was determined with 1 μl of total RNA on a Bioanalyzer small RNA kit (Agilent; 5067-1548) prior to small RNA library preparation.

2.6.3 RNA extraction from mouse serum

For purification of total RNA from mouse serum, 200 μl of naïve and infected sera were thawed on ice for 45 min and spun down at 10,000g to make sure any cell debris was removed prior extraction. Total RNA was purified using the miRNeasy mini Kit (Qiagen; 217004). Briefly, thawed serum was mixed with 700 μl of Qiazol (Qiagen; 217004) and vortex thoroughly for 15 seconds before adding 140 μl of chloroform. Samples containing Qiazol and chloroform were vortexed thoroughly for an additional 15 seconds and incubated 3 min at RT. After centrifugation at 12,000g for

15 min the aqueous phase was obtained and mixed with 1.5 volumes of 100% Ethanol and passed through a miRNeasy column. The columns were washed three times with buffers included in the kit and RNA was eluted in 50 µl of nuclease-free distilled water. RNA samples were quantified by Qubit fluorimeter (Invitrogen; Q32866), and stored at -80^{o}C until small RNA library preparation or qRT-PCR analysis.

2.6.4 RNA extraction from *O. ochengi* nodule fluids and human serum/plasma

Total RNA was extracted from 20 µl of pooled nodule fluids from cattle (*O. ochengi* infection), 200 µl of serum pooled from 12 infected individuals in Cameroon (pooled prior to RNA extraction), or pooled from equal volumes of RNA extracted from 13 infected or 13 uninfected individuals from Ghana (total equivalent of 50 µl plasma per sample). Samples were shipped in liquid nitrogen and stored at -80°C for 3-4 years (Cameroon samples) or 5 years (Ghana samples). The serum was thawed on ice and serum or plasma was spun down at 16,000 g for 5 min at 4°C to remove any additional cell debris. The cleared serum was then transferred to a new 2 mL Eppendorf tube and RNA extracted using the miRCURY RNA isolation kit for Biofluids (Exiqon; 300112) according to manufacturers' protocols. In both cases, RNA was eluted in 50 µL of 0.1 mM EDTA (0.5M stock – Gibco; 15575). RNA was stored at -20 °C prior to further analysis. The relative small RNA content from these samples was determined with 1 µl of total RNA on a Bioanalyzer small RNA kit (Agilent; 5067-1548). Before proceeding with small RNA library preparation from serum or plasma RNA, samples were subjected to a clean-up protocol similar to what has been previously described (Burgos, Javaherian, et al., 2013). Briefly, 50 µl of eluted RNA was diluted to 100 µl with Nuclease-free distilled water followed by addition of 1 µl glycoblue 15 mg/ml (Life technologies; AM9516), 60 µl of Sodium acetate 3 M pH 5.2 (AppliChem; A3947,0250) and 500 µl of ethanol 100% (Fisher; BP2818500). The RNA was precipitated for 30 min at -80°C then spun at 16,000xg for 30 min at 4°C and washed twice with 75% Ethanol. The pellets were air-dried at room temperature for 15 minutes and re-suspended in 8 µl of 0.1 mM EDTA pH 8.0 (0.5M stock – Gibco; 15575).

2.6.5 RNA extraction from adherent macrophages

After adhesion (see 2.13), adherent cells were washed 5 times with warm (37^{o}C) PBS 1X (Sigma; D8537-500ML). The absence of non-adherent cells and microfilariae was verified under the microscopy, after which a total of 1 mL of Trizol (Ambion; 15596026) was added per well. The entire well surface was then scraped using a cell scraper. The lysed cells in Trizol were placed onto 1.5 mL Eppendorf tubes and kept at -80^{o}C until RNA extraction with miRNeasy mini kit (Qiagen; 217004). Total RNA was purified from 700 µl of lysed cells in Trizol according to manufacturer's recommendations, and eluting in 25 µl of nuclease-free distilled water.

2.7 Small RNA library preparation and deep sequencing

2.7.1 Small RNA library preparation from *L. sigmodontis* ES products, gerbil serum, body cavity exudates and adherent macrophages

For the analysis of small RNA content by next generation sequencing, libraries were prepared from 2.5 µl of total RNA from all the replicates harvested (detailed in 2.4.1), using the CleanTag small RNA Library Prep kit (TriLink; L-3206) according to the manufacturer's protocol, using a 1:12 dilution of the adapters and final PCR amplification of 22 cycles. PCR products of the expected molecular weight (140-160bp) were size selected and samples were sequenced in three independent sequencing projects on an Illumina HiSeq high output v4 50bp single-end at Edinburgh Genomics (http://genomics.ed.ac.uk/) (**Figure 2.2**).

2.7.2 Small RNA library preparation from human and murine (mouse and gerbil) serum, and *O. ochengi* nodule fluids

For the analysis of small RNA content in the nodule fluids, murine serum or human serum and plasma, libraries were prepared from 2.5 µl total RNA using the Illumina TruSeq small RNA Preparation kit (Illumina; RS-200-0012), according to the manufacturers' protocol, and using 1:10 dilution of adapters. The final purified

libraries were sequenced on an Illumina HiSeq 2500 instrument using v3 reagents at Edinburgh Genomics (http://genomics.ed.ac.uk/).

2.7.3 Small RNA library purification protocol

After barcoding, samples were pooled together and the PCR products were run on a 6% TBE acrylamide gel (Invitrogen; EC62652BOX) using Novex 1X TBE Running buffer (Life technologies; LC6675) for ~1.5h at room temperature. The gel was then stained with 1/10,000 dilution of SYBR gold (Invitrogen; S11494) diluted in 1X TBE running buffer, and incubated for ~20 min at room temperature. The PCR products of the expected molecular weight (140-160 bp) were size selected with sterile scalpels. The acrylamide gel fragments were crushed by spinning down through a 0.2 mL Eppendorf tube, with a punctured hole in the bottom, inside a 1.5 mL Eppendorf tube. The fragmented acrylamide flow-through was incubated with 300 µL of 1X PBS (Sigma; D8537-500ML) overnight in a rotor at 4°C. The following day, the gel pieces were removed using 0.22 µm filters (Costar), and the DNA was precipitated using a solution containing 1 µl glycoblue 15 mg/ml (Life technologies; AM9516), 60 µl of Sodium acetate 3 M pH 5.2 (AppliChem; A3947,0250) and 600 µl of ethanol 100% (Fisher; BP2818500). This mix was incubated for 1h at -80°C, pelleted by centrifugation at 16,000xg for 20 min at 4°C, followed by two consecutive washes with 75% EtOH. The final pellet was air-dried and resuspended in 15 µl of EB Buffer (Qiagen; 19086). The DNA concentration was quantified using a Qubit dsDNA High Sensitivity kit (Invitrogen; Q32851) and the Qubit Fluorimeter (Invitrogen; Q32866). Similarly, the samples were also analysed on a Bioanalyzer using the high sensitivity DNA kit (Agilent; 5067-46260), as represented in Figure 2.2.

2.8 Bioinformatic analysis

Analysis carried out by Dr. A. Ivens from the University of Edinburgh.

All libraries were analysed by first clipping the 3' sRNA adapter using cutadapt (N, & Martin, 2011), searching for at least a 6 bases match to the adapter sequence. For analysis of small RNAs, only sequences that contained the adapter, were >16 nt in length, and were present in ≥ 2 copies were retained for further analysis.

2.8.1 Bioinformatic analysis of *L. sigmodontis* ES products, gerbil serum, body cavity exudates and adherent macrophages

Given the lack of a genome draft from *M. unguiculatus*, we decided to align the sequences against the mouse genome (mm10) or to the *L. sigmodontis* genome draft (v 2.1) using bowtie, requiring perfect matches along the full length of the sequence. Sequences were analysed for known classes of RNA based on Rfam. The best hit with at most two mismatches was used to classify the reads. Analysis of miRNA content was carried out using miRDeep2 with the following settings: 1) reads map perfectly to the genome, 2) cut off –v 1, 3) employing the "-s option" using all mature sequences from miRBase (version 21), 4) only read lengths (18 to 30 nt) were analysed. Folding analyses of the predicted novel pre-miRNA detected in ES products, serum or PEC/PLEC were carried out using the RNAfold Vienna package with default settings. Pairwise comparisons between lifecycle stages to detect differentially expressed miRNAs were conducted using the Bioconductor DESeq2 package (Love, Huber, et al., 2014), with default settings. miRNA read counts were normalised in DESeq2 using the rlog method which corrects for different library sizes and reduces differences between samples for low read counts. Gene-specific dispersion values were estimated by an empirical Bayes method called Cook's dispersion. Pairwise differential expression testing between ESP from lifecycle stages was performed using the adjusted *T*-test once negative bimodal models were fitted and dispersion values estimated. Significance was assessed as having an experiment-wide false discovery rate (FDR) <0.05 (calculated using the Benjamini Hochberg method). miRNAs which had log2 fold-change values ≥1.5 or ≤-1.5 were further filtered and prioritised. Although we considered all significantly differentially expressed miRNAs which had a FDR<0.05 and an adjusted *p* value <0.05 biologically relevant, we applied an arbitrary fold-change cut-off to a level we considered relevant to limit the set of differentially expressed genes to a workable number for further analysis without applying too stringent cut-offs. The rlog values (log2 fold-change) of the most differentially expressed miRNAs calculated with DESeq2 were used to create Principal Component Analysis (PCA) plots and unsupervised hierarchical clustering analysis plots using R package. The bioinformatics workflow is represented in **Figure 2.3**.

2.8.2 Bioinformatic analysis from mouse serum, human serum/plasma, and *O. ochengi* nodule fluids

Sequences were analysed for alignment to the following genome versions: Bovine (ftp://ftp.ensembl.org/pub/release71/fasta/bos_taurus/dna/Bos_taurus.UMD3.1.71.dna.toplevel.fa.gz), human (version hg19), *O. ochengi* (version 1.1; from http://onchocerca.nematod.es; unpublished genome sequence from M. Blaxter, B. Makepeace and colleagues) and *O. volvulus* (ftp://ftp.sanger.ac.uk/pub/project/pathogens/Onchocerca/volvulus/OVOC.V3.fa). Bowtie (Langmead, Trapnell, et al., 2009) was used, requiring perfect matches along the full length of the sequence. Sequences were analysed for known classes of RNA based on Rfam (Griffiths-Jones, 2003) sequences (version 11, obtained from ftp://ftp.sanger.ac.uk/pub/databases/Rfam/11.0/). For analysis of mouse serum from animals infected with *L. sigmodontis*, we aligned the sequencing reads against either the *M. musculus* genome (mm9) or the *L. sigmodontis* genome draft (v 2.1) genome. The best hit with no mismatches was used to classify the reads. Analysis of miRNA content was carried out using miRdeep2 (Friedländer, Mackowiak, et al., 2012) with the following default settings: 1) requiring that reads map perfectly to the genome, 2) using cut-off -v 1, 3) the "-s option" was employed, using all mature sequences from miRBase (version 20) (Kozomara, & Griffiths-Jones, 2014), 4) read length (18 to 30) were employed. Folding analyses of the novel pre-miRNAs detected in nodule fluids were carried out using the RNAfold Vienna package with default settings (Gruber, Lorenz, et al., 2008) (**Figure 2.3**).

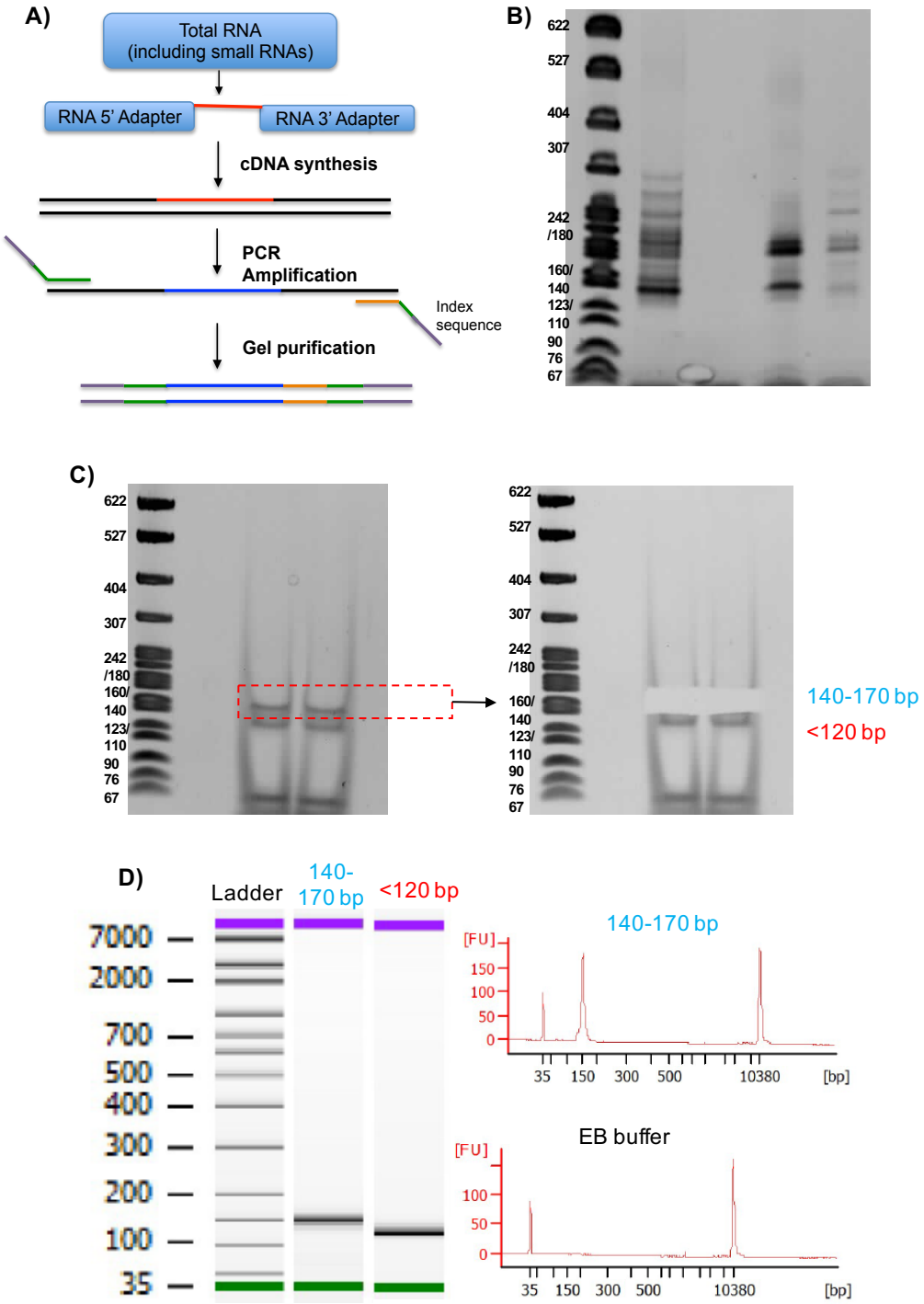

Figure 2.2 Small RNA cloning protocol. A) Schematic representation of the small RNA cloning protocol. The expected size of an amplicon containing 20-30 nt in length is between 140-160 bp. Similarly, the expected size of an amplicon lacking an insert (e.g. adapter dimers – "empty amplicons" - and other unspecific PCR products in <120 bp). B) Barcoded PCR products obtained after reverse transcription of the di-tagged RNA. C) After pooling samples together, PCR products of 140-170 bp we excised from the gel and purified as described. D) Bioanalyzer results of purified PCR products. The PCR products <120 bp in length were included as control to determine the lack of "empty amplicons" in the purified libraries ("140-170 bp").

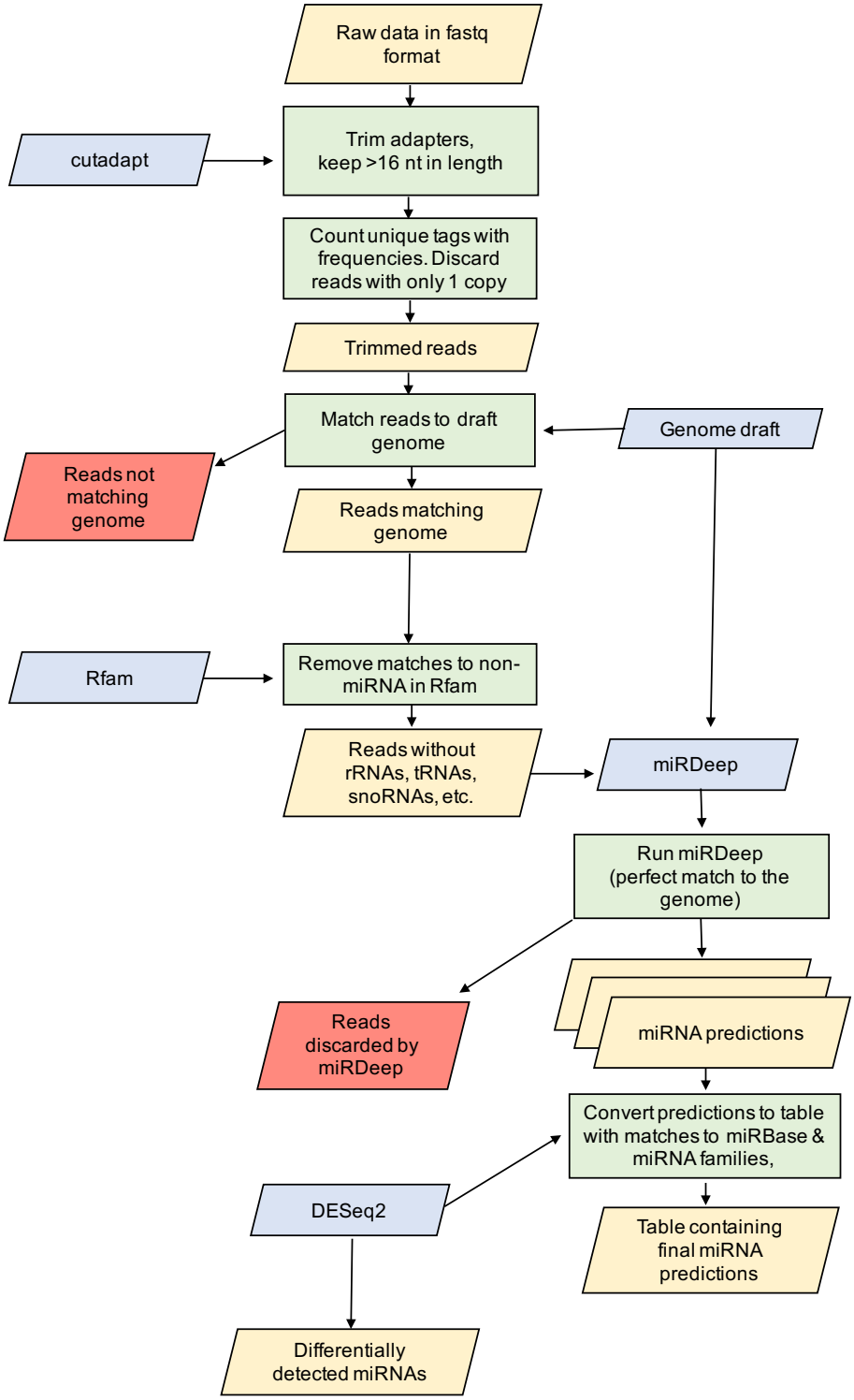

Figure 2.3 Bioinformatic workflow for the analysis of the small RNA libraries. Yellow boxes indicate outputs from specific analysis, blue boxes indicate bioinfomatic packages used, green boxes represent tasks conducted by the bioinformatics packages and red boxes indicate reads that were discarded at each step.

2.9 Quantitative RT-PCR (qRT-PCR)

2.9.1 Detection of parasite-derived miRNAs by qRT-PCR

For cDNA synthesis using RNA from serum, a fixed volume of 2.5 μL of total RNA, derived from 10 μL of serum, was used as input and 0.1 pM of the synthetic cel-miR-39 RNA (5'-UCACCGGGUGUAAAUCAGCUUG-3') was spiked into the reverse transcription reaction mix. This is included to control for inhibitors present in the samples that could influence efficiency of the RT or PCR. Similarly, a spiked water control was included to monitor for the presence of potential inhibitors that may affect the efficiency of the reverse transcription. For cDNA synthesis using RNA extracted from ES products, a total of 2.5 μL of purified RNA, equivalent to ~ 150 μL of total ES products, was used and 0.1 pM of the synthetic Spike 1 (5'-ACUGUACGUCUGCCAUUAGCUU-3') added to the reverse transcription reaction mix for normalisation. The synthetic Spike 1 does not show homology to any known nematode miRNA in miRBase, therefore we do not expect any cross-amplification with endogenous parasite-derived miRNAs in ES products. For analysis of gravid adult female worm tissues and adherent macrophages, a total of 50 ng of total RNA was used, adding 0.1 pM of the synthetic Spike 1 to the reverse transcription reaction mix for normalisation. Reverse transcription reactions were performed using the miScript RT II System (Qiagen; 218161) according to manufacturer's protocol, containing 0.5 μL of miScript Reverse Transcriptase, 1 μL of 5X miScript Hiflex RT Buffer, 0.5 μL of 10X Nucleic acid mix, and 0.5 μL of the corresponding spike-in RNA, in a total volume of 5 μL. Samples were incubated for 60 min at 37^{o}C followed by 5 min at 95^{o}C. cDNAs were diluted 1:10 by adding 45 μL of nuclease-free distilled water. Quantitative PCR was carried out with the QuantiTec SYBR Green PCR kit (Qiagen; 204145), which includes a universal (reverse) primer, according to manufacturer's protocol. Primers for *L. sigmodontis*-specific miRNAs and synthetic spike-in RNAs were used at a working concentration of 2 μM, and were purchased from Invitrogen. Human and mouse miScript miRNA primers, as well as the universal (reverse) primer, were all purchased from Qiagen and were provided as 2 μM ready-to-use primers stocks. 1 μL of 1:10 diluted cDNA was added to 9 μL master mix containing 5 μL 2X SYBR green master mix and, 2 μL of nuclease-free distilled water, 1 μL of forward (miRNA-specific) primer and 1 μL of universal reverse primer.

The qPCR reactions were set up in 384-well plates, with two technical replicates for each sample tested and a nuclease-free water (no-template) control. The temperature profile used was as follow: 1) pre-denaturation for 15 min at 95^{o}C, 2) 50 cycles of denaturation 15s at 94^{o}C, annealing 30s at 55 ^{o}C, and elongation 30s at 70 ^{o}C. Fluorescence data collection was performed at the end of each annealing step. Data was collected on a Light Cycler 480 System (Roche). A list of the primers used is given in **Table 2.2**.

2.9.2 Generation of standard curves and primer efficiency

Serial dilutions (1:10) of known input amounts of total RNA from mixed adult female worms were used to construct standard curves to assess primer efficiency for parasite miRNA detection in serum, PLEC and ES products. The Ct values obtained were plotted against the logarithm of input ng of RNA and a linear regression model was fitted to generate a formula, where the slope directly correlates with the qPCR efficiency. We assumed that a slope (m) of ~3.33 correspond to an efficiency (*E*) of 1 ± 0.1 (**Table 2.2**). The primers ordered through Qiagen (cel-miR-39, hsa-miR-16-5p, hsa-miR-21-3p) are already optimized and were used according to recommendations from the manufacturer, whereas the primer for the synthetic spike 1 has been already optimized in our laboratory and used as shown here. The sequences for these primers are shown in **Table 2.3**.

Table 2.2 Parasite miRNA primers used for qRT-PCR

miRNA	DNA Sequence (5' – 3')	Slope	Amplification factor	Efficiency (*E*)
miR-993-3p	TAAGCTCGTCTCTACAGGCAGG	-2.945	2.19	118.5%
miR-100a-5p	AACCCGTAGTTTCGAACATGTGT	-3.051	2.13	112.7%
miR-100d	TACCCGTAGCTCCGAATATGT	-3.205	2.05	105.1%
miR-5866	TTACCATGTTGATCGATCTCC	-3.679	1.87	87%
miR-5364-3p	CGAGGTATTGTTTATTGGCTGA	-3.703	1.86	86.2%
Lin-4-5p	TCCCTGAGACCTCTGCTGCGA	-3.987	1.78	78.16%
miR-71-5p	TGAAAGACATGGGTAGTGAGAC	-4.093	1.76	75.5%
miR-228-5p	AATGGCACTAGATGAATTCACGG	-3.807	1.83	83.1
miR-5360	ACGAATCGTCGAATCGGA	-5.154	1.56	57%

Table 2.3 Host miRNA primers and synthetic controls used for qRT-PCR analysis

miRNA	DNA Sequence (5' – 3')	Company	Catalogue number
cel-miR-39-3p	TCACCGGGTGTAAATCAGCTTG	Qiagen	MS00019789
hsa-miR-16-5p	TAGCAGCACGTAAATATTGGCG	Qiagen	MS00031493
hsa-miR-21-5p	TAGCTTATCAGACTGATGTTGA	Qiagen	MS00009079
Spike 1	ACTGTACGTCTGCCATTAGCTT	IDT	Not assigned

2.9.3 qRT-PCR data analysis

For analysis of miRNAs in serum and PEC/PLEC exudates, Ct values were median-normalised to mmu-miR-16-5p, relative change was calculated as 2^{-Ctn}, were Ctn stands for normalised Ct values. For validation of deep sequencing results from *L. sigmodontis* secretomes, Ct values were Log2 transformed and the relative abundance was plotted in Log10 scale. For analysis of the effect of IVM on miRNA secretion by gravid adult female worms, Ct values were Log2 transformed and the fold change was estimated compared to the signal of samples before treatment (Time "0h"). For biomarker studies, the relative fold change between naïve and infected samples was calculated using the average of the naïve group as reference and plotted in logarithmic scale. For the cumulative analysis of miRNAs, the arithmetic mean of fold changes for miR-71 and miR-100a were used. The fold change values were used to calculate sensitivity and specificity of the biomarker assay employing the Receiver Operating Characteristic (ROC) curves in GraphPad Prism (version 7) software.

2.10 RT-PCR

2.10.1 Dissection of gravid adult female worms

Kindly assisted by Dr. Nathaly Vallarino Lhermitte and Dr. Coralie Martin, at The National Museum of Natural History, Paris, France.

A total of >60 *L. sigmodontis* adult gravid female worms were recovered from infected gerbils at day 90 post-infection. To separate anatomical structures, worms were chilled at 4^{o}C and dissected using a stereomicroscope, and fine tipped forceps. One set of forceps was used to grip and steady the centre of the parasite after chilling and placement onto a glass slide containing 200 µL of PBS 1X (Sigma; D8537-500ML). The other set of forceps was used to grasp and gently twist the parasite close to the first set of forceps, resulting in a break in the body wall. The cephalic tip

(anterior end) of the body wall was then grasped and gently peeled away from the rest of the organs, which exposes the digestive tissue (darker) and the reproductive tissue (lighter). The digestive tissue was then pull away from the reproductive tissue and the body wall (cuticle). The reproductive tissue was subsequently pulled away by holding the body wall with one set of forceps. The empty carcase after removing the digestive and the reproductive tissue is what we assigned here as "cuticle". Each anatomical fraction was kept in separate tubes containing 1 mL of Trizol (Ambion; 15596026), and the same tissue from multiple female worms were pooled together. The RNA was purified as described in 2.6.1.

2.10.2 RT-PCR analysis

After purifying total RNA from gravid adult female worms, the RNA concentration (2 μL) was measured with the Qubit High Sensitivity RNA kit (Invitrogen; Q32855) using Qubit 2.0 Fluorimeter (Invitrogen; Q32866). A total of 20 ng of RNA was then incubated with 20 U/μL of Turbo DNase (Thermo Scientific; AM2238) at 37^{o}C for 10 min, followed inactivation at 75^{o}C for 10 min, in a final volume of 10 μL. Then, 6 μL of this reaction was reverse transcribed using the SuperScript III First Strand kit (Thermo Scientific; 18080051) as follow:

1. First reaction: 6 μL of DNAse-treated RNA + 1 μL of 50 μM Oligo-$dT_{(15)}$ (Promega; C1101) + 1μL Annealing buffer (Final volume = 8 μL). These samples were incubated for 5 min at 65^{o}C.
2. Second reaction: 8 μL from the first reaction were then incubated with 10 μL of 2X First strand buffer and 2 μL of the SuperScript III RNase Out RT enzyme (Final volume = 20 μL). These samples were incubated for 50 min at 50^{o}C, followed by an incubation at 85^{o}C for 5 min. A sample containing 20 ng of total RNA from female worms was incubated with nuclease-free distilled water without the RT enzyme and is reported as "No RT" control.

After preparing the cDNAs, the samples were PCR amplified using the Phusion High fidelity PCR Master Mix (NEB; M0531L). Per sample and gene, 2 μL of cDNA was incubated with 2.5 μL of 10 μM primer mix (containing equimolar concentrations of forward and reverse primers), 12.5 μL of 2X Phusion Enzyme mix, and 8 μL of nuclease-free distilled water, to a final volume of 25 μL. The primers used for these studies are listed in **Table 2.4**. The samples were incubated as follow: 1) 30s at 98^{o}C, 2) 35 cycles of 10s at 98^{o}C, 30s at 55^{o}C, and 15s at 72^{o}C, 3) 10 min at 72^{o}C, and a

final incubation step at 4^{o}C kept on hold until tubes were removed from the cycler. 10 µL of the final PCR products were mixed with 5 µL gel loading Dye (Thermo; F-350) and loaded into a gel made of 2% UltraPure Agarose (Invitrogen; 16500-500) dissolved in 1X TAE buffer (Fisher; BP1332-4) and containing a 1/10,000 dilution of SYBR gold (Invitrogen; S11494). Samples were run at 150V for ~1h at room temperature, and gel images were acquired on an INGENIUS gel dock (SYNGENE). We also ran 4 µL of the 100 bp DNA ladder (NEB; N323L) to identify the size of the PCR product.

Table 2.4 Parasite mRNA primers used for RT-PCR analysis

mRNA	DNA Sequence (5' – 3')
Lsi-avr-14_Forward	GACCACACAAAGTTCGGGTAT C
Lsi-avr-14_Reverser	ATGTGACCGGTGTAGTGTTTT G
Lsi-18S rRNA_Forward	GTACAAAGGGCAGGGACGTA
Lsi-18S rRNA_Forward	CATTGCCGAAAGGTACTGGT

2.11 Statistical analysis

Statistical analyses were done using Prism 7 (GraphPad Software Inc., USA). The choice of the statistical test was based on initial normality tests conducted using Prism. Depending upon the number of samples, the normality tests used were either D'Agostino & Pearson normality test (when >8 samples were tested) or the Kolmogorov-Smirnov test (when > 3 and < 8 samples were tested). Based on the results from the normality test, we then proceeded to statistically analyse our data using either parametric (normally distributed data) or non-parametric (non-normally distributed data). The information regarding the specific statistical analysis conducted in each experiment is provided in each figure legend. Significance was denoted by the resulting *p* value, applying the following cut-offs: * $p < 0.05$, ** $p < 0.005$, *** $p <$ 0.00

Chapter 3: **Developmental regulation of microRNA release by filarial parasites**

3.1 Introduction

3.1.1 Helminth Excretory/Secretory products

A fascinating aspect in the interplay between parasitic nematodes and their hosts is the sophisticated myriad of interactions they have co-evolved during their longstanding evolutionary relationship. In this context, parasites have evolved multiple mechanisms to circumvent the strong immune reaction mounted against them. One of such mechanisms involves the release of factors with immunomodulatory properties. These products, broadly termed Excretion/Secretion (ES) products, have been extensively studied in multiple parasitic nematodes (Hewitson, Grainger, et al., 2009).

The composition of the ES products derived from helminths is complex (Hewitson, Grainger, et al., 2009) and includes soluble protein factors including cytokine homologues of the TGF-β family and the macrophage migration inhibitory factor (MIF), cathepsins, and aspartyl endopeptidases, among several others (Hewitson, Grainger, et al., 2009; McSorley, Hewitson, et al., 2013). These are known to impair the function of several immune cell types, enabling the parasite to fully develop and ensure fitness. Moreover, the composition of the ES products differs between lifecycle stages, perhaps reflecting the specific challenges faced by each developmental stage within a given (insect or vertebrate) host. For instance, *Litomosoides sigmodontis* gravid females secrete a plethora of proteins solely identified in this stage, with other lifecycle stages exhibiting a more restricted composition of ES products (Armstrong, Babayan, et al., 2014). Sex- and stage-specific proteomic analyses of ES products have also been conducted in other parasites, including the heartworm *Dirofilaria immitis* (Geary, Satti, et al., 2012), the filarial parasite *Brugia malayi* (Hewitson, Harcus, et al., 2008; Moreno, & Geary, 2008; Zang, Atmadja, et al., 2016) and the gastrointestinal nematodes *Aascaris suum* (Chehayeb, Robertson, et al., 2014; Wang, Van Steendam, et al., 2013) and *Nippostrongylus brasiliensis* (Sotillo, Sanchez-Flores, et al., 2014). Although the function of the secreted proteins is thought to be immunomodulation of the host, other

interactions, such as parasite-to-parasite interactions (e.g. adult males and adult females), are also plausible but this is generally less well studied.

However, the interactions with the host are not likely to be solely mediated by protein factors, as other components of the ES products are thought to actively be involved. For example, the release of extracellular vesicles (EVs) have been described in several helminthic parasites, including trematodes (*Schistosoma mansoni*, *Fasciola hepatica*, among others) and nematodes of medical and veterinary importance (Cwiklinski, de la Torre-Escudero, et al., 2015; Fromm, Trelis, et al., 2015; Hansen, Kringel, et al., 2015; Nowacki, Swain, et al., 2015; Tzelos, Matthews, et al., 2016; Wang, Li, et al., 2015; Zamanian, Fraser, Agbedanu, & Harischandra, 2015). The EV cargo includes a diverse suite of molecules that are thought to be encapsulated within a lipid bilayer. In some cases, these cargoes contain protein markers thought to be associated with intracellular trafficking processes (e.g. endosomal pathway), including several RAB proteins and ALIX (Buck, Coakley, Simbari, McSorley, et al., 2014), actively involved in vesicle transport, tethering and fusion (Raposo, & Stoorvogel, 2013). Moreover, it has been demonstrated that EVs derived from the gastrointestinal nematode *Heligmosomoides polygyrus* possess a greater proportion of plasmalogen and ether glycerophospholipids when compared to host cell-derived EVs, which are typically enriched in sphingolipids and cholesterol. These differences could be important for EV fluidity and stability upon release (Simbari, Mccaskill, et al., 2016). Intriguingly, it has also been demonstrated that EVs are loaded with small non-coding RNAs, including miRNAs, in association with RNA-binding proteins actively involved in RNAi effector function (Buck, Coakley, Simbari, McSorley, et al., 2014). This observation supports the hypothesis that parasites use extracellular RNAi machinery to actively regulate gene expression in the host cell for their own benefit. Consistent with this hypothesis, it has been demonstrated that *H. polygyrus* EVs downregulate expression of genes important for an adequate innate immune response, including *dusp1* and *il33r* (Buck, Coakley, Simbari, McSorley, et al., 2014).

3.1.2 Extracellular parasite-derived miRNAs *in vitro* and *in vivo*

There are, however, some fundamental questions that require addressing to better understand the role of miRNAs released by parasites, and whether and how these act as mediators of the parasite-to-host crosstalk. The secretion of miRNAs by parasitic nematodes have now been shown *in vivo* in a multitude of organisms (reviewed in Coakley, Maizels, et al., 2015), and their potential as biomarkers for infections is exciting and promising (discussed in detail in chapter 5 and in Quintana, Babayan, et al., 2016). Nonetheless, it is still unclear whether all developmental stages have the capacity to secrete RNAs (and miRNAs) or if this is restricted to a given developmental stage. Previous studies have demonstrated differences in the protein content of the secretomes of different developmental stages of parasitic nematodes (Chehayeb, Robertson, et al., 2014; Hewitson, Harcus, et al., 2008; Kwan-Lim, Gregory, et al., 1989; Moreno, & Geary, 2008; Sotillo, Sanchez-Flores, et al., 2014). These differences have been proposed to reflect potentially different interactions between each life stage and the hosts. Moreover, in the context of development and nematode physiology, several miRNA families display distinctive expression patters across nematode lifecycle stages, thought to regulate distinct processes including moulting (Britton, Winter, et al., 2014; Poole, Gu, et al., 2014; Resnick, McCulloch, et al., 2010; Winter, Gillan, et al., 2015; Xu, Fu, et al., 2013) Therefore, one might expect that there should be specific extracellular miRNA "signatures" in the secretomes from multiple developmental stages of the same parasite. During the preparation of this PhD thesis, two articles were published that partially addressed this question. First, Zamanian et al., characterised EVs derived from infective L3 and adult stages from the human pathogen *B. malayi* by transmission electron microscopy (TEM) (Zamanian, Fraser, Agbedanu, & Harischandra, 2015). Moreover, the same study reported that the EVs derived from the infective L3 stage also contained miRNAs, as previously reported in adult stages of other parasitic nematodes (Buck, Coakley, Simbari, McSorley, et al., 2014; Zamanian, Fraser, Agbedanu, & Harischandra, 2015). In a separate report, Tritten et al. concluded that there are differences in the released miRNA found in ES products from adult males, females and mf from the heartworm *D. immitis* (Tritten, Clarke, et al., 2016). These studies suggest that the secretion of EVs containing miRNAs is not likely to be restricted to adult worm stages, and could be found in other developmental stages. Here, we

contribute further to these two studies by examining specific differences in the miRNAs of ES products derived from several developmental stages of *L. sigmodontis*. We also address other aspects of miRNA release by parasitic nematodes, including temporal dynamics of secretion, effect of anthelminthic chemotherapy upon miRNA secretion, as well as their potential as biomarkers for filariasis in different hosts. This chapter is dedicated to the study of small RNA composition in the secretome of several developmental stages of the filarial parasite *L. sigmodontis*.

3.2 Specific aims

1. To determine whether there are stage and/or sex-specific miRNAs differentially detected in the secretome from the filarial parasite *Litomosoides sigmodontis*
2. To identify miRNAs specifically secreted by *Litomosoides sigmodontis* gravid female worms
3. To investigate the association of secreted miRNAs with extracellular vesicles *in vitro*.

3.3 Results

3.3.1 Larval and adult stages secrete RNA *in vitro*

As discussed above, miRNAs have been shown to be released by several parasitic nematodes both *in vitro* and *in vivo*. However, factors dictating release of RNAs are not well characterized, including whether this is developmentally regulated. Therefore, our first aim was to describe the RNA composition, with an emphasis on miRNAs, in ES products from larval and adult stages of the filarial nematode *L. sigmodontis*. Total RNA was purified from *in vitro* ES products from larval (vector-derived L3s - vL3s, host-derived L3s - hL3s, L4s, and mf) and adult stages (juvenile males – jAM, pre-gravid females – pgAF, adult males – AM, and gravid adult females – gAF) obtained as described in Chapter 2. The total RNA extracted was quantified by both Nanodrop and Qubit however we failed to detect a signal in the accurate range of quantification (data not shown), perhaps due to the relative low worm density used to generate ES products from lifecycle stage. We next sought to profile the small RNA content, defined as the population of total RNA <150 nt in length, using a small RNA lab-on-a-chip technology of the Bioanalyzer 2100, as described in Chapter 2. Our results indicate that the small RNA fraction in ES products from larval and adult stages is composed of two main populations, 20-30 nt in length and 40-60 nt in length (**Figure 3.1A & B**). However, there are clear differences in the relative intensity of the signal detected between lifecycle stages, which is likely to be associated with different RNA concentrations of total RNA present in the ES products (**Figure 3.1B**). For downstream analysis, we focussed on the shorter, 20-30 nt, RNA population, as this should include sequences of the expected size for mature miRNAs (21-24 nt in length). Given that we could not obtain reliable measurements of RNA concentration in these samples, we decided to use equivalent volumes of RNA for small RNA library preparation, as described in Chapter 2. The resulting PCR products for each sample were pooled at equimolar concentrations and subjected to small RNA sequencing on a HiSeq2500 to obtain 50bp, single-end reads as described in Chapter 2.

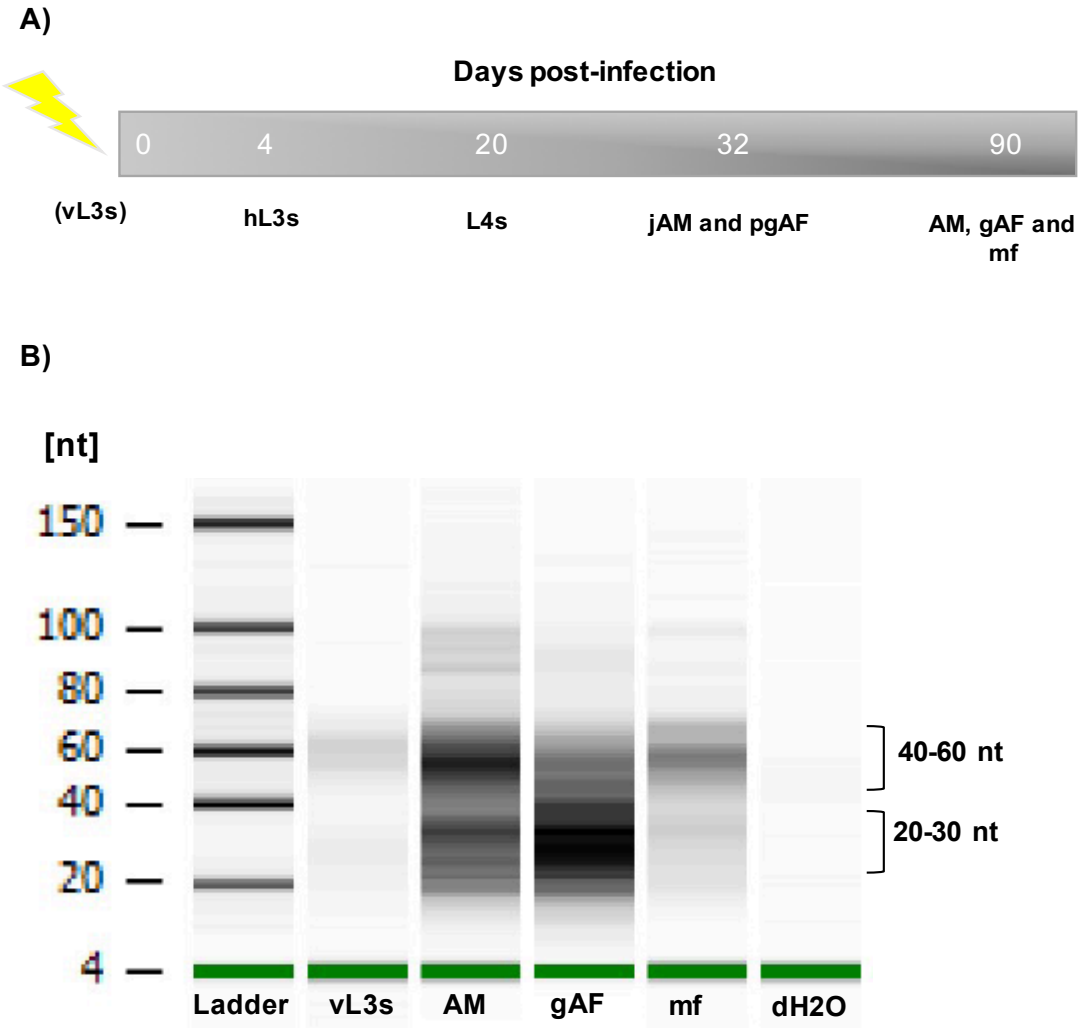

Figure 3.1 Small RNA profile of ES products from larval and adult stages of *L. sigmodontis*. A) time points at which worms were harvested from infected gerbils. Vector-derived L3s were harvested from infected mites immediately before infection (indicated by a yellow thunderbolt). Thereafter host-derived L3s (hL3s) were harvested at day 4 post-infection, L4s at day 20 post-infection, juvenile males (jAM) and pre-gravid females (pgAF) at day 32 post-infection, and adult males (AM), gravid adult females (gAF) and microfilariae (mf) at day 90 post-infection. B) Total RNA (1 µL from 25 µL in total) purified from the *in vitro* ES products was loaded into a Bioanalyzer small RNA chip. Representative electropherograms are shown indicating two clear populations of RNAs in ES products with different lengths: 20-30 nt and 40-60 nt. A well containing H_2O was also included as negative control.

3.3.2 The RNA composition of the ES product from larval and adult stages is predominantly composed of rRNAs, tRNA fragments and miRNAs

On average, we obtained 7,569,695 raw reads from ES products from vL3s (*n*= 2), 6,281,894 raw reads from hL3s (*n*= 2), 12,471,046 raw reads for L4s (*n* = 2), 4,493,814 raw reads for jAM (*n* = 2), 11,043,195 raw reads from pgAF (*n* = 2), 6,833,171 raw reads from AM (*n* = 10), 8,892,543 raw reads from gAF (*n* = 12) and 5,944,094 raw reads from mf (*n* = 8) (**Table 3.1 & Supplementary table 1**). It is important to note that some of the replicates were variable in terms of their raw read counts; e.g. vL3s and jAM, where we observed ~10X and ~3X differential depth of coverage between replicates (**Supplementary table 3.1**). After trimming the 3' adapter and discarding all reads that were <17 nt in length, we obtained on average 86.5% high-quality reads for vL3s, 72.5% high-quality reads for hL3s, 62.8% high-quality reads for L4s, 64.44% high-quality reads for jAM, 75.32% high-quality reads for pgAF, 78.4% high-quality reads for AM, 84.78% high-quality reads for gAF and 83.65% high-quality reads for mf (**Figure 3.2A, Table 3.1 & Supplementary table 1**). We then classified reads as mapping perfectly and unambiguously to either *L. sigmodontis* or the *M. musculus* reference genomes. To date, there is no reference genome available for gerbils, and there are limitations to using alternative genomes to answer mappability questions. Nevertheless, to discard sequences unlikely to be parasite-derived, we assumed that the *M. musculus* genome used in this study was sufficient, given that this is one the closest rodent relative to gerbils, for which there is a good genome annotation available. This analysis led us to identify 12.2% *L. sigmodontis*-specific reads in ES products from vL3s, 1.5% in hL3s, 0.94% in L4s, 2.46% in jAM, 35.5% in pgAF, 12.4% in AM, 45.11% in gAF, and 15.97% in mf (**Table 3.1 & Supplementary table 3.1**). On the other hand, we detected >25% of the total high-quality reads in hL3s and L4s that mapped perfectly and unambiguously to the *M. musculus* genome, which contrasts with the <5% total *M. musculus*-specific reads detected in ES products of the remaining lifecycle stages (**Figure 3.2B, Table 3.1 & Supplementary table 3.1)**. The differences between the percentage of parasite reads in each sample could reflect the differential secretory capacity between developmental stages (consistent with Bioanalyzer results), however it is difficult to test this and several factors can influence the quality of a library (discussed further below).

The next step was to determine the general RNA biotypes of the *L. sigmodontis*-specific sequences. To do so, we used the Rfam repository (Burge, Daub, et al., 2013), which allows us to discriminate between the conserved RNA families reported in the literature, including rRNAs, tRNAs, small nucleolar RNAs (snoRNAs), Y RNAs, among others (Burge, Daub, et al., 2013). For practical reasons, we report in here rRNAs, tRNAs and miRNAs as three main individual groups and define a fourth group, called "other Rfam", that contains all the other RNA families. Based on Rfam analysis, we detected different proportions of reads being classified as rRNAs or tRNAs between the larval and adult stages. The data also suggests the presence of less RNA sequences classified as tRNAs in the ES products from larval stages (vL3s, hL3s, L4s, and mf) when compared to adult stages (**Figure 3.2C**, **Table 3.1 & Supplementary table 3.1)**. Conversely, the proportion of reads classified as rRNAs was higher in ES products larval stages when compared to ES products from adult stages. Nevertheless, both rRNAs and tRNAs represent the top two most abundantly RNA biotypes detected in ES products from both larval and adult stages. We also noted that a proportion of the *L. sigmodontis*-specific reads could not be classified using Rfam (termed "Non-Rfam"; **Figure 3.2B and C, and Table 3.1**). At present, these sequences are not annotated and therefore it is unclear whether they represent true biologically relevant sequences or potential contaminations.

A third class of RNA biotypes corresponded to miRNAs. However, one limitation of identifying miRNAs using Rfam is that it only identifies known miRNA families. To more accurately profile miRNAs in these ES products, we curated these datasets using miRDeep2 (Friedländer, Mackowiak, et al., 2012), which predicts known and potentially novel miRNAs using as a reference the miRNAs reported in the latest version of miRBase (Kozomara, & Griffiths-Jones, 2014). We used the total *L. sigmodontis*-specific reads as input for miRNA identification using miRDeep2, based on the criteria described in chapter 2. For this analysis, and based on the variable number of reads in ES products across lifecycle stages (**Table 3.1**), we decided to arbitrarily set a cut-off of at least 100,000 *L. sigmodontis*-specific reads in each sample for downstream analysis and miRNA identification by miRDeep2. This led to the exclusion of samples from hL3s, L4s and jAM as their overall *L. sigmodontis*-specific read counts were below this threshold (**Table 3.1**).

Table 3.1 RNA diversity in the ES products of larval and adult stages of *Litomosoides sigmodontis*

ES product[1,2]	vL3s	hL3s	L4s	jAM	pgAF	AM	gAF	mf
Input reads	7,596,695 (10,720,434)	6,281,894 (6,378,787)	12,471,046 (12,744,267)	4,493,814 (5,501,542)	11,043,195 (12,509,154)	5,079,075 (9,489,535)	7,175,484 (9,950,704)	6,493,083 (7,823,877)
High-quality reads	6,571,665 (9,372,767)	4,553,588 (4,697,848)	7,840,378 (7,977,987)	2,895,861 (3,488,358)	8,317,514 (9,722,226)	3,849,365 (8,166,739)	6,577,228 (8,939,823)	5,207,592 (6,989,296)
% High-quality reads	79.9% (83.9%)	72.5% (73.6%)	62.9% (63.1%)	65.9% (67.4%)	73.8% (76.7%)	78.1% (86.4%)	89.7% (91.5%)	83,1% (88.7%)
***M. musculus* reads**	467,424 (681,772)	1,620,514 (1,683,092)	2,267,466 (2,339,368)	142,110 (162,823)	242,416 (279,780)	256,816 (351,738)	177,444 (266,406)	151,564 (186,608)
***L. sigmodontis* reads**	**803,555 (1,152,021)**	**68,157 (73,260)**	**73,500 (76,256)**	**71,118 (74,655)**	**2,952,875 (4,124,719)**	**542,449 (692,607)**	**2,858,480 (4,700,570)**	**698,580 (813,256)**
rRNAs	330,111 (474,840)	10,884 (11,495)	13,962 (14,170)	18,467 (19,172)	1,080,446 (1,520,564)	69,944 (101,291)	854,148 (1,614,902)	212,606 (281,256)
tRNAs	65,773 (93,354)	20,788 (21,901)	736 (748)	1,140 (1,468)	797,239 (1,118,407)	327,758 (444,546)	1,336,480 (1,632,588)	253,601 (357,182)
miRNAs	5,597 (7,009)	46 (51)	142 (159)	76 (80)	10,372 (15,018)	986 (1,172)	14,622 (31,364)	2,154 (4,183)
Other Rfam	7,956 (11,143)	331 (334)	1,038 (1,144)	1,095 (1,332)	69,077 (93,716)	10,701 (14,663)	64,572 (122,489)	20,175 (26,486)
Non-Rfam	394,117 (565,674)	36,107 (39,484)	57,622 (60,509)	50,339 (54,011)	995,740 (1,377,012)	117,685 (145,575)	780,201 (1,273,977)	205,969 (282,146)

[1]The following samples and replicates were subjected to deep sequencing: vector-derived L3s (vL3s; n = 2), host-derived or "migratory" L3s (hL3s; n = 2), L4s (n = 2), juvenile males (jAM) and pre-gravid adult females (pgAF) at day 32 post-infection (n = 2, per sex), and adult males (AM; n = 10), gravid adult females (gAF; n = 12), and microfilariae (mf; n = 8).

[2] The median and the upper limit for the 75% of the total reads (in bracket) are reported for each lifecycle stage

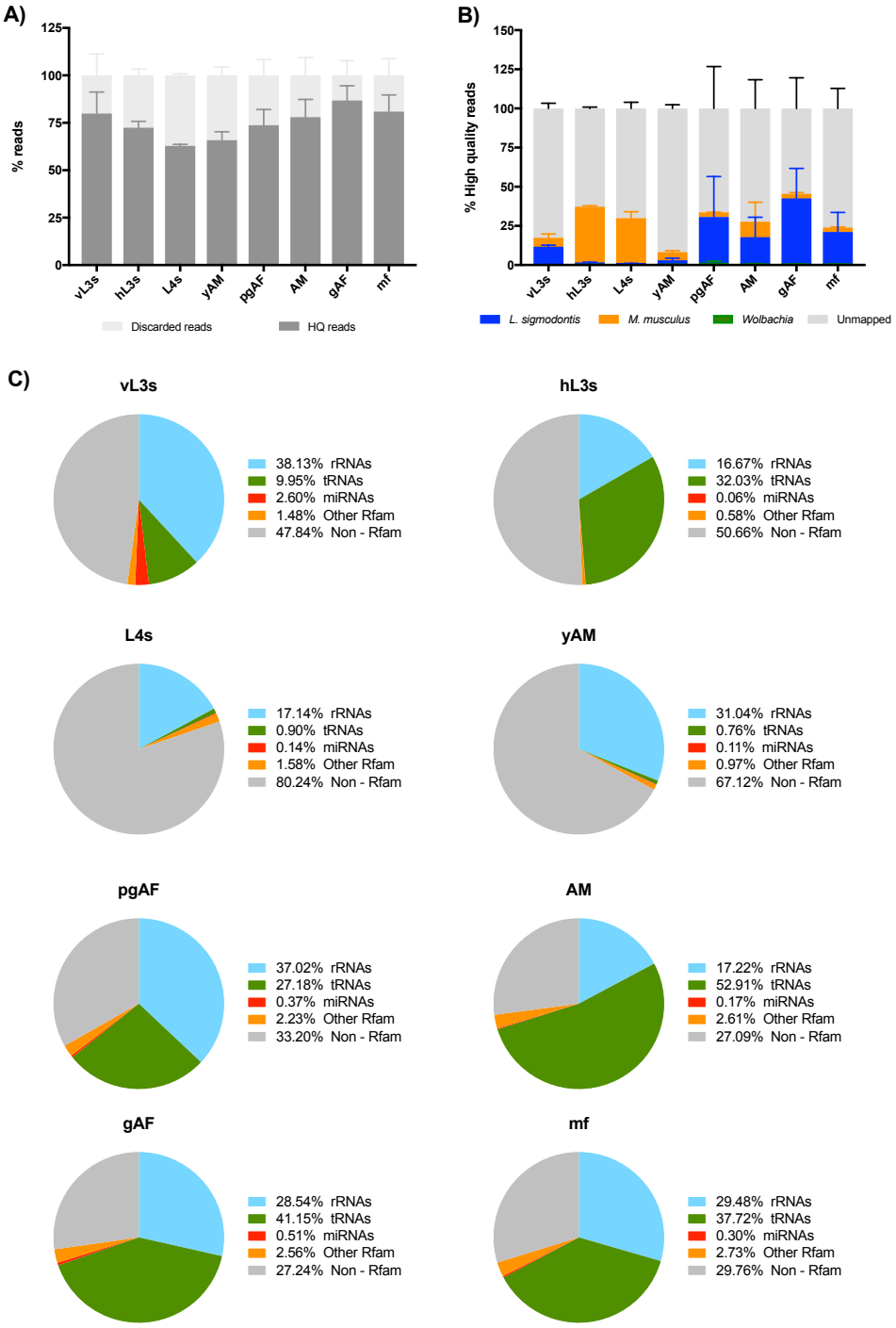

Figure 3.2 *L. sigmodontis* ES products contain small RNAs. A) Initial filtering step of the raw reads produced high-quality (HQ) reads (those containing the sequence of the 3' adapter), and those that did not contain the 3' adapter sequence were discarded. B) Mapping analysis against the relevant genomes were carried using HQ reads as inputs. C) Proportion of *L. sigmodontis* small RNA biotypes (<30 nt) identified in sequencing libraries from ES products from larval and adult stages.

Following this filtering, we ended up analysing a total of 34 samples and from these, a total of 208 mature miRNA sequences, mapped to 221 genomic loci, were detected in > 2 copies in at least 1 of the samples (**Supplementary table 3.2**). It is important to note that in some cases a miRNA could derive from multiple genomic loci with hairpin-like structures and cannot be unambiguously mapped to a single location, thus explaining why there are more genomic loci than actual mature miRNA sequences. We detected a total of 60 miRNAs in the ES products from vL3s, 74 miRNAs in ES products from pgAF, 78 miRNAs in ES products from AM, 203 miRNAs in ES products from gAF and 98 miRNAs in ES products from mf (**Supplementary table 3.2**). Of the 208 miRNAs, 76 (36.5%) had >100 counts when tallying reads across all replicates, whereas the remaining 132 miRNAs (63.5%) had <100 read counts (**Supplementary table 3.2**). The 20 most abundant miRNAs detected in ES products across developmental stages account for ~92% of the total miRNA reads identified by miRDeep2 (**Table 3.2)**. These are mostly composed of miRNAs belonging to families broadly conserved miR-10 and lin-4/miR-125 miRNA families, as well as the Bantam family. **Figure 3.3** represents the log2 transformed read counts of each miRNA normalised to the total miRNA reads in that sample and demonstrates that ES products from gAF worms contain a more diverse suite of miRNAs at this level of detection. Further Principal Component Analysis (PCA) broadly segregates the ES products into two main clusters, each corresponding to ES products from AM and gAF, whereas the cluster formed by mf was more variable (**Figure 3.4A**). The miRNA content observed in ES products from vL3s and pre-gravid females were variable and with only two replicates could not be attributed to a cluster (**Figure 3.4A**). The most abundant miRNA family detected was the miR-10 family, with three members (miR-100a, miR-100d and miR-993-3p) representing ~22% of the total miRNAs identified by miRDeep2 across the samples (**Table 3.2**). This family is highly conserved across the animal kingdom, and is found in both parasitic nematodes and their vertebrate hosts. To compare the sequence identity of the mature miRNAs detected by miRDeep2, these were aligned with the mature miRNA sequence of the miR-100s identified in mice and humans using EMBL-EBI Multiple Sequence Comparison by Log-Expectation (MUSCLE) (Edgar, 2004), setting up the alignment to the same start position in all cases (first nucleotide in the 5' end). In line with their family classification, all these miRNAs shared the same seed sequence, defined as nucleotides in position 2-8 of the 5' end (**Figure 3.5A and B**). However, the 3' end is

more heterogeneous and shows poor conservation between sequences identified in parasitic nematodes and vertebrates (**Figure 3.5A and B**). Beyond the conserved families, a total of 26 novel miRNAs were also predicted by miRDeep2 (**Table 3.3**) which could derive from up to 30 different loci in the genome, these accounted for ~0.1% of the total miRNAs counts identified by miRDeep2 (**Table 3.3**). Four of these novel miRNAs, called novel-1 to novel-4 based on their relative abundance accounted for 51% of the total read counts assigned as novel miRNAs. Interestingly, several of these potentially novel miRNAs were highly abundant in the ES products of mf (e.g. lsi-novel-1, novel-4, novel-5, novel-7) when compared to AM and/or gAF, whereas lsi-novel-3 was predominantly enriched in the of AM when compared to gAF (**Table 3.3**). The secondary structures of the four most abundant predicted pre-miRNA hairpins showed the canonical 3' 2-nt overhang, and suggesting these are *bona fide* Dicer-derived miRNAs (**Figure 3.6**).

Table 3.2 Top 20 most abundant miRNAs detected in the secretome of *Litomosoides sigmodontis*

miRNA	Mature RNA sequence (5' – 3')	Genomic locus	Total RPM[1]	RPM[1,2] in AM secretome (*n* = 10)	RPM[1,2] in gAF secretome (*n* = 12)	RPM[1,2] in mf secretome (*n* = 8)
miR-100a[3]	aacccguaguuucgaacaugugu	nLs.2.1.scaf00144	203,082	24,816 (124,797)	195,384 (264,137)	58,731 (85,273)
miR-92-5p	uauugcacucgucccggccuga	nLs.2.1.scaf00001	185,757	94,888 (147,518)	244,141 (336,294)	351,549 (529,561)
miR-71-5p	ugaaagacauggguagugagacg	nLs.2.1.scaf00472	173,120	85,954 (113,177)	119,381 (181,402)	48,083 (62,943)
Lin-4-5p	ucccugagaccucugcugcga	nLs.2.1.scaf00367	109,094	134,917 (176,235)	55,825 (71,360)	1,220 (12,267)
miR-8805-5p[4]	ggaggaaucagcgugcugu	nLs.2.1.scaf00006	74,752	11,363 (21,743)	92,784 (94,633)	47,878 (73,264)
miR-9146-5p[4]	gccuggaugaaucucggug	nLs.2.1.scaf00457	29,436	98,699 (257,689)	19,504 (32,664)	39,579 (47,357)
miR-5364-5p	cgagguauuguuuauuggcuga	nLs.2.1.scaf00070	24,417	1,414 (17,814)	21,217 (26,977)	0 (0)
miR-5866-5p	uuaccauguugaucgaucucc	nLs.2.1.scaf01139	21,351	0 (1,699)	23,909 (36,241)	4,213 (6,298)
Bantam-a-3p	ugagaucauugugaaagcuauu	nLs.2.1.scaf01674	16,673	1,029 (7,733)	12,561 (20,054)	1,589 (5,375)
miR-6659-3p[4]	cuuggcugggaggugacucgcgauc	nLs.2.1.scaf00364	16,481	17,936 (45,270)	18,790 (19,787)	15,490 (29,419)
miR-9887-5p[4]	cagggcugcacgcgcgc	nLs.2.1.scaf00003	16,078	22,088 (38,655)	14,822 (18,353)	27,642 (31,826)
miR-100d-5p	uacccguagcuccgaauaugugu	nLs.2.1.scaf00144	13,994	0 (8,461)	23,208 (27,267)	3,242 (10,294)
miR-993-3p	uaagcucgucucuacaggcagg	nLs.2.1.scaf00199	12,793	0 (1,236)	11,164 (17,448)	5,977 (8,477)
Bantam-b	ugagaucacguuacauccgccu	nLs.2.1.scaf02066	11,992	4,385 (9,685)	5,903 (7,726)	2,785 (4,021)
miR-34-5p	uggcaguguguuagcugguugu	nLs.2.1.scaf00918	11,217	10,026 (39,442)	13,664 (24,588)	10,902 (18,795)
miR-6077-3p[4]	uggaagagauaggaacagagc	nLs.2.1.scaf00282	8,970	7,719 (16,924)	7,898 (9,210)	14,565 (25,918)
miR-8319-3p[4]	gaauuagcucgugcgguacggc	nLs.2.1.scaf00584	8,377	37,259 (75,989)	7,636 (7,864)	2,097 (9,625)
miR-36c-5p[4]	ucaccggagacauuguuccgca	nLs.2.1.scaf00392	7,596	0 (0)	4,260 (8,352)	0 (8,713)
miR-6717-5p[4]	gggcgaugaugguaugaagggua	nLs.2.1.scaf00382	7,545	14,962 (36,662)	15,750 (16,492)	22,086 (31,056)
miR-4942-3p[4]	acgaugacaguaauaggauuauu	nLs.2.1.scaf01227	7,341	0 (356)	6,004 (6,294)	0 (916)

[1] RPM = Reads per million miRNA reads; [2] The median of the sequencing reads and the upper limit for the 75% of the total reads (in bracket) are reported for AM, gAF and mf
[3]A shorter miR-100a, lacking the first four nucleotides in the 5' end, was also abundantly detected; [4] miRNA name assigned based on seed sequence homology with other miRNAs.

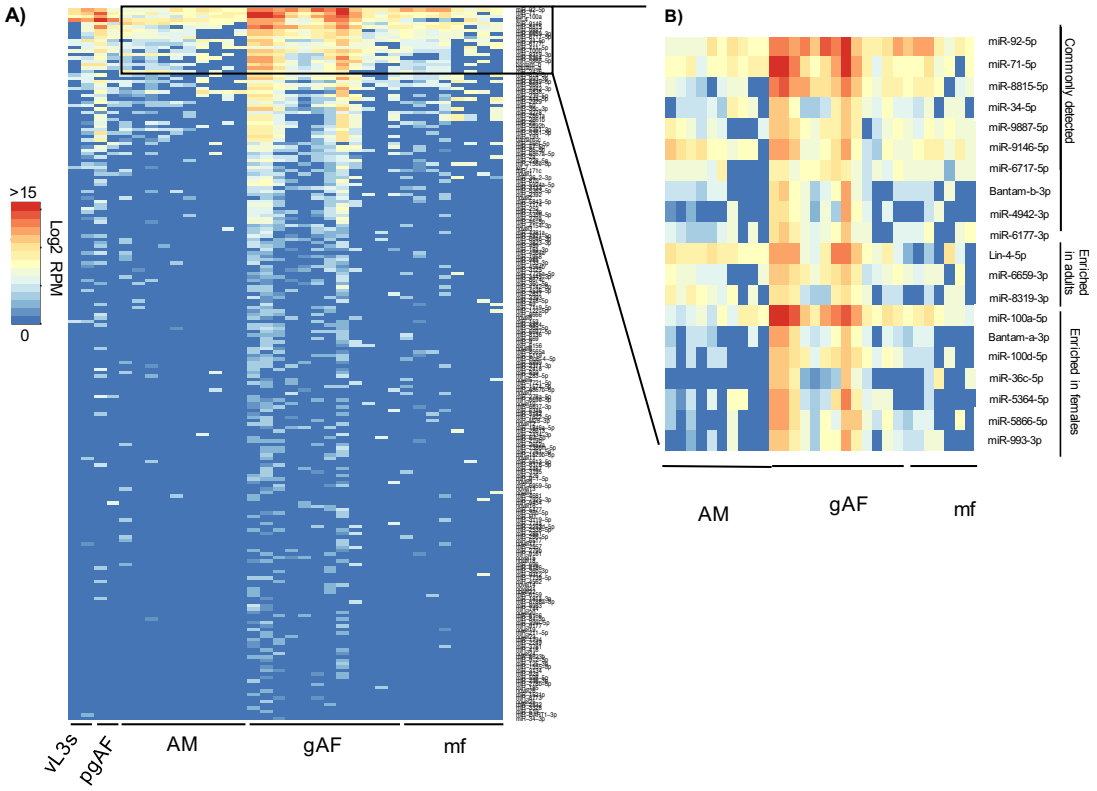

Figure 3.3 miRNA identification in the secretome of *L. sigmodontis*. (A) Heat map of the abundance level of the 208 miRNAs detected in all the secretomes screened by deep sequencing, (B) The top 20 miRNAs that account for >90% of the total miRNA reads across developmental stages, depicting their levels in adult males (AM), gravid adult females (gAF), and microfilariae (mf). vL3s = vector-derived L3s; pgAF = pre-gravid adult females. Of the top 20, 11 are enriched in adults or gAF compared to mf, whereas the remaining 10 are commonly detected in all the secretomes based on DEseq2 analysis.

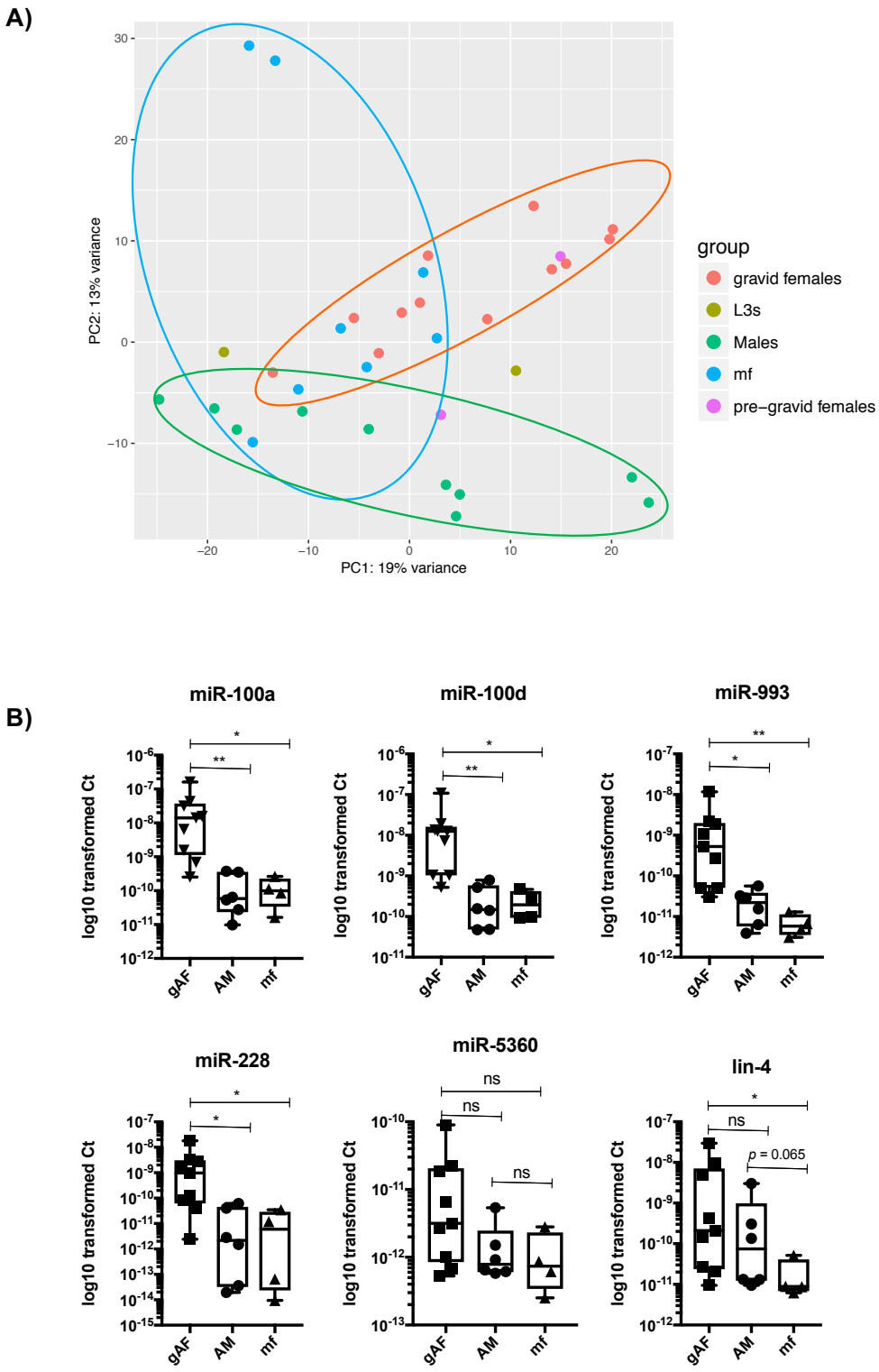

Figure 3.4 Differentially detected miRNAs in the secretome of larval and adult stages of *L. sigmodontis*. A) Principal Component Analysis (PCA) of the miRNAs detected in the secretome of larval and adult stages of *L. sigmodontis*. B) qRT-PCR validations were conducted using 2.5 µL of total RNA from ES products (same volume used for small RNA library preps). The miRNAs measured were selected based on their differentially detection from the DESeq2 analysis as in Figure 3.3 (* $p < 0.05$; ** $p < 0.005$; ns = not significant; Kruskal-Wallis test for Multiple comparisons).

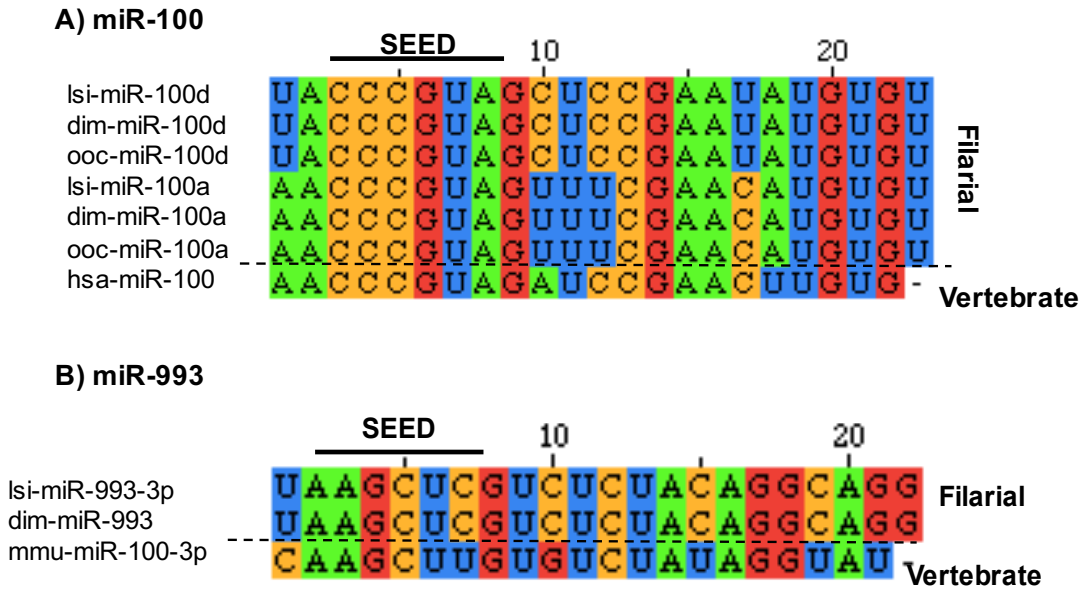

Figure 3.5 Mature miRNA sequences of extracellular miR-10 family members detected in ES products from larval and adult stages of *L. sigmodontis*. Several members of the miR-10 family were found to be enriched in the secretome of gAF worms when compared to adult males and/or mf. The vertebrate homologues to these sequences were included as references, alongside the sequences reported in other filarial nematodes. A) sequence of the miR-100s detected in several ES products showing the seed sequence, defined as nucleotides in position 2-8 in the 5' end, is broadly conserved between filarial nematodes and vertebrates. On the other hand, the 3' is highly heterogeneous between filarial nematodes and vertebrates. B) The seed sequence of miR-993-3p is only conserved between nucleotides 2-6, with poor homology between miR-993 from filarial parasites and vertebrate hosts.

Table 3.3 novel miRNAs detected in the secretome of *L. sigmodontis*

miRNA	RNA sequence (5' – 3')	Length (nt)	Genomic location	Average RPM[1] vL3s	Average RPM[1] pgAF	Average RPM[1] AM	Average RPM[1] gAF	Average RPM[1] mf
lsi-Novel-1	agcuugagguaggaugaacaacu	23	nLs.2.1.scaf00725_36299; nLs.2.1.scaf00725_36308	68.78	328.40	138.49	137.85	2142.20
lsi-Novel-2	uaggcgcaucagaacuagacggc	23	nLs.2.1.scaf00643_34575	103.17	0	1191	163.86	785.47
lsi-Novel-3	ucaggaugagaugauggaugaau	23	nLs.2.1.scaf00419_28137	0	0	2188.12	152.16	0
lsi-Novel-4	ucucuguaauguuccucucuccc	23	nLs.2.1.scaf00012_2609	0	0	0	6.50	2356.42
lsi-Novel-5	aacccuccucucagcccauccc	22	nLs.2.1.scaf00323_24399	0	0	0	14.31	1999.39
lsi-Novel-6	ugccccgccuucuucucccgc	21	nLs.2.1.scaf00559_32469	68.78	231.10	0	58.52	0
lsi-Novel-7	ggugcgaagcgcaguuggaugagc	24	nLs.2.1.scaf00428_28447	0	0	0	36.41	880.68
lsi-Novel-8	uggguguguagguauggauaauc	24	nLs.2.1.scaf00093_11380; nLs.2.1.scaf00074_9579	0	182.45	0	55.92	0
lsi-Novel-9	uacuggguguuggcaguggggu	23	nLs.2.1.scaf00336_25049	0	0	0	67.63	0
lsi-Novel-10	auggcguuggcguuggcuacc	21	nLs.2.1.scaf00415_28022	0	0	0	63.67	0
lsi-Novel-11	gagauacguuugaaggagcucaac	24	nLs.2.1.scaf00565_32616	378.29	0	0	39.02	0
lsi-Novel-12	accaucaguagucuugugauc	21	nLs.2.1.scaf00142_14716	0	0	0	45.52	0
lsi-Novel-13	cccgaagguggcuuugacgcu	21	nLs.2.1.scaf00315_23858	0	0	498.56	14.31	0
lsi-Novel-14	gagcgagaucggcggcguggagaga	25	nLs.2.1.scaf01553_45817; nLs.2.1.scaf00923_39792	0	0	0	32.51	0
lsi-Novel-15	guuagcgguuucgagcgugguga	23	nLs.2.1.scaf00371_26475	0	0	0	31.21	0
lsi-Novel-16	gguuccgccgguggagugacc	21	nLs.2.1.scaf00292_22935	0	0	0	31.21	0
lsi-Novel-17	uaaugaaacuuagauuccugagc	23	nLs.2.1.scaf00764_37032	103.70	0	0	14.31	142.81
lsi-Novel-18	aggguuagauuugguauaaauc	22	nLs.2.1.scaf00831_38112	0	0	0	22.11	0
lsi-Novel-19	agcgguaguaguaguagu	18	nLs.2.1.scaf02071_47669	0	0	0	18.21	71.41
lsi-Novel-20	uggugcgagaucugugac	18	nLs.2.1.scaf00165_16219	0	0	55.40	18.21	0
lsi-Novel-21	gaacucguugaacauugaacua	22	nLs.2.1.scaf01711_46585	0	0	0	20.81	0
lsi-Novel-22	gaacucguugaacauugaac	20	nLs.2.1.scaf01711_46596	0	0	0	20.81	0
lsi-Novel-23	gacauuagccugguuucaucggacc	25	nLs.2.1.scaf00518_31313	0	0	0	16.91	0
lsi-Novel-24	auaauauuauuauuguugucg	21	nLs.2.1.scaf01227_43436	0	0	0	16.90	0
lsi-Novel-25	uuacggguaauugugaugaugc	22	nLs.2.1.scaf00152_15430	0	0	0	14.31	0
lsi-Novel-26	aagcaaucacagcggccggau	21	nLs.2.1.scaf01015_41090; nLs.2.1.scaf01015_41095	0	0	0	10.40	0

[1] Reads per million of miRNAs reads (RPM) detected in all the ES samples tested for each individual lifecycle stage.

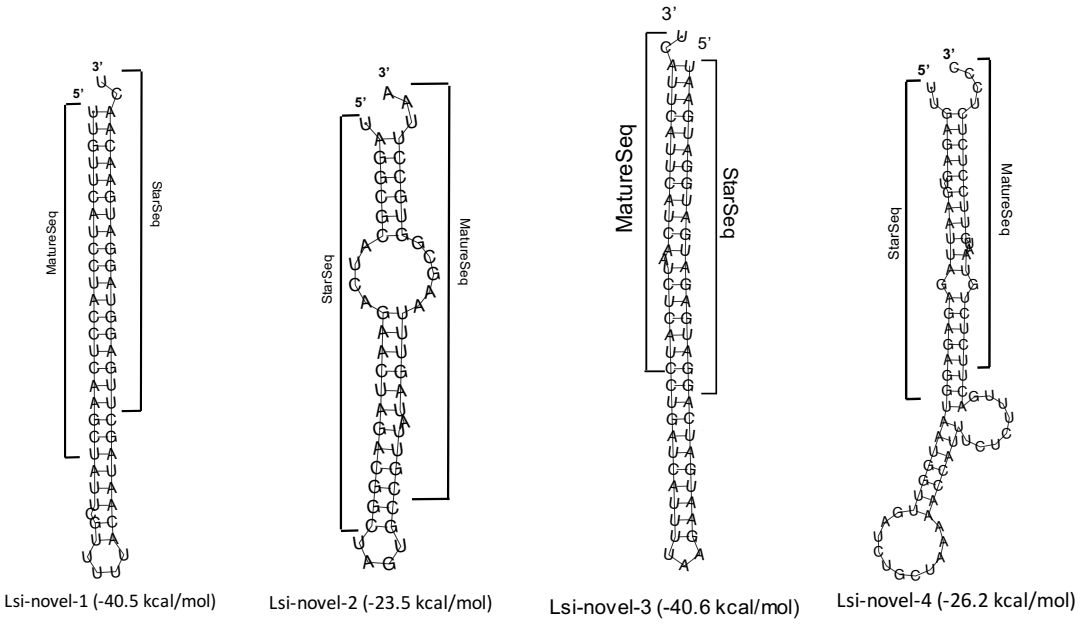

Figure 3.6 Secondary structure of the four most abundant novel pre-miRNAs identified in ES products from larval and adult stages of *L. sigmodontis*. The secondary structures were predicted using the pre-miRNA sequenced identified by miRDeep2 (table 3.3) using the Vienna RNAfold package. Lines indicate the mature and the star sequences predicted by deep sequencing.

A recent report showed that the vector-derived L3s from the human filarial pathogen *B. malayi* secrete EVs loaded with miRNAs, which have been proposed as a route for communication with the mosquito vector (Zamanian, Fraser, Agbedanu, & Harischandra, 2015). We detected a total of 60 parasite-derived miRNAs in ES products from *L. sigmodontis* vector-derived L3s (**Supplementary table 3.2**), out of which 6 (lin-4, miR-92, miR-71, miR-34, bantam-b and miR-100a) accounted for >90% of the miRNA read counts for this stage (**Supplementary table 3.2**). Moreover, these miRNAs were also detected in ES products from *B. malayi* L3s (Zamanian, Fraser, Agbedanu, & Harischandra, 2015). However, it is difficult to make direct comparisons between both studies due to technical differences in small RNA library preparation and sequencing analysis. Moreover, we did not perform a side-by-side comparison with ES products from other parasites (including *B. malayi*), thus making it difficult to control for depth of sequencing coverage and sequence filtering criteria.

3.3.3 *Wolbachia*-derived RNA sequences detected in ES products from *L. sigmodontis*

Previously, it has been demonstrated that a small fraction of the proteins detected in pre-gravid and gravid females are derived from the endosymbiont *Wolbachia* (e.g. GroELS) (Armstrong, Babayan, et al., 2014). It is important to highlight that *Wolbachia* is found in most of the developmental stages within the filarial host, however its population undergoes expansion during the transition to the L4 stage and in young adults, particularly in the primordial reproductive tissues and germline cells (Fischer, Beatty, et al., 2011). Therefore, we next sought to examine whether any of the RNA sequences could derive from the endosymbiont. After discarding reads that mapped perfectly to either the *M. musculus* or *L. sigmodontis* genomes, we detected ~6X more high-quality reads mapping perfectly to the *Wolbachia* genome in ES products from adult stages (young and fully reproductive adults) compared to larval stages (**Table 3.4**). Moreover, we observed ~6X more high-quality reads mapping to *Wolbachia* in ES products from pgAF and gAF compared to jAM and AM (**Table 3.4**). Of all the lifecycle assessed, we detected most of the *Wolbachia*-specific high-quality reads in the ES products from pgAF (136,074 reads) compared to other lifecycle stages with a comparable number of high-quality reads. Taken together, these data suggest that the ES products from *L. sigmodontis* contain not only parasite-derived RNAs, but could also a small fraction of RNAs (<1.5% of the high-quality

reads) that align to the symbiont *Wolbachia*. Interestingly, these *Wolbachia*-derived sequences are more abundantly detected in ES products from pgAF and gAF, consistent with previous proteomic characterisations of the ES products from these lifecycle stages. Nevertheless, further and more thorough investigation is required to determine whether these RNA sequences are *bona fide Wolbachia*-derived RNA products, or are rather derived from other sources or contaminants.

Table 3.4 *Wolbachia*-derived RNAs detected in the secretome of larval and adult stages of *L. sigmodontis*

Secretome[1,2]	vL3s	hL3s	L4s	jAM	pgAF	AM	gAF	mf
Input reads	7,596,695 (10,720,435)	6,281,894 (5,501,542)	12,471,046 (12,744,268)	4,493,814 (5,501,542)	11,043,195 (12,509,154)	5,079,075 (9,489,535)	7,175,484 (9,950,704)	6,493,084 (7,823,877)
High-quality reads	6,571,666 (9,372,768)	2,895,861 (3,488,258)	7,840,378 (7,977,988)	2,895,861 (3,488,358)	8,317,514 (9,722,226)	3,849,365 (8,166,739)	6,577,228 (8,939,823)	5,207,592 (6,989,296)
***Wolbachia* Reads**	3,119 (4,259)	4,744 (4,919)	5,484 (5,933)	5,299 (5,563)	136,074 (187,290)	16,821 (34,229)	25,085 (55,548)	19,923 (26,994)
rRNAs	2,184 (3,007)	2,700 (2,721)	3,189 (3,350)	3,204 (3,369)	26,420 (34,438)	6,468 (18,102)	8,355 (14,992)	10,930 (12,928)
tRNAs	123 (148)	311 (316)	376 (405)	189 (209)	27,240 (38,412)	3,802 (6,363)	10,085 (22,747)	1,922 (2,502)
Other Rfam	135 (175)	710 (720)	737 (860)	442 (526)	15,384 (21,412)	1,662 (2,693)	1,102 (1,934)	1,142 (1,562)
Non-Rfam	677 (930)	1,022 (1,171)	1,182 (1,318)	1,463 (1,469)	67,030 (93,026)	4,888 (7,069)	5,542 (15,872)	5,929 (10,001)

[1]After mapping analysis, all the reads that mapped perfectly and unambiguously to the *Wolbachia* genome draft, and not to either to *L. sigmodontis* genome draft or the *M. musculus* genome, were retrieved and classified based on Rfam, as described in Chapter 2. The following samples and replicates were subjected to deep sequencing: vector-derived L3s (vL3s; $n = 2$), host-derived or "migratory" L3s (hL3s; $n = 2$), L4s ($n = 2$), juvenile males (jAM) and pre-gravid adult females (pgAF) at day 32 post-infection ($n = 2$, per sex), and adult males (AM; $n = 10$), gravid adult females (gAF; $n = 12$), and microfilariae (mf; $n = 8$). Values indicate range of number of reads (min to max) for each category.

[2] The median of the sequencing reads and the upper limit for the 75% of the total reads (in bracket) are reported for all the lifecycle stages tested

3.3.4 Differentially detected miRNAs in the secretome of *L. sigmodontis*

Next, we determined whether we can identify lifecycle stage miRNA "signatures" in the secretomes evaluated by deep sequencing. For this analysis, we focussed on AM, gAF, and mf, as it is important to identify biomarkers that 1) can inform about the presence and/or the relative adult/female worm burden in a patient and/or population, 2) discriminate between adults and mf worms. Similarly, these lifecycle stages co-exist within the host, so it becomes important to address whether we can discriminate between the presence of different stages based on the miRNA profile of their secretome. For statistical analysis, we employed a Bayesian statistical method called DESeq2 which, apart from performing well with relatively low number of biological replicates, also corrects for differential library size, (Love, Huber, et al., 2014). We used the 208 miRNAs identified by miRDeep2 (**Supplementary table 3.2**) as an input for analysis, without any previous filtering or normalisation. A total of 17 miRNAs were differentially detected in ES products based on pairwise comparisons, as shown in **Table 3.5**. Statistical analysis indicates that some miRNAs were significantly enriched in ES products of AM compared to gAF and mf (e.g. miR-5838), in adult worms (AM and gAF) compared to mf (e.g. miR-5360 and lin-4), as well as 11 miRNAs enriched in the secretome of gAF (e.g. miR-100a, miR-100b, among others) (**Table 3.5**). These differences were further confirmed by qRT-PCR (**Figure 3.4B**). Of the 17 differentially detected miRNAs, 9 miRNAs were within the top 20 most abundant miRNAs, whereas the remaining 6 miRNAs were not within the most abundant miRNAs (**Table 3.2 and Supplementary table 3.2**). This suggests that the method is not biased to only detect differences among abundant miRNAs. Taken together, our data suggests that a subset of the miRNAs detected in the secretome of *L. sigmodontis* can be confidently attributed to stage- and sex-enriched markers, mostly associated with gAF worms.

Table 3.5 Most differentially detected miRNAs in the secretome of *L. sigmodontis*

Enriched in adult females					
miRNA	**RNA Sequence (5' – 3')**	**RPM[A]**	**Log2 FC**	**Adj *p* value**	**Previously reported as excreted/secreted *in vitro* & *in vivo*? [B]**
miR-5364-5p	cgagguauuguuuauuggcuga	22,829.8	6.53	3.37E-07	*O. volvulus*[1], *O. ochengi*[1], *D. immitis*[2,3]
miR-240	uacuggccuuucaaacucuaga	3,857.49	6.08	5E-4	Not reported
miR-36c	cgguacaacguuucacgguagagc	7,598.27	5.18	3E-4	Not reported
miR-57-5p	uacccugugguaccgagcugugucu	11,53.21	4.18	1.4E-2	*D. immitis*[2,3]
miR-2860b	agcuguauuggcugugauaug	3,741.85	4.08	4.8E-2	Not reported
miR-239-5p	uuuguacuucggcuaaggugcug	5,017.06	3.45	4.4E-2	*O. ochengi*[1], *D. immitis*[3]
miR-86-5p	uaagugaaugcuuugccacagucu	671.6	3.33	4.8E-2	*L. sigmodontis*[4], *O. ochengi1, D. immitis*[2,3]
miR-44a-5p	cuggaugugcaucgugguuga	3,495.71	3.04	4.8E-2	Not reported
Bantam-a-3p	ugagaucauugugaaagcuauu	16,983.1	2.94	4.9E-2	*L. sigmodontis*[4], *O. volvulus*[1,5], *O. ochengi*[1], *D. immitis*[2,3]
miR-100d-5p	uacccguagcuccgaauaugugu	13,504.4	2.70	3.4E-2	*L. sigmodontis*[4], *O. volvulus*[1,2], *O. ochengi*[1,6], *D. immitis*[2,3], *L. loa*[5]
miR-100a	aacccguaguuucgaacaugugu	200,810	2.17	5E-3	*L. sigmodontis*[4], *O. volvulus*[1,2], *O. ochengi*[1,6], *D. immitis*[2,3], *L. loa*[5]
Enriched in males					
miRNA	**RNA Sequence (5' – 3')**	**RPM[1]**	**Log2 FC**	**Adj *p* value**	**Previously reported *in vitro* & *in vivo*? [B]**
miR-5838	ugaguauuuucgguuucgcauc	5,319.43	5.50	3.2E-4	*O. ochengi*[1]
miR-2426	gaggaagugaugaggagcc	4,921.58	4.76	5.3E-4	Not reported
miR-9146-5p	gccuggaugaaucucggug	29,753.3	4.36	3.3E-6	Not reported
miR-8319-3p	gaauuagcucgugcgguacggc	8,175.41	3.98	3.2E-4	Not reported
Enriched in adult stages					
miRNA	**RNA Sequence (5' – 3')**	**RPM[1]**	**Log2 FC**	**Adj *p* value**	**Previously reported *in vitro* & *in vivo*? [B]**
miR-5360-5p	acgaaucgucgaaucgga	1,838.3	4.61	4.4E-2	*O. ochengi*[1], *D. immitis*[2,3]
Lin-4-5p	ucccugagaccucugcugcga	108,025	3.15	3.4E-2	*L. sigmodontis*[4], *O. volvulus*[1,2], *O. ochengi*[1,6], *D. immitis*[2,3], *L. loa*[5]

[A] RPM = reads per million. miRNAs with >7,000 reads per million were classified in the top 20 most abundant miRNAs. Using this classification, from 17 differentially enriched miRNAs, 9 miRNAs were amongst the top 20 most abundant miRNAs, whereas the remaining 6 miRNAs were lowly abundant.

[B] Superscripts indicate references: 1) (Quintana, Makepeace, et al., 2015), 2) (Tritten, Burkman, et al., 2014), 3) (Tritten, Clarke, et al., 2016), 4) (Buck, Coakley, Simbari, McSorley, et al., 2014), 5) (Tritten, Neill, et al., 2014)

3.3.5 Comparison of the secretome of pre-gravid versus gravid adult female worms *in vitro*

The data presented thus far indicates that gAF worms secrete a myriad of miRNAs, many of which are enriched in this developmental stage but not in other stages (AM and/or mf). One of the most outstanding traits of gAF worms is their reproductive capacity, where a single female worm can secrete thousands of mf per day (Ziewer, Hübner, Dubben, Hoffmann, Bain, Martin, Hoerauf, Specht, et al., 2012). Therefore, one plausible hypothesis is that the secretion of female-enriched miRNAs is associated with reproductive status ("virgin" females vs. "gravid" females). To test this hypothesis, we compared the ES products from "virgin" females (pgAF) to the fully reproductive adults (gAF). *In silico* analysis using DESeq2 suggests that some of the female-enriched miRNAs, including one of the miR-10 family member (miR-993-3p), are strongly associated with gAF worms, whereas other miRNAs (lin-4 and miR-278a-5p) are more highly detected in pgAF (**Figure 3.7A**). Nevertheless, the differences were not significant between these samples by qRT-PCR, at least for miR-993 and lin-4 (**Figure 3.7B**), due perhaps to technical limitations associated with the detection of lowly abundant miRNAs by qRT-PCR, and thus could not validate the results from DESeq2 analysis. It is also worth noting that we were limited with the number of replicates that were obtained for the pgAF (n = 2), and further replicates will be necessary to clarify if there are differences in the secretome of female worms before and after they actively produce mf.

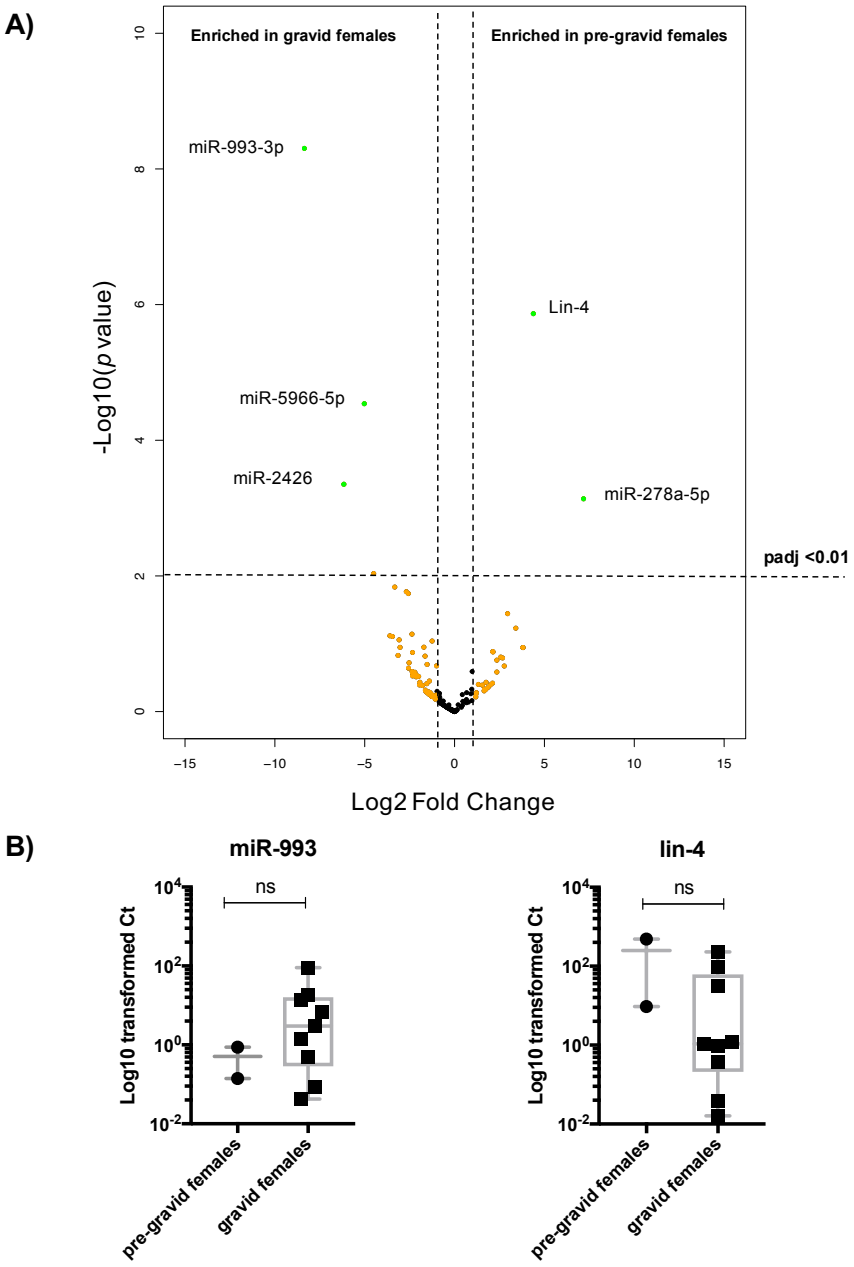

Figure 3.7 Volcano plot of miRNAs differentially detected in ES products comparing pre-gravid female worms vs. gravid adult females. A) The volcano plot shows fold changes (Log2 scale) and adjusted *p* values for individual miRNAs determined by DESeq2 analysis. The horizontal dotted line represents the chosen cut-off (*padj* < 0.01) to determine significantly different miRNAs between juvenile and gravid females, whereas the vertical dotted lines represent Log2FC >1 or <-1. Orange dots represent miRNAs with Log2FC > 1 or <-1, whereas green dots represent miRNAs with Log2FC > 1 or <-1 and *padj* <0.01. Gravid female worms were used as a reference group for analysis. B) qRT-PCR validation of the *in-silico* prediction of the differential miRNA composition of the secretome from pre-gravid females vs. adult gravid females (ns = not significant; Mann-Whitney test)

3.3.6 Gravid adult female worms secrete extracellular vesicles (EVs) containing miRNAs *in vitro*

We next sought to determine whether the signal of miRNAs enriched in gAF secretome was associated with extracellular vesicles (EVs). To assess this, we pooled equivalent volume of ES products from gAF harvested at 24, 48 and 72h in culture and purified EVs using the cold acetone precipitation (Gallart-Palau, Serra, et al., 2015). This approach enables the separation of soluble proteins by precipitation with acetone (protein pellet), leaving a supernatant enriched in organic-soluble, lipid-containing EVs (supernatant) (Gallart-Palau, Serra, et al., 2015). TEM analysis revealed the presence of vesicle-like structures ~50-100 nm in diameter in the supernatant fraction of the ES products from gAF worms but not in the protein-enriched pellet fraction or in the negative control, consistent with previous reports of nematode-derived EVs (**Figure 3.8A & B**). Furthermore, we confirmed the size of these vesicles by nanoparticle tracking analysis (NTA) to be between 50 and 112 nm in length (average = 87 nm), and the concentration was 8x10^7 particles/mL (**Figure 3.9A**). Based on qRT-PCR, the signal of several miRNAs enriched in the secretome of gravid female worms was higher in the fraction containing the EVs when compared to the vesicle-depleted (pellet) fraction (**Figure 3.9B**), thus suggesting that these miRNAs are likely to be released in association with EVs *in vitro*, corresponding with previous studies of *H. polygyrus* adult worms (Buck, Coakley, Simbari, McSorley, et al., 2014).

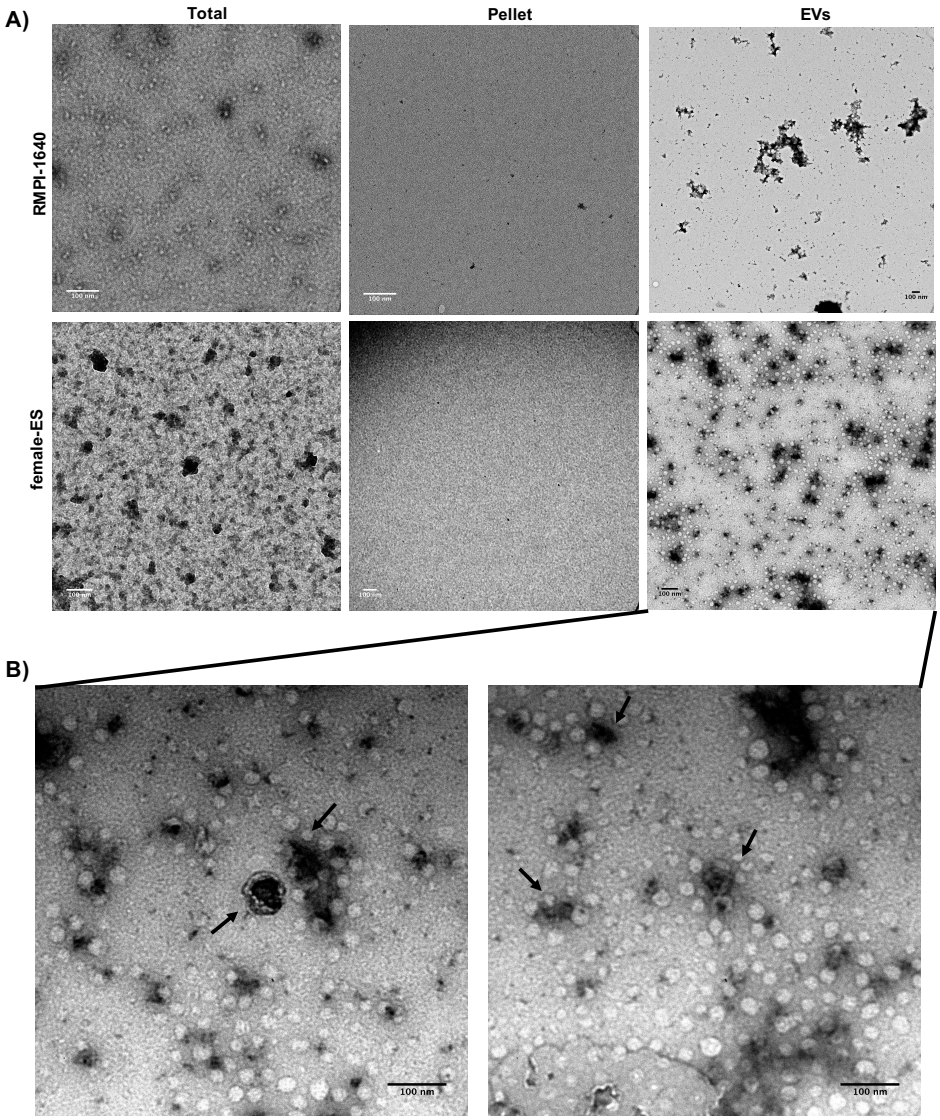

Figure 3.8 Gravid adult female worms secrete extracellular vesicles *in vitro*. A) Extracellular vesicles were purified from pooled ES products by Protein Organic Solvent Precipitation (PROSPR) using cold acetone. RPMI-1640 media was included as negative control. Transmission electron microscopy of three fractions after purification (Total, pellet and EVs) in the EVs are readily detected in the "EVs" fraction. B) Zoom-in of the EVs fraction, were arrows indicate potential EVs. Bar scale = 100 nm.

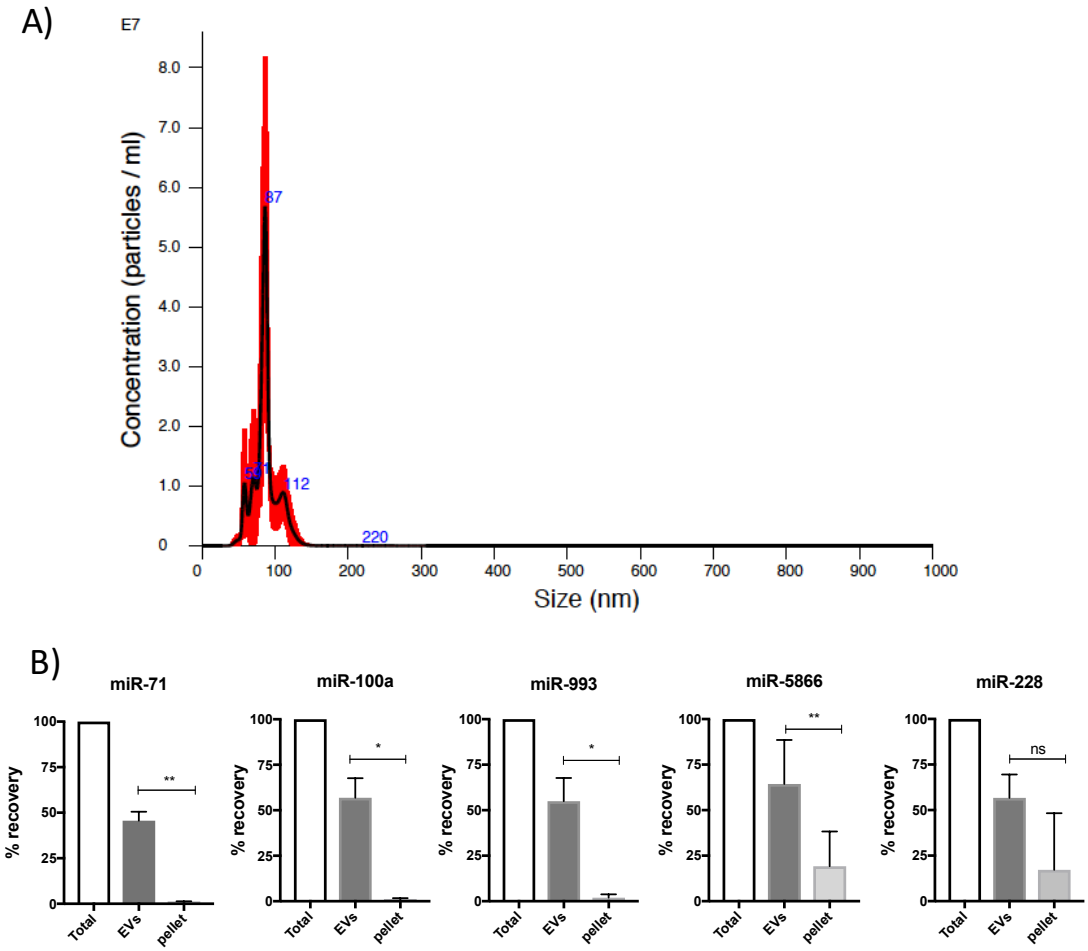

Figure 3.9 Gravid adult female-enriched miRNAs are mainly released within extracellular vesicles *in vitro*. A) The quantification and size distribution of EVs obtained from the ES products from gravid adult female worms were confirmed by Nanoparticle Tracking Analysis (NTA) and, B) When using equivalent amounts of material for RNA extraction and analysis by qRT-PCR, we observed that the signal of several female-enriched miRNAs were found to be enriched in the fraction containing the EVs but not in the fraction depleted of EVs (* $p<0.05$; ** $p< 0.005$; ns = not significant; *t* test).

3.4 Summary

- 208 mature miRNAs are found in the secretomes of *L. sigmodontis*.
- Of the 208, 26 are novel miRNA candidates with no homology to other nematode miRNAs. Based on structural features, four of these were classified as *bona fide* Dicer-derived miRNAs.
- Potential *Wolbachia*-derived RNA sequences were abundantly detected in the secretome of pgAF and gAF.
- 17 miRNAs were differentially detected in the secretome of adult and mf stages (Log2Fold change >1, *padj* <0.05), with 11 being associated with gAF worms.
- Several members of the miR-10 family (miR-100a, miR-100d and miR-993), which are the most abundant miRNAs detected in the secretome of *L. sigmodontis*, are detected in gAF. Other miRNAs exhibited a more ubiquitous secretion pattern and were consistently detected in ES products of all the developmental stages tested (e.g. miR-71, miR-92, miR-34).
- Gravid adult female worms secrete extracellular vesicles of around 50-110 nm in length that are associated with the miRNAs *in vitro*.

3.5 Discussion

The overarching goal of this chapter was to determine whether the secretion of small RNAs, with an emphasis on miRNAs, is developmentally regulated in filarial parasites. A second goal was to statistically assess whether a group of miRNA could be confidently assigned as stage- and/or sex-specific markers. The release of excretory/secretory (ES) products by parasitic nematodes has been extensively studied (Hewitson, Grainger, et al., 2009; Hoerauf, Satoguina, et al., 2005), and it is recognised that these products provide powerful mechanisms by which these parasites can effectively manipulate their host's immune system to establish an infection. However, the complexity of these ES products has recently been re-evaluated with several lines of enquiry now indicating that they also contain extracellular vesicles containing components of the RNAi machinery, thus opening the possibility that the parasite can also interfere with gene expression within host cells (Coakley, Maizels, et al., 2015). Nonetheless, the information regarding the RNA cargo of EVs has only been reported in individual developmental stages of different parasites (Buck, Coakley, Simbari, McSorley, et al., 2014; Tritten, Clarke, et al., 2016; Zamanian, Fraser, Agbedanu, & Harischandra, 2015). A thorough and robust side-by-side comparison of both larval and adult stages is still lacking. It is important to mention that a separate study evaluating the miRNA secretion by individual replicates of several developmental stages in the clade III heartworm *Dirofilaria immitis* was published during the preparation of this PhD thesis (Tritten, Clarke, et al., 2016). This study will be used as a point of reference for comparisons as *D. immitis* belongs to the same nematode clade as *L. sigmodontis,* and thus provides an opportunity to contextualise and validate our results. To broadly characterise the overall small RNA population in ES products, we first decided to profile the total RNA obtained from these samples using analysis by a Bioanalyzer. This analysis revealed that the *in vitro* ES products from all the developmental stages examined in this study contain small RNA of between 20-30 nt in length and "longer" RNAs of between 40-60 nt in length (**Figure 3.1B**). It is important to stress that we only focussed in the shorter RNA populations (20-30 nt) for the studies presented in here, but did not study the longer RNA population (40-60 nt) also noted in the Bioanalyzer assay. We chose the shorter RNA population because we anticipated it should contain small RNA molecules such as miRNAs. The characterisation of the longer RNA population may be also

important as it may hold interesting RNA candidates to understand pathogen-to-host interactions as well as potential novel biomarker candidates. This aspect certainly merits further investigation.

Next, we prepared small RNA libraries from total RNAs, which rendered PCR products of varying sizes. We rationalised that given the size of mature miRNAs (21-24 nt in length), we would focus on PCR products of between 140 to 160 bp in length, to account for inserts of between 20 to 40 nt in length (described in Chapter 2). We pooled equimolar concentrations of these libraries and subjected these to next generation sequencing using the Illumina HiSeq platform. Interestingly, at a similar depth of coverage, we consistently observed a greater proportion of sequences that mapped to the *L. sigmodontis* genome in ES products from both pgAF and gAF when compared to other developmental stages (**Figure 3.2B and Table 3.1**). Similar observations in terms of diversity and richness of the secretomes of both pgAF and gAF worms have been previously documented in proteomic studies of *L. sigmodontis* (Armstrong, Babayan, et al., 2014).

We also noted that the RNA sequences identified in the secretomes tested here did not derive exclusively from *L. sigmodontis,* and a fraction of the high-quality reads mapped unambiguously to the *Wolbachia* genome draft. More specifically, there was a greater proportion of *Wolbachia*-specific sequences in the secretome of pgAF, which were on average 3X more abundant than in the secretome of gAF and AM (**Table 3.4**). This observation is consistent with previous reports, which have shown that this endosymbiont undergoes extensive multiplication in the lateral cords and female reproductive tissue of L4s and pgAF during development (Fischer, Beatty, et al., 2011). Moreover, *Wolbachia* proteins (e.g. GroELS) have also been detected in the secretome of both pgAF and gAF *L. sigmodontis* worms but not in the ES products from other developmental stages, including AM and mf (Armstrong, Babayan, et al., 2014). These results suggest that *Wolbachia* may exist in the uterine tissue and/or fluids from *L. sigmodontis* female worms, representing a likely release route for this material *in vitro*, although this remains speculative, as other secretion routes (e.g. secretory pore, cuticle, etc.) are also plausible routes for secretion and release (Armstrong, Xia, et al., 2016). However, it is important to emphasise that bacterial contaminants have often been reported in deep sequencing studies (Laurence, Hatzis, et al., 2014; Strong, Xu, et al., 2014), and our analysis does not rule out the possibility that these might be bacterial contaminants and, therefore, may not

represent a true biological phenomenon. Further and more thorough analyses to identify common bacterial contaminants in our libraries will be necessary to robustly determine whether these are derived from *Wolbachia*.

In terms of the *L. sigmodontis* RNA sequences, our small RNA libraries were dominated by rRNAs, tRNA fragments as well as miRNAs. These results are consistent with previous findings in several parasites, including parasitic nematodes (Buck, Coakley, Simbari, McSorley, et al., 2014) but also in pathogenic flukes such as *S. mansoni* (Nowacki, Swain, et al., 2015) and *S. japonica* (Zhu, Wang, et al., 2016). We decided to explore the miRNA content of the ES products further and used the package miRDeep (Friedländer, Mackowiak, et al., 2012), to identify known and novel miRNAs. A total of 208 miRNAs were detected in all the samples analysed by deep sequencing, as opposed to a total of 131 mature miRNAs previously reported in the secretome of *D. immitis* (Tritten, Clarke, et al., 2016). These differences can relate to multiple factors, including different sample preparation, different genome annotations, analysis criteria and cut-offs used to discriminate between high and low abundant miRNAs. For example, we required for a miRNA to be detected in at least two biological replicates, in at least one developmental stage, at >2 copies, whereas in previous studies it was required to be found in at least one developmental stage and present at >10 copies (Tritten, Clarke, et al., 2016). In *D. immitis*, a total of 12 highly abundant miRNAs were detected as common to all the developmental stages tested; amongst these, several are likely of parasite origin: miR-92, miR-57, miR-36a, miR-100a, miR-100b, miR-100d, lin-4, miR-71-5p, miR-279-3p, let-7-5p, whereas three (let-7-5p, PC-5p-799_1592 and PC-3p-389-2939) were also found in the genome of dogs, the natural host of *D. immitis* (Tritten, Clarke, et al., 2016). We also detected several of these miRNAs within the top 20 most abundant miRNAs in the combined secretome of *L. sigmodontis*, including miR-92, miR-71, miR-100a and lin-4 (**Table 3.2**). This suggests similarities in the miRNAs that are robustly secreted by filarial parasites.

The miRNA profiling of the secretomes assessed in this study provides important insights into the differences between developmental stages. One interesting observation is that the secretome of infective L3s contain miRNAs not only reported in this study but also previously shown in the same stage of the human pathogen *B. malayi,* including miR-71, miR-92, lin-4 and miR-100a (Zamanian, Fraser, Agbedanu, & Harischandra, 2015). This could imply important and potentially specific

interactions established by the infective stage during invasion of the vertebrate host, where the L3s-derived EVs have been demonstrated to be internalised and to induce a classically activated status in macrophages (Zamanian, Fraser, Agbedanu, & Harischandra, 2015). On the other hand, during the chronic stage of the infection, both adult worms and the mf co-exist within the vertebrate. Our findings suggest that gAF secrete several female-enriched miRNAs that may be important for long-lasting and sustained interactions with the vertebrate host. It is therefore tempting to speculate that the miRNAs released by gAF (or adult worms) are central for any potential parasite-to-host interaction mediated by miRNAs However, this cannot be supported by the results presented in here and merit further investigation.

From a diagnostic standpoint, it is important to understand if we can discriminate adult worms (or even gAF worms) from mf based on the miRNA profiles of their secretomes. We demonstrated that a total of 11 miRNAs are enriched in the secretome of gAF worms, and offer the possibility to further understand if these female-enriched miRNAs can be used as biomarkers for filarial infections (discussed in chapter 5). Some examples of the female-enriched miRNAs are miR-100a and miR-100d which belong to the broadly conserved miR-10 family (Tehler, Høyland-Kroghsbo, et al., 2011). Other miRNAs are known to be exclusively expressed by filarial nematodes. For example, miR-5364 is a novel member of the let-7 family that is found exclusively in filarial nematodes and it has been shown to be abundantly expressed in post-infective stages (including adult worms) and is thought to mediate developmental transitions (Winter, Gillan, et al., 2015). The differences in the miRNA composition detected in the secretomes of *L. sigmodontis* gAF compared to mf are consistent with the extraordinary secretory capacity of gAF worms. Interestingly, a further *in silico* comparison between pre-gravid versus gravid female worms suggested potential differences between these two stages, based on the signal of miR-993-3p (enriched in gravid adult female worms) and lin-4 (enriched in pre-gravid female worms) but we failed to validate this. One caveat of these studies is the low number of biological replicates we obtained from pgAF (n = 2), compared to gAF worms (n = 12). Further experiments are required to robustly detect specific differences between “virgin” and gravid females. This information is relevant to delineate a subset of extracellular miRNAs that can be confidently assigned to reproductively active female worms.

Lastly, the potential role of the parasite-derived miRNAs and EVs during infection are yet to be fully elucidated. In this regard, several reports have shown that parasite-

derived miRNAs could in theory target messenger RNAs in host cells, and it has been shown that several of the most abundant miRNAs and EVs secreted by parasitic nematodes (including miR-71, let-7 and miR-239) can regulate genes important for innate immunity, such as *il33r* and *dusp1* (Buck, Coakley, Simbari, McSorley, et al., 2014). On the other hand, the function of most of the miRNAs is not understood, and the role of the extracellular miR-10 miRNA family is not clear. It is thought that several members of this family act cooperatively with miR-196b to regulate expression of the Homeobox (*hox*) gene family during early haematopoietic cell development, inside the nematode (O'Connell, Rao, et al., 2010; Tehler, Høyland-Kroghsbo, et al., 2011). These observations may suggest that, at the molecular level, gravid adult female worms secrete a plethora of miRNAs that could interfere with the expression of host genes important for immune homeostasis and activation, with important consequences not only for the parasite-to-host crosstalk but also for further diagnostic applications.

Chapter 4: **Effect of anthelminthic chemotherapy on miRNA secretion by filarial gravid adult female worms**

4.1 Introduction

Filariases comprise a group of chronic infections that result in the development of highly debilitating symptoms, with serious socio-economical and health burdens (Taylor, Hoerauf, et al., 2010). At present, there are no vaccines available to prevent these infections (Hotez, Strych, et al., 2016), and they are treated with anthelminthic chemotherapy (Panic, Duthaler, et al., 2014). Other strategies, such as vector control, are also of importance (Erickson, Thomsen, et al., 2013; Mackenzie, Homeida, et al., 2012). Therefore, mass drug administration (MDA) programmes, currently underway in Africa and Latin America (Coffeng, Stolk, et al., 2013), aim to interrupt transmission and diminish morbidity by administering anthelminthic compounds (Babalola, 2011; Babayan, Allen, et al., 2012; Utzinger, Becker, et al., 2012). Since the late 1980's, control of onchocerciasis has primarily relied on the administration of Ivermectin (IVM) (Babalola, 2011; Murdoch, Asuzu, et al., 2002; Taylor, Hoerauf, et al., 2010). Conversely, therapeutic regimes for Lymphatic Filariasis (LF) includes annual, single-dose combinations of either IVM or Diethylcarbamazine (DEC) alongside Albendazole (ABZ) (Fischer, King, et al., 2017). Most of these anthelminthic therapies have a potent effect on killing microfilariae (microfilaricidal activity), whereas very limited treatment options actually affect the viability of adult worms (macrofilaricidal activity) (Panic, Duthaler, et al., 2014). Compounds such as Doxycycline (DOX) are thought to target the *Wolbachia* endosymbiont, and have been shown to have macrofilaricidal activity (Debrah, Specht, et al., 2015; Panic, Duthaler, et al., 2014).

4.1.1 Glutamate-gated chloride channels and the mode of action of Ivermectin

Ivermectin (IVM) belongs to the group of macrocyclic lactones (ML) that comprise one of the few classes of drug used to treat filarial infections (Panic, Duthaler, et al., 2014; Wolstenholme, Maclean, et al., 2016). They selectively paralyse the parasite by

increasing muscle Cl^- permeability through directly binding to glutamate-gated chloride (GluCl) channels (Laing, Gillan, et al., 2017; Martin, 1997). The GluCl channels are members of the membrane-bound, ligand-gated ion channels, composed of two (α and β) subunits (Wolstenholme, & Rogers, 2005). The receptor is composed of four transmembrane domains (M1 to M4), with both the C and N terminal located in the extracellular space, alongside several loops connecting the transmembrane domains (Wolstenholme, 2012) (**Figure 4.1**) Expression of the α subunit alone results in the appearance of an IVM-gated channel, whereas co-expression of both α and β subunits lead to the formation of an IVM-sensitive, glutamate-gated channel (Wolstenholme, & Rogers, 2005). In *C. elegans*, there are six genes encoding α and β subunits of the GluCl channel (Williamson, Walsh, et al., 2007). Of these, the *avr-15* and *avr-14* genes produce two α subunits by alternative splicing to form the GluClα2A and GluClα2B isoforms, and the GluClα3A and GluClα3B isoforms, respectively (Laing, Gillan, et al., 2017; Wolstenholme, & Rogers, 2005). Gene-wise comparisons between the free-living nematode *C. elegans* and other parasitic nematodes have shown a very distinctive pattern in the evolution of the GluCl channel across nematodes clades. Interestingly, comparisons between the free-living *Caenorhabditis elegans* and the parasitic nematode *Haemonchus contortus* (both belonging to clade the V) have identified *avr-14* homologs in both species, but not for all the repertory of GluCl genes described in *C. elegans* (Wolstenholme, & Rogers, 2005) (**Figure 4.1A**). Moreover, the *avr-14* gene (and its two splicing products) is conserved across clades (including several clade III nematodes such as *D. immitis* and *O. volvulus*), whereas other genes (e.g. *glc-1, glc-3* and *avr-15*) were only found in *C. elegans* (Williamson, Walsh, et al., 2007; Wolstenholme, & Rogers, 2005) (**Figure 4.1A-C**).

4.1.2 *In vitro* and *in vivo* effects of IVM on filarial nematodes

The effects of IVM on the nervous system on some nematodes, including *Ascaris spp.*, are well-characterised, and it has been demonstrated that this compound inhibits pharyngeal pumping and impairs nematode feeding (Laing, Gillan, et al., 2017; Martin, 1997). However, the mode of action of IVM against filarial nematodes has been widely disputed, and the exact mechanism underlying this process remains controversial, as there is conflictive evidence regarding the *in vitro* effect of this

compound in several parameters, including survival, motility and reproduction (Reviewed by Carithers, 2017). One hypothesis suggests that this compound acts synergistically with the immune system to mediate worm killing (Carithers, 2017). In this scenario, IVM impairs the capacity of parasitic nematodes to secrete immunomodulatory effectors that are otherwise require to dampen the immune response against them (Carithers, 2017). Consistent with this hypothesis, a recent study has demonstrated that the GluCl channels targeted by IVM are specifically detected surrounding the Excretory/Secretory (ES) apparatus in *B. malayi* microfilariae (mf), which is a specialised organ responsible for the release of soluble material into the milieu (Moreno, Nabhan, et al., 2010). Through a combination of biochemical and immunofluorescence methods, it was demonstrated that IVM blocks the *in vitro* secretion of proteins by mf in a time- and dose-dependent manner, including immunomodulatory proteins typically found in the ES products of mf (e.g. venom allergen-like 1 protein (VAL-1), tumour protein-like protein (TCTP) and Macrophage migration inhibitory factor-1 (MIF-1), among others) (Moreno, Nabhan, et al., 2010). Similar observations have been reported in *D. immitis*, where *in vitro* exposure with IVM concentrations ranging from 0.01 to 0.1 mM leads to increase binding of peripheral blood mononuclear cells and neutrophils to the *D. immitis* mf, thought to be due to the incapacity of the mf to secrete immunomodulatory molecules (Vatta, Dzimianski, et al., 2014). However, the macrofilaricidal (adult worm killing) effect of IVM remains controversial. In adult filarial worms, IVM is known to induce sterility, although the exact mechanism remains elusive (Li, Rush, et al., 2014a). Based on *in situ* hybridisation studies, the expression of the IVM receptor subunit *avr-14* was highly detected in the reproductive tissue (Li, Rush, et al., 2014a), thus leading to the hypothesis that IVM preferentially acts upon the reproductive organ, explaining its sterility effects observed *in vitro* and *in vivo* (Bronsvoort, Renz, et al., 2005; Tompkins, Stitt, et al., 2010) (**Figure 4.2**). The sterilising effect of IVM on adult female worms was further confirmed by RNA sequencing (Ballesteros, Tritten, ONeill, et al., 2016; Laing, Gillan, et al., 2017). At the transcriptomic level, treatment of *B. malayi* gravid adult females (gAF) with physiological doses of IVM (~100 nM) induces a strong global dysregulation of genes with gene ontology (GO) terms associated with meiosis, calcium signalling and embryogenesis (Ballesteros, Tritten, ONeill, et al., 2016; Laing, Gillan, et al., 2017). Interestingly, the effects of IVM on the *B. malayi* transcriptome seems to change in a dose-dependent manner (Ballesteros,

Tritten, ONeill, et al., 2016). At low concentrations (100 nM), most of the dysregulated genes were associated with cuticle remodelling, growth, locomotion and nematode larval development (Ballesteros, Tritten, ONeill, et al., 2016). Conversely, at higher concentrations of IVM (1 μM), there was an enrichment of dysregulated genes associated with fatty-acyl-CoA binding, structural constituents of cuticle, double-strand break repair via non-homologous end joining, cytokinesis and reproduction, which is consistent with the sterilising effects reported for IVM in several filarial nematodes (Ballesteros, Tritten, ONeill, et al., 2016). These observations strongly indicate that IVM has potent effects on the parasite physiology that extend beyond reproduction, including motility, viability and secretion. Indeed, treatment with low concentrations of IVM induces paralysis *in vitro* in studies with *B. malayi* adult males (AM) and gAF (Tompkins, Stitt, et al., 2010). In gAF, an effect in motility with low concentrations of IVM (0.15 μg/mL = ~0.2nM) was observed after 3 days of exposure, whereas higher drug concentrations (170 μg/mL – 5000 μg/mL = 0.2 mM - ~5.7 mM) induced paralysis in gAF as soon as 1 day post-exposure (Tompkins, Stitt, et al., 2010). However, the effects are not similar between sexes, as motility declined faster in AM after 24h compared to gAF, but in both cases they did not recover from treatment and were considered dead after 8 days of exposure to IVM (Tompkins, Stitt, et al., 2010). Conversely, motility of *B. malayi* mf was only impaired at high drug concentrations (>1.2 mg/ml = ~1.4 mM). Apart from the effects of IVM on gAF motility, the fertility was also impaired in *in vitro* studies, with the number of released mf by gAF declining progressively in a dose- and time-dependent fashion (Tompkins, Stitt, et al., 2010). Nevertheless, the main caveat of this study is that the concentrations used were far higher than the ones achieved in plasma of patients treated with IVM (~50 ng/mL = ~50 pM) (Baraka, Mahmoud, et al., 1996; Canga, Prieto, et al., 2008), once again demonstrating the discrepancies between *in vitro* and *in vivo* data on studies regarding the effect of IVM on adult filarial nematodes. Despite these discrepancies, one common observation is that IVM impairs the reproductive capacity of filarial adult female worms, demonstrated at the transcriptional level but also in the overall mf output (Ballesteros, Tritten, ONeill, et al., 2016; Tompkins, Stitt, et al., 2010). In the previous result chapter, we have demonstrated that gravid adult female worms secrete a plethora of miRNAs enriched in the secretome of this lifecycle stage when compared to adult males and mf.

However, the precise tissue origin of these female-enriched miRNAs remains unclear. Our hypothesis is that the uterine fluid is a likely source of some of the miRNAs detected in the secretome of adult female worms. Here, using IVM to induce an impaired reproductive capacity in female worms, we attempt to address whether the reproductive organs are involved in the secretion of miRNAs. It is important to mention that there is no previous information on the effect that anthelminthic chemotherapy has upon small RNA release in filarial nematodes, and these studies constitute an effort to shed light into this. To test our hypothesis, we first studied the temporal dynamics for both EV and miRNA secretion from gravid adult females, as well as the worm tissue expression of both IVM receptor and miRNAs enriched in the secretome of gAF. We then examined whether an impairment on the reproductive capacity of adult female worms mediated by IVM is also accompanied by a reduction in the secretion of miRNAs.

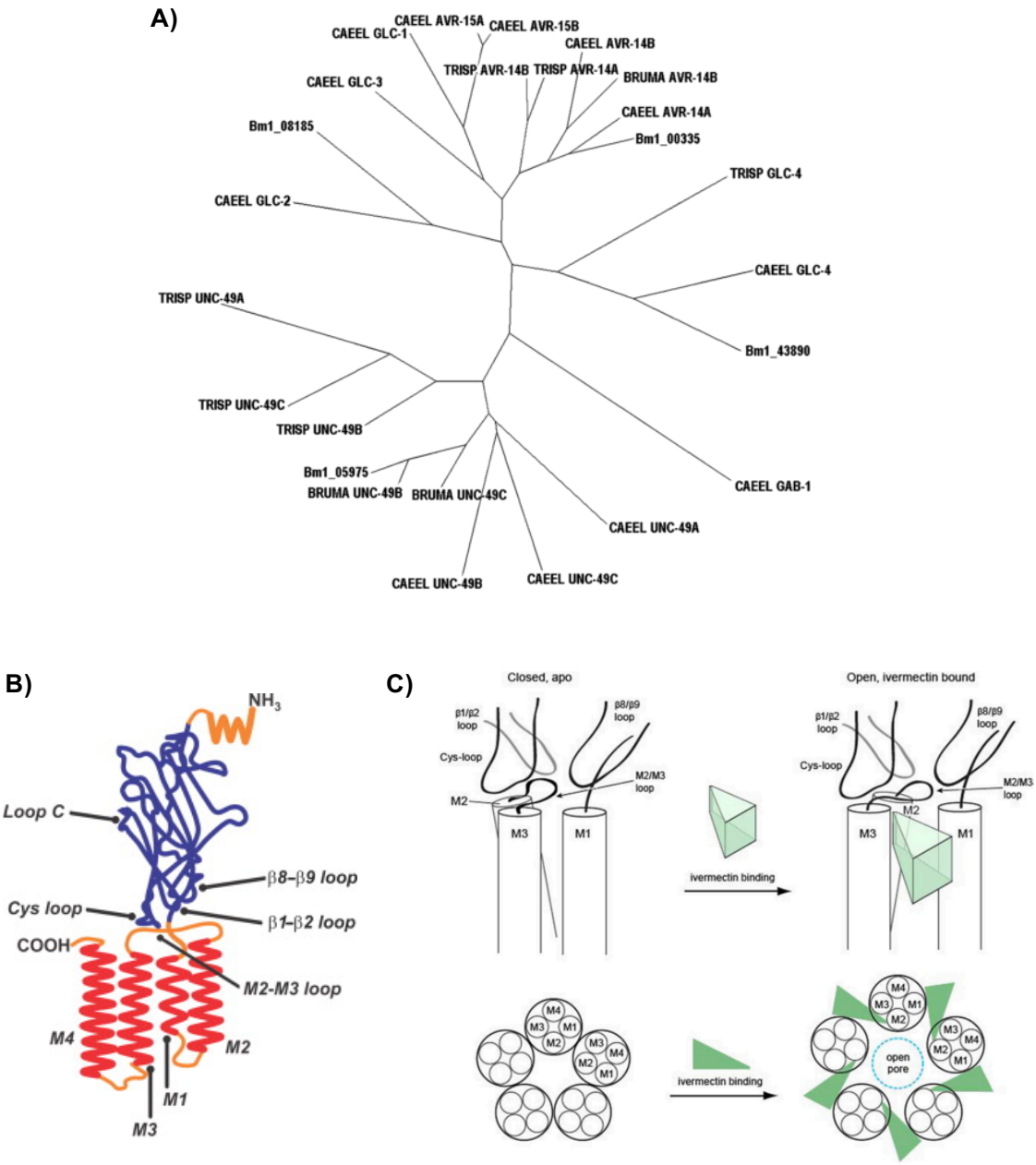

Figure 4.1 Mechanism of action of IVM. A) Boot-Strapped neighbour-joining tree of the glutamate and GABA-gated chloride channel sequences of the clade-III *B. malayi* (BMA), clade-I *T. spiralis* (TRISP), and clade-V *C. elegans* (CAEEL) (taken from: Williamson, Walsh, et al., 2007). B) Illustration of the structure of a Cys-loop ligand-gated ion channel (e.g. GluCl channel), displaying the extracellular moiety (N- and C-terminal, M2-M3 loop, etc.), and the four transmembrane domains (M1 to M4). C) Side and top view of the putative binding sites of IVM. In this model, IVM binds between the M1 and M3 membrane-spanning domains of adjacent subunits, and tends to induce opening of the channel by interfering with the position of the subunits (taken from: Wolstenholme, 2012)

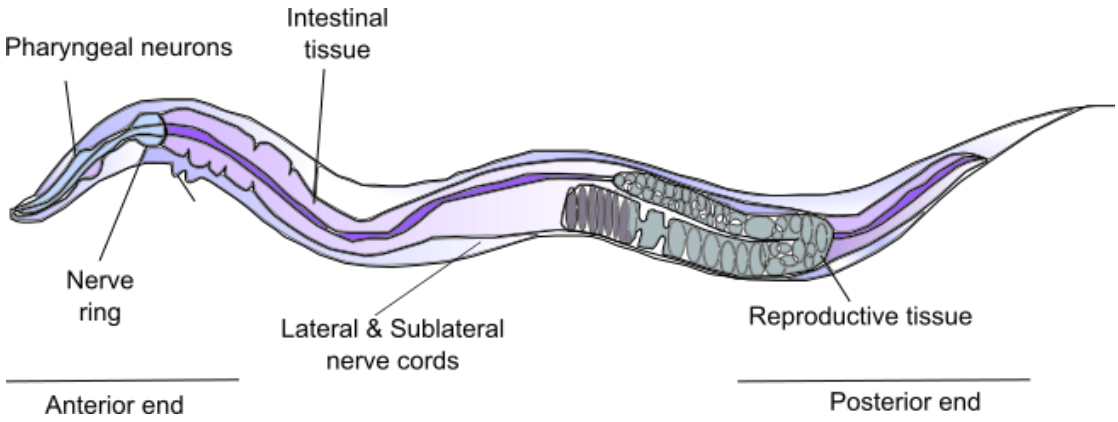

Figure 4.2 Proposed tissues that are likely to be targeted by IVM. The illustration depicts an adult female worm. Studies in *C. elegans* and several parasitic nematodes have demonstrated that IVM affects motility and feeding behaviour. These observations correlate with electrophysiological studies on the depolarizing effects of IVM on synaptic and pre-synaptic neurons (Wolstenholme, 2012), mostly localized in the anterior end, and along the soma of the worm (nerve cords). Given its sterilizing effects, it is thought that IVM also targets the reproductive tissues (Ballesteros, Tritten, ONeill, et al., 2016; Bronsvoort, Renz, et al., 2005)**.**

4.2 Specific aims

1. To examine the temporal dynamics of miRNA and extracellular vesicle release by gAF worms
2. To examine the effect of IVM treatment on miRNA release by gAF worms *in vitro*
3. To determine whether the reproductive organs and/or uterine fluid is a likely source of the secreted miRNAs detected in the secretome of gAF worms

4.3 Results

4.3.1 Temporal dynamics of EV and miRNA release by gravid adult female worms *in vitro*

In chapter 3, we demonstrated that gAF female worms secrete a myriad of miRNAs, some of which are female-enriched miRNAs, in association with EVs *in vitro*. Here, our main goal is to determine the effects of IVM on miRNA release from gravid adult female worms, and to determine whether the female-enriched miRNAs derive from the reproductive tissue. However, little is known about the temporal dynamics of EV and small RNA secretion by parasitic nematodes. This information is essential for studies where a time-dependent hypothesis (e.g. effect of IVM on miRNA secretion over time) is tested. Therefore, our first goal was to determine whether the release rate of EVs and miRNAs changes over the short time course when the gAF are in culture (up to 72 hours). We prepared small RNA libraries from total RNA purified from ES products from gravid adult females collected during the first 24 hours or after 2 days (48-72 hours) *in vitro*, as described in chapter 2. Alongside this, we also monitored the viability of these worms with the MTT assay, as described in other studies (Lakshmi, Joseph, et al., 2010; Rao, Mehta, et al., 1991; Voronin, Bachu, et al., 2016), to help correlate any changes in miRNA and EV release with the viability *in vitro*. To measure the particle concentration and size, we used a nanoparticle tracking system that, based on the pore size of the instrument, allow use to accurately measure particles between 70 and 420 nm in length (Coumans, Pol, et al., 2014). Therefore, particles of other sizes could not be screened with this approach. Our data show that gAF worms were viable over 3 days *in vitro* (**Figure 4.3A and B**), but the amount of EVs (70-100 nm in length) significantly decreased ~10X between 0-24h and 48-72h (**Figure 4.3C**), without significant changes in the EV size (**Figure 4.3D**). Similar results have been previously reported in EVs derived from *B. malayi* L3s, where the release rate was reported to decay in a time-dependent manner (Zamanian, Fraser, Agbedanu, & Harischandra, 2015). We then purified total RNA and prepared small RNA libraries from 5 biological replicates of ES products harvested at early (0-24h) and later (48-72h) time points, as described in chapter 2. Libraries were sequenced at a similar depth of coverage at these two time points (8,777,156 reads at 0-24h vs. 11,625,404 reads at 48h-72h) (**Supplementary table 4.1A and Table 4.1**). After trimming the 3' adapter, on average we obtained a total of 7,122,913 and 8,395,193 high quality reads at 0-24h and 48-72h, respectively (**Supplementary table 4.1A and**

Table 4.1). Interestingly, we noted a ~2.2X decrease in the number of *L. sigmodontis*-specific reads over time (21.44% of the high-quality reads at 0-24h vs. 9.65% of the high-quality reads at 48-72h) (**Supplementary table 4.1A**). However, the relative proportions of the *L. sigmodontis*-specific RNA biotypes detected by deep sequences was similar at both time points: 24,11% vs. 18.40% of rRNA reads at 0-24h vs 48-72h, respectively, 46.20% vs 52.31% tRNA reads at 0-24h vs 48-72h, respectively, 0.41% vs 0.31% miRNA reads at 0-24h vs 48-72h, respectively, and 26.93% vs 26.01% other unmapped reads at 0-24h vs 48-72h, respectively. These results suggest a reduction in the overall RNA content at later time points compared to early time points, without changes in the proportion or the RNA biotypes that are secreted over time (**Supplementary table 4.1A, and Table 4.1**). Further unsupervised hierarchical clustering analysis of the secreted miRNAs population revealed that the ES products can be broadly grouped into two main clusters based on the time point at which they were harvested: 0-24h vs 48-72h, with some degree of variability between biological replicates (**Figure 4.4A**). Based on Cook's distances (CD) for estimation of influential samples (outliers) and establishing a cut-off of 3 (Cook, 1977), we did not detect the presence of outliers in our datasets (**Figure 4.4B**). Despite this, statistical analysis using DESeq2 did not reveal significant changes in the relative levels of individual miRNAs over time (using a significance cut-off *padj*<0.05) (**Supplementary table 4.1B**, **Table 4.2 and Figure 4.4C**). These results indicate that in fully viable gAF worms, the secretion of a subset of miRNAs remains unchanged over time, whereas there is a ~10X decrease in the concentration of vesicles released over time.

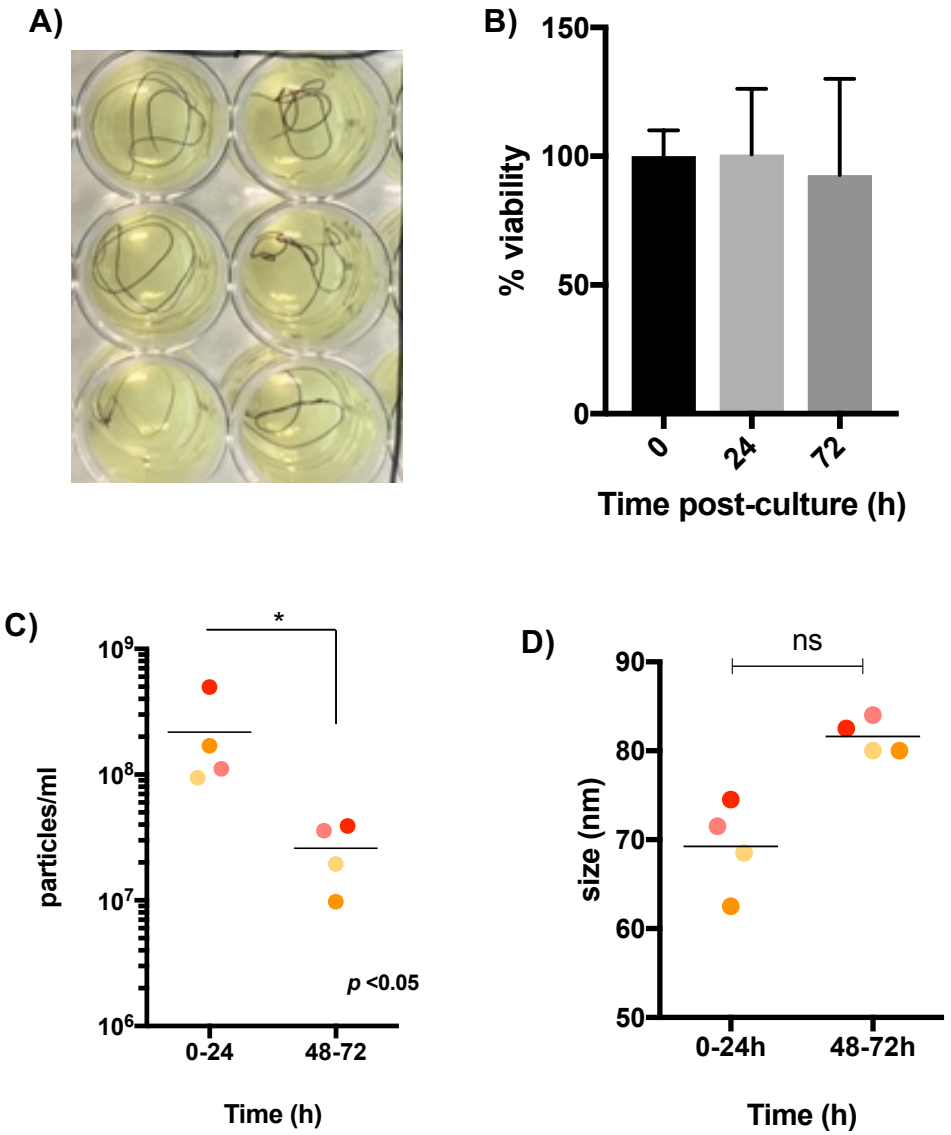

Figure 4.3 Release of EVs by viable gAF decays in a time-dependent manner. A) Worm viability was monitored by MTT assay, in which intracellular NAD(P)H-dependent oxidoreductase enzymes mediate the reduction the tetrazolium dye MTT to a water-insoluble, purple formazan crystal, thus turning worms purple (as shown in picture); B) Using this method, the % of survival can be calculated in relation to worms at time 0 (adult female worms freshly retrieved from the host; $n = 2$). C) The number and D) size of the particles released over time were calculated using nanoparticle tracking analysis, showing a significant decrease in the concentration of particles over time (colours indicate independent replicates; $n = 4$). (* $p < 0.05$, ns = not significant; Mann-Whitney test).

Table 4.1 RNA diversity in the secretome of gravid adult *L. sigmodontis* female worms over time

Time point	ES products 0 – 24h (n = 5)[1]	ES products 48 – 72h (n = 5)[1]
Input reads	6,686,464 (11,989,234)	10,084,909 (12,845,248)
High quality reads	5,842,129 (8,715,012)	7,093,858 (9,211,574)
% High quality reads	86.40% (88.4%)	71.7% (73.4%)
***M. musculus* reads**	232,675 (264,446)	199,203 (250,323)
***L. sigmodontis* reads**	**1,137,223 (1,315,579)**	**440,121 (939,378)**
rRNAs	292,752 (313,614)	111,551 (180,813)
tRNAs	510,997 (766,856)	243,583 (513,506)
miRNAs	**6,090 (6,318)**	**2,033 (2,393)**
Other Rfam	32,232 (40,303)	12,842 (26,210)
Non-Rfam	354,087 (452,646)	130,594 (216,816)

[1] The median and the upper limit for the 75% of the total sequencing reads (brackets) are reported for each time point.

Table 4.2 Top 20 most abundant miRNAs detected in the secretome of gravid adult *L. sigmodontis* female worms over time

miRNA	Mature RNA sequence (5' – 3')	Genomic locus	Total RPM[1]	Log2FC[3]	*padj*[3]	RPM[1,2] in 0-24h secretome (*n* = 5)	RPM[1,2] in 48-72h secretome (*n* = 5)
miR-92-5p	uauugcacucgucccggccuga	nLs.2.1.scaf00001	446,726.7	2.085	>0.99	281,963 (559,154)	378,436 (504,086)
miR-100a	aacccguaguuucgaacaugugu	nLs.2.1.scaf00144	160,974.8	0.972	0.64	115,974 (125,148)	229,826 (249,336)
miR-71-5p	ugaaagacauggguagugagacg	nLs.2.1.scaf00472	129,923.9	-1.738	0.4769	111,968 (191,473)	12,257 (52,370)
miR-8805-5p	ggaggaaucagcgugcugu	nLs.2.1.scaf00006	75,371.7	1.220	>0.99	93,878 (113,655)	2,554 (13,019)
Lin-4-5p	ucccugagaccucugcugcga	nLs.2.1.scaf00367	41,049.8	-0.609	0.870	43,138 (48,164)	34,123 (39,743)
miR-100d-5p	uacccguagcuccgaauaugugu	nLs.2.1.scaf00144	23,842.4	4.465	>0.99	25,633 (28,425)	473 (41,113)
miR-5866-5p	uuaccauguugaucgaucucc	nLs.2.1.scaf01139	18,060.1	-1.826	0.615	21,882 (47,375)	0 (1,021)
miR-6659-3p	cuuggcugggaggugacucgcgauc	nLs.2.1.scaf00364	14,665.1	-0.082	>0.99	13,033 (13,956)	14,304 (24,004)
miR-9146-5p	gccuggaugaaucucggug	nLs.2.1.scaf00457	14,277.5	-0.135	>0.99	11,566 (12,746)	1,532 (30,578)
miR-5364-5p	cgagguauuguuuauuggcuga	nLs.2.1.scaf00070	13,409.4	-1.899	0.0615	21,196 (28,425)	0 (0)
Bantam-b	ugagaucacguuacauccgccu	nLs.2.1.scaf02066	11,146.1	-3.678	0.367	4,689 (4,869)	0 (15,846)
miR-4292-3p	acgaugacaguaauaggauuauu	nLs.2.1.scaf01227	11,006.6	2.744	>0.99	0 (2,077)	0 (11,649)
miR-993-3p	uaagcucgucucuacaggcagg	nLs.2.1.scaf00199	6,836.5	0.818	0.870	4,698 (10,526)	0 (0)
miR-9887-5p	cagggcugcacgcgcgc	nLs.2.1.scaf00003	6,433.4	-4.899	0.0556	8,665 (9,714)	0 (0)
miR-34-5p	uggcaguguggguuagcugguugu	nLs.2.1.scaf00918	5,704.8	-5.482	0.060	7,896 (13,462)	0 (0)
miR-6077-3p	uggaagagauaggaacagagc	nLs.2.1.scaf00282	5,565.3	-4.969	0.080	9,378 (9,486)	0 (0)
miR-8319-3p	gaauuagcucgugcgguacggc	nLs.2.1.scaf00584	5,053.7	1.303	0.779	1,575 (4,378)	0 (6,852)
Bantam-a-3p	ugagaucauugugaaagcuauu	nLs.2.1.scaf01674	4,929.7	1.684	0.615	6,015 (7,502)	0 (0)
miR-239-5p	uuuguacuucggcuaaggugcug	nLs.2.1.scaf00430	4,929.7	1.01	>0.99	0 (2,600)	0 (0)
miR-36c	cgguacaacguuucacgguagagc	nLs.2.1.scaf00392	93.01	-3.127	0.476	0 (295)	0 (0)

[1]RPM = miRNA reads per million total miRNA reads for each barcode.
[2]The median and the upper limit for the 75% of the sequencing reads (brackets) for each miRNA are reported at each time point.
[3]The lo2 Fold-change (Log2FC) and *padj* values were calculated using DESeq2, using the "0-24h" samples as the reference group.

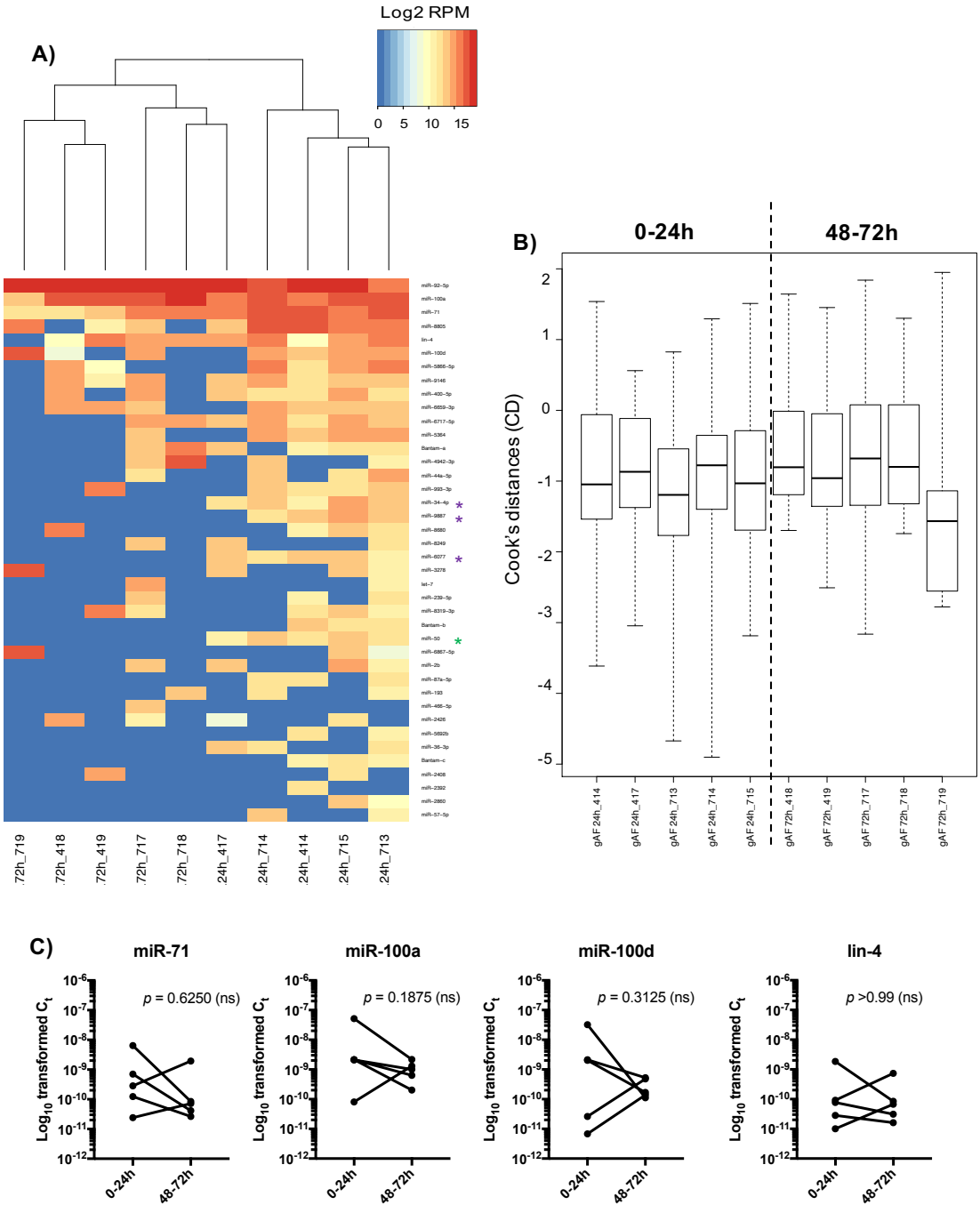

Figure 4.4 miRNA composition of the ES products from gravid adult *L. sigmodontis* female worms over time. A) Log-2 normalised miRNAs (per million total miRNAs) with > 100 read counts are represented in this heat map. Unsupervised hierarchical clustering segregated samples into two main clusters: samples from 0-24h and samples from 48-72h, with some degree of biological variability between replicates (represented in heat map). Green asterisk represents miRNAs (miR-50) that changes significantly between 0-24h compared to 48-72h when cut-off *padj*<0.05 is applied in DESeq2 analysis. Purple asterisks represent miRNAs (miR-9887-5p, miR-34-5p, and miR-6077-3p) that changes significantly between 0-24h compared to 48-72h when cut-off *padj*<0.1 is applied in DESeq2 analysis. B) Boxplot (Average ± Standard Deviation) of Cook's distance (CD) for the presence of potential outliers (CD > 3 indicates potential outliers) C) 2.5 µL of total RNA from ES products were used for qRT-PCR validations. The transformed Ct values of several parasite miRNAs (log10 scale; y axis) for each of the corresponding samples (n = 5) are displayed over time (x axis) (*ns* = not significant; Wilcoxon test).

4.3.2 Low concentration of IVM blocks the release of proteins and microfilariae by gravid adult female worms without impairing worm viability

Next, we sought to investigate the effect of IVM upon miRNA release. As discussed previously in this chapter, IVM could have multiple effects on the adult worms. Therefore, our working hypothesis is that low concentrations of IVM impairs the release of mf, protein and miRNAs without compromising the viability of the gAF *in vitro*. This hypothesis is depicted as a schematic in **Figure 4.5**. To our knowledge, there is no previous information regarding the minimum concentration of IVM required to impair protein release by gAF worms. Therefore, we decided to use two drug concentrations based on results from the close relative *Brugia malayi*; **1 μM**, which is below the reported IC_{50} concentration (2.22 μM) and 10-fold higher than the plasmatic concentration in patients subjected to MDA (~0.1 μM) (Ballesteros, Tritten, ONeill, et al., 2016; Storey, Marcellino, et al., 2014), and **10 μM**, which is above the reported IC50 and has been shown to severely impair motility and mf release (Storey, Marcellino, et al., 2014; Tompkins, Stitt, et al., 2010). As mentioned above, IVM is known to bind directly to the IVM-sensitive glutamate-gated chloride channel *avr-14* (Laing, Gillan, et al., 2017; Wolstenholme, & Rogers, 2005). Therefore, we first determined the expression of the *avr-14* gene in several tissues from gAF worms. A genome browser search using the WormBase ParaSite repository (Howe, Bolt, et al., 2016), revealed that the latest *L. sigmodontis* genome draft (nLs.2.1.2) contains a single copy of the avr-14 gene (ID nLs.2.1.2.g09042), located in the forward strand of the genomic scaffold 01332, between nucleotides 1,250 and 5,391 (**Figure 4.6**). This gene is composed of 9 exons, which encode for a protein of 328 amino acids with at least two putative neurotransmitter-gated ion channel transmembrane domains, as expected for a member of the glutamate-gated chloride channel (Wolstenholme, 2012). **Figure 4.6** indicates the region of the mature mRNA that we selected for subsequent RT-PCR studies. The *L. sigmodontis avr-14* is closely related to the *avr-14* gene in other filarial nematodes, included *B. malayi*, where the expression of this receptor is well characterised (Li, Rush, et al., 2014a) (**Figure 4.7**). Therefore, we hypothesise that, as shown for *B. malayi*, *avr-14* is highly expressed in the reproductive tissue of adult female worms. To test this hypothesis, we dissected >60 gravid adult female worms, recovered from gerbils at day ~90 post-infection, and harvested the anterior end (containing the head, the pharynx and nerve ring), the reproductive tissue,

digestive tissue, cuticle and eggs/mf released during dissection (**Figure 4.8A-E**). Images of some of the tissues harvested are shown in figure **4.8B-E**. The tissues from individual worms were pooled and kept in Trizol until RNA extraction, as discussed in chapter 2. Our RT-PCR data show that the IVM receptor is highly expressed in the reproductive tissue, and to a lower extent in the digestive tissue (**Figure 4.8F**). This is consistent with previous studies on *avr-14* expression in *B. malayi* gAF (Li, Rush, et al., 2014). This result suggests that IVM could bind to and acts upon the reproductive tissue in gAF worms, although other tissues (e.g. nerve ring, pharynx, digestive tissue) may also be susceptible to IVM.

We next decided to determine the expression pattern of some of the miRNAs abundantly detected in the secretome of gAF, as demonstrated in chapter 3. We observed a differential expression pattern of miRNAs in tissues from gravid adult female worms. miR-993 was predominantly expressed in the cuticle and in the digestive tissue but lowly expressed in the reproductive tissue (**Figure 4.8G**), whereas miR-228, miR-100a and miR-100b were highly abundant in the reproductive and digestive tissue, and poorly detected in the cuticle (**Figure 4.8G**). Other miRNAs, such as miR-5364 and miR-5866, were lowly expressed in the cuticle or in the reproductive tissue, respectively (**Figure 4.8G**).

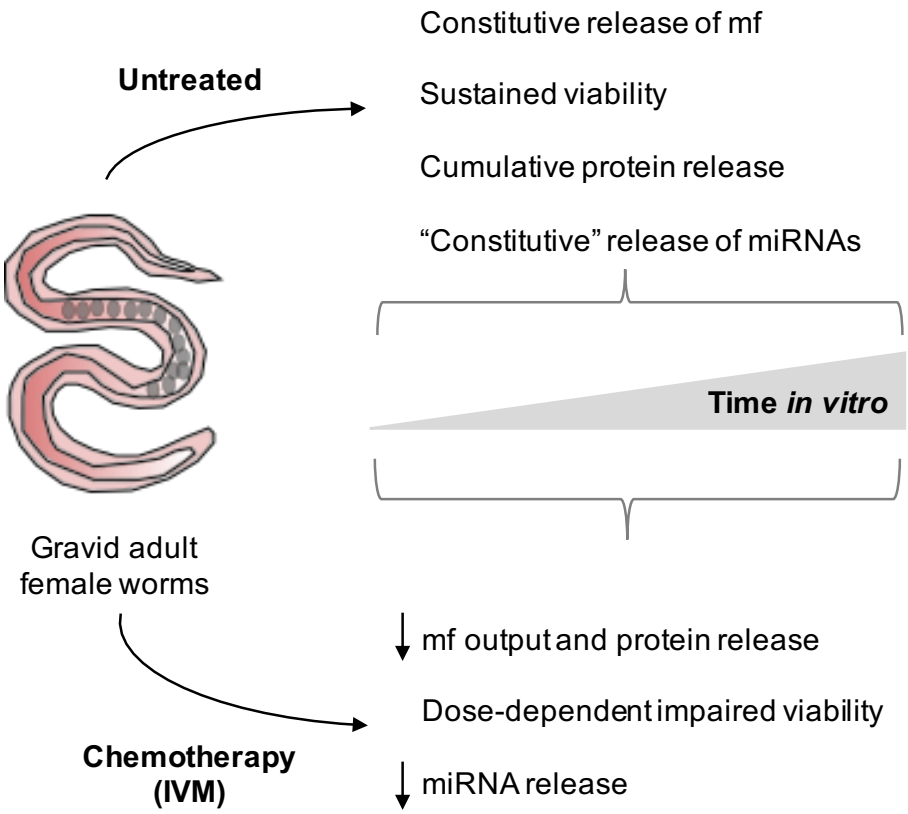

Figure 4.5 Schematic representation of the potential effect of IVM on miRNA release by gravid adult *L. sigmodontis* female worms. Our hypothesis is that in untreated worms, there is a constitutive release of mf over time, and the viability, protein and miRNA release are not impaired. Conversely, anthelminthic chemotherapy impairs mf output, worm viability and miRNA *in vitro*.

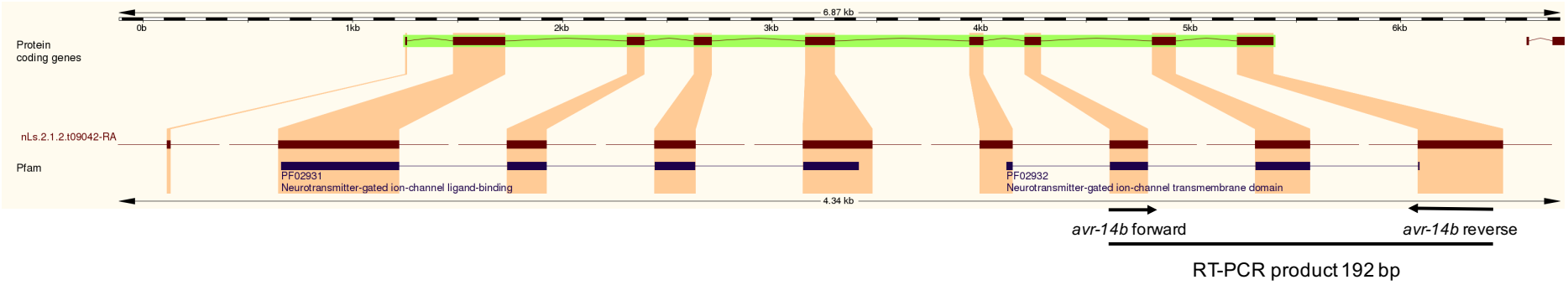

Figure 4.6 The *L. sigmodontis avr-14* gene. The *avr-14* gene (ID nLs.2.1.2.g09042) is in the genomic scaffold 01332 of the latest annotation of the *L. sigmodontis* genome draft (nLs.2.1.2) and, as shown here, contains 9 exons (thick red bars). The ligand-binding domains were predicted using Pfam (thick blue bars). The detection of the mature mRNA in *L. sigmodontis* gravid adult female tissues was conducted by RT-PCR using total RNA from female tissues, and is discussed in figure 4.6 and in chapter 2. The forward primer was designed against the exon 7, whereas the reverse primer was designed against the exon 9 of the mature mRNA sequence. The expected amplicon size is of 192bp.

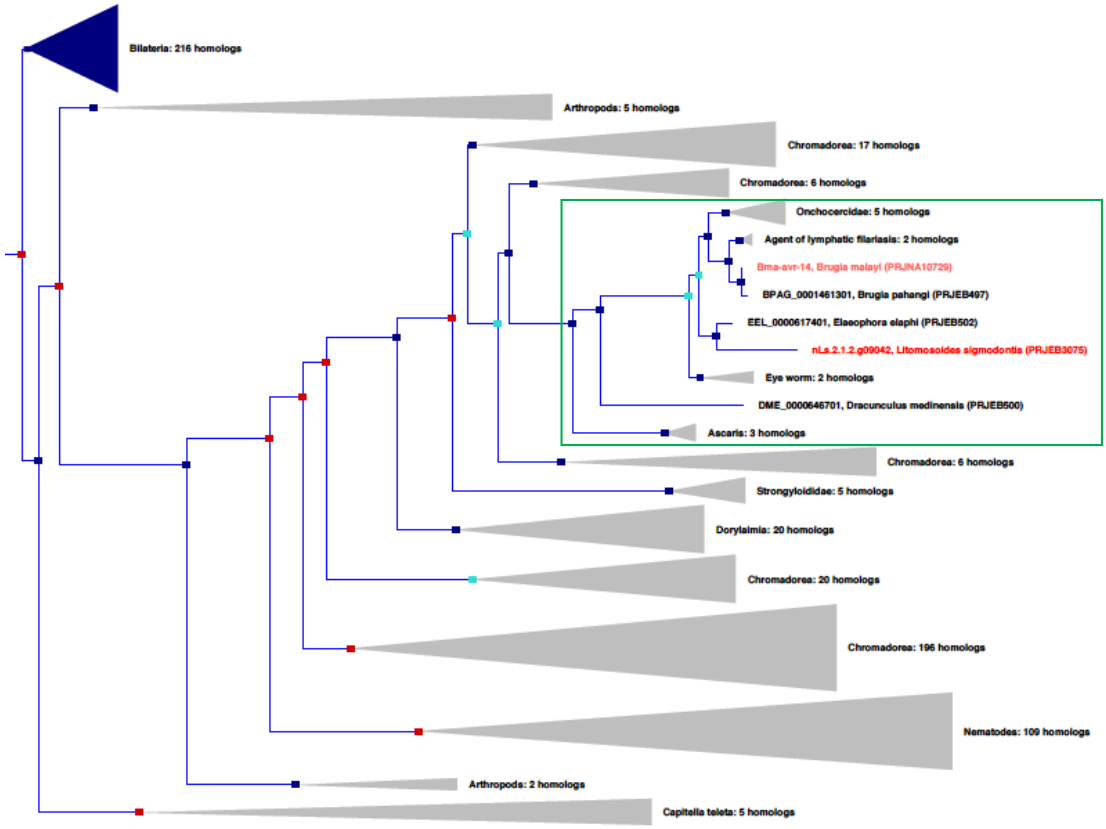

Figure 4.7 Evolutionary relationships of *L. sigmodontis* avr-14 gene to other clade III nematodes. Only one gene is detected in the *L. sigmodontis* transcriptome (gene ID nLs.2.1.2.g09042), which share a high degree of homology to the b isoform of the *avr-14* gene in *B. malayi* (*Bma-avr-14b*) (gene ID WBGene00221971) (both genes are highlighted in red). The green square correspond to the expanded branch derived from all the clade III nematodes included in this analysis. Grey collapsed nodes at the end of each branch represent sub-trees (Note: the nematode branch representing 109 homologs includes results from all non-clade III nematodes), whereas blue nodes represent collapsed paralogs sequences. Blue squares represent speciation nodes, red squares represent duplication nodes, green nodes represent ambiguous nodes, and orange squares represent gene split events.

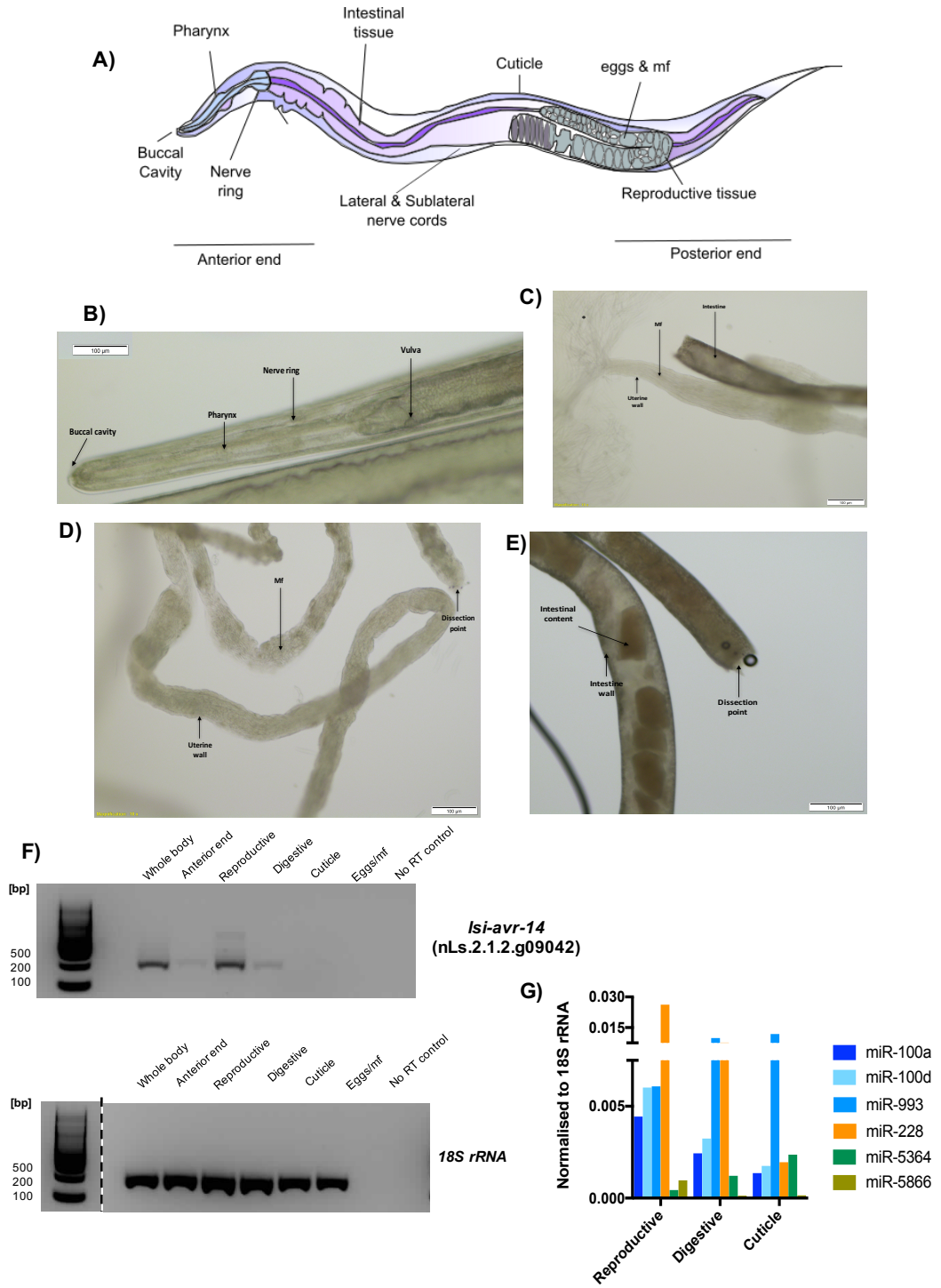

Figure 4.8 Tissue-specific expression of miRNAs previously identified in the secretome of gravid adult *L. sigmodontis* female worms. A) Simplified schematic representation of the tissues taken from gravid female worms at day 90 post-infection from gerbils. (B) The anterior end (containing the pharynx and the nerve ring), (C & D) reproductive, (C & E) digestive and cuticle tissues were harvested and placed directly into Trizol (as described in chapter 2). The expression of *Lsi-avr-14* was assessed by RT-PCR from purified gravid adult female tissues. The signal of 18S rRNA was used as housekeeping, and a reaction lacking Reverse Transcriptase enzyme was included as "No RT" control. G) qRT-PCR of miRNAs identified as enriched in the secretome of gravid female worms, normalised to the signal of *18S rRNA*.

Next, we treated gAF worms *in vitro* with either 1 or 10 μM final concentration of IVM and measured 1) viability, 2) motility, 3) mf release and 4) protein concentration of the ES products, to monitor the effect of these compounds on gAF. As a control, we treated gAF worms with either 0.01% or 0.1% DMSO (vehicle controls), which correspond to the final concentrations of this compound at 1 and 10 μM IVM, respectively. The viability of gAF was significantly reduced (>50%) in gAF worms treated with 10 μM IVM, whereas this was not impaired at low concentrations (1 μM), when compared to DMSO-treated worms (**Figure 4.9A**). Similar results were observed in terms of gAF motility, were 10 μM of IVM significantly impairs the motility gAF after 72h of exposure, whereas 1 μM of IVM did not impair motility (**Figure 4.10**) We also observed that IVM treatment impaired the mf output at all the concentrations tested, with a more pronounced impairment on mf output at 72h post-treatment (**Figure 4.9B and C**), consistent with previous results in other filarial parasites (Storey, Marcellino, et al., 2014; Tompkins, Stitt, et al., 2010). Based on these results, we decided to use low concentrations of these compounds (1 μM) to determine the effect on release of proteins and miRNAs by gAF. The protein concentration as well as the miRNA content was assessed in the ES products harvested before treatment and 24h after incubating the gAF with either 0.01% DMSO or 1 μM IVM (**Figure 4.11A**). In DMSO-treated worms, we expect a sustained release of proteins and miRNAs by gAF over time, resulting in a significant cumulative increase in the concentration of both molecules (**Figure 4.5**). Conversely, in IVM-treated worms, we expect a reduction in the release of proteins and miRNAs over time, and so we anticipate no significant differences in the measurement of both molecules before and after exposure to IVM (**Figure 4.5**). Consistent with our hypothesis, the protein concentration significantly increased in ES products from gAF worms after 24h of treatment with 0.01% DMSO compared to the time right before exposure ("0h"), whereas we did not detect a significant difference in the protein concentration of ES products from worms before and after treatment with 1 μM IVM (**Figure 4.11B**). These differences were more evident when we calculated the fold increase (compared to 0h time point) in protein concentration after adding either 0.01% DMSO or 1 μM IVM (**Figure 4.11C**). This analysis shows that there is a cumulative release of proteins over time in worms exposed to 0.01% DMSO, whereas we did not

observe an increase in the proportion of proteins released before and after addition of 1 μM IVM (**Figure 4.11C**). These results indicate that low concentrations of IVM impair both mf and protein release by gAF worms over time, without compromising their viability or motility.

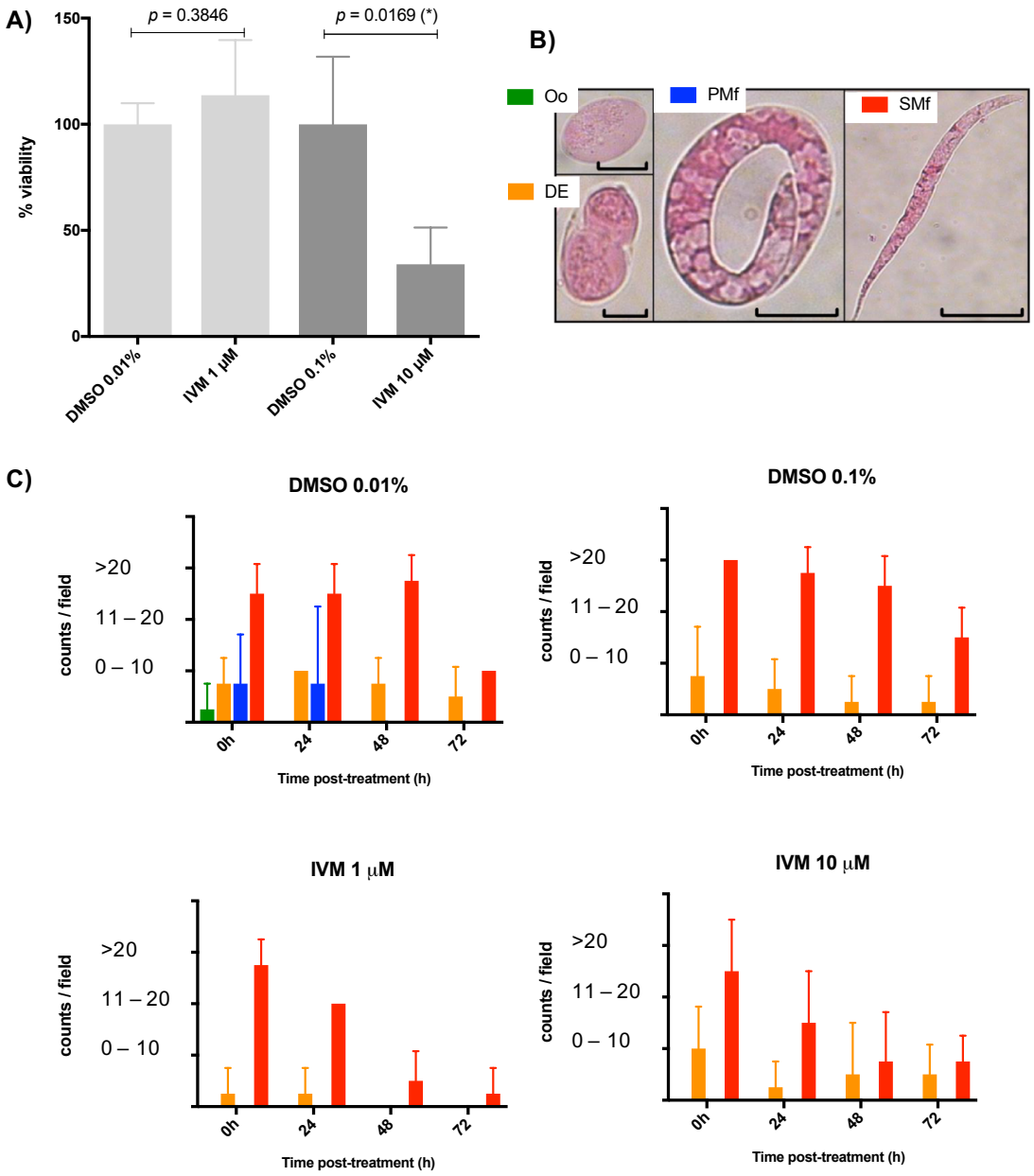

Figure 4.9 Effect of IVM on viability and mf output from gravid adult *L. sigmodontis* female worms. A) The survival of gravid adult female worms exposed to either 1 or 10 µM IVM for 72h was monitored by MTT assay. The % of survival was calculated using the DMSO-treated worms as control (* $p < 0.05$; *t* test). B) The number of oocytes (Oo), developing embryos (DE), pretzel-like mf (PMf) and stretched mf (SMf) (as described by Ziewer, Hübner, et al., 2012) were assessed semi-quantitatively (counts/field) in samples before (0h) and after (24h) addition of either untreated or treated with 1 or 10 µM Ivermectin over 72h (C).

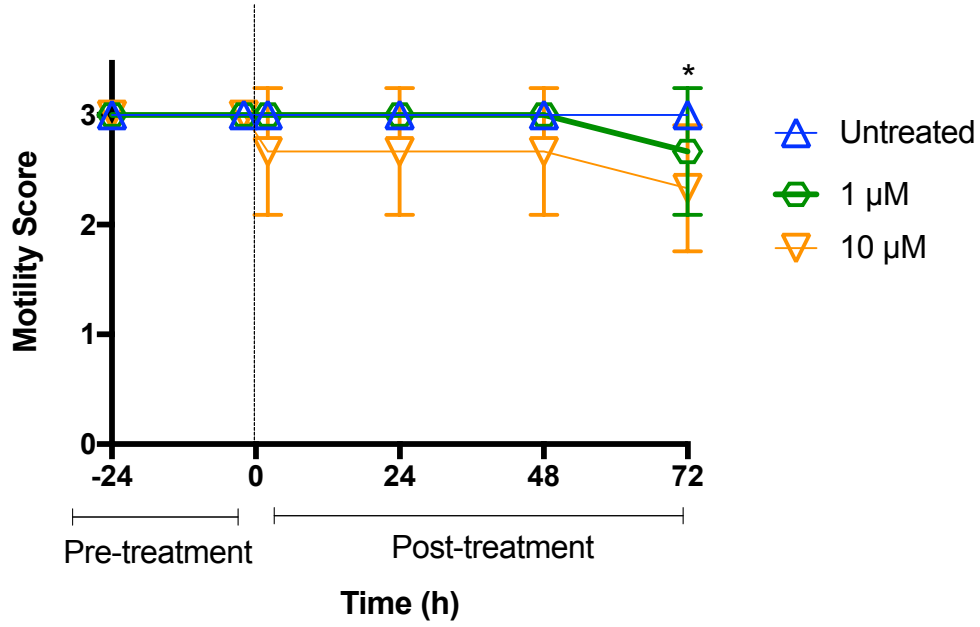

Figure 4.10 Effect of IVM on motility of gravid adult *L. sigmodontis* female worms. Mean motility (+/- SD) of gravid adult female worms after exposure to IVM. Parasite motility was assessed as described in chapter 2; Motility was scored based on head-to-tail movement as: 1) immotile and slightly motile, 2) Moderately motile with slow sinusoidal movements, 3) highly motile and comparable to untreated worms. (* p <0.05; *** p <0.0005; Dunnett's ANOVA multiple comparisons test using the untreated worms as reference group)

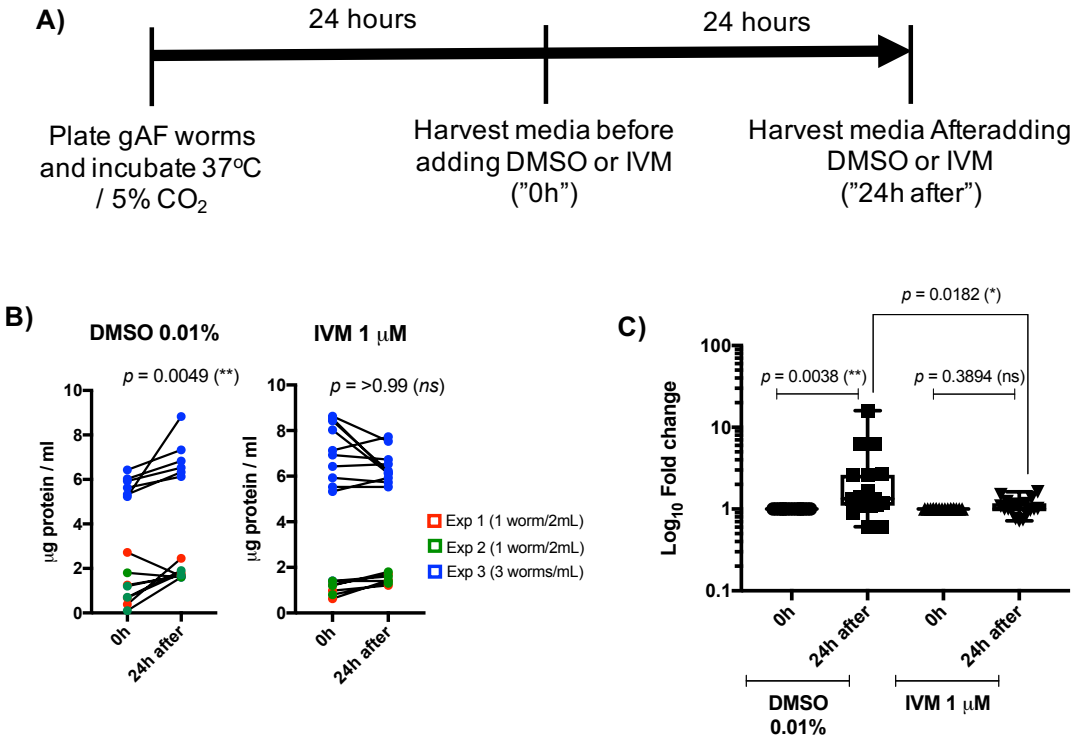

Figure 4.11 Effect of IVM on protein secretion by gravid adult *L. sigmodontis* female worms *in vitro*. A) Schematic representation of the experimental setup. B) Pooled data from three independent experiments (colour-coded). The cumulative protein concentration (micrograms of protein/ml) of the ES products was measured 24h before and 24h after addition of either 0.01% DMSO (n = 14) or 1 μM IVM (n = 17). C) The fold change in the protein concentration (compared to before treatment) was also assessed (* p <0.05; ** p < 0.005; ns = not significant. Wilcoxon test).

4.3.3 IVM partially impairs the release of miRNAs from gravid adult female worms *in vitro*

Next, we determine whether IVM also impairs the release of miRNAs shown in the previous result chapter to be enriched in the ES products of gAF worms *in vitro* (miR-100a, miR-100d and miR-228). These miRNAs were also confirmed to be expressed in the reproductive tissue of gAF worms (**Figure 4.8G**), thought to be one of the target sites of IVM, based on the expression of *avr-14* gene (**Figure 4.8F**). The results from three independent experiments (n = 3-4 replicates/experiment) are shown in **Figure 4.12**. As demonstrated for protein concentration, we noted a significant increase in the signal of all the miRNAs (except perhaps miR-228) in the ES products from worms treated with 0.01% DMSO, when compared to the signal at 0h (based on schematic in Figure 4.11A) (**Figure 4.12**). Conversely, we did not observe a significant increase in the signal of extracellular parasite miRNAs in worms after treatment with 1 μM IVM when compared to the 0h time point (**Figure 4.12**). These results are consistent with our findings on protein secretion (**Figure 4.11B & C**), and may indicate that 1 μM IVM could impair the secretion of miRNAs by gAF *in vitro*. Nevertheless, we failed to observe a significant difference on the relative miRNA signal in the ES products of DMSO-treated gAF and IVM-treated worms at the same time point (24h after incubation) (**Figure 4.12**), which could be partially attributed to the degree of variability observed in response to the treatments, or to the presence of alternative routes for secretion, derived perhaps from tissues that are insensitive to IVM. For instance, the cuticle is likely to be insensitive IVM given that it does not express *avr-14* (**Figure 4.8F**). These results indicate that sub-lethal concentrations of IVM impairs the release of proteins and the mf output by *L. sigmodontis* gAF, and partially impairs the release of miRNAs derived from gAF worms *in vitro*.

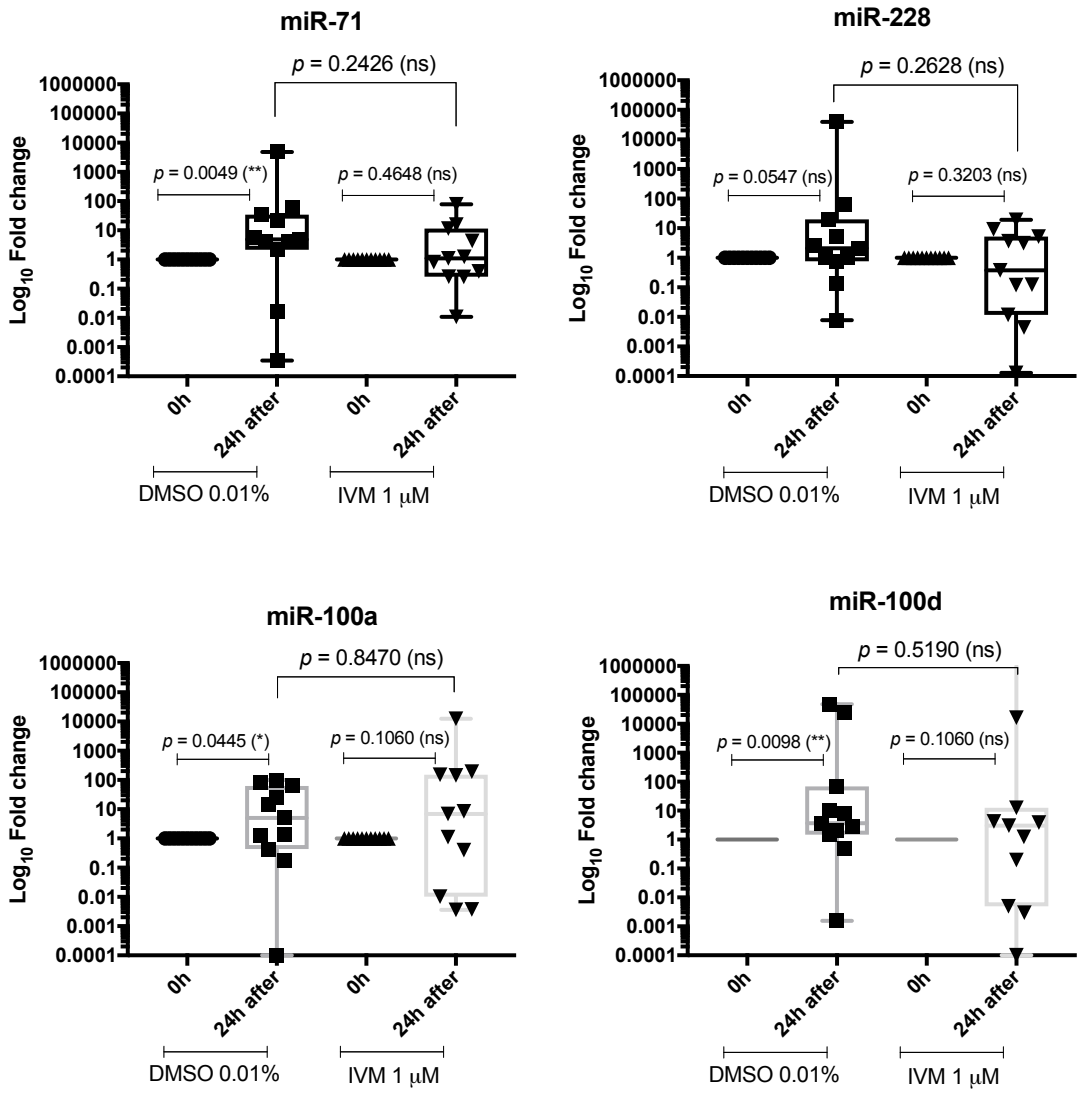

Figure 4.12 Effect of IVM on miRNA secretion by gravid adult *L. sigmodontis* female worms *in vitro*. The signal of several female-enriched miRNAs (miR-100a, miR-100d and miR-228), as well as miR-71, was measured in ES products 24h before and 24h after addition of either 0.01% DMSO or 1 μM IVM. Each dot represents a single worm, from a total of 3 independent experiments. In each condition, the fold change was estimated to the ES product before addition of the compounds mentioned before and the results shown represent pooled data from two independent experiments (ns = not significant; Wilcoxon test).

4.4 Summary

- The EV release rate by gravid adult female worms decreases in a time-dependent manner. However, the relative abundance of a subset of the secreted miRNA does not seem to significantly change over time.
- The miRNAs shown to be enriched in the secretome of gAF worms are expressed in different tissues; miR-228, miR-100a and miR-100d are abundantly expressed in the reproductive tract, whereas miR-993-3p is abundantly expressed in the digestive tissue and the cuticle.
- IVM impairs the release of proteins and the microfilariae output, and partially impairs the release of miRNAs that were previously identified to be enriched in the secretome of gAF worms.

4.5 Discussion

The release of ES products by parasitic nematodes, including gAF worms, is likely to be associated with tissues and organs with glandular or secretory capacity. Examples of these structures are the Excretory/Secretory system, the digestive tissue, the reproductive tissue, and the glandular pharynx, among others (Avery, & Shtonda, 2003; Branicky, & Hekimi, 2006; Buechner, 2002; Madathiparambil, Kaleysa, et al., 2009). Proteomic analysis of the ES products from gAF worms suggest that the uterine fluid is a rich source of proteins normally released during birth in several species including *L. sigmodontis* and *A. suum* (Armstrong, Babayan, et al., 2014; Chehayeb, Robertson, et al., 2014); However, the packaging, trafficking and release of the components typically found in ES products, including EVs and miRNAs, are thought to be dynamic processes yet to be fully elucidated. In a recent report, it has been demonstrated that *Brugia malayi* L3s release EVs, but that this process decays in a time dependent manner, thought to be associated with a poor viability of this developmental stage *in vitro* (Zamanian, Fraser, Agbedanu, & Harischandra, 2015). Our data demonstrate that gAF worms release EVs of 70-100 nm in length but the overall concentration of EVs decreased ~10 fold between the first and third day in culture, without significant changes in their size. Moreover, we did not observe a decrease in worm viability *in vitro* over time, thus suggesting that the slight reduction in EV output observed over time is not explained by worm death, and could potentially be explained by specific adaptations to the *in vitro* culture conditions, as it has been demonstrated at the transcriptional level in *B. malayi* gAF (Ballesteros, Tritten, O'Neill, et al., 2016). Importantly, we observed an overall reduction in the signal of most of the secreted miRNA in ES products at later time points (48-72h) when compare to early time points (0-24h) by deep sequencing, although these results were not significant in further statistical analysis by DESeq2 or qRT-PCR analysis. These results led us to propose that the population of miRNAs that are selected, sorted, and packaged for excretion/secretion (likely within, but not exclusively associated to, EVs) does not change in a time-dependent manner, but the overall RNA secretion (including miRNAs) is reduced instead. However, further experimental evidence, including more biological replicates as well as the evaluation of other RNA biotypes, is require to validate this hypothesis.

To date, little is known about the true biological diversity of the EV population secreted by parasites. Indeed, most of the studies thus far have described the presence of EVs in the secretome of a multitude of parasites based solely in their size and shape by either transmission electron microscopy (reviewed by Coakley, Maizels, et al., 2015) or by nanoparticle tracking systems (Tritten, Clarke, et al., 2016; Zamanian, Fraser, Agbedanu, & Harischandra, 2015). However, different EVs may be released under determine environmental conditions, particularly in response to environmental stressors such as starvation or exposure to drugs (as proposed by de la Torre-Escudero, Bennett, et al., 2016). One limitation of our studies is that is does not address whether other types of EVs (smaller than 70 nm or bigger than 400 nm), or other types of RNAs, also reported in the secretome of helminthic parasites (e.g. Y RNAs and siRNAs), are dynamically released over time. As mentioned before, gAF worms undergo extensive metabolic adaptations in response to *in vitro* culture conditions, including changes in the expression of cuticle collagens and serpins, which are markers of stress (Ballesteros, Tritten, O'Neill, et al., 2016). It is therefore tempting to speculate that under stressful conditions, the production of one type of EV decreases whereas other types of EVs, of varying sizes and biogenesis pathways (e.g. microvesicles, apoptotic bodies; reviewed by Colombo, Raposo, et al., 2014), or even stress-induced membrane blebs (de la Torre-Escudero, Bennett, et al., 2016) could increase in a time-dependent manner. Given the range of particle sizes that we can confidently detect with the nanoparticle tracking platform used in the studies presented in here (70 – 420 nm), this cannot be addressed with the data presented here. The anthelminthic compound IVM, traditionally used to treat filarial infections, is documented to disrupt the reproductive capacity of *B. malayi* and *O. volvulus* adult worms, with a concomitant reduction in embryogenesis and mf output by gravid adult female worms *in vitro* and *in vivo* (Ballesteros, Tritten, ONeill, et al., 2016; Li, Rush, et al., 2014; Osei-Atwen*).* A recent report also demonstrated that IVM has profound effects on the transcriptional landscape of *B. malayi* gravid adult females, with a strong down-regulation of genes associated with embryogenesis and meiosis (Ballesteros, Tritten, ONeill, et al., 2016). Together with the tissue localization of the IVM receptor in the gonadal tissue (Li, Rush, et al., 2014) this may explain the sterilizing effect that IVM has on gravid adult female worms. Interestingly, it has been demonstrated that the IVM receptor is abundantly expressed in the lateral and sublateral cords in *H. contortus* (Portillo, Jagannathan, et al., 2003), *B. malayi* (Li,

Rush, et al., 2015), and *Ascaris suum* (Holden-Dye, Joyner, et al., 2013), among others, also indicating an effect of IVM on the nervous system in many parasitic nematodes. The effects of IVM are not limited to adult worms, as IVM has also been shown to impair the capacity of mf to release immunomodulatory effectors, with important consequences for their viability and survival (Moreno, Nabhan, et al., 2010; Vatta, Dzimianski, et al., 2014). This is the basis for the current hypothesis that IVM does not kill filarial nematodes *per se*, but acts synergistically with the immune system to mediate worm killing (Carithers, 2017). Importantly, we only observed a reduction in worm viability at concentrations (10 μM) far exceeding those previously used *in vivo* (~50 pM) (Baraka, Mahmoud, et al., 1996; González Canga, Sahagún Prieto, et al., 2008), demonstrating the inability of IVM to induce macrofilaricidal activity against *L. sigmodontis* at the plasmatic concentrations normally reached *in vivo*. Nevertheless, as reported in other adult filarial nematodes, our results demonstrate that IVM impairs the mf production by *L. sigmodontis* adult worms in a time- and dose-dependent manner. This observation helped us to address whether an impairment in the reproductive capacity of adult female worms leads to a reduction in the secretion of miRNAs found to be enriched in the secretome of this lifecycle stage. Consistent with our hypothesis, our data demonstrates that *L. sigmodontis* gAF worms exposed to sub-lethal concentrations of IVM have an impaired capacity to secrete proteins *in vitro* without measurable effects on worm viability. Moreover, we observed low concentrations of IVM partially impairs the release of some miRNAs by adult female worms, consistent with the effects observed in protein release and mf output. One possibility to explain this partial effect of IVM upon miRNA secretion is that these miRNAs may also derived from tissues insensitive to IVM based on the expression of the IVM receptor avr-14 (e.g. cuticle, and less likely, the digestive tissue). In line with this hypothesis, EVs from the gastrointestinal nematode *H. polygyrus* are thought to derived from the intestinal tract of the parasite (Buck, Coakley, Simbari, McSorley, et al., 2014), whereas other routes of secretion, including the tegument in trematodes (comparable to the cuticle in nematodes), have also been proposed in several parasites (reviewed by de la Torre-Escudero, Bennett, et al., 2016). Alternatively, other tissues may still be sensitive to IVM but may require a higher dose concentrations to exert an effect on miRNA and protein release. It is also possible that other anthelminthic compounds with similar efficacy to IVM, including

Levamisole (LEV), Flubendazole (FBZ) and Doxycycline (DOX) might influence miRNA secretion in different ways, depending on their mechanisms of action and targeted tissues. LEV, for example, binds to the nicotinic acetylcholine receptor in synaptic connections at the neuromuscular junctions (Martin, Robertson, et al., 2012), whereas FBZ inhibits microtubule polarisation in the intestinal epithelial cells of several parasitic nematodes (Martin, 1997). Similarly, DOX specifically targets the endosymbiont *Wolbachia*, abundantly found in the reproductive tissue and lateral cord, and induces its elimination (Debrah, Specht, et al., 2015; Kon, Pattison, et al., 1998). Given the variety of worm tissues and organs that these compounds actively act upon, it would be informative to address whether any of these can be specifically targeted with chemotherapy to further understand likely routes for secretion of EV and small RNAs (as discussed by de la Torre-Escudero, Bennett, et al., 2016).

Nonetheless, it is important to stress that we did not test a battery of IVM concentrations and we cannot rule out that the variability observed in some of our experimental replicates could be due to off-target effects. Moreover, we did not address whether IVM impairs the detection of circulating parasite-derived miRNAs *in vivo*. These studies become even more relevant in the context of potentially developing a miRNA-based biomarker assay for diagnosis of filarial infections. As mentioned before, the plasmatic concentration of IVM reported in patients subjected to MDA is ~50 ng/mL (~50 pM) (Ballesteros, Tritten, ONeill, et al., 2016; Baraka, Mahmoud, et al., 1996; González Canga, Sahagún Prieto, et al., 2008), which is 100-fold lower than the concentration used in the studies presented in here (1μM). Therefore, we anticipate that IVM may not interfere with the detection of miRNAs derived from the adult females in human biofluids (e.g. serum and/or plasma). We are currently conducting experiments to shed light into this. The potential detection and application of filarial-derived miRNAs as diagnostics for infections are discussed in more detail in chapter 5.

Chapter 5: **Extracellular filarial-derived small RNAs in host biofluids and potential as biomarkers for filarial infections**

5.1 Introduction

Filarial infections affect more than 150 million people in tropical and subtropical regions, with almost one billion thought to be at risk of infection (Knopp, Steinmann, et al., 2012) (Hotez, Alvarado, et al., 2014). For more than 25 years, Ivermectin (IVM) has been used in mass drug administration (MDA) programmes to control onchocerciasis in Africa and Latin America. Following the success of the onchocerciasis Elimination Program for the Americas, which has used MDA of IVM alone to abrogate transmission in most endemic foci, the goal of the African Program for onchocerciasis Control (APOC; which covers a vastly greater area) has shifted from control to eradication (Crump, Morel, et al., 2012). However, major challenges to this endeavour remain, such as the emergence of IVM resistance (Osei-Atweneboana, Eng, et al., 2007), the potential for severe adverse reactions to IVM in loiasis-endemic areas (Gardon, Gardon-Wendel, et al., 1997), and significant limitations in the accurate and rapid diagnosis of infection (Boatin, Toé, et al., 2002). As discussed in chapter 1, parasitological diagnosis of human onchocerciasis relies on the presence of palpable nodules (onchocercoma) containing adult worms and/or the detection of mf in skin snips (Boatin, Toé, et al., 2002). These methods perform well in highly endemic regions where the overall parasitic burden is high, but performs poorly in the detection of pre-patent, early infections or in regions where the infection intensity is low (Taylor, Keyvan-Larijani, et al., 1987). Other methods rely on the detection of parasite antigens such as Ov16 (Park, Dickerson, et al., 2008), N-acetyltyramine-O-β-glucuronide (NATOG) (Globisch, Moreno, et al., 2013), among others. Interestingly, the newly identified biomarker NATOG can be detected in both plasma and urine, and suggest that multiple biofluids can be used for further diagnostic applications in onchocerciasis (Lagatie, Ediage, et al., 2016). Even though some of these are commercially available and currently used in the regional programmes for onchocerciasis control and elimination (Fischer, Bonow, et al., 2005), these methods sometimes render cross-reactivity with sera from patients infected with

other filarial infections, thus compromising its specificity (Fischer, Bonow, et al., 2005). Alternatively, the detection of parasite-derived nucleic acids has become increasingly popular for human diagnostics as well as for molecular xenomonitoring of blackflies and mosquitoes (Alhassan, Li, et al., 2015). The *O. volvulus* DNA repetitive sequence O-150 (Zimmerman, Guderian, et al., 1994), the *Brugia HhaI* repetitive family (Fink, Fahle, et al., 2011), among others (reviewed by Alhassan, Li, et al., 2015), are a few examples of promising candidates for a nucleic acid-based diagnostic test. PCR-based methods such as Loop-Mediated Isothermal Amplification (LAMP) are popular and attractive alternatives for standard diagnostic methods as they are less vulnerable to inhibitors typically detected in clinical samples (Notomi, Mori, et al., 2015). LAMP methods can also detect very low copy numbers without the need for sophisticated equipment (Alhassan, Makepeace, Lacourse, et al., 2014; Drame, Fink, et al., 2014; Poole, Tanner, et al., 2012), and are generally cheap (<1.00 USD per sample; (Han, 2013). However, little is known about the potential use of other types of nucleic acids (e.g. small RNAs) for filarial infections (reviewed by Quintana, Babayan, et al., 2016)

5.1.1 miRNAs as diagnostics for parasitic infections

Small non-coding RNAs (sncRNAs) are important regulators of many processes in animals, from development to immunity. MicroRNAs (miRNAs) are the best characterized class of sncRNA which operate by guiding the RNA-induced silencing complex (RISC) to specific messenger RNAs (mRNAs) inside cells, where they inhibit translation and de-stabilize the targeted mRNAs (Fabian, & Sonenberg, 2012). However, their functions do not seem to be confined within the limits of the cells. For examples, studies in the last 10 years have demonstrated that miRNAs can also exist in a cell-free form in extracellular fluids in many vertebrates, where they may play endocrine signalling roles (Turchinovich, Samatov, et al., 2013). For parasitic species, an outstanding hypothesis is whether these species are capable of interacting with and manipulating this signalling system for their own benefit. Nonetheless, due to their biophysical properties (e.g. encapsulation within extracellular vesicles, stability in a wide range of biofluids) and biochemical properties (e.g. primary sequence poorly conserved between parasites and vertebrate hosts) (Hoy, & Buck, 2012), the parasite-derived circulating miRNAs offer new possibilities for the development of a new

generation of biomarkers for helminthic infections, including filariasis (Hoy, Lundie, et al., 2014; Quintana, Babayan, et al., 2016).

In the previous result chapters, we have shown that all lifecycle stages secrete small RNAs, including miRNAs, *in vitro* (e.g. miR-71), with a clear subpopulation of miRNAs found to be enriched in the secretome of gAF worms compared to AM and/or mf (e.g. miR-100a, miR-100d, among others). Similarly, other miRNAs are comparatively enriched in the secretome of adult worms (AM and gAF) worms when compared to mf (e.g. miR-5360, lin-4) and thus offer opportunities for the detection of adult stages. Here, we aim to address two main questions using samples from hosts infected with *L. sigmodontis, O. ochengi or O. volvulus*:

1. Where are extracellular parasite-derived miRNAs detected within the host during an infection?
2. Do filarial-derived miRNAs hold promise as biomarkers for filarial infections?

5.2 Specific aims

1. To investigate the parasite-derived small RNA content from biofluids during infection with *L. sigmodontis* (gerbils and BALB/c mice) and validate their presence in serum.

2. To examine the diagnostic potential of parasite-derived miRNAs in serum as biomarkers for filarial infections

3. To investigate the small RNA profile of nodular fluids from cattle infected with *O. ochengi*

4. To investigate the small RNA profile of *O. volvulus*-infected human serum and plasma samples

5.3 Results

5.3.1 Parasite-derived miRNAs are found in multiple tissues and body compartments simultaneously during infection

Our results thus far have shown that gAF worms secrete a diverse population of miRNAs likely to be associated with EVs. Moreover, we have also demonstrated that the traditional anthelminthic chemotherapy used to treat filarial infections does not impair the secretion of miRNAs by gAF worms. However, little is known about the relative *in vivo* localization of the miRNAs secreted by parasites within the host during an infection. Therefore, we sought to simultaneously screen matched biofluids from gerbils infected with *L. sigmodontis* by next generation sequencing. At day 90 post-infection, we harvested blood and body cavity exudates (pleural/peritoneal; PLEC/PEC, respectively), from which we also purified adherent cells by adhesion to plastic, as described in chapter 2. It is important to mention that, given the lack of specific antibodies against gerbil epitopes, we failed to phenotype the adherent cells as macrophages by Flow cytometry (data not shown). Henceforth, these cells will be generically referred to as "adherent cells". We then proceeded to prepare small RNA libraries from total RNA purified from serum, PLEC/PEC and adherent cells, as described in chapter 2. Our sequencing results are summarised in **Table 5.1**. We obtained a similar depth of coverage for libraries prepared from gerbil serum (3,8 million reads the naïve group vs 5.9 million reads for the infected group), body cavity exudates (5.01 million reads for the naïve group vs 3.4 million reads for the infected group) and adherent cells (1.6 million reads for the naïve group vs 7.16 million reads for the infected group) **(Table 5.1 and supplementary table 5.1)**. The proportion of high quality reads, defined as those containing the 3' adapter and >17 nt after adapter trimming, was consistently >80% for all the samples tested (**Table 5.1 and supplementary table 5.1**). Intriguingly, we noted a greater proportion of reads mapping perfectly and unambiguously to the *L. sigmodontis* genome in infected sera compared to naïve controls, but not in the PLEC/PEC or adherent cells (**Table 5.1 and supplementary table 5.1**). The presence of *L. sigmodontis*-specific reads in naïve samples could be attributed to sequences that are conserved between parasites and hosts, although a potential cross-contamination between samples could not be ruled out. However, this does not explain the differential abundance of parasite RNA in different biofluids, and this may suggest differential accumulation rates or turnover in different body compartments or biofluids. For downstream analyses, we decided to

discard *L. sigmodontis*-specific sequences that could be perfectly conserved between the parasite and the host, and that are detected in naïve and infected samples, as we assumed these holds little biomarker potential. Further miRNA identification using *L. sigmdontis*-specific reads revealed the presence of 38 miRNAs (**Supplementary table 5.2 and Figure 5.1**). The top 10 most abundant miRNAs (>1,000 reads per million total miRNA reads) detected in these datasets are reported in **Table 5.2**. Of these, the most abundant miRNAs were miR-71, miR-92, let-7, miR-100a and miR-34, which were detected in more than 10,000 copies per million of miRNA reads, whereas the other miRNAs were comparatively less abundant (**Table 5.2 and Figure 5.1**). Both miR-92 and let-7 are highly conserved between nematodes and mammals. There can be some heterogeneity in the terminal nucleotides of these miRNAs based on non-templated additions (Landgraf, Rusu, et al., 2007), as is common for miRNAs, such that they could technically align better to parasite than host. The exact origin(s) of these miRNAs cannot be inferred and thus were not attributed as potential filarial-derived miRNAs. Importantly, the miRNA profile differs greatly between samples obtained from the same animal; overall, the sera from infected animals seem to contain a greater diversity of parasite-derived miRNAs when compared to PLEC/PEC or adherent cells from the same animals (**Table 5.2 and Figure 5.1**), which may suggest a differential turnover or stability in different tissues *in vivo*.

Table 5.1 RNA diversity of *L. sigmodontis*-derived small RNAs in serum, body cavity exudates and adherent cells

Sample type	**Serum**[1]		**Body cavity exudates**[1]		**Adherent cells**[1]	
Experimental group	**Naïve (*n* = 3)**	**Infected (*n* = 5)**	**Naïve (*n* = 3)**	**Infected (*n* = 5)**	**Naïve (*n* = 3)**	**Infected (*n* = 5)**
Total reads	3,862,124 (4,994,884)	5,945,559 (6,538,304)	5,011,624 (8,496,866)	3,412,170 (3,665,746)	1,599,366 (2,723,559)	7,168,523 (8,780,109)
High quality reads	3,696,777 (4,802,151)	5,195,779 (5,587,832)	4,777,937 (7,665,433)	3,023,290 (3,447,559)	1,325,089 (2,288,593)	6,324,530 (7,786,544)
% High quality reads	95.72% (96.06%)	86.45% (87.39%)	95.16% (95.25%)	90.07% (92.96%)	82.85% (83.69%)	88.23% (88.68%)
***M. musculus* reads**	2,709,665 (3,404,703)	3,014,914 (3,021,699)	3,260,851 (4,265,803)	2,025,732 (2,068,098)	758,211 (1,372,950)	4,360,474 (5,982,157)
***L. sigmodontis* reads**	3,272 (3,722)	60,750 (81,492)	3,302 (6,226)	4,429 (6,709)	4,411 (6,943)	6,910 (8,134)
% *L. sigmodontis* reads	0.058% (0.131%)	1.443% (1,568%)	0.087% (0.093%)	0.167% (0.260%)	0.333% (0.371%)	0.110% (0.215%)
rRNAs[2]	2,385 (2,668)	3,099 (3,306)	1,897 (3,602)	2,331 (3,396)	553 (819)	502 (524)
tRNAs[2]	18 (128)	4,569 (6,810)	31 (250)	244 (630)	13 (15)	114 (155)
miRNAs[2]	31 (58)	41,781 (66,088)	187 (463)	237 (290)	3,577 (5,401)	4,629 (6,800)
Other Rfam[2]	85 (92)	1,088 (1,344)	117 (143)	141 (218)	202 (307)	457 (644)

[1] The median and the upper limit for the 75% of the total reads (in bracket) are shown for all the biofluids tested.
[2] Rfam classification using sequencing reads mapping unambiguously and perfectly to the *L. sigmodontis* genome draft.

Table 5.2 Top 10 most abundant *L. sigmodontis*-derived miRNAs identified in biofluids and adherent cells from naive and infected gerbils.

			Serum[2]		Body cavity exudates (PEC/PLEC)[2]		Adherent cells[2]	
miRNA	**Mature RNA Sequence (5' – 3')**	**RPM[1]**	**Naïve (*n* = 3)**	**Infected (*n* = 5)**	**Naïve (*n* = 3)**	**Infected (*n* = 5)**	**Naïve (*n* = 3)**	**Infected (*n* = 5)**
miR-71-5p	ugaaagacauggguagugagacg	631,921	2 (43)	50,569 (65,511)	3 (47)	0 (7.5)	0 (1)	171 (475)
miR-92-5p	uauugcacucgucccggccuga	194,873	0 (0)	13,621 (17,629)	21 (112)	84 (126)	0 (0)	133 (184)
Let-7-5p	ugagguaguagguuguauaguua	116,594	2 (14)	3 (52)	185 (302)	132 (195)	3,564 (5,377)	2,932 (3,590)
miR-100a[3]	aacccguaguuucgaacaugugu	17,318	0 (0)	1,262 (1415)	0 (8)	0 (0)	0 (0)	30 (63)
miR-34-5p	uggcagugugguuagcugguugu	16,136	0 (0)	1007 (1638)	0 (0)	0 (0)	0 (0)	26 (67)
miR-100d-5p	uacccguagcuccgaauaugugu	6,985	0 (0)	293 (543)	0 (12)	0 (0)	0 (0)	0 (2)
miR-50-5p	ugauaugucugauauucuuggguu	3,282	0 (0)	145 (279)	0 (0)	0 (0)	0 (0)	2 (4)
miR-1	uggaauguaaagaaguauguag	3,098	0 (0)	193 (256)	0 (0)	0 (0)	0 (0)	7 (7)
miR-6077-3p	uggaagagauaggaacagagc	2,242	0 (0)	119 (144)	0 (11)	0 (0)	0 (0)	0 (2)
miR-87a-5p	gugagcaaaguuucagguguu	1,501	0 (0)	127 (142)	0 (0)	0 (0)	0 (0)	0 (3)

[1] miRNA reads normalized per million of total miRNA reads detected by miRDeep2
[2] The median of the sequencing reads and the upper 75% limit of the distribution (in brackets) of the total reads is reported for each experimental condition
[3] A shorter miR-100a, lacking the first four nucleotides ("aacc") in the 5' end, was also abundantly detected in our datasets.

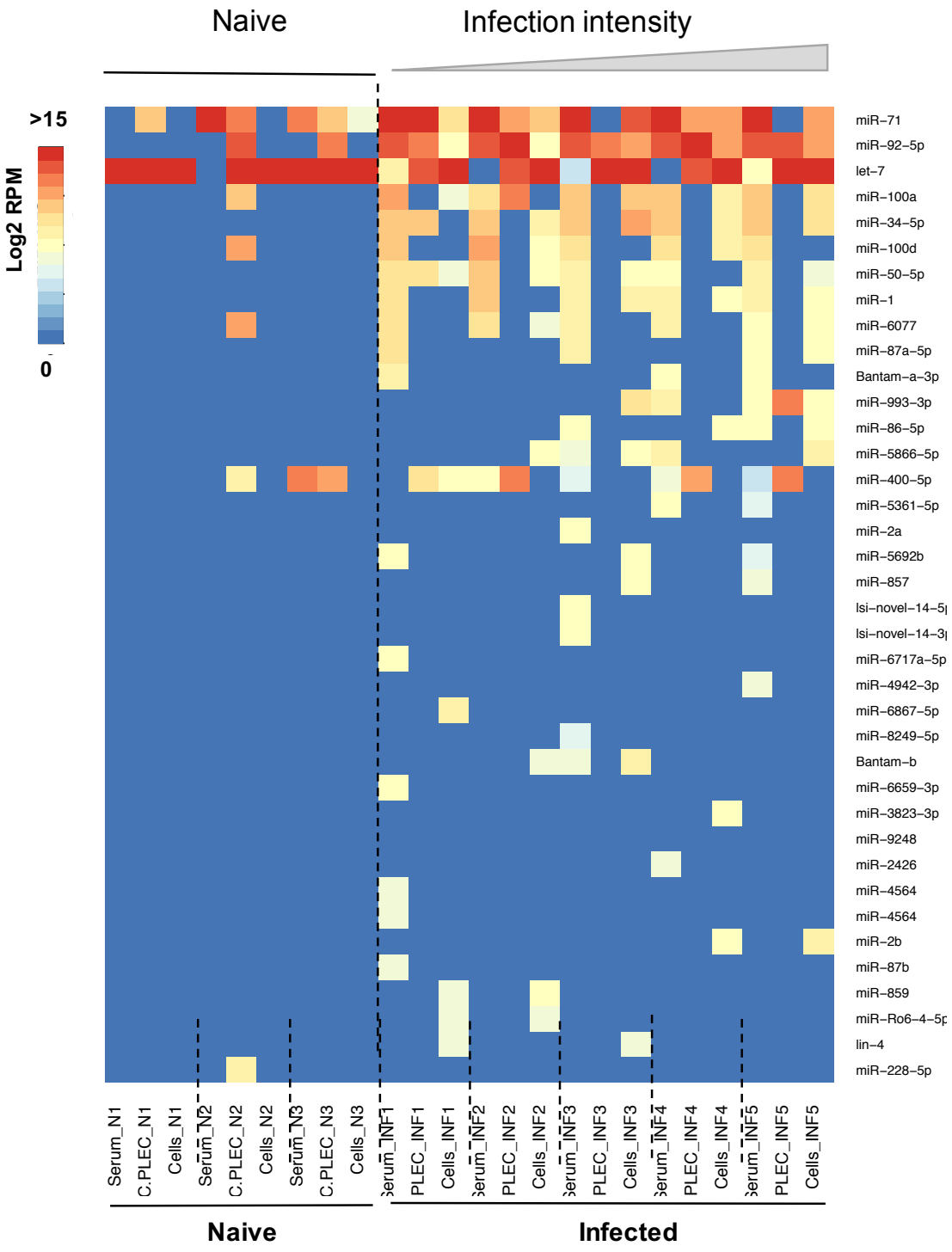

Figure 5.1 Co-localization of *L. sigmodontis*-derived miRNAs *in vivo*. Parasite derived miRNAs were screened by deep sequencing in matched serum, pleural/peritoneal exudates and macrophages from both naïve (n = 3) and *L. sigmdontis*-infected (n = 5) gerbils. The heat map represents the log2-transformed reads per million (RPM) in columns, and samples from naïve (N) and Infected (Inf) samples in rows. Log2 RPM of "0" indicates no detection in that sample. The infected samples were organised from low to high infection intensity, defined as the number of microfilariae counted in the body cavity (PEC/PLEC) exudates (**Supplementary table 5.2**).

5.3.2 Parasite-derived miRNAs are found in murine pleural/peritoneal macrophages during infection

Several reports have demonstrated that the parasite-derived extracellular vesicles (EVs) can be actively internalised by macrophages, thereby affecting their polarisation during infection (Buck, Coakley, Simbari, McSorley, et al., 2014; Coakley, McCaskill, et al., 2017; Zamanian, Fraser, Agbedanu, & Harischandra, 2015). Moreover, it has been shown that the parasite-derived miRNAs found within EVs can manipulate the expression of genes important for the establishment of an adequate innate immune response, including *dusp1* and *il33r* (Buck, Coakley, Simbari, McSorley, et al., 2014). However, these studies have been conducted *in vitro*; hence, evidence of a potential interaction between the parasite-derived miRNAs and macrophages *in vivo* is still lacking. To examine this further in a model where we could phenotype the cells, we analysed macrophages of *L. sigmodontis*-infected BALB/c mice by adhesion to plastic (as described by Helgason, & Miller, 2005), followed by qRT-PCR analysis. Our results show a recovery of between 60% to 100% of $CD11b^{+}/F480^{+}$ from the PLEC/PEC of naïve and infected BALB/c mice (**Figure 5.2 A and B**). Moreover, we found that the signal of several female-derived miRNAs was significantly enriched in macrophages from infected animals but not in naïve controls (**Figure 5.2C**), indicating that the macrophages inside the body cavities are likely to internalize the parasite-derived miRNAs *in vivo*.

BALB/c mice are also susceptible to the infection by *L. sigmodontis* (Maréchal, Le Goff, et al., 1997). Therefore, we hypothesized that, as shown in serum from infected gerbils, we are likely to detect parasite-derived miRNAs in serum from infected BALB/c mice but not from naïve controls. To test this, we prepared small RNA libraries from total RNA purified from naïve and infected sera, and sequencing results analysed as described in chapter 2. A total of 1,188 reads mapped perfectly and unambiguously to the *L. sigmodontis* draft genome and 761 of these derived from 16 nematode miRNAs, found exclusively during the patent stage of the infection (**Table 5.3**). The most abundant miRNAs in serum from infected animals included several members of the miR-10 family (miR-100a, miR-100b, miR-100c), miR-86, bantam (Bantam-a, -b and –c). Interestingly, most of the abundant miRNAs detected in infected gerbil and mouse sera are homologues of those found in extracellular vesicles derived from *H. polygyrus*, including miR-100, bantam, miR-71 and miR-263 (Buck, Coakley, Simbari, McSorley, et al., 2014), and were shown to be enriched in adult and

female secretomes in chapter 3.

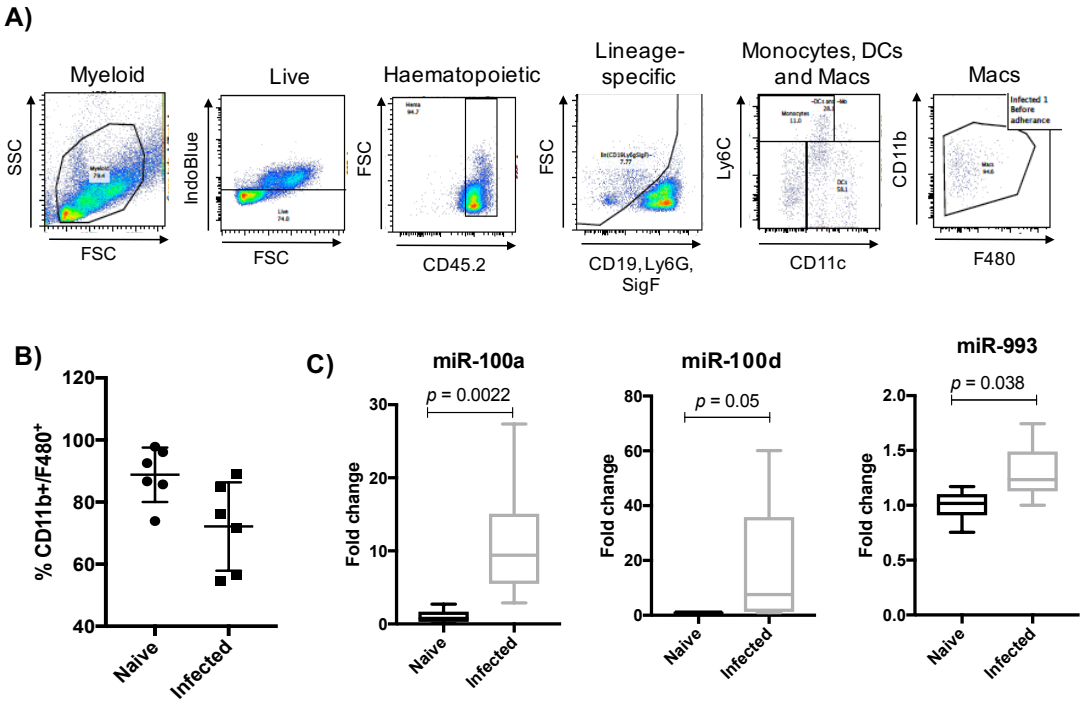

Figure 5.2 *L. sigmodontis*-derived miRNAs in pleural/peritoneal macrophages *in vivo*. A) Flow cytometry gating strategy to phenotype macrophages, B) BALB/c-derived macrophages were purified by adhesion to plastic and phenotype based on expression of surface markers $CD11b^{+}/F480^{+}$ (Naïve = 6 animals; Infected = 6 animals), C) The signal of several female-derived miRNAs were significantly detected in adhered macrophages after extensive washes. (* $p<0.05$; Boxplots represents median ± 95% range; Mann-Whitney test)

Table 5.3 *L. sigmodontis*-derived miRNAs found in mouse serum during the patent stage of the infection (day 60 post-infection)[1]

miRNA name	RNA Mature sequence (5' – 3')	Number of reads (Infected)
miR-100d-5p[2]	uacccguagcuccgaauaugugu	479
miR-86	uaagugaaugcuuugccacagucu	57
Bantam-a-3p	ugagaucauugugaaagcuauu	45
Bantam-b	ugagaucacguuacauccgccu	45
miR-100a[2]	aacccguaguuucgaacaugugu	40
miR-71-5p	ugaaagacauggguagugagacg	32
miR-100c	aacccguagaauugaaaucgugu	22
miR-50-5p	ugauaugucugauauucuuggguu	10
miR-34-5p	uggcagugugguuagcugguugu	8
miR-228-5p[2]	aauggcacuagaugaauucacgg	7
Bantam-c	ugagaucaugccacauccgucu	4
miR-50-3p	ccagcaucucagacguaucggc	3
miR-153	uugcauagucacaaaagugaug	3
miR-87-5p	cgccugggacuucgacucaaccu	2
miR-2	uaucacagccagcuuugaugu	2
miR-5866-5p	uuaccauguugaucgaucucc	2

([1]Reported in Buck, Coakley, et al., 2014). [2] Some of the miRNAs reported in this table have been re-named from the published version to maintain consistency with the sequences and nomenclature used in chapter 2, 3, and 4.

5.3.3 Two parasite-derived miRNAs discriminate *L. sigmodontis* infected BALB/c mice from naïve controls with high sensitivity and specificity

Our *in vivo* data in gerbils show the presence of parasite-derived miRNAs in multiple biofluids, including serum and body cavity exudates, as well as in adherent cells recovered from the site of infection. These results were further confirmed in macrophages from infected BALB/c mice, where the signal of several parasite-derived miRNAs were statistically enriched in these cells when compared to those harvested from naïve controls (**Figure 5.3**). Importantly, we have demonstrated the presence of 16 circulating, parasite-derived miRNAs in serum from infected BALB/c mice during the patent stage of the infection (**Table 5.3**) (Buck, Coakley, Simbari, McSorley, et al., 2014), including several miRNAs that are enriched in the secretome of gAF worms (**Chapter 3**). However, our data does not provide enough evidence to propose a hypothesis to explain how these parasite-derived miRNAs reach different tissues, biofluids and even body compartments during an infection. It is tempting to speculate that the migration of mf from the body cavities (e.g. pleural cavity) to the bloodstream, as well as potential migratory antigen-presenting macrophages, may all function as "vehicles" to facilitate the distribution and dissemination of female-derived miRNAs into the bloodstream. Nevertheless, as discussed in the introduction, there is a need for diagnostic tools that can help to determine the presence of gAF worms during infection. Therefore, to determine the biomarker potential of these filarial-derived miRNAs, we decided to measure the signal of several parasite miRNAs in serum from naïve and infected BALB/c animals by qRT-PCR in two independent experiments. We did not observe differences in the relative abundance of endogenous host miRNAs (miR-16-5p and miR-21-3p) (**Figure 5.3A and table 5.4**). Similarly, the signal of the synthetic miRNA cel-miR-39, spiked at the reverse transcription step to monitor potential inhibition, was not different between naïve and infected samples and was comparable to the spiked water control (**Figure 5.3A and table 5.4**). Receiver Operating Characteristic (ROC) curve analyses were used to statistically assess the performance of the parasite miRNA-diagnostic test, including parameters such as specificity, sensitivity and accuracy of the platform (Florkowski, 2008). Statistical analysis shows that miR-71 and miR-100d can discriminate between infected and naïve animals with high sensitivity (>80%) and specificity (100%) (**Figure 5.3.B**). Moreover, a combination of these two miRNAs robustly

discriminated both experimental groups (>90%/100% Sensitivity/specificity) (**Figure 5.3B**). The results presented in chapter 3 demonstrated that miR-71 is commonly detected in the secretome of multiple developmental stages, whereas miR-100d was enriched in the secretome of gAF worms. However, we failed to observe a correlation between the parasite burden (number of AM, gAF or mf) and the signal of the parasite-derived miRNAs in serum (**Table 5.4**). These results highlight the robustness of the circulating filarial-derived miRNAs as biomarkers for infection.

Table 5.4 In vivo detection of circulating *L. sigmodontis*-derived miRNAs in BALB/c during the patent stage of the infection (day 60 post-infection)

Experiment 1 Naive	Adult males	Adult females	Mf[2]	mmu-miR-16-5p[3]	mmu-miR-21-3p[3]	Filarial miR-71[3]	Filarial miR-100d[3]
1	0	0	0	1.22	0.78	1.41	1
2	0	0	0	0.51	1.16	0.73	1
3	0	0	0	0.38	0.53	0.65	1
4	0	0	0	1.86	1.61	0.93	1
5	0	0	0	1.66	1.43	1.43	1
6	0	0	0	0.35	0.47	0.81	1
Infected							
1	ND[1]	ND[1]	0	1.84	4.04	0.47	10.37
2	4	4	67	0.029	0.39	127.5	29.04
3	ND[1]	ND[1]	0	1.92	3.99	10.36	4138.8
4	0	4	10	0.15	1.20	495.9	260333.2
5	2	1	10	0.54	4.64	23.7	84110.6
6	4	8	53	0.11	0.85	22.01	56.89
Experiment 2 Naive	**Adult males**	**Adult females**	**Mf[2]**	**mmu-miR-16-5p[3]**	**mmu-miR-21-3p[3]**	**Filarial miR-71[3]**	**Filarial miR-100d[3]**
1	0	0	0	0.56	0.70	0.19	0.92
2	0	0	0	0.60	0.50	0.20	0.99
3	0	0	0	0.52	0.53	0.20	0.97
4	0	0	0	2.05	2.32	0.21	1.04
5	0	0	0	1.64	1.38	0.21	1.04
6	0	0	0	0.61	0.59	0.21	1.01
Infected							
1	5	3	13	0.58	0.71	39.23	0.88
2	1	4	0	0.47	0.52	0.17	0.84
3	0	3	14	2.39	2.30	594.5	7767.4
4	1	4	89	0.49	0.61	146.5	783.4
5	0	5	25	0.89	0.90	2855.3	24019.2
6	3	5	3	0.91	1.58	0.21	1.06

[1] ND = not detected due to the presence of granulomas.
[2] Number of microfilariae in 30 µL of blood
[3] Fold change compared to the average of the naïve group

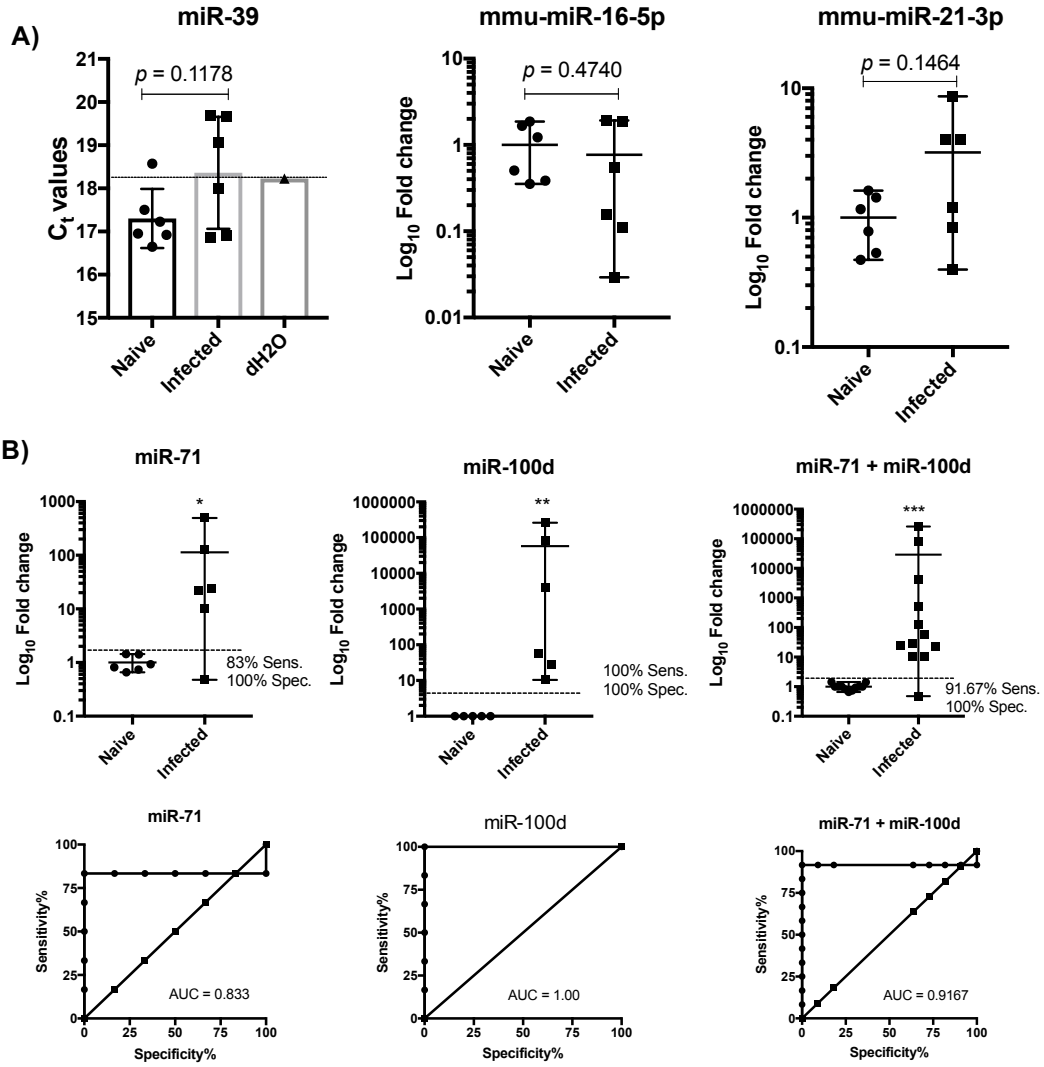

Figure 5.3 Biomarker potential of two *L. sigmodontis*-derived miRNAs. Serum from naïve (n = 6) and infected (n = 6) animals were obtained at day 60 post-infection and the signal of two parasite-derived miRNAs was measured by qRT-PCR. A) Signal of the synthetic cel-miR-39, as well as endogenous host mmu-miR-16-5p and mmu-miR-21-5p suggest a similar amplification efficiency and relative total RNA content between naïve and infected samples. B) Using either miR-100d or miR-71, or a combination of both parasite miRNAs, it is possible to discriminate between experimental groups with >80% sensitivity and 100% specificity. (* p <0.05; ** p <0.005; *** p < 0.0005; Kolmogorov-Smirnov test)

5.3.4 *O. ochengi* small RNAs are present in bovine nodule fluids

Widely distributed in west Africa, *Onchocerca ochengi* is a closely related species to the human pathogen *O. volvulus*, and is the causative agent of bovine onchocerciasis (Trees, 1992). Owing to their geographical distribution, vector transmission and morphology of mf and infective stage, *O. volvulus* and *O. ochengi* were considered sister species, with some evidence of sympatric speciation within the *Onchocerca* genus (Morales-Hojas, Cheke, et al., 2006). Indeed, both *O. volvulus* and *O. ochengi* exhibit similar biological features, including genomes (Cotton, Bennuru, et al., 2016), proteomes (Armstrong, Xia, et al., 2016), and reproductive behaviour. In this regard, *O. ochengi* adult worms induce the formation of subcutaneous nodules (onchocercomata), as observed in *O. volvulus* infections (Hildebrandt, Eisenbarth, et al., 2014). For these reasons, *O. ochengi* offers an attractive opportunity to study specific aspects of the biology of *Onchocerca spp* infections that, for ethical reasons, are not possible to test in *O. volvulus* (Trees, 1992).

The onchocercoma fluid is a rich source of parasite material and can be regarded as a source of ES products secreted by worms under physiological conditions (Armstrong, Xia, et al., 2016). Given the biological relevance of this material, we wanted to address what is the parasite-specific small RNA content of onchocercomata fluids. As discussed in chapter 2, total RNA from 20 μL of *O. ochengi* nodular fluid was purified using miRNeasy mini kit (Qiagen) and analysed for total small RNA content using the Agilent Bioanalyzer. Two populations were observed between 20-30 nt and 50-70 nt (**Figure 5.4**), similar to the small RNA profile previously observed for the *in vitro* ES products from larval and adult stages of *L. sigmodontis* (chapter 3), and *in vitro* secretion products of the gastrointestinal nematode *H. polygyrus* (Buck, Coakley, Simbari, McSorley, et al., 2014). Small RNA libraries were prepared using total RNA as input, sequenced to identify the small RNAs between 17 and 40 nt and analysed as described in chapter 2. To further increase confidence and stringency of our bioinformatics pipeline, we required that only reads containing the 3' adapter and aligned along their full length to the bovine or *O. ochengi* draft genomes were included. Since some small RNA sequences can be post-transcriptionally edited this method may miss true positives (Ebhardt, Tsang, et al., 2009). Following these criteria, a total of 15,022,278 reads were analysed of which 11,912,199 aligned to the bovine genome and 157,633 aligned to the *O. ochengi* genome (**Table 5.5**). A total of

6,301 reads that could be equivalently aligned to both genomes were not included in the analysis since their origin could not be determined.

The small RNA content was initially classified based on sequence identity (assessed using BLAST (Altschul, Gish, et al., 1990) to known RNA classes in Rfam and revealed a predominance of tRNA fragments (**Table 5.5**), as previously observed in other extracellular fluids (Dhahbi, Spindler, et al., 2013; Hoy, Lundie, et al., 2014; Yeri, Courtright, et al., 2017). Identification of miRNAs was carried out using miRdeep2 which not only identifies matches to miRNAs already present in miRBase but also identifies novel miRNAs based on the ability of the reads to map to potential hairpins in the genome (Friedländer, Mackowiak, et al., 2012). From this analysis, a total of 62 mature miRNAs were identified including 23 that are identical to previously described nematode miRNAs (primarily *Ascaris suum* and *Brugia malayi*), 18 that are only identical in their seed sites (nucleotides 2 to 8) to other nematode miRNAs, and 21 of which did not share homology in their seed sites (**Supplementary Table 5.1**). These 21 derived from 16 novel pre-miRNA candidates that are not conserved in other nematodes. The top 20 most abundant *O. ochengi* miRNAs detected in nodular fluids are reported in **Table 5.6**. Six of these have reads mapping specifically to both arms of the hairpin with 3' overhangs (**Figure 5.5**) and we therefore assigned confidence to their classification as Dicer-derived miRNAs. To determine whether these small RNAs are conserved in the closely related human parasite *O. volvulus*, miRdeep2 analysis of the reads sequenced in the *O. ochengi* nodule material was carried out using the *O. volvulus* draft genome as the mapping substrate, allowing for up to 2 mismatches. All sequences aligned perfectly and were derived from hairpins, apart from three miRNAs (Ooc-novel-3-3p, Ooc-novel-15, Ooc-miR-49) where a 1 nt mismatch was present (**Supplementary Table 5.1**). The most abundant miRNAs detected in the nodular fluids belong to several miRNA families, including bantam, miR-279, lin-4/miR-125 and miR-10 (**Table 5.5**), accounting for more than 95% of the total miRNA reads in nodular fluids.

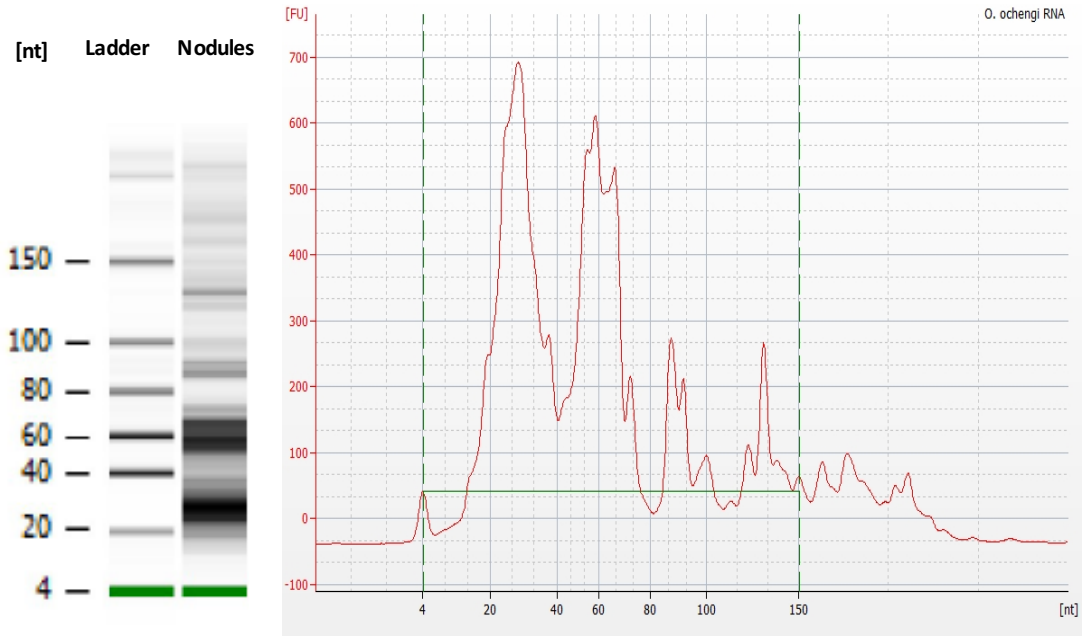

Figure 5.4 Small RNA profile of onchocercoma fluids from cattle infected with *O. ochengi*. Gel and electropherogram of total RNA (1µL) from nodule fluids based on a Agilent Bioanalyzer small RNA chip (Reported in Quintana, Makepeace, et al., 2015).

Table 5.5 Classification of small RNAs from onchocercoma fluids from cattle infected with *O. ochengi* infection[1]

Trimmed reads	**15,022,278**
***B. taurus* genome match**	11,912,199
Unambiguous reads	11,905,898
rRNAs	20,836
tRNAs	11,335,037
miRNAs	382,791
Other Rfam	25,716
***O. ochengi* genome match**	157,633
Unambiguous	151,332
rRNAs	2,616
tRNAs	120,733
miRNAs	11,455
Other Rfam	2,344

([1]Reported in Quintana, Makepeace, et al., 2015).

Table 5.6 Top 20 most abundant miRNAs detected in onchocercoma fluids from cattle infected with *O. ochengi*

miRNA	RNA Sequence (5' – 3')	miRDeep score	*O. ochengi* genomic scaffold	Total reads	Enrichment in *L. sigmodontis* in *vitro* secretome[1]
ooc-bantam-a-3p	ugagaucauugugaaagcuauu	5	>nOo.2.0.Scaf00917_323	4,924	gAF
ooc-miR-279a	ugacuagaaccauacucagcu	5.3	>nOo.2.0.Scaf00355_160	1,822	ND
ooc-novel-7	uuaccugauuagacucuucgc	5.1	>nOo.2.0.Scaf03280_769	1,276	ND
ooc-lin-4-5p	ucccugagaccucugcugcga	272.4	>nOo.2.0.Scaf01957_508	524	Adult worms
ooc-miR-100d-5p	uacccguagcuccgaauaugugu	5.3	>nOo.2.0.Scaf01476_420	375	gAF
ooc-miR-5364-5p	cgagguauuguuuauuggcuga	5.3	>nOo.2.0.Scaf02997_686	341	gAF
ooc-novel-1-5p	acuguaucgguugugacaugu	129	>nOo.2.0.Scaf19423_1506	247	ND
ooc-miR-5360	acgaaucgucgaaucggaugucu	5.1	>nOo.2.0.Scaf00322_144	203	Adult worms
ooc-miR-2a	uaucacaggccugaugcagcuagc	5.2	>nOo.2.0.Scaf06237_1056	165	ND
ooc-novel-8	augcaauuguaguucagaucauu	5.2	>nOo.2.0.Scaf00261_135	163	ND
ooc-bantam-b	ugagaucacguuacauccgucu	5.1	>nOo.2.0.Scaf11849_1321	157	ND
ooc-bantam-c	ugagaucaugucacauccgucu	3	>nOo.2.0.Scaf10764_1296	147	ND
ooc-miR-239	uuuguacuucggcuaaggugcug	5.1	>nOo.2.0.Scaf02964_682	128	gAF
ooc-novel-9	ucacuuggaguacuauucacu	4.3	>nOo.2.0.Scaf09890_1264	109	ND
ooc-novel-2-5p	ugaaucgugauuuuauuugaucu	46.1	>nOo.2.0.Scaf00874_319	80	ND
ooc-novel-3-5p	aggaauaguuguucacgguagagc	41.3	>nOo.2.0.Scaf06237_1053	75	ND
ooc-miR-71-5p	ugaaagacauggguagugagacg	5.2	>nOo.2.0.Scaf00541_22	49	Multiple
ooc-miR-240	uacuggccuuucaaacucuggga	5	>nOo.2.0.Scaf00527_220	48	ND
ooc-novel-10	aucccgacucguggcaccaaauc	5.5	>nOo.2.0.Scaf01927_501	48	ND
ooc-miR-5838	ugaguauuuucgguuucgcauc	4.4	>nOo.2.0.Scaf02307_562	43	AM

[1] Based on DESeq2 results presented in chapter 3. Lifecycle stage enrichment was established based on differential expression, as discussed in chapter 2 and 3. gAF = gravid adult females, AM = adult males, Multiple = miRNAs that were similarly detected in multiple secretomes (e.g. adult worms and mf). ND = not detected as differentially enriched by DESeq2. Note: miR-100d has been re-named from the published version to maintain consistency in the miRNA nomenclature used in chapters 2, 3, and 4.

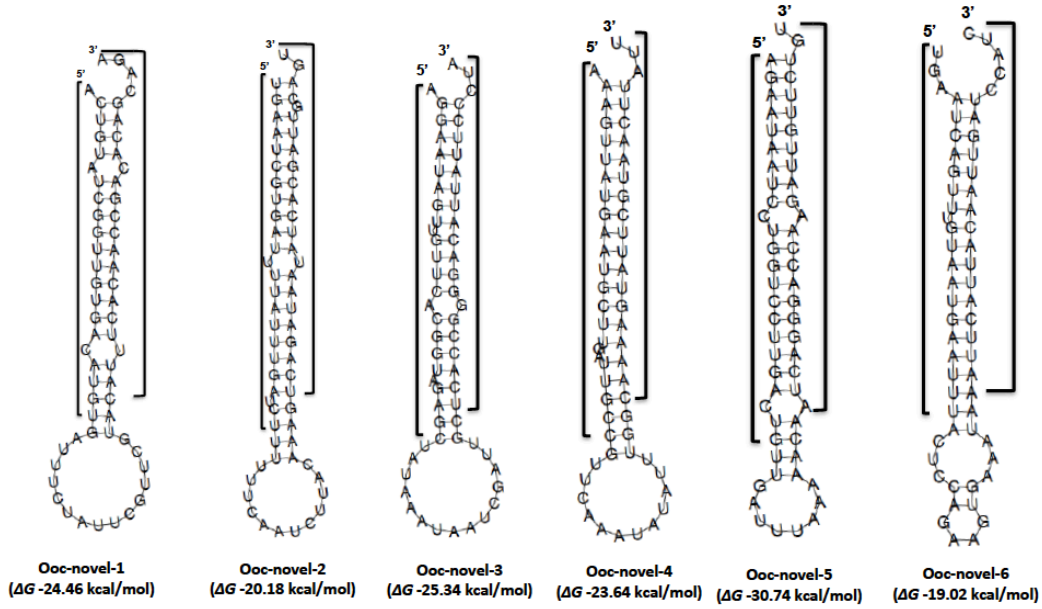

Figure 5.5 Novel *O. ochengi* miRNAs identified in bovine onchocercoma fluids and their predicted pre-miRNA secondary structure. Predicted secondary structures of the novel pre-miRNAs identified by presence of reads mapping to both 5p and 3p arms (indicated in brackets). The minimum free energies (MFE) are indicated according to prediction by RNAfold (Reported in Quintana, Makepeace, et al., 2015).

5.3.5 Six parasite-derived miRNAs are detected in serum or plasma of humans infected with *O. volvulus*

To date very little is known about the factors that dictate the stability of extracellular RNA in fluids or whether and how these molecules traffic within the body. The nodules are highly vascularized (George, Palmieri, et al., 1985) and provide a direct route to the blood system for parasite-derived molecules. To determine whether *O. volvulus*-derived miRNAs are present in serum and plasma, we carried out two parallel analyses of samples pooled from infected humans obtained from two geographically relevant regions in Africa, Cameroon (Zouré, Noma, et al., 2014) and Ghana (Turner, Osei-Atweneboana, et al., 2013), and compared these to pooled endemic or European controls. Small RNA sequencing libraries were prepared, sequenced and analysed as above. A total of 10-25 million reads were analysed per sample, of which 39-51% mapped to the human genome and 1.0-1.5% mapped to the draft *O. volvulus* genome (**Table 5.7**). Most of the reads from human serum that mapped to *O. volvulus* were identified as rRNA fragments, but these were detected at comparable levels in European control and infected samples (**Table 5.7**). It is possible these are of human origin but are edited or that they derive from other organisms or dietary sources as shown in several systems (Beatty, Guduric-fuchs, et al., 2014; Wang, Li, et al., 2012). Similarly, the source of many reads that map to *O. volvulus* genome and are annotated as tRNA fragments (Dhahbi, Spindler, et al., 2013) cannot be reliably assigned (**Table 5.7**).

Here we focus on the miRNAs detected in the serum from humans testing positive for *O. volvulus* that can be assigned a nematode origin. From the combined datasets, we identify a total of six *O. volvulus* miRNAs (**Table 5.8**). The nematode origin of these is evident from several criteria: 1) they map perfectly to regions that fold into hairpin structures within the *O. volvulus* genome; 2) they are not other classes of sncRNA and 3) they are not present in the sera of European controls. Of the six miRNAs identified, all were identical to the *O. ochengi* miRNAs found in nodules (**Table 5.6, Table 5.8 and supplementary figure 5.1**). Two of the miRNAs, miR-71 and lin-4, are detected in infected samples from both Ghana and Cameroon but neither endemic nor European controls. Two are detected only in the infected pooled sample from Ghana (miR-100d, miR-87) and two of these are present in infected and endemic control samples from Ghana (miR-100a, bantam-a). Of note, the sequences of miR-100a and

miR-100d are identical to the members of the miR-100s sequence found in ES products from *L. sigmodontis*, serum and adherent macrophages from *L. sigmodontis*-infected BALB/c mice, serum from *L. sigmodontis*-infected gerbils, and nodule fluids from *O. ochengi* onchocercomata. Similarly, As the endemic control sample was a pool of 13 individuals, it is possible that these miRNAs could derive from an individual misdiagnosed as negative for onchocerciasis or co-infected with other co-endemic nematode parasites in these regions. As mentioned in previous sections, miR-92 and let-7 are highly conserved across the animal kingdom (including vertebrates and nematodes) and therefore cannot be confidently assigned as exclusively derived from nematodes.

Table 5.7 Classification of small RNA reads in human serum and plasma from uninfected and infected individuals[1]

Human serum/plasma	Uninfected serum (European control)	Infected serum (Cameroon)	Uninfected plasma (Ghana)	Infected plasma (Ghana)
Trimmed reads	**25,519,512**	**23,734,119**	**24,992,446**	**10,015,190**
Human genome match	**9,998,552**	**9,331,113**	**12,936,180**	**4,791,645**
Unambiguous	9,937,398	9,102,817	12,846,400	4,742,963
rRNA	15,854	26,512	13,022	6,744
tRNA	2,568,803	82,382	6,442,858	1,724,586
Y RNA	1,149,988	2,408,124	1,004,222	476,464
other Rfam	198,310	33,516	8,497	3,791
miRNA	5,589,367	5,924,748	5,266,797	2,472,450
***O. volvulus* genome match**	**304,991**	**583,693**	**328,590**	**157,005**
Unambiguous	243,837	355,397	238,810	108,323
rRNA	140,174	108,351	132,900	49,797
tRNA	358	400	1,884	1,929
Y RNA	50	0	0	0
other Rfam	2,434	2,712	3,013	688
miRNA	0	75	344	743

([1]Reported in Quintana, Makepeace, et al., 2015)

Table 5.8 Nematode-derived miRNAs detected in serum and plasma from individuals who tested positive for *O. volvulus*[1]

miRNA	RNA sequence (5' – 3')	Genomic coordinates	Uninfected serum (European control)	Infected serum (Cameroon)	Uninfected serum (Ghana)	Infected serum (Ghana)
miR-71	ugaaagacauggguagugagac(g)	>OVOC.OM1b_40, >OVOC.OM1b_58	0	43	0	98
lin-4-5p	ucccugagaccucugcugcga	>OVOC.OM4_217, >OVOC.OM4_213	0	32	0	73
miR-100a	aacccguaguuucgaacaugugu	>OVOC.OM1a_27	0	0	121	314
miR-87	gugagcaaaguuucagguguuc	>OVOC.OM2_148	0	0	0	85
miR-100d-5p	uacccguagcuccgaauaugugu	>OVOC.OM1a_25	0	0	0	102
bantam-a-3p	ugagaucauugugaaagcuauu	>OVOC.OM2_134	0	0	223	71

[1] Numbers indicate read counts for each miRNA within each dataset (Reported in Quintana, Makepeace, et al., 2015). Brackets in the miR-71 sequence indicate heterogeneity in the 3' terminal nucleotide between datasets. Note: Both miR-100s reported in this table have been re-named from the published version to maintain consistency with the sequences and nomenclature used in chapter 2, 3, and 4.

5.3.6 Common and distinct circulating miRNA signatures in filarial infections

So far, we have identified parasite-derived miRNAs in a wide range of host biofluids, including nodule fluids from *O. ochengi* infection, *L. sigmdontis* infected mouse and gerbil serum, and *O. volvulus* infected human serum and plasma. Of these, four of the 16 miRNAs detected in infected mouse serum are identical to the *O. volvulus* miRNAs detected in human serum (mir-71, two miR-100 members, and one bantam family member) and one is derived from the other arm of the hairpin of a *O. volvulus* miRNA (miR-87). Six of these are identical to *O. ochengi* miRNAs found in the nodule fluid and three (miR-50-3p and Bantam-b, -c) differ by 1 nt outside of the seed region (**Figure 5.6**). Strikingly multiple miR-100 and bantam family members also dominated the ES product of *L. sigmodontis* gAF worms (chapter 3) as well as the secretome of the gastrointestinal nematode *H. polygyrus* (Buck, Coakley, Simbari, McSorley, et al., 2014). As demonstrated in chapter 3, the miR-100 and bantam miRNAs identified in ES products from several parasites have distinct sequences outside of their seed regions from other organisms, including vertebrates. To compare relative quantities across the datasets and to qualify our limit of detection, we used total host miRNA read counts in the same samples as a normalizer. The individual parasite miRNAs are detected at a range of 26 to 12,863 reads per million bovine miRNA reads (*O. ochengi* nodule fluid), 5 to 127 per million human miRNA reads (serum/plasma from *O. volvulus* positive individuals) and 2 to 367 reads per million mouse miRNAs (serum from *L. sigmodontis* infected mice) as shown in **Table 5.9**. We anticipate these relative proportions will vary depending on the intensity of infection. Importantly, this provides a baseline for comparing relative levels of parasite miRNAs between studies and understanding the limits of detection in each study.

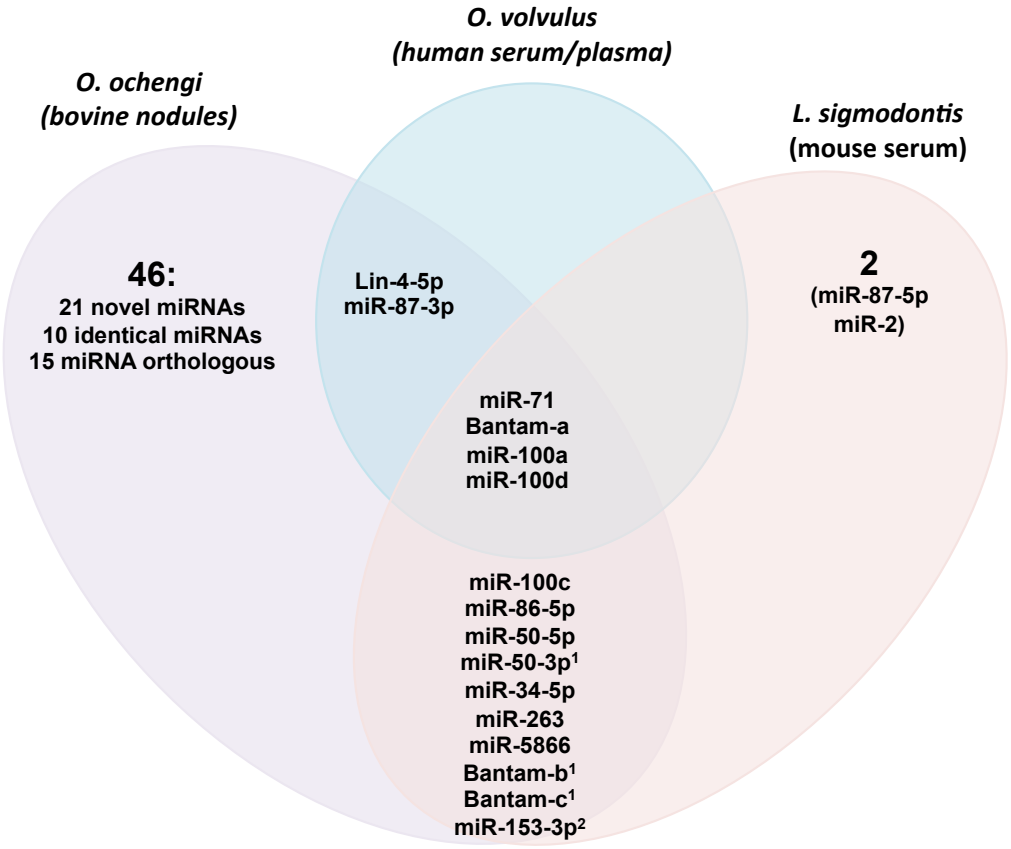

Figure 5.6 Venn diagram depicting overlap in extracellular parasite-derived miRNAs identified in filarial infections. Overlapping mature miRNAs sequences identified in cattle nodule fluids (*O. ochengi*), serum/plasma from infected patients in Cameroon and Ghana (*O. volvulus*) and infected mouse serum (*L. sigmodontis*). [1]These miRNAs differ by 1 nt outside the seed sequence (nt in position 2-8) in *L. sigmodontis* and *O. ochengi*. [2]miR-153-3p is identical to mammalian miR-153-3p from nucleotides 1-21. The miRNAs assigned as "identical" are those that showed 100% homology with miRNAs found in vertebrates, whereas orthologue miRNAs are those that shared the same seed sequence and are thought to be functionally similar (Reported in Quintana, Makepeace, et al., 2015).

Table 5.9 Relative abundance of nematode miRNAs in biofluids in comparison to host miRNAs

miRNA	RNA sequence (5' – 3')	*O. ochengi* Nodules	*O. volvulus* (Ghana)	*O. volvulus* (Cameroon)	*L. sigmodontis*
Ooc-miR-71-5p	ugaaagacauggguagugagacg	117.6	39.6	7.3	25.1
Ooc-lin-4-5p	ucccugagaccucugcugcga	1,355.8	29.5	5.4	ND (<0.8)
Ooc-miR-100a[1]	aacccguaguuucgaacaugugu	86.2	48.9	ND (<0.3)	31.4
Ooc-miR-87	gugagcaaaguuucagguguuc	26.1	34.4	ND (<0.3)	ND (<0.8)
Ooc-miR-100d-5p[1,2]	uacccguagcuccgaauaugugu	979.6	127.0	ND (<0.3)	376.0
Ooc-bantam-a-3p[2]	ugagaucauugugaaagcuauu	12,863.4	28.7	ND (<0.3)	35.3
Ooc-miR-86	uaagugaaugcuuugccacagucu	65.3	ND (<0.8)	ND (<0.3)	44.7
Ooc-miR-228-5p[1]	aauggcacuagaugaauucacgg	44.4	ND (<0.8)	ND (<0.3)	5.5
Ooc-miR-50	ugauaugucugauauucuuggguu	31.3	ND (<0.8)	ND (<0.3)	7.9
Ooc-miR-34-5p	uggcagugugguuagcugguugu	70.5	ND (<0.8)	ND (<0.3)	6.3
Ooc-miR-5866-5p	uuaccauguugaucgaucucc(a)[3]	70.5	ND (<0.8)	ND (<0.3)	1.60
	Total host miRNAs	**382,791**	**2,472,450**	**5,924,748**	**1,273,839**

[1] Some of the miRNAs reported in this table have been re-named from the published version to maintain consistency with the sequences and nomenclature used in chapter 2, 3, 4.
[2] Also detected in healthy endemic Ghanaian controls.
[3] Brackets indicate heterogeneity in the 3' terminal nucleotide between datasets
ND = not detected; the limit of detection is shown in brackets, based on the number of total host miRNAs sequenced, and assuming that 2 reads are required to identify a parasite sequence.

5.3.7 Detection of parasite-derived miRNAs in human plasma

Our analyses demonstrated that several filarial-derived miRNAs can be readily detected in human serum and plasma by deep sequencing (**Table 5.8**). Moreover, we have demonstrated that two of these miRNAs, miR-71 and miR-100d, can significantly discriminate between naïve and infected animals with high sensitivity and specificity in a murine model of infection (**Figure 5.3 and Table 5.4**). Therefore, we next evaluated whether we can detect these two parasite-derived miRNAs in human plasma using a standard qRT-PCR detection method (**detailed in chapter 2**). A second goal was to determine whether these two miRNAs can specifically be detected in *O. volvulus*-infected patients compared to other filarial infections. To address these questions, we using plasma samples from three non-endemic healthy donors, 6 plasma samples from patients infected with *L. loa*, 7 samples from patients infected with *O. volvulus*, and 5 samples from patients infected with *W. bancrofti* (**Table 5.10**). Using the Ct values of the synthetic cel-miR-39 spike-in, we did not detect the presence of inhibitors in any of the samples tested compared to the spiked water control (**Figure 5.7A**). Similarly, we did not observe differences in the Ct values of the human endogenous hsa-miR-16-5p in serum between healthy donors and infected patients, although the Ct values for hsa-miR-21-5p were higher in non-endemic control samples compared to infected samples (**Figure 5.7B**). Nevertheless, we did not detect reliable Ct values for the two parasite miRNAs (miR-71 and miR-100d) in any of the samples tested (**Figure 5.7C**). These results are consistent with a recent report that describes the challenges of detecting filarial-derived miRNAs in human plasma using conventional qRT-PCR-based methods (Lagatie, Batsa Debrah, et al., 2017).

Table 5.10 Clinical and parasitological information of the human samples used in the pilot qRT-PCR study

Subject ID	Group	Age	Sex	Mf count	No. nodules
215	EC[1]	N/D[2]	N/D	N/D	0
219	EC	N/D	N/D	N/D	0
220	EC	N/D	N/D	N/D	0
38/31	*L. loa*[3]	45	Male	740	0
K/83	*L. loa*	56	Male	700	0
38/106	*L. loa*	40	Female	320	0
L/11	*L. loa*	52	Male	34	0
L/17	*L. loa*	44	Female	25	0
L/84	*L. loa*	49	Female	13	0
L/42	*L. loa*	57	Male	17	0
K/20	*O. volvulus*[4]	11	Female	28	0
K/19	*O. volvulus*	45	Male	81	3
K/5	*O. volvulus*	34	Male	89	1
K/32	*O. volvulus*	10	Male	78	0
38/203	*O. volvulus*	43	Male	32	2
38/205	*O. volvulus*	33	Female	26	0
K/33	*O. volvulus*	10	Male	20	0
39/115	*M. perstans*[3]	64	Male	80	0
39/64	*M. perstans*	30	Male	20	0
38/202	*M. perstans*	26	Female	1	0
36/51	*M. perstans*	35	Male	60	0

[1] EC = endemic control; [2] N/D = not detected or not recorded; [3] mf counts were conducted in blood smears; [4] mf counts were conducted using skin biopsies ("skin snips).

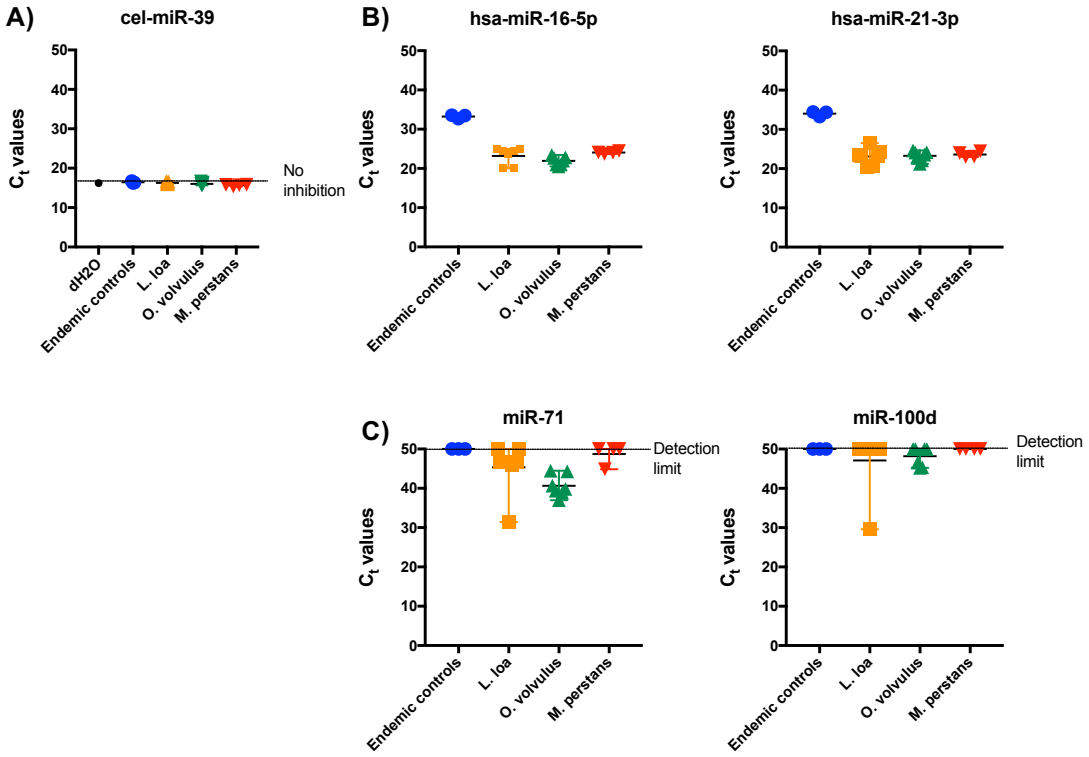

Figure 5.7 Detection of parasite-derived miRNAs in human plasma. The Ct values obtained for different qRT-PCR assays are plotted from healthy endemic controls (*n* = 3), *L. loa*-infected patients (*n* = 7), *O. volvulus*-infected patients (*n* = 7), and *M. perstans*-infected patients (*n* = 4). A) cel-miR-39 is used to monitor the presence of potential inhibitors often found in human plasma, compared to the spiked water control. B) Additionally, two endogenous host miRNAs, hsa-miR-16-5p and hsa-miR-21-5p, are used to determine the relative RNA abundance in the samples. C) Similarly, two filarial miRNAs, miR-71 and miR-100d, were also measured in these samples.

5.4 Summary

- Parasite-derived miRNAs were simultaneously detected in serum, body cavity exudates and adherent macrophage-like cells from gerbils and BALB/c mice
- A total of 16 *L. sigmodontis*-derived miRNAs were detected in serum from infected BALB/c mice during the patent stage of the infection
- Two filarial-derived miRNAs (miR-71 and miR-100d) discriminate between infected animals from naïve controls with 100% specificity and >80% sensitivity.
- A total of 62 nematode-derived miRNAs, including 16 potentially novel miRNAs were detected in *O. ochengi* onchocercomata fluids from infected cattle.
- Six parasite-derived miRNAs were detected in serum and plasma from *O. volvulus* infected patients from Cameroon and Ghana but not in endemic controls. These parasite miRNAs were also detected in nodular fluids from *O. ochengi* infection.
- Despite of the identification of parasite-derived miRNAs in human serum/plasma by deep sequencing, we did not detect reliable signal of parasite-derived miRNAs in human plasma by qRT-PCR.

5.5 Discussion

The discovery that RNA is secreted by parasitic nematodes opens many avenues for further investigation into their functional properties and diagnostic utility. However, the mechanisms or pathways that act as vehicles for dissemination to other tissues or body compartments (e.g. bloodstream) are unclear. Here we have demonstrated that parasite-derived miRNAs, including several miRNAs enriched in the secretome of adult females, are found abundantly in serum of infected animals when compared to body cavity exudates or macrophages. Interestingly, our data suggest that during an infection macrophages may be physiological targets for the miRNAs secreted by *L. sigmodontis*. In chapter 3, we have demonstrated that gravid adult female worms actively release stage- and sex-enriched/specific miRNAs when compared to adult males or mf *in vitro*. Based on these results and the data presented in this chapter, one likely hypothesis to explain the accumulation of parasite-derived miRNAs in serum is they reach circulation as by-products of mf migration. Alternatively, it is plausible that macrophage trafficking to and from the bloodstream can also contribute to this effect, although this remains speculative and merits further investigation. Regardless of the mechanism underlying trafficking of parasite material to the bloodstream, our results also demonstrated that the filarial-derived miRNAs can be readily detected in the serum of animals infected with *L. sigmodontis*. Moreover, we have also demonstrated that sncRNAs derived from *Onchocerca spp*. are present in host tissues, both at a concentrated site of infection (nodule fluid) and in the circulatory system (serum/plasma) of their hosts. Six *O. volvulus* miRNAs were identified in human plasma, all of which are identical to those found in *O. ochengi* nodule fluid, and four of which are also identical to those found in serum of mice infected with the related filarial nematode *L. sigmodontis* (Figure 5.3). This suggests extensive overlap in the identity of extracellular parasite-derived miRNAs in filarial infections and gives confidence in the conserved nature of RNA secretion among these pathogens. This is further supported by several other reports that identified miRNA candidates of potential nematode origin in the biofluids from multiple filarial infections (Quintana, Makepeace, et al., 2015; Tritten, Burkman, et al., 2014; Tritten, Neill, et al., 2014): 4 of the 6 miRNAs that we identify in *O. volvulus*-infected humans are among the 22 miRNA candidates found in *Loa loa*-infected baboons and 2 of the 62 *O. ochengi*

miRNAs in nodules are among the 10 candidates found in bovine plasma (**Supplementary Table 5.1**).

A common feature in all the infections is the presence of miR-71, bantam family and miR-100 family miRNAs (where family is defined based on identical seed sequences, nucleotides 2-8). We previously identified 5 miR-100 family members within the top 20 most abundant miRNAs secreted by *H. polygyrus* (Buck, Coakley, Simbari, McSorley, et al., 2014). The factors dictating the expansion of this miRNA family are not known; miR-100 is one of the oldest miRNAs, having evolved in the last common ancestor of Eumetazoa (Tehler, Høyland-Kroghsbo, et al., 2011). This family has expanded in some animal lineages: in *C. elegans* it is referred to as the miR-51 family and is redundantly required for embryonic development (Shaw, Armisen, et al., 2010) and also involved in developmental timing and buccal cavity formation (Brenner, Kemp, et al., 2012; Shaw, Armisen, et al., 2010). Why members of this family are secreted by parasitic nematodes is unknown and raises interesting questions regarding whether these would interact with host targets (**Figure 5.8**). We also identify bantam family members in serum of both *L. sigmodontis* and *O. volvulus* infected hosts, which show some diversity in sequence between these nematodes species (Chapter 3). One of the bantam members identified here appears conserved and secreted in all Clade III nematodes. We identified this miRNA in *O. ochengi* nodule fluid, serum from *O. volvulus*-infected individuals and serum from mice infected with *L. sigmodontis*. However, this miRNA sequence was also present in endemic controls from the Ghana cohort. This may represent a false negative individual or may occur if another parasite in one or more of the control individuals also secretes bantam orthologues. The secretion of bantam family members also occurs in trematodes; we previously identified a bantam family member (distinct in sequence from those identified here, Figure 5.4) in the serum of mice and humans infected with *S. mansoni* (van der Werf, de Vlas, et al., 2003), and demonstrated its utility as a biomarker for schistosomiasis (Hoy, Lundie, et al., 2014).

Recent studies reported putative *O. volvulus* miRNAs in human serum (Tritten, Burkman, et al., 2014), some of which we annotate here as human ribosomal RNAs (**Supplementary table 5.3**). This does not rule out that human sequences could also serve as a marker of infection, but it is imperative to compare serum from uninfected individuals to avoid false positives and to build a better context for when and why these sequences can be detected. As observed in the *L. sigmodontis* dataset the *O.*

volvulus miRNAs are much less abundant than host miRNAs in serum or plasma: in the Ghana samples, we mapped 743 reads to 6 different nematode-derived miRNAs, compared to approx. 2.5 million human miRNAs reads in the same library. Low-abundance is a challenge when detecting any type of parasite-derived molecule in host fluid. An advantage of the miRNAs is that these can be amplified by PCR prior to detection. However, we failed to detect reliable signals for parasite miR-71 and miR-100a in human plasma, although these were confidently detected in serum from infected mice. These observations may suggest that multiple factors affect the detection of parasite-derived miRNAs in biofluids. In this regard, a recent study addressed the difficulties of detecting filarial-derived miRNAs by conventional SYBR green-based qRT-PCR methods in human serum (Lagatie, Debrah, et al., 2017), which is expected given the relative low abundance shown by our studies. We are currently testing better conditions for a reliable detection of filarial-derived miRNAs in complex human samples, including serum, plasma and urine. We anticipate that methods for enriching parasite material are likely to be advantageous in terms of maximizing the specificity and sensitivity of detection, as well as to increase the robustness for the detection of parasite-derived miRNAs in complex biofluids such as serum. In this regard, in chapter 3 we demonstrated that filarial nematodes are likely to secrete miRNAs in association with extracellular vesicles, consistent with other reports (Buck, Coakley, Simbari, McSorley, et al., 2014; Zamanian, Fraser, Agbedanu, & Harischandra, 2015). Further work is required to understand whether parasite and host miRNAs exist in similar or distinct complexes in host fluids, and/or whether these can be further purified prior to RNA extraction to reduce the possibility of cross-contamination. Other considerations such as costs and training make it unlikely to develop a field-friendly, qRT-PCR based diagnostic method for onchocerciasis, whereas other cheaper methods (e.g. LAMP-based detection of miRNAs) are more suitable platforms to take this work forward (reviewed in Quintana, Babayan, et al., 2016). Finally, the biology and dynamics of secreted miRNAs remain very open topics of research. Our results shed light onto the extent to which different parasite life stages secrete miRNAs, as well as their relative localisation in different biofluids from infected hosts. Moreover, we have also demonstrated that the serum is an attractive and reliable source of material for detection of filarial-derived miRNAs. However, it is still unclear exactly what their half-lives are in host tissues including

blood, the degree to which RNA secretion is regulated, the mechanism by which the small RNAs enter circulation and the stability of each RNA species in different fluids.

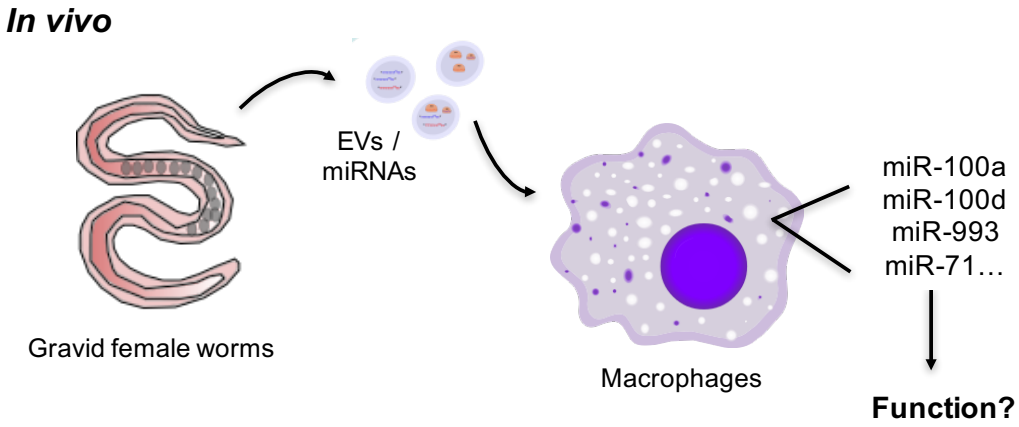

Figure 5.8 Schematic representation of the potential parasite-to-host interactions mediated by EVs and miRNAs *in vivo*. The functions of the parasite-derived miRNAs incorporated by macrophages *in vivo* remain speculative and merits further investigation.

Chapter 6: **Concluding remarks and Future Directions**

6.1 Rational and objectives of this thesis

Filarial infections represent one of the most debilitating diseases in tropical and subtropical regions, imposing a tremendous socio-economic burden on many economically deprived countries (Taylor, Hoerauf, et al., 2010). Recent estimates suggest that nearly 150 million people are either infected or at risk of infection due to high endemicity, mostly in sub-Saharan countries (Hotez, Strych, et al., 2016; Taylor, Hoerauf, et al., 2010). Depending on the pathogen, these infections can be broadly classified into lymphatic filariasis (LF; produced by *Brugia malayi, L. loa* or *Wuchereria bancrofti*) and onchocerciasis, that in humans is only produced by *Onchocerca volvulus* (Babayan, Allen, et al., 2012; Lawrence, & Devaney, 2001; Taylor, Hoerauf, et al., 2010). LF, also known as elephantiasis, is characterised by a swelling of the lymphatic system and a concomitant malformation of the lower limbs (Babayan, Allen, et al., 2012). Onchocerciasis, on the other hand, is characterised by an exacerbated immune response against the mf that normally reside in the skin and ocular tissues, leading to skin depigmentation, severe skin rash, visual impairment and blindness (Babayan, Allen, et al., 2012). Despite huge progress made towards understanding the immunological bases of filarial infections, and the mechanisms by which these parasites harmoniously establish a crosstalk with their hosts, little progress has been made towards the development of an effective and reliable vaccine strategy for prevention (Babayan, Allen, et al., 2012; Hotez, Strych, et al., 2016). Therefore, these diseases are currently treated with the use of anthelminthic compounds such as Ivermectin (IVM), normally distributed through several programs under a mass drug administration (MDA) scheme (Hotez, Strych, et al., 2016). Similarly, cost-effective and reliable diagnostic methods are still lacking, and the detection of microfilariae in either blood smears (for LF) or skin biopsies (for onchocerciasis) remain the gold standard techniques. These diagnostic methods have clear limitations as multiple factors affect the accurate detection of mf in these samples (Discussed by Alhassan, Li, et al., 2015; and Quintana, Babayan, et al., 2016).

Similarly, IVM has potent microfilaricidal activity but has little effect on adult worms, leading to potential misdiagnosis of infection in populations subjected to MDA (Wolstenholme, Maclean, et al., 2016). In this regard, it has been proposed that skin snips are not useful as a diagnostic method in post-MDA surveillance and will not be sufficient to monitor the progress of onchocerciasis elimination programs (Eberhard, Cupp, et al., 2017). Consequently, the development of novel biomarker assays is paramount to successfully achieve the goals of the African and American programme for control and elimination of onchocerciasis and LF (Babayan, Allen, et al., 2012; Coffeng, Stolk, et al., 2013; Murdoch, Asuzu, et al., 2002; Zouré, Noma, et al., 2014). In the context of these control and elimination programmes, an ideal biomarker for filarial infections (or for onchocerciasis) should at least meet two main criteria: 1) It should be capable to account for the presence of reproductively competent adult female worms, and 2) it should be able to diagnose the presence of adult female worms during the sub-clinical stages of the infection (e.g. before the presence of mf in skin snips or blood smears is evident).

An alternative to detect circulating mf in biopsies could be to measure extracellular products released by adult worms that are highly stable in biofluids. The study of these products, broadly termed Excretory/Secretory (ES) products has led to the identification of leading candidates for therapeutic and diagnostic potential (Hewitson, Grainger, et al., 2009). More recently, several studies have demonstrated that the ES products derived from helminths not only contain protein effectors, but also other types of metabolites, including lipids, carbohydrates and microRNAs (miRNAs) (Buck, Coakley, Simbari, McSorley, et al., 2014). Interestingly, these small non-coding RNAs are released within extracellular vesicles and have been shown to be stable in biofluids (Buck, Coakley, Simbari, McSorley, et al., 2014). These are an attractive prospect as biomarkers, as the mature miRNA sequences are often poorly conserved (or absence) between their vertebrate hosts (Alhassan, Li, et al., 2015; Quintana, Babayan, et al., 2016). This could help to identify miRNA sequences that are uniquely derived from the parasite and not from the vertebrate host. Previous studies demonstrated that these circulating parasite-derived miRNAs are readily detectable in serum from *Schistosoma mansoni* infected patients and can discriminate between uninfected and infected patients with high sensitivity and specificity (Hoy, Lundie, et al., 2014). These studies prompted us to further investigate the potential use of miRNAs as novel diagnostics for filarial infections. Using the filarial nematode

Litomosoides sigmodontis, this thesis aims to answer three main questions:

- Can we identify stage- and sex-specific miRNA markers in the secretome of larval and adult stages of *L. sigmodontis*?
- Does IVM affect the secretion of miRNAs by gravid adult female worms? Is the reproductive tissue a likely source for the secretion of the female-enriched extracellular miRNAs?
- Can we identify filarial-derived miRNAs in biofluids from vertebrate hosts? If so, can they be used to discriminate between naïve and infected individuals?

6.2 Conclusions

It is important to stress that at the time of conducting the studies for this PhD thesis, there was a paucity of information regarding the presence of filarial-derived miRNAs *in vitro* or *in vivo*. We demonstrated that both larval and adult stages of *L. sigmodontis* secrete miRNAs *in vitro*, and that the gravid adult females secrete a plethora of miRNAs that, based on statistical analysis with many biological replicates, can be assigned as sex-enriched markers (e.g. miR-100a, miR-100d, miR-5866, miR-228), when compared to adult males and mf. Similarly, other miRNAs were commonly detected in the secretome of adult males and gravid adult females, and can be viewed as stage-enriched markers (miR-5360 and lin-4) when compared to mf. Other miRNAs were detected at a high level in every secretome examined, and could be viewed as common markers to larval and adult stages (e.g. miR-71, miR-92, miR-34). Moreover, we have demonstrated that these extracellular miRNAs are abundantly detected extracellular vesicles (EVs) released from the gravid adult females. Therefore, we propose that miRNAs are released within EVs in filarial nematodes, as demonstrated for many other parasitic nematodes and trematodes (reviewed by Coakley, Maizels, et al., 2015). These results are consistent with studies conducted in the heartworm *Dirofilaria immitis*, which is a close relative to *L. sigmodontis* (Tritten, Clarke, et al., 2016). More specifically, the authors found that the gAF have a prolific capacity to release proteins and miRNAs *in vitro* (Tritten, Clarke, et al., 2016). Importantly, this study also demonstrated the presence of several proteins linked to EVs in the secretomes of larval and adult *D. immitis* (Tritten, Clarke, et al., 2016), further confirming our model in which miRNAs are likely to be released in association with EVs by filarial nematodes. Similarly, a separate study revealed that the *Brugia malayi* infective stage secretes EVs containing miRNAs *in vitro*

(Zamanian, Fraser, Agbedanu, & Harischandra, 2015), consistent with our results from the infective stage of *L. sigmodontis*, and we observed a great deal of overlap between the miRNAs detected in the secretomes from both nematodes. These results highlight the potential regulation of miRNA secretion throughout development, and may reflect specific interactions established by each developmental stage. In the case of the infective stage, it is tempting to speculate that these miRNAs play important roles in mediating communication with the insect vector, whereas other miRNAs from the adult worms or microfilariae might be required for a fine-tuned communication with the vertebrate host. Whilst experimental evidence is lacking with respect to the internalization of miRNAs by host cell *in vivo*, several studies with other helminths have reported that macrophages may be a primary target of the secreted miRNAs and EVs *in vitro*. More specifically, it has been demonstrated that EVs can modulate, and in some instances, impair the phenotypic polarisation of macrophages *in vitro*, and may confer protection against infections (Coakley, McCaskill, et al., 2017; Olmos-Ortiz, Barajas-Mendiola, et al., 2017; Zamanian, Fraser, Agbedanu, & Harischandra, 2015). The results presented in this PhD thesis also provide *in vivo* evidence to support these *in vitro* observations, and we propose that, under physiological conditions, the EV/miRNA-mediated parasite-to-host communication may require a direct crosstalk between parasites and macrophages. It is known that the balance in the communication between parasites and immune cells eventually leads to the establishment of chronic infections, observed not only in experimental models of infection (e.g. Gerbils or Balb/c mice), but also in human populations (Babayan, Ungeheuer, et al., 2003). It is intriguing to think that extracellular parasite miRNAs could contribute to this chronicity. It is important to mention, however, that these studies, including the ones presented in this PhD thesis, did not examine the potential role of other immune cells in this dynamic interplay. In this regard, it has been demonstrated that granulocytes such as neutrophils and eosinophils are important for modulating and eliminating filarial infections (Attout, Martin, et al., 2008; Hansen, Trees, et al., 2011; Nfon, Makepeace, et al., 2006; Pionnier, Brotin, et al., 2016; Vatta, Dzimianski, et al., 2014). It is also important to mention that miRNAs are not the most abundant RNA biotype secreted by parasitic nematodes. Our results demonstrated that rRNAs and tRNA fragments are more abundant that miRNAs in the secretomes tested in here. Our overarching goal was to understand and to determine whether parasite-derived miRNA hold promises as biomarkers for filarial infections,

but other RNA biotypes (including other type of small non-coding RNAs such as siRNAs) may also actively play a role in other processes, such as communicating and manipulating host's cells. We have not provided further experimental evidence for any other type of RNAs, and this merits further investigation.

One potential application of these extracellular miRNAs is as biomarkers of infection. In this regard, we have demonstrated in this PhD thesis that filarial-derived miRNAs can be detected in a wide range of biofluids, including *O. ochengi* onchocercomata fluids, serum and plasma from patients infected with *O. volvulus*, as well as serum from gerbils and mice infected with *L. sigmodontis*. Our results are consistent with similar reports demonstrating the presence of filarial-derived miRNAs in serum and plasma from baboons infected with *L. loa*, serum from cattle infected with *O. ochengi*, dog serum infected with *B. pahangi and D. immitis*, and human patients infected with *O. volvulus* (Tritten, Burkman, et al., 2014; Tritten, Neill, et al., 2014). Moreover, we have demonstrated that several of the *L. sigmodontis*-derived miRNAs are likely to derived from gravid adult females or from adult worms, and these can discriminate infected mice from naïve controls with high sensitivity and specificity. Using mouse serum, these parasite-derived miRNAs performed similarly, or even better than the reported specificity/sensitivity for the gold standard technique for filarial detection (mf in skin biopsies or blood smears), or for alternative diagnostic methods (Boatin, Toé, et al., 2002; Guzmán, Awadzi, et al., 2002; Taylor, Keyvan-Larijani, et al., 1987; Thiele, Cama, et al., 2016). However, we and others have encountered difficulties in further developing a miRNA-based diagnostic assay for human samples (Lagatie, Batsa Debrah, et al., 2017). According to a recent report, the relative abundance of these miRNAs is simply too low to be accurately detected by RT-qPCR (Lagatie, Batsa Debrah, et al., 2017), although we could readily detect them by more sensitive approaches such as deep sequencing. Nonetheless, neither next gen sequencing or qRT-PCR are particularly field-friendly and further technological developments are clearly required to take these ideas forward. One possibility to overcome these issues could the development of Loop-mediated Isothermal Amplification (LAMP) for the detection of miRNAs, as shown for the detection of other nucleic acids in infected samples (Alhassan, Makepeace, Lacourse, et al., 2014; Drame, Fink, et al., 2014; Notomi, Mori, et al., 2015; Poole, Tanner, et al., 2012). This method is cost-effective, does not require advanced infrastructure or equipment, and could be conducted by medical or laboratory personal without the need of advanced training (Alhassan, Li, et

al., 2015). One outstanding question is how and when do *L. sigmodontis*-derived miRNAs reach the bloodstream? Our data suggest that *L. sigmodontis*-derived miRNAs are detected in circulation during the patent stage of infection (e.g. when mf are detected in blood) but not during pre-patent stages of infection (e.g. when no mf are detected in blood). However, this was done with a limited number of samples and a relatively low depth of coverage. Given that most of the miRNAs detected in circulation are either enriched in the secretome of adult worms or gravid female worms, it is possible that one likely route for dissemination requires mf migration from the pleural space, where the adult worms reside, to the bloodstream. However, we have not provided experimental evidence to mechanistically support this hypothesis and remains speculative based on the data presented in this thesis. Interestingly, we demonstrated a comparatively lower abundance of parasite-derived miRNAs in the pleural space when compared to serum from infected gerbils. Based on our findings, we also propose that at the site of tissue residency of adult worms, macrophages (and perhaps other immune cells) are either actively involved in mediating the clearance of these products, or are being targeted by the parasites. Nevertheless, this may explain why the parasite-derived are less abundant in the body cavity exudates than in serum. It is unclear, however, if these cells can also act as "vehicles" for dissemination to the bloodstream. Importantly, little is known about the half-life of the parasite-derived miRNAs in circulation, which can be helpful for discrimination between past and ongoing infections. Further investigation into these aspects will shed light into the dynamics of parasite-derived miRNA detection in specific biofluids, and will help to determine whether these can be used to diagnose infections at early time points. Lastly, we have provided important insights into the influence of anthelminthic chemotherapy over miRNA secretion by gravid adult worms. Our data suggest that sub-lethal concentrations of IVM partially impair mf output, as well as protein and miRNA secretion by gravid adult female worms, as soon as 24h of exposure to the drug. We propose that the uterine fluid/reproductive tissue is a likely route for secretion of miRNAs, but not the only one, thus explaining the partial impairment observed in miRNA secretion mediated by IVM. These results also have important implications for diagnostics, and might suggest that at the plasmatic concentrations typically achieved in patients receiving anthelminthic treatment (~50 pM) should not pose a problem for the detection of parasite-derived miRNAs in serum from treated patients. We foresee that a miRNA-based diagnostic

platform for filarial infections might be developed in a post-MDA context, as an alternative to skin snip examinations. However, additionally to the technical limitations for the detection of parasite-derived miRNAs in human biofluids, it is important to test whether other anthelminthic compounds (e.g. Flubendazole, Levamisole, and Doxycycline) influence miRNA secretion by adult worms.

6.3 Limitations and caveats

6.3.1 Chapter 3

In this chapter, we demonstrated that adult female worms secrete a myriad of miRNAs associated with extracellular vesicles. Further statistical analyses demonstrated that a subset of these extracellular miRNAs are enriched in the secretome of adult female worms, whereas a second subset was differentially enriched in adult worms (both male and female) when compared to mf. However, given the lack of enough replication, we could not address whether the reproductive status of the adult female worms ("virgin" female vs. gravid females) could be linked to a subset of extracellular miRNAs. This is relevant to identify miRNAs that are particularly enriched in reproductively active female worms. Although the EV purification method used in this PhD thesis, that is based on solvent-based purification of EVs using cold acetone, rendered reliable results that are consistent with previous publications in extracellular miRNAs secreted by helminths, it is not a gold standard technique used to purify EVs. Importantly, we tried different EV purification methods, including ultracentrifugation, size exclusion, and molecular crowding, but failed to obtain reliable EV preparations with these methods (data not shown). We therefore anticipate that further work is required to improve the method by which EVs are purified from *L. sigmodontis* ES products. This would also enable proteomic analysis on purified EVs, and may lead to the development of antibody-based capture system for cleaner EV purifications in future.

6.3.2 Chapter 4

In this chapter, we demonstrated that sub-lethal concentrations of Ivermectin (IVM), induce an overall impairment in mf output and protein secretion but only partially impair miRNA secretion *in vitro*. However, we did not determine whether the detection of parasite-derived miRNAs is not impaired *in vivo* between untreated and IVM-treated infected mice with *L. sigmodontis*. Based on our *in vitro* results, we hypothesise that IVM will not affect the detection of parasite miRNAs in serum, but

this clearly needs to be tested. Furthermore, the studies presented in this chapter were limited to address the effect of IVM upon miRNA secretion. Other anthelminthic drugs are currently used as part of the mass drug administration (MDA) programmes in Africa and America, including Albendazole and Flubendazole (Fischer, King, et al., 2017; Mackenzie, & Geary, 2011; Taylor, Hoerauf, et al., 2010). Therefore, it becomes important to address whether any of these compounds have a detrimental effect on miRNA secretion. Understanding this aspect is beneficial for the development of a miRNA-based diagnosis platform that is suitable for post-MDA surveillance and control.

6.3.3 Chapter 5

In this chapter, we demonstrated that parasite-derived miRNAs can be readily detectable in macrophages purified from the site of infection *in vivo*. However, from a parasite-to-host crosstalk point of view, we showed limited experimental evidence regarding the functional capacity of parasite-derived miRNAs in macrophages *in vivo*. Therefore, it remains elusive whether the filarial miRNAs detected in macrophages are functionally relevant. A recent report demonstrated that helminth-derived EVs can be internalised by macrophages, impairing the onset of classical and alternative activation macrophages *in vitro* (Coakley, McCaskill, et al., 2017). It is not clear, however, if the parasite-derived miRNAs function in the same manner in both cell subsets, or if their function is dependent upon the context of the cell they target (e.g. classically vs. alternatively activated macrophages). Moreover, we did not extend our studies into other types of immune cells important for the immune response against helminths, such as neutrophils and eosinophils. It would be important to clarify if the macrophages are the sole targets of these extracellular miRNAs, and if so, what host genes are likely to be targeted.

We also demonstrated that parasite-derived miRNAs are found in a wide range of host biofluids, including nodular fluids, serum and plasma. Using the *L. sigmodontis* model, we also demonstrated that two parasite-derived miRNAs, including one miRNA enriched in the secretome of adult female worms (miR-100d), significantly discriminate between naïve and infected animals with high sensitivity and specificity (>80% / 100%). Importantly, we failed to observe a correlation between parasite burden, *L. sigmodontis*-specific antibodies in serum, and signal of parasite miRNAs in serum by qRT-PCR, consistent with previous results in dogs infected with *B. pahangi*

(Tritten, Burkman, et al., 2014). Unfortunately, our qRT-PCR data in human plasma RNA was not as promising as the results obtained in the mouse model, illustrating the technical challenges of detecting lowly abundant parasite material in biofluids. This has been recently discussed by Lagatie, et al. (Lagatie, Debrah, et al., 2017). However, this report did not provide hypotheses to explain these challenges, or solutions to overcome these issues. We propose that one potential explanation for the low abundance of parasite miRNAs in human samples compared to other filarial infections (including *L. sigmodontis* and *B. pahangi*) may be associated with overall parasitic burden, tissue localisation of the adult stages within the host (lymphatic system vs skin), among others. Alternatively, the issues could also be technical, requiring the development of alternative ways to improve the detection of these molecules in complex samples such as serum or plasma. The detection in other biofluids (e.g. such as urine,), as well as the development of other detection platforms (e.g. LAMP) could improve the detection. We foresee that coupling antibody-based capture assays to purify EVs with LAMP methods to detect and amplify RNAs ("IP-LAMP") could improve the detection in human serum and/or plasma.

Using parasite miRNAs as biomarkers, could it be possible to discriminate between filarial species that are co-endemic with *O. volvulus*, or even with other helminth infections that are highly prevalent in the field (e.g. schistosomiasis)? As mentioned before, we could not address this question owing the technical limitations using human plasma. Nevertheless, there is evidence that demonstrates that some parasite miRNA families (e.g. miR-10, Bantam) are also in serum from patients infected with *S. mansoni* (Hoy, Lundie, et al., 2014), and in serum from other filarial infections (Tritten, Burkman, et al., 2014; Tritten, Clarke, et al., 2016; Tritten, Neill, et al., 2014). However, these sequences display heterogeneity in the mature miRNA sequence between parasites (Quintana, Makepeace, et al., 2015). Moreover, it not clear yet if parasite miRNAs can be detected in during soil-transmitted helminth infections (Buck, Coakley, Simbari, McSorley, et al., 2014), but given the high prevalence of these types of infections in the field (Boatin, Basáñez, et al., 2012; Boon, & Vickers, 2013; Padmasiri, Montresor, et al., 2006), this warrants further investigation. Based on the reports thus far describing the parasite miRNA component in biofluids from infected hosts, several of the most abundant miRNAs (e.g. miR-71, miR-100a, miR-100d, lin-4, among others) are commonly detected in several of these infections. Therefore, we foresee that these miRNAs are not likely to robustly discriminate between filarial

species. One possibility would be to develop a "pan-filarial" detection assay, but this approach would not fit the goals of the current control and elimination programmes. Alternatively, we could turn our attention to either RNA sequences classified in here as "novel miRNAs", not reported in other filarial species or vertebrate hosts, or to host miRNAs that could be dysregulated upon filarial infection. We did not address any of these two possibilities but acknowledge that these could also be attractive candidates to put forward towards subsequent studies.

6.4 Future directions

The findings presented in this PhD thesis provide a solid rational for the development of miRNA-based diagnostic platforms for filarial infections of medical and veterinary importance. Moreover, based on the detection of gravid adult female-derived miRNAs in serum, these studies also provide an alternative diagnostic method to mf detection in blood or skin biopsies. We anticipate that this technology could help to monitor the presence of ongoing infections, especially in situations where the mf counts are low or undetectable due to treatment with IVM. These studies also open multiple avenues for research, and thus there are many questions yet to be addressed:

Regarding parasite tissue origin, small RNA trafficking and secretion:

- What factors determine the fate of miRNAs for transport to the extracellular space?
- Which RNA-binding protein partners are necessary for sorting and transport?
- Which specific tissues are involved in release of small RNAs and extracellular vesicles in filarial nematodes?

Regarding parasite-to-host communication:

- Are the parasite-derived miRNAs functional in host cells under physiological conditions? If so, how do parasite-derived miRNAs operate upon internalization by the host cell?
- Do parasite-derived miRNAs require endogenous host factors for functional activity?
- What is the turnover of the parasite-derived miRNAs upon internalization by the host cell?
- Are there other classes of small non-coding RNAs also being secreted by parasites and internalised by host cells?

Regarding diagnostic application of filarial-derived miRNAs:

- What is the half-life of parasite-derived miRNAs in serum?
- Apart from qRT-PCR, which other methods are well suited for a field-friendly miRNA-based diagnostic platform for filarial infection?
- Does the level of parasite-derived miRNA decrease upon infection clearance?
- Is it possible to detect parasite-derived miRNAs in other biofluids such as urine or saliva?

Chapter 7: **Appendices**

7.1 Chapter 3

7.1.1 Supplementary table 3.1 Diversity of RNA biotypes detected in *L. sigmodontis in vitro* ES products by deep sequencing

Supplementary file 3.1.xlsx is available on the CD
This table shows all the RNA biotypes detected in the small RNA libraries prepared from total RNA purified from *in vitro* ES products from larval (A) and adult stages (B) of *L. sigmodontis* using the Rfam package. The reads were first mapped against the *L. sigmodontis* genome draft, the *M. musculus* genome and the *Wolbachia* genome draft, as described in chapter 2 - Materials and methods. The RNA diversity was determined on the reads that mapped perfectly and unambiguously to the *L. sigmodontis* genome draft. The table contains the following samples for the ES from larval stages: two biological replicates for vector-derived L3s (vL3s), two biological replicates host-derived L3s (hL3), two biological replicates of L4 stage (L4s), eight biological replicates of microfilariae (mf). The following samples for the ES products from adult stages are also included in this table: two biological replicates of juvenile adult males (jAM), two biological replicates of pre-gravid adult females (pgAF), ten biological replicates of adult males (AM), and twelve biological replicates of gravid adult female worms (gAF).

7.1.2 Supplementary table 3.2 – Prediction of known and novel *L. sigmodontis* miRNAs in ES products obtained *in vitro*

Supplementary file 3.2.xlsx is available on the CD
This table shows all the predictions (only predictions with a miRDeep2 score > 0 and with > 2 copies are included in the text). The prediction of miRNAs was conducted with reads that mapped perfectly and unambiguously to the *L. sigmodontis* genome draft. We set up an arbitrary cut-off of 100,000 *L. sigmodontis*-specific reads for a robust miRNA identification. Some libraries did not meet this cut-off and were therefore excluded from miRNA identification. The table contains the following samples for the ES from larval stages: two biological replicates for vector-derived L3s (vL3s), and eight biological replicates of microfilariae (mf). The following samples for the ES products from adult stages are also included in this table: two biological replicates of pre-gravid adult females (pgAF), ten biological replicates of adult males (AM), and twelve biological replicates of gravid adult female worms (gAF).

7.2 Chapter 4

7.2.1 Supplementary table 4.1 – RNA diversity and Prediction of known and novel *L. sigmodontis* miRNAs in gravid adult female ES products obtained *in vitro* at early (0 - 24h) and late time points (48 - 72h)

Supplementary file 4.1.xlsx is available on the CD
This table contains two sections:

1) RNA diversity in the *in vitro* ES products from gravid adult female worms harvested at early (0 -24h) and late (48 – 72h) time points, five replicates in total for each time point. The reads were first mapped against the *L. sigmodontis* genome draft, the *M. musculus* genome and the *Wolbachia* genome draft, as described in chapter 2 - Materials and methods. The RNA diversity was determined on the reads that mapped perfectly and unambiguously to the *L. sigmodontis* genome draft.
2) Prediction of known and novel miRNAs in the *in vitro* ES products from gravid adult female worms harvested at early (0 -24h) and late (48 – 72h) time points, five replicates in total for each time point. This table shows all the predictions (only predictions with a miRDeep2 score > 0 and with > 2 copies are included in the text). The prediction of miRNAs was conducted with reads that mapped perfectly and unambiguously to the *L. sigmodontis* genome draft. We set up an arbitrary cut-off 100,000 *L. sigmodontis*-specific reads for a robust miRNA identification.

7.3 Chapter 5

7.3.1 Supplementary table 5.1 - Diversity of RNA biotypes detected in serum, body cavity exudates (PEC/PLEC), and adherent cells from naïve and infected gerbils

Supplementary file 5.1.xlsx is available on the CD
This table shows all the RNA biotypes detected in the small RNA libraries prepared from total RNA purified from serum, body cavity exudates (PEC/PLEC) and macrophages form naïve (n = 3) and *L. sigmodontis*-infected (n = 5) gerbils, using the Rfam package. The reads were first mapped against the *L. sigmodontis* genome draft, the *M. musculus* genome and the Wolbachia genome draft, as described in chapter 2 - Materials and methods. The RNA diversity was determined on the reads that mapped perfectly and unambiguously to the *L. sigmodontis* genome draft.

7.3.2 Supplementary table 5.2 – Prediction of known and novel *L. sigmodontis* miRNAs in serum, body cavity exudates, and adherent cells from naïve and infected gerbils

Supplementary file 5.2.xlsx is available on the CD
This table shows all the predictions (only predictions with a miRDeep2 score > 0 and with > 2 copies are included in the text). The prediction of miRNAs was conducted with reads that mapped perfectly and unambiguously to the *L. sigmodontis* genome draft. We set up an arbitrary cut-off of 10,000 *L. sigmodontis*-specific reads for a robust miRNA identification. Some libraries did not meet this cut-off and were therefore excluded from miRNA identification. The samples included in here are derived from total RNA purified from serum, body cavity exudates (PEC/PLEC) and macrophages form naïve (n = 3) and *L. sigmodontis*-infected (n = 5) gerbils.

7.3.3 Supplementary table 5.3 – miRNA candidates found in *O. ochengi* nodules and comparison to *Loa loa* and *O. ochengi* miRNA candidates reported by Tritten, et al. Molecular & Biochemical Parasitology, 2014.

Supplementary file 5.1.xlsx is available on the CD, or at:
https://static-content.springer.com/esm/art%3A10.1186%2Fs13071-015-0656-1/MediaObjects/13071_2015_656_MOESM2_ESM.xlsx
This table shows all the predictions (only predictions with a miRDeep2 score > 0 and with > 2 copies are included in the text).

7.4 Extracellular *Onchocerca*-derived small RNAs in host nodules and blood

Juan F. Quintana, Benjamin L. Makepeace, Simon A. Babayan, Alasdair Ivens, Kenneth M. Pfarr, Mark Blaxter, Alexander Drebrah, Samuel Wanji, Henrietta F. Ngangyung, Germanus S. Bah, Vincent T. Tanya, David W. Taylor, Achim Hoerauf, Amy H. Buck

Parasites & Vectors (2015), 8(1): 58
Available at: https://parasitesandvectors.biomedcentral.com/articles/10.1186/s13071-015-0656-1#Sec8

Quintana *et al. Parasites & Vectors* (2015) 8:58
DOI 10.1186/s13071-015-0656-1

Parasites & Vectors

RESEARCH Open Access

Extracellular *Onchocerca*-derived small RNAs in host nodules and blood

Juan F Quintana[1], Benjamin L Makepeace[2], Simon A Babayan[3], Alasdair Ivens[1], Kenneth M Pfarr[4], Mark Blaxter[1], Alexander Debrah[5], Samuel Wanji[6], Henrietta F Ngangyung[7], Germanus S Bah[7], Vincent N Tanya[8], David W Taylor[2,9], Achim Hoerauf[4] and Amy H Buck[1*]

Abstract

Background: microRNAs (miRNAs), a class of short, non-coding RNA can be found in a highly stable, cell-free form in mammalian body fluids. Specific miRNAs are secreted by parasitic nematodes in exosomes and have been detected in the serum of murine and dog hosts infected with the filarial nematodes *Litomosoides sigmodontis* and *Dirofilaria immitis*, respectively. Here we identify extracellular, parasite-derived small RNAs associated with *Onchocerca* species infecting cattle and humans.

Methods: Small RNA libraries were prepared from total RNA extracted from the nodule fluid of cattle infected with *Onchocerca ochengi* as well as serum and plasma from humans infected with *Onchocerca volvulus* in Cameroon and Ghana. Parasite-derived miRNAs were identified based on the criteria that sequences unambiguously map to hairpin structures in *Onchocerca* genomes, do not align to the human genome and are not present in European control serum.

Results: A total of 62 mature miRNAs from 52 distinct pre-miRNA candidates were identified in nodule fluid from cattle infected with *O. ochengi* of which 59 are identical in the genome of the human parasite *O. volvulus*. Six of the extracellular miRNAs were also identified in sequencing analyses of serum and plasma from humans infected with *O. volvulus*. Based on sequencing analysis the abundance levels of the parasite miRNAs in serum or plasma range from 5 to 127 reads/per million total host miRNA reads identified, comparable to our previous analyses of *Schistosoma mansoni* and *L. sigmodontis* miRNAs in serum. All six of the *O. volvulus* miRNAs identified have orthologs in other filarial nematodes and four were identified in the serum of mice infected with *L. sigmodontis*.

Conclusions: We have identified parasite-derived miRNAs associated with onchocerciasis in cattle and humans. Our results confirm the conserved nature of RNA secretion by diverse nematodes. Additional species-specific small RNAs from *O. volvulus* may be present in serum based on the novel miRNA sequences identified in the nodule fluid. In our analyses comparison to European control serum illuminates the scope for false-positives, warranting caution in criteria that should be applied to identification of biomarkers of infection.

Keywords: microRNAs, Extracellular RNA, Filarial nematode, Onchocerciasis, Host-pathogen

*Correspondence: a.buck@ed.ac.uk
[1]Centre for Immunity, Infection and Evolution, Ashworth Laboratories, University of Edinburgh, West Mains Road, Edinburgh, UK
Full list of author information is available at the end of the article

Background

Small non-coding RNAs (sncRNAs) have emerged as important regulators of many processes in animals, from development to immunity. MicroRNAs (miRNAs) are the best characterized class of sncRNA which operate by guiding the RNA-induced silencing complex (RISC) to specific messenger RNAs (mRNAs) inside cells, where they inhibit translation and de-stabilize the targeted mRNAs [1]. In parasitic nematodes and flatworms, miRNAs have been shown to have core roles in the physiology of development, differentiation and homeostasis and potentially drug resistance [2]. Studies in the last 7 years have demonstrated that miRNAs can also exist in a cell-free form in extracellular fluids, where they may play endocrine signalling roles, reviewed in [3]. For parasitic species, interacting with this signalling system offers another potential mechanism of host manipulation. We and others have identified miRNAs from nematodes and trematodes in the serum of infected animals [4-6] and initial studies with *S. mansoni* demonstrated the utility of these molecules in distinguishing uninfected and infected humans [4]. The exact origin of these circulating parasite RNAs is unknown, but proteomic analysis of *Dicrocoelium dendriticum* suggests RNAs are associated with exosomes secreted from the parasite surface [7] and it is possible that previously described microvesicles in schistosomes could also contain RNA [8]. Recently we showed that miRNAs are packaged within vesicles secreted by the gastrointestinal nematode *Heligmosomoides polygyrus* and that these derive from the intestine of the nematode. These secreted vesicles (and their cargoes) suppress Th2 innate immune responses *in vivo* and the miRNAs within them are transferred to host cells *in vitro* [9]. Homologues of some of the miRNAs secreted by *H. polygyrus* miRNAs were also found in serum of hosts infected with the filarial nematodes *Litomosoides sigmodontis* [9] and *Dirofilaria immitis* [5]. The miRNAs secreted by nematodes and platyhelminth parasites may be a new axis of host-parasite interaction. Here we characterize the extracellular, parasite-derived miRNAs associated with the important human disease onchocerciasis.

Filarial infections currently affect over 150 million people in tropical and subtropical regions [10], with *Onchocerca volvulus* accounting for approximately 30.4 million [11] of which more than 99% occur in Africa. Onchocerciasis is characterised by skin disease, which can be very severe, and is also the second leading cause of infectious blindness. *Onchocerca ochengi*, a filarial parasite of cattle, is the closest relative of *O. volvulus*, with which it is sympatric, and shares several key features with the human parasite [12,13]. Specifically, *O. ochengi* induces the formation of onchocercomata with very similar histological structure to human nodules [14], and both *O. ochengi* and *O. volvulus* present comparable mating behaviour within the nodules and subsequent Mf production, leading to a patent infection over a similar timescale [12]. The phylogenetic closeness means that the two species have very similar genomes, and thus very closely related (sometimes identical) antigens are present in both. There is evidence of cross-protection [15]. Therefore, *O. ochengi* represents the most relevant experimental model to understand the crosstalk between the parasite and the host in the context of onchocerciasis.

Since 1989, ivermectin has been used in mass drug administration (MDA) programmes to control onchocerciasis in Africa and Latin America. Following the success of the Onchocerciasis Elimination Program for the Americas, which has used MDA of ivermectin alone to abrogate transmission in most endemic foci, the goal of the African Programme for Onchocerciasis Control (APOC; which covers a vastly greater area) has shifted from control to eradication [13]. However, major challenges to this endeavour remain, such as the emergence of ivermectin resistance [16], the potential for severe adverse reactions to ivermectin in loiasis-endemic areas [17], and significant limitations in the accurate and rapid diagnosis of infection [18]. Currently, diagnosis relies on identification of microfilariae in skin snips, which are laborious and notoriously insensitive; additionally, this procedure can cause considerable discomfort. The availability of immunoassays such as the Ov16 serological test [19] has greatly enhanced the ability to detect residual transmission or the re-emergence of infection by using young children as "sentinels"; however, the longevity of immune responses in onchocerciasis renders this assay unsuitable as a tool to confirm elimination of infection from adults [20].

Detection of parasite DNA in a wide variety of bodily fluids by either polymerase chain reaction (PCR) or high-throughput deep sequencing has proven to be successful in the diagnosis of infections caused by *S. mansoni*, gastrointestinal parasitic nematodes [21] and *Leishmania* [22], among others. DNA-based tests thus represent an alternative diagnostic platform to conventional parasitological or antigen-based assays. sncRNAs are another class of diagnostic biomarker that can be amplified and are detectable by qRT-PCR. miRNAs are generally ~22 nt in length and have been detected outside of cells in many mammalian body fluids indicating that these molecules can be rendered highly stable and protected against extreme conditions (i.e. low pH, degradation by extracellular RNases, etc.) [23]. The functional significance of their extracellular existence is still elusive [3,23] but they have been shown to act locally in cell-to-cell communication in mammalian systems [3] and can also be moved from parasite to host via exosomes [9].

Here we report the detection and identification of *Onchocerca* spp. miRNAs from bovine nodular fluid *ex vivo* and the detection of a subset of these molecules in the serum

and plasma of human onchocerciasis patients from Ghana and Cameroon. Several of these miRNAs are orthologs of (and in some cases have identical sequence to) those previously identified in serum of mice infected with *L. sigmodontis* as well as miRNAs secreted by *H. polygyrus in vitro*. Our findings indicate that miRNA secretion by nematodes is conserved in *Onchocerca* species.

Methods

O. ochengi nodule fluid

Bovine skins containing numerous *O. ochengi* onchocercomata were obtained from Ngaoundéré abattoir, Adamawa Region, Cameroon [24]. Freshly excised nodules were screened visually, and discarded if hard or discoloured, which are signs of calcification. Nodules were rinsed in PBS, dried thoroughly, and pricked with a 21G hypodermic needle. The nodules were gently squeezed, and the expressed fluid (~0.5 µl) collected with a micropipette, pooling from >10 nodules per biological replicate. The fluid was spun at 500 g for 5 min to pellet any cellular material or Mf, and the supernatant was stored at -80°C. The samples were shipped to the UK on dry ice and remained frozen prior to analysis.

Human serum samples

Archived human plasma from *O. volvulus* infected and uninfected volunteers was collected as part of a European Union Seventh Framework Programme Research grant, contract 131242 "Enhanced Protective Immunity Against Filariasis (EPIAF)", (http://cordis.europa.eu/project/rcn/94066_en.html). Infected individuals were those with palpable nodules and microfilaridermia by skin snip. Uninfected individuals were defined as persons with no palpable nodules and microfilariae negative skin snips. Serum or EDTA plasma was collected as previously described [25].

Ethics statement

The Committee on Human Research Publication and Ethics at the University of Science and Technology in Kumasi, Ghana, and the Ethics Committee at the University of Bonn, Germany approved the use of archived plasma samples. Collection of sera from onchocerciasis patients in Cameroon was approved by the Cameroon Ethics Committee and the Ministry of Public Health as part of the EU FP7 contract 131242 (EPIAF) and in compliance with the Helsinki declaration on the use of humans in biomedical research. Prior to recruitment, the nature and objectives of the study were explained to potential participants and those who agreed to take part in the study signed a consent form while an assent was obtained from parents or guardians of children who were enrolled in the study. Participation was voluntary.

RNA extraction and library preparation

RNA was extracted from 20 µL of pooled nodule fluids from cattle (*O. ochengi* infection), 200 µL of serum pooled from 12 infected individuals in Cameroon (pooled prior to RNA extraction), or pooled from equal volumes of RNA extracted from 13 infected or 13 uninfected individuals in Ghana (total equivalent of 50 µL plasma). Samples were shipped in liquid nitrogen and stored at –80°C for 3–4 years (Cameroon samples) or 5 years (Ghana samples). The serum was thawed on ice and serum or plasma was spun down at 16,000 g for 5 min at 4°C to remove any additional cell debris. The cleared serum was then transferred to a new 2 mL Eppendorf tube and RNA extracted using the miRCURY RNA isolation kit for Biofluids (Exiqon) according to manufacturers' protocols. In both cases, RNA was eluted in 50 µL of 0.1 mM EDTA. RNA was stored at –20°C prior to further analysis. The relative small RNA content from these samples was determined with 1 µL of total RNA on a Bioanalyzer small RNA chip (Agilent).

Before proceeding with small RNA library preparation from serum or plasma RNA, samples were cleaned up as in [26]. Briefly, 50 µL of eluted RNA was diluted to 100 µL with Nuclease-free MiliQ water followed by addition of 1 µL glycoblue 15 mg/ml (Life technologies), 60 µL of Sodium acetate 3 M pH 5.2 (AppliChem) and 500 µL of ethanol 100%. The RNA was precipitated for 30 min at –80°C then spun at 16,000 g for 30 min at 4°C and washed twice with 75% Ethanol. The pellets were air-dried at room temperature for 15 minutes and re-suspended in 8 µL of 0.1 mM EDTA pH 8.0.

For the analysis of small RNA content in these nodule fluids or human serum and plasma, libraries were prepared from total RNA using the Illumina TruSeq small RNA Preparation kit, according to the manufacturers' protocol, and using 1:10 dilution of adapters. PCR products of the expected molecular weight (140–160 bp) were size selected and sequenced on an IlluminaHiSeq2500 instrument using v3 reagents in Edinburgh Genomics (http://genomics.ed.ac.uk/).

Bioinformatic analysis

All libraries were analysed by first clipping the 3' sRNA adapter using cut adapt [27], searching for at least a 6 base match to the adapter sequence. For analysis of small RNAs, only sequences that contained the adapter, were >16 nt in length, and were present at ≥ 2 copies were retained for further analysis. Sequences were analyzed for alignment to bovine (ftp://ftp.ensembl.org/pub/release-71/fasta/bos_taurus/dna/Bos_taurus.UMD3.1.71.dna.toplevel.fa.gz), human (version hg19), *O.ochengi* (version 1.1; from http://onchocerca.nematodes; unpublished genome sequence from M. Blaxter, B. Makepeace and colleagues) or *O. volvulus* (ftp://ftp.sanger.ac.uk/pub/project/pathogens/Onchocerca/volvulus/

OVOC.V3.fa) using bowtie [28], requiring perfect matches along the full length of the sequence. Sequences were analyzed for known classes of RNA based on Rfam [29] (version 11, obtained from ftp://ftp.sanger.ac.uk/pub/databases/Rfam/11.0/). The best hit with at most two mismatches was used to classify the reads. Analysis of miRNA content was carried out using miRdeep2 [30] with the following settings: 1) reads map perfectly to the genome, 2) cut off -v 1, 3) employing the "-s option" using all mature sequences from mirbase (version 20) [31], 4) only read lengths (18 to 30 nt) were analyzed. Folding analyses of the novel pre-miRNAs detected in nodule fluids were carried out using the RNAfold Vienna package with default settings [32].

Results

O. ochengi small RNAs are present in bovine nodule fluid

RNA from the fluid of nodules of cattle infected with *O. ochengi* was analysed for small RNA content using the Agilent Bioanalyzer. Two populations were observed between 20–30 nt and 50–70 nt (Figure 1), similar to the small RNA profile previously observed for the *in vitro* secretion products of the gastrointestinal nematode *H. polygyrus* [9]. Small RNA libraries were prepared and sequenced to identify the small RNAs between 17 and 40 nt and analysed as previously described [4]. Importantly, to avoid analysis of sequencing artefacts, reads that were present in < 2 copies were discarded and according to default criteria of miRdeep2 alignments only reads > 16 nt were analysed. To further increase confidence in our assignments, we required that reads contained the 3' adapter and aligned along their full length to the bovine or *O. ochengi* draft genomes. Since some small RNA sequences can be post-transcriptionally edited this method may miss true positives. Following these criteria, a total of 15,043,191 reads were analysed of which 11,905,898 aligned to the bovine genome and 151,332 aligned to the *O. ochengi* genome (Table 1). A total of 6,301 reads that could be equivalently aligned to both genomes were not included in the analysis since their origin could not be determined.

The small RNA content was initially classified based on sequence identity (assessed using BLAST [33]) to known RNA classes in Rfam and revealed a predominance of tRNA fragments (Table 1), as previously observed in other extracellular fluids [4,34]. Identification of miRNAs was carried out using miRdeep2 which not only identifies matches to miRNAs already present in miRbase but also identifies novel miRNAs based on the ability of the reads to map to potential hairpins in the genome [30]. From this analysis a total of 62 mature miRNAs were identified including 23 that are identical to previously described nematode miRNAs (primarily *Ascaris suum* and *Brugia malayi*), 18 that are only identical in their seed sites (nucleotides 2 to 8) to other nematode miRNAs, and 21 of which did not

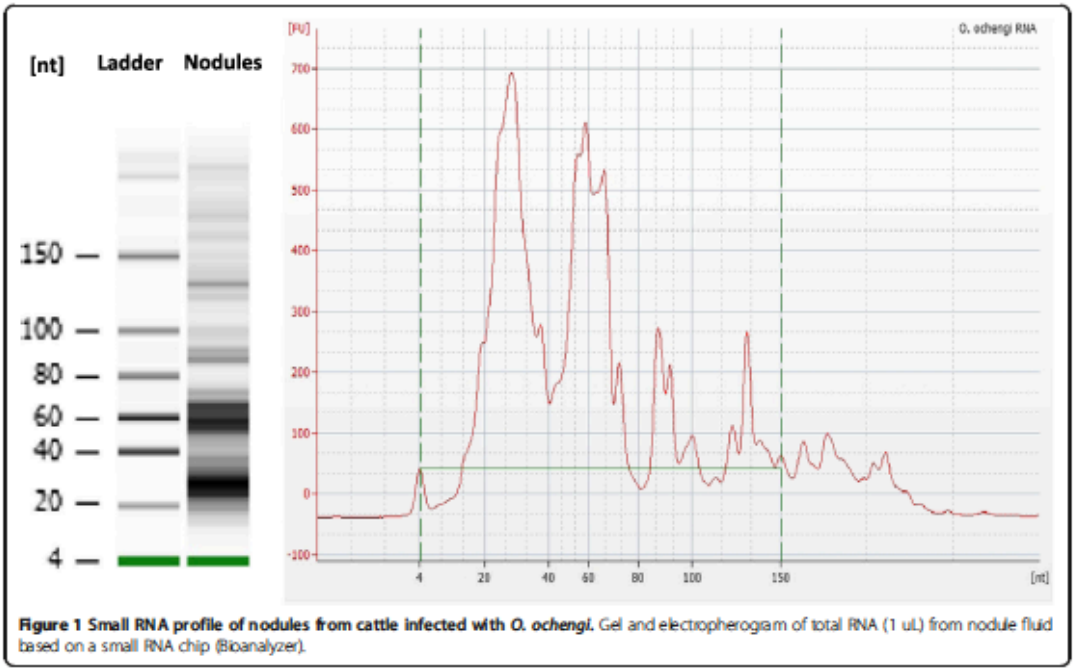

Figure 1 Small RNA profile of nodules from cattle infected with *O. ochengi*. Gel and electropherogram of total RNA (1 uL) from nodule fluid based on a small RNA chip (Bioanalyzer).

Table 1 Bovine and *O.ochengi* small RNA classification in nodules

Trimmed reads	**15022278**
Bovine genome match	**11912199**
Unambigious	11905898
rRNA	20836
tRNA	11335037
Y RNA	51307
Other Rfam	25716
miRNA	382791
***O. ochengi* genome match**	**157633**
Unambigious	151332
rRNA	2616
tRNA	120733
Y RNA	0
Other Rfam	2344
miRNA	11455

share homology in their seed sites (Additional file 1: Table S1). From these analyses we identify 16 novel pre-miRNA candidates that are not homologs of other known nematode pre-miRNAs. Six of these have reads mapping specifically to both arms of the hairpin with 3′ overhangs (Figure 2) and we therefore assign confidence to their classification as Dicer-derived miRNAs. To determine whether these small RNAs are conserved in the closely related human parasite *O. volvulus*, miRdeep2 analysis of the reads sequenced in the *O. ochengi* nodule material was carried out using the *O. volvulus* draft genome as the mapping substrate, allowing for up to 2 mismatches. All sequences aligned perfectly and derived from hairpins, apart from three miRNAs (Ooc-novel-3-3p, Ooc-novel-15, Ooc-miR-49) where a 1 nt mismatch was present (Additional file 1: Table S1).

Six parasite-derived miRNAs are detected in serum or plasma of humans infected with *O. volvulus*

To date very little is known about the factors that dictate the stability of extracellular RNA in fluids or whether and how these traffic within the body. The nodules are highly vascularized [35] and provide a direct route to the blood system for parasite-derived molecules. To determine whether *O. volvulus*-derived miRNAs are present in serum and plasma we carried out two parallel analyses of samples pooled from infected humans obtained from two geographically relevant regions in Africa, Cameroon [36] and Ghana [37], and compared these to pooled endemic or European controls. At present there is no standardized way to assess the integrity or quality of RNA extracted from serum since the intact large ribosomal RNAs (rRNAs) are not present. However we observed a distinct population of small RNA that is 20–30 nt in length based on Bioanalyzer analyses. This population was more prominent when using the Exiqon biofluids extraction kit compared to the Qiagen miRNA easy kit (Additional file 2: Figure S1). Small RNA sequencing libraries were prepared, sequenced and analysed as above. A total of 10–25 million reads were analysed per sample, of which 39-51% mapped to the human genome and

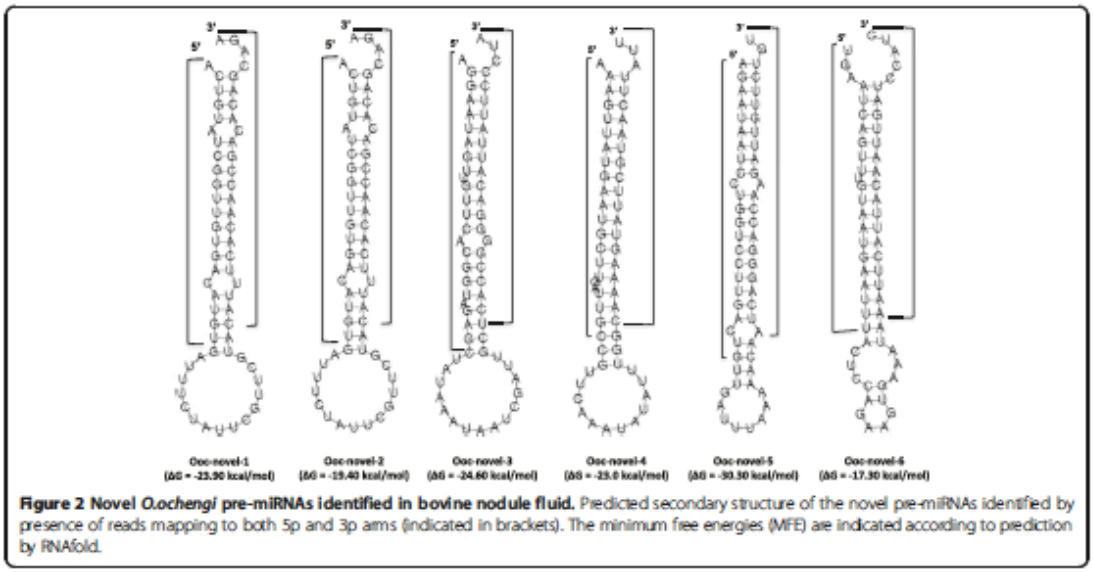

Figure 2 Novel *O.ochengi* pre-miRNAs identified in bovine nodule fluid. Predicted secondary structure of the novel pre-miRNAs identified by presence of reads mapping to both 5p and 3p arms (indicated in brackets). The minimum free energies (MFE) are indicated according to prediction by RNAfold.

1.0-1.5% mapped to the draft *O. volvulus* genome. The majority of the reads from human serum that mapped to *O. volvulus* were identified as rRNA fragments, but these were detected at comparable levels in European control and infected samples. It is possible these are of human origin but are edited or that they derive from other organisms or dietary sources as shown in several studies [38,39]. Similarly the source of many reads that map to *O. volvulus* genome and are annotated as tRNA fragments [34] cannot be reliably assigned (Table 2).

Here we focus on the miRNAs detected in the serum from humans testing positive for *O. volvulus* that can be assigned a nematode origin. From the combined datasets we identify a total of six *O. volvulus* miRNAs. The nematode origin of these is evident from a number of criteria: 1) they map perfectly to regions that fold into hairpin structures within the *O. volvulus* genome; 2) they are not other classes of sncRNA and 3) they are not present in the sera of European controls. Of the six miRNAs identified, all were identical to the *O. ochengi* miRNAs found in nodules (Table 3). Two of the miRNAs, miR-71 and lin-4, are detected in infected samples from both Ghana and Cameroon but neither endemic nor European controls. Two are detected only in the infected pooled sample from Ghana (miR-100a, miR-87) and two of these are present in infected and endemic control samples from Ghana (miR-100d, bantam-a). As the endemic control sample was a pool of 13 individuals, it is possible that these miRNAs could derive from an individual misdiagnosed as negative for onchocerciasis or co-infected with other co-endemic nematode parasites in these regions. Of note, miR-92 and let-7 were detected in some of the libraries however the mature miRNAs are perfectly conserved between nematodes and mammals. There can be some heterogeneity in the terminal nucleotides of these miRNAs based on non-templated additions [40] (as is common for miRNAs) such that they could technically align better to parasite than host. The exact origin(s) of these miRNA cannot be inferred.

Common and distinct circulating miRNA signatures in filarial infections

We recently identified 16 miRNAs in the serum of mice infected with the filarial nematode *L. sigmodontis* and four of these are identical to the *O. volvulus* miRNAs detected in human serum (mir-71, two miR-100 members, and one bantam family member) and one is derived from the other arm of the hairpin of a *O. volvulus* miRNA (miR-87). A further seven of the *L.sigmodontis* miRNAs are identical to *O. ochengi* miRNAs found in the nodule fluid and three (miR-50-3p and Bantam-b,c) differ by 1 nt outside of the seed region (Figure 3). Strikingly multiple miR-100 and bantam family members are present in the datasets. These also dominate the secretion product of the gastrointestinal nematode *H. polygyrus* [9]. The *O. volvulus* miR-100 and bantam miRNAs identified have distinct sequences outside of their seed regions from the miRNAs in *H. polygyrus* (Figure 4).

To compare relative quantities across the datasets and to qualify our limit of detection, we used total host miRNA read counts in the same samples as a normalizer. The individual parasite miRNAs are detected at a range of 26 to 12,863 per million bovine miRNA reads (*O. ochengi* nodule fluid), 5 to 127 per million human miRNA reads (serum/

Table 2 Small RNA classification in human serum and plasma from uninfected and infected individuals

Human serum/plasma	Uninfected serum (European control)	Infected serum (Cameroon)	Uninfected plasma (Ghana)	Infected plasma (Ghana)
Trimmed reads	**25519512**	**23734119**	**24992446**	**10015190**
Human genome match	**9998552**	**9331113**	**12936180**	**4791645**
Unambiguous	**9937398**	**9102817**	**12846400**	**4742963**
rRNA	15854	26512	13022	6744
tRNA	2568803	82382	6442858	1724586
Y RNA	1149988	2408124	1004222	476464
Other Rfam	198310	33516	8497	3791
miRNA	5589367	5924748	5266797	2472450
***O. volvulus* genome match**	**304991**	**583693**	**328590**	**157005**
Unambiguous	**243837**	**355397**	**238810**	**108323**
rRNA	140174	108351	132900	49797
tRNA	358	400	1884	1929
Y RNA	50	0	0	0
Other Rfam	2434	2712	3013	688
miRNA	0	75	344	743

Table 3 Read numbers of nematode-derived miRNAs detected in serum or plasma from individuals who tested positive for *O. volvulus*

miRNA	RNA sequence	Precursor coordinates	Uninfected serum (European control)	Infected serum (Cameroon)	Uninfected serum (Ghana)	Infected serum (Ghana)
miR-71	UGAAAGACAUGGGUAGUGAGAC[G][1]	OVOC.OM1b:9907432..9907494:+	**0**	**43**	**0**	**98**
lin-4	UCCCUGAGACCUCUGCUGCGA	OVOC.OM4:5453650..5453708:-	**0**	**32**	**0**	**73**
miR-100d	AACCCGUAGUUUCGAACAUGUGU	OVOC.OM1a:1762729..1762789:-	**0**	**0**	**121**	**314**
miR-87-3p	GUGAGCAAAGUUUCAGGUGUUC	OVOC.OM2:17655901..17655965:-	**0**	**0**	**0**	**85**
miR-100a	UACCCGUAGCUCCGAAUAUGUGU	OVOC.OM1a:1763611..1763671:-	**0**	**0**	**0**	**102**
bantam-a	UGAGAUCAUUGUGAAAGCUAUU	OVOC.OM2:1211194..1211257:-	**0**	**0**	**223**	**71**

[1]Brackets indicate heterogeneity in the 3' terminal nucleotide between datasets.

plasma from *O. volvulus* positive individuals) and 2 to 367 reads per million mouse miRNAs (serum from *L. sigmodontis* infected mice) as shown in Table 4. We anticipate these relative proportions will vary depending on the intensity of infection. Importantly, this provides a baseline for comparing relative levels of parasite miRNAs between studies and understanding the limits of detection in each study.

A recent analysis of serum from humans infected with *O. volvulus* using deep sequencing reported 20 putative *O. volvulus* miRNAs that have no overlap with those we identify here [5]. Thirteen of the reported sequences were < 17 nt long, or detected in only one read and thus are not analysed by our criteria. Of the seven additional sequences three of these perfectly align to human ribosomal RNA and two of these (PC-5p-31768_12, PC-3p-46055_7) are found as a part of longer sequences in European control serum. One of the sequences, let-7, is also found in our datasets but we do not confidently assign this to nematode origin given its conservation in the mammalian host.

Discussion

The discovery that RNA is secreted by nematodes opens up many avenues for further investigation into their functional properties and diagnostic utility. Here we report that small noncoding RNAs derived from *Onchocerca spp.* are present in host tissues, both at a concentrated site of infection (nodule fluid) and in the circulatory system (serum/plasma) of their hosts. Six *O. volvulus* miRNAs were identified in human plasma, all of which are identical to those found in *O. ochengi* nodule fluid, and four of

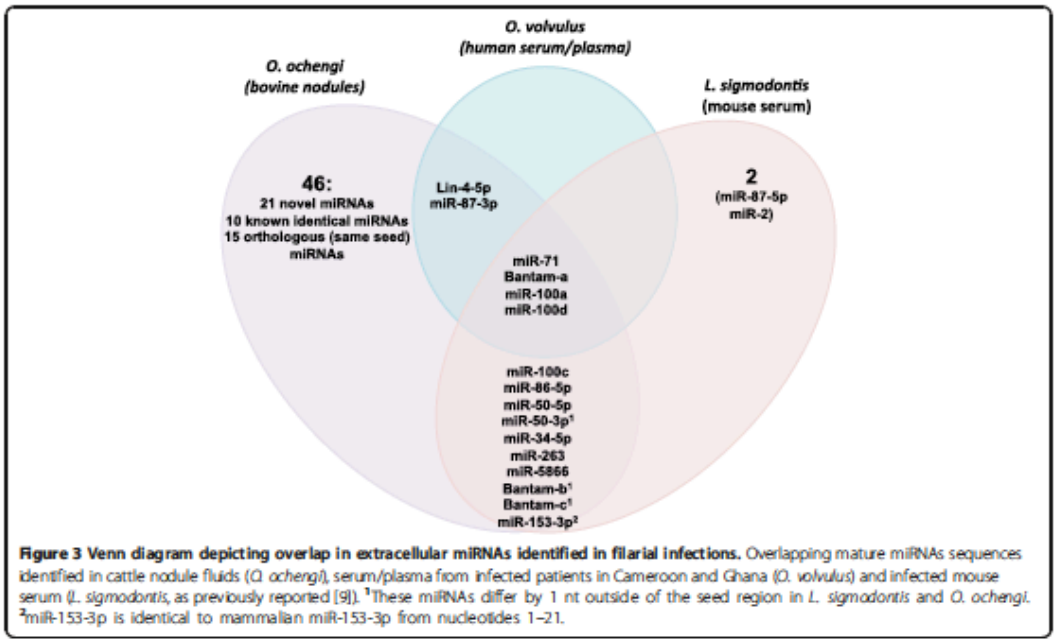

Figure 3 Venn diagram depicting overlap in extracellular miRNAs identified in filarial infections. Overlapping mature miRNAs sequences identified in cattle nodule fluids (*O. ochengi*), serum/plasma from infected patients in Cameroon and Ghana (*O. volvulus*) and infected mouse serum (*L. sigmodontis*, as previously reported [9]). [1]These miRNAs differ by 1 nt outside of the seed region in *L. sigmodontis* and *O. ochengi*. [2]miR-153-3p is identical to mammalian miR-153-3p from nucleotides 1–21.

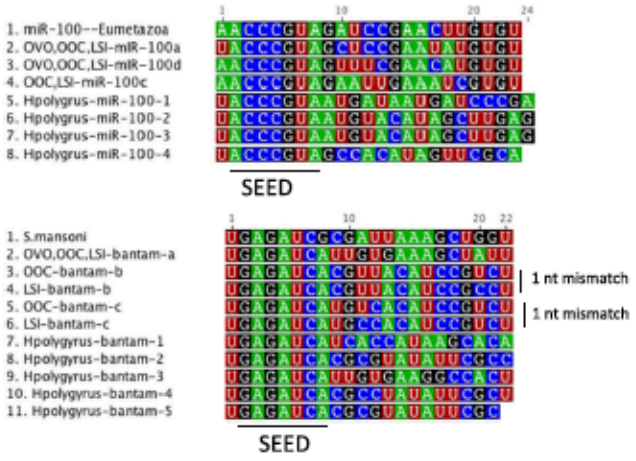

Figure 4 Sequences of extracellular miR-100 and bantam family members in nematode parasites. The conserved miR-100 sequence (Eumetazoa) is shown in relation to the nematode family members identified in these datasets: *O. volvulus* (OVO), *O. ochengi* (OOC), *L. sigmodontis* (LSI) or *H. polygyrus* (Hpolygyrus). The *S. mansoni* bantam sequence is taken from Hoy et al., PLos NTDS 2014 [4]. The naming of family members is arbitrary.

which are also identical to those found in serum of mice infected with the related filarial nematode *L. sigmodontis* (Figure 3). This suggests extensive overlap in the identity of extracellular parasite-derived miRNAs in filarial infections and gives confidence in the conserved nature of RNA secretion among these pathogens. This is further supported by a report published while this manuscript was in preparation which identified miRNA candidates of potential nematode origin in the plasma of baboons infected with *Loa loa* and the plasma of an *O. ochengi*-infected cow [41]: 4 of the 6 miRNAs that we identify in *O. volvulus*-infected humans are among the 22 miRNA candidates found in *Loa loa*-infected baboons and 2 of the 62 *O. ochengi* miRNAs in nodules are among the 10 candidates found in bovine plasma (Additional file 1: Table S1).

A common feature in all the infections is the presence of miR-71, bantam family and miR-100 family miRNAs (where family is defined based on identical seed sequences, nucleotides 2–8). We previously identified 5 miR-100 family members within the top 20 most abundant miRNAs secreted by *H. polygyrus* [9]. The factors dictating the expansion of this miRNA family are not known; miR-100 is

Table 4 Relative abundance of nematode miRNA in fluids in comparison to host miRNAs (reads per million)

miRNA	Sequence	*O. ochengi*	*O. volvulus* (Ghana)	*O. volvulus* (Cameroon)	*L. sigmodontis*
Ooc-miR-71	UGAAAGACAUGGGUAGUGAGAC[G][3]	117.6	39.6	7.3	25.1
Ooc-lin-4	UCCCUGAGACCUCUGCUGCGA	1355.8	29.5	5.4	ND (<0.8)[2]
Ooc-miR-100d[1]	AACCCGUAGUUUCGAACAUGUGU	86.2	127.0	ND (<0.3)[2]	31.4
Ooc-miR-87-3p	GUGAGCAAAGUUUCAGGUGUUC	26.1	34.4	ND (<0.3)[2]	ND (<0.8)[2]
Ooc-miR-100a	UACCCGUAGCUCCGAAUAUGUGU	979.6	41.3	ND (<0.3)[2]	376.0
Ooc-bantam-a[1]	UGAGAUCAUUGUGAAAGCUAUU	12863.4	28.7	ND (<0.3)[2]	35.3
Ooc-miR-86	UAAGUGAAUGCUUUGCCACAGUCU	65.3	ND (<0.8)[2]	ND (<0.3)[2]	44.7
Ooc-miR-263/183	AAUGGCACUAGAUGAAUUCACGG	44.4	ND (<0.8)[2]	ND (<0.3)[2]	5.5
Ooc-miR-50-5p	UGAUAUGUCUGAUAUCUUGGGUU	31.3	ND (<0.8)[2]	ND (<0.3)[2]	7.9
Ooc-miR-34	UGGCAGUGUGGUUAGCUGGUUGU	70.5	ND (<0.8)[2]	ND (<0.3)[2]	6.3
Ooc-miR-5866	UUACCAUGUUGAUCGAUCUCC[A][3]	70.5	ND (<0.8)[2]	ND (<0.3)[2]	1.60
	Total host miRNAs	**382791**	**2472450**	**5924748**	**1273839**

[1]Also found in endemic Ghanaian controls.
[2]ND = not detected; the limit of detection is shown in (), based on the number of total host miRNAs sequenced and assuming 2 reads are required to identify a parasite sequence.
[3]Brackets indicate heterogeneity in the 3' terminal nucleotide between datasets.

one of the oldest miRNAs, having evolved in the last common ancestor of Eumetazoa (the highly conserved sequence is noted in Figure 4 and is identical across parasitic nematodes and all of their mammalian hosts). This family has expanded in some animal lineages: in *C. elegans* it is referred to as the miR-51 family and is redundantly required for embryonic development [42] and also involved in developmental timing and buccal cavity formation [42,43]. Why members of this family are secreted by parasitic nematodes is unknown and raises interesting questions regarding whether these would interact with host targets. From a diagnostic standpoint it is worth noting that the sequences outside the seed region differ between the filarial nematodes and *H. polygyrus* (Figure 4). We also identify bantam family members in serum of both *L. sigmodontis* and *O. volvulus* infected hosts. Two of the bantam family members found in the serum of *L. sigmodontis* infected mice have a 1 nt mismatch to the family members in *O. ochengi* and *O. volvulus* (Figure 4). One of the bantam members identified here appears conserved and secreted in all Clade III nematodes. We identified this miRNA in *O. ochengi* nodule fluid, serum from *O. volvulus*-infected individuals and serum from mice infected with *L. sigmodontis*. However, this miRNA sequence was also present in endemic controls from the Ghana cohort. This may represent a false negative individual or may occur if another parasite in one or more of the control individuals also secretes bantam orthologs. According to miRbase, this sequence is specific to filarial nematodes and is not present in the Clade V nematodes (Rhabditida; strongyles including *H. polygyrus*, free-living rhabditids and relatives). Interestingly, the secretion of bantam family members also occurs in trematodes; we previously identified a bantam family member (distinct in sequence from those identified here, Figure 4) in the serum of mice and humans infected with *S. mansoni* [44], and demonstrated its utility as a biomarker for schistosomiasis [4].

A key criterion in our analysis is the requirement that the annotated nematode miRNAs do not have a match in the host genome. A recent study reported putative *O. volvulus* miRNAs in human serum [5], some of which we annotate here as human ribosomal RNAs. This does not rule out that human sequences could also serve as a marker of infection, but it will be imperative to compare serum from uninfected individuals to avoid false positives and to build a better context for when and why these sequences can be detected.

We previously identified miRNAs derived from *L. sigmodontis* in mouse serum during patent infection [9]. However using the same library preparation methodology and sequencing at the same depth of coverage we did not detect miRNAs derived from the gastrointestinal nematode *H. polygyrus* in the serum of infected mice (at day 14, when the adult worms reside in the small intestine). Since the adult *H. polygyrus* worms secrete miRNAs within exosomes *in vitro* [9] it seems likely that lack of detection in serum relates to the localization of the parasite in the host. In support of this a recent report identified 245 putative parasite miRNAs in the serum of dogs infected with the heartworm *D. immitis* [5]. Individuals infected with this species of filaria would be expected to have a higher concentration of circulating parasite-derived miRNAs (relative to other filariae) due to the presence of both Mf in the blood and adult worms in the pulmonary artery and heart.

As observed in the *L. sigmondontis* dataset the *O. volvulus* miRNAs are much less abundant than host miRNAs in serum or plasma: in the Ghana samples we mapped 743 reads to 6 different nematode-derived miRNAs, compared to approx. 2.5 million human miRNAs reads in the same library. Low-abundance is a challenge when detecting any type of parasite-derived molecule in host fluid. An advantage of the miRNAs is that these can be amplified by PCR prior to detection. Nonetheless, methods for enriching parasite material are likely to be advantageous in terms of maximizing the specificity and sensitivity of detection. In this regard, we have shown nematode miRNAs are secreted within extracellular vesicles *in vitro* [9]. Further work is required to understand whether parasite and host miRNAs exist in similar or distinct complexes in host fluids, and/or whether these can be further purified prior to RNA extraction to reduce the scope for cross-contamination.

The biology and dynamics of secreted miRNAs are thus very open topics. Nothing is known at present about the extent to which different parasite life stages secrete miRNAs or what their half-lives are in host tissues including blood. We anticipate that the diagnostic utility of these molecules will also depend on the degree to which RNA secretion is regulated, the mechanism by which the small RNAs enter circulation and the stability of each RNA species in different fluids.

Conclusions

We have identified a total of 62 miRNAs derived from *O. ochengi* in bovine nodule fluids, including miRNAs that are perfectly conserved in other filarial nematodes and some that do not have homology to other nematodes. Six of the conserved miRNAs are present in serum or plasma from humans testing positive for *O. volvulus* in Cameroon and Ghana. Four of these are also identical to those found in the serum of mice infected with *L. sigmodontis* including miR-100 and bantam family members. These findings support the conserved nature of RNA secretion by nematode parasites and identify miRNAs as a new potential biomarker for filarial infections that could

significantly improve the diagnostic outlook for these neglected conditions. Further studies investigating exactly which parasite life stage(s) secrets such miRNAs, their stability, half-lives and localization within the host will drive forward the applications of parasite-specific miRNAs as biomarkers for onchocerciasis.

Additional files

Additional file 1: Table S1. miRNA candidates found in *O.ochengi* nodules and comparison to *Loa loa* and *O.ochengi* miRNA candidates reported in Tritten et al., Molecular & Biochemical Parasitology 2014 [41].

Additional file 2: Figure S1. Small RNA profile of human serum comparing two different extraction kits. Gel of total RNA (1 uL) extracted from three replicates of human European control serum using two different kits: miRNeasy serum/plasma kit (Qiagen) and miRCURY RNA Isolation kit Biofluids (Exiqon) based on small RNA chip (Bioanalyzer).

Competing interests
The authors declare that they have no competing interests.
The data discussed in this publication have been deposited in NCBI's Gene Expression Omnibus (Barrett *et al.* 2013) and are accessible through GEO Series accession number GSE63933 (http://www.ncbi.nlm.nih.gov/geo/query/acc.cgi?acc = GSE63933).

Authors' contributions
JFQ performed experiments, co-designed studies and co-wrote the manuscript with AHB; BM, SAB, DWT, KMP and AH coordinated accessibility of material, edited manuscript and co-conceived project with AHB; AI, JFQ and AHB analysed the data, MB provided genome data, advice and edited manuscript, AD, SW, HFN, GSB, VNT provided crucial sample material. AHB wrote paper with JFQ and supervised the work. All authors read and approved the final version of the manuscript.

Acknowledgements
Funding was provided by the Institute for Medical Microbiology, Immunology and Parasitology, University Hospital of Bonn, Germany as part of a consortium grant funded by the Bill and Melinda Gates Foundation to the University Hospital of Bonn as well as a Wellcome Trust RCDF (WT097394AIA) to A. Buck. Funding for Cameroonian human sera and nodule fluid was provided by the 7th Framework Programme of the European Commission (project identifier HEALTHF3-2010-242131). We thank Kat Gordon and Kashyap Chhatbar for helpful discussions on this work.

Author details
[1]Centre for Immunity, Infection and Evolution, Ashworth Laboratories, University of Edinburgh, West Mains Road, Edinburgh, UK. [2]Institute of Infection and Global Health, University of Liverpool, Liverpool, Merseyside, UK. [3]Institute of Biodiversity, Animal Health and Comparative Medicine, College of Medical, Veterinary and Life Sciences, University of Glasgow, Glasgow, UK. [4]Institute of Medical Microbiology, Immunology and Parasitology, University Hospital of Bonn, Bonn, Germany. [5]Kumasi Centre for Collaborative Research (KCCR) and Kwame Nkrumah University of Science and Technology, Kumasi, Ghana. [6]Research Foundation in Tropical Diseases and Environment and University of Buea, Buea, Cameroon. [7]Institut de Recherche Agricole pour le Développement, Regional Centre of Wakwa, Ngaoundéré, Cameroon. [8]Cameroon Academy of Sciences, Yaoundé, Cameroon. [9]Division of Pathway Medicine, School for Biomedical Sciences, University of Edinburgh, Little France, Edinburgh, UK.

Received: 5 December 2014 Accepted: 12 January 2015
Published online: 27 January 2015

References
1. Fabian MR, Sonenberg N. The mechanics of miRNA-mediated gene silencing: a look under the hood of miRISC. Nat Struct Mol Biol. 2012;19:586–93.
2. Devaney E, Winter AD, Britton C. microRNAs: a role in drug resistance in parasitic nematodes? Trends Parasitol. 2010;26:428–33.
3. Turchinovich A, Samatov TR, Tonevitsky AG, Burwinkel B. Circulating miRNAs: cell-cell communication function? Front Genet. 2013;4(June):119.
4. Hoy AM, Lundie RJ, Ivens A, Quintana JF, Nausch N, Forster T, et al. Parasite-derived microRNAs in host serum as novel biomarkers of helminth infection. PLoS Negl Trop Dis. 2014;8:e2701.
5. Tritten L, Burkman E, Moorhead A, Satti M, Geary J, Mackenzie C, et al. Detection of circulating parasite-derived MicroRNAs in filarial infections. PLoS Negl Trop Dis. 2014;8:e2971.
6. Cheng G, Luo R, Hu C, Cao J, Jin Y. Deep sequencing-based identification of pathogen-specific microRNAs in the plasma of rabbits infected with *Schistosoma japonicum*. Parasitology. 2013;140:1751–61.
7. Bernal D, Trelis M, Montaner S, Cantalapiedra F, Galiano A, Hackenberg M, et al. Surface analysis of *Dicrocoelium dendriticum*. The molecular characterization of exosomes reveals the presence of miRNAs. J Proteomics. 2014;105:232–41.
8. Gobert GN, Stenzel DJ, McManus DP, Jones MK. The ultrastructural architecture of the adult *Schistosoma japonicum* tegument. Int J Parasitol. 2003;33:1561–75.
9. Buck AH, Coakley G, Simbari F, Mcsorley H, Quintana J, Le BT, et al. Exosomes secreted by nematode parasites transfer small RNAs to mammalian cells and modulate innate immunity. Nat Commun. 2014;5:5488.
10. Knopp S, Steinmann P, Hatz C, Keiser J, Utzinger J. Nematode infections: filariases. Infect Dis Clin North Am. 2012;26(2):359–81.
11. Hotez PJ, Alvarado M, Basáñez M-G, Bolliger I, Bourne R, Boussinesq M, et al. The global burden of disease study 2010: interpretation and implications for the neglected tropical diseases. PLoS Negl Trop Dis. 2014;8:e2865.
12. Morales-Hojas R, Cheke RA, Post RJ. Molecular systematics of five *Onchocerca* species (Nematoda: Filarioidea) including the human parasite, O. volvulus, suggest sympatric speciation. J Helminthol. 2006;80:281–90.
13. Crump A, Morel CM, Omura S. The onchocerciasis chronicle: from the beginning to the end? Trends Parasitol. 2012;28:280–8.
14. Nfon CK, Makepeace BL, Njongmeta LM, Tanya VN, Bain O, Trees AJ. Eosinophils contribute to killing of adult *Onchocerca ochengi* within onchocercomata following elimination of *Wolbachia*. Microbes Infect. 2006;8:2698–705.
15. Wahl G, Enyong P, Ngosso A, Schibel JM, Moyou R, Tubbesing H, et al. *Onchocerca ochengi*: epidemiological evidence of cross-protection against *Onchocerca volvulus* in man. Parasitology. 1998;116(Pt 4):349–62.
16. Osei-Atweneboana MY, Eng JKL, Boakye DA, Gyapong JO, Prichard RK. Prevalence and intensity of *Onchocerca volvulus* infection and efficacy of ivermectin in endemic communities in Ghana: a two-phase epidemiological study. Lancet. 2007;369:2021–9.
17. Gardon J, Gardon-Wendel N, Demanga-Ngangue, Kamgno J, Chippaux JP, Boussinesq M. Serious reactions after mass treatment of onchocerciasis with ivermectin in an area endemic for *Loa loa* infection. Lancet. 1997; 350:18–22.
18. Boatin BA, Toé L, Alley ES, Nagelkerke NJD, Bonsboom G, Habbema JDF. Detection of *Onchocerca volvulus* infection in low prevalence areas: a comparison of three diagnostic methods. Parasitology. 2002;125(Pt 6):545–52.
19. Park J, Dickerson TJ, Janda KD. Major sperm protein as a diagnostic antigen for onchocerciasis. Bioorg Med Chem. 2008; 16:7206–9.
20. Weil GJ, Steel C, Liftis F, Li B, Mearns G, Lobos E, et al. A rapid-format antibody card test for diagnosis of onchocerciasis. J Infect Dis. 2000;186:1796–9.
21. Taniuchi M, Verweij JJ, Noor Z, Sobuz SU, Van Lieshout L, Petri Jr WA, et al. High throughput multiplex PCR and probe-based detection with luminex beads for seven intestinal parasites. Am J Trop Med Hyg. 2011;84:332–7.
22. Srivastava P, Mehrotra S, Tiwary P, Chakravarty J, Sundar S. Diagnosis of Indian visceral leishmaniasis by nucleic acid detection using PCR. PLoS One. 2011;6:4–8.
23. Hoy AM, Buck AH. Extracellular small RNAs: what, where, why? Biochem Soc Trans. 2012;40:886–90.
24. Wahl G, Achu-Kwi MD, Mbah D, Dawa O, Renz A. Bovine onchocerciasis in North Cameroon. Vet Parasitol. 1994;52:297–311.
25. Arndts K, Specht S, Debrah AY, Tamarozzi F, Klarmann Schulz U, Mand S, et al. Immunoepidemiological profiling of onchocerciasis patients reveals associations with microfilaria loads and ivermectin intake on both individual and community levels. PLoS Negl Trop Dis. 2014;8:e2679.
26. Burgos KL, Javaherian A, Bomprezzi R, Ghaffari L, Rhodes S, Courtright A, et al. Identification of extracellular miRNA in human cerebrospinal fluid by next-generation sequencing. RNA. 2013;19:712–22.

27. Martin M. Cutadapt removes adapter sequences from high-throughput sequencing reads. Bioinformatics Act. 2011;17:10–2.
28. Langmead B, Trapnell C, Pop M, Salzberg SL. Ultrafast and memory-efficient alignment of short DNA sequences to the human genome. Genome Biol. 2009;10:R25.
29. Griffiths-Jones S. Rfam: an RNA family database. Nucleic Acids Res. 2003;31:439–41.
30. Friedländer MR, Mackowiak SD, Li N, Chen W, Rajewsky N. miRDeep2 accurately identifies known and hundreds of novel microRNA genes in seven animal clades. Nucleic Acids Res. 2012;40:37–52.
31. Kozomara A, Griffiths-Jones S. miRBase: annotating high confidence microRNAs using deep sequencing data. Nucleic Acids Res. 2014;42(Database issue):D68–73.
32. Gruber AR, Lorenz R, Bernhart SH, Neuböck R, Hofacker IL. The Vienna RNA websuite. Nucleic Acids Res. 2008;36(Web Server issue):W70–4.
33. Altschul SF, Gish W, Miller W, Myers EW, Lipman D. Basic Local Alignment Search Tool.pdf. J Mol Biol. 1990;215:403–10.
34. Dhahbi JM, Spindler SR, Atamna H, Yamakawa A, Boffelli D, Mote P, et al. 5' tRNA halves are present as abundant complexes in serum, concentrated in blood cells, and modulated by aging and calorie restriction. BMC Genomics. 2013;14:298.
35. George GH, Palmieri JR, Connor DH. The onchocercal nodule: interrelationship of adult worms and blood vessels. Am J Trop Med Hyg. 1985;34:1144–8.
36. Zouré HGM, Noma M, Tekle AH, Amazigo UV, Diggle PJ, Giorgi E, et al. The geographic distribution of onchocerciasis in the 20 participating countries of the African Programme for Onchocerciasis Control: (2) pre-control endemicity levels and estimated number infected. Parasit Vectors. 2014;7:326.
37. Turner HC, Osei-Atweneboana MY, Walker M, Tettevi EJ, Churcher TS, Asiedu O, et al. The cost of annual versus biannual community-directed treatment of onchocerciasis with ivermectin: Ghana as a case study. PLoS Negl Trop Dis. 2013;7:e2452.
38. Wang K, Li H, Yuan Y, Etheridge A, Zhou Y, Huang D, et al. The complex exogenous RNA spectra in human plasma: an interface with human gut biota? PLoS One. 2012;7:e51009.
39. Beatty M, Guduric-fuchs J, Brown E, Bridgett S, Chakravarthy U, Hogg RE, et al. Small RNAs from plants, bacteria and fungi within the order Hypocreales are ubiquitous in human plasma. BMC Genomics. 2014;15:933.
40. Landgraf P, Rusu M, Sheridan R, Sewer A, Iovino N, Aravin A, et al. A mammlian microRNA expression atlas based on small RNA library sequencing. Cell. 2007;129:1401–14.
41. Tritten L, Nelli MO, Wanji S, Njouendoui A, Fombad F, Kengne-ouaffo J, et al. *Loa loa* and *Onchocerca ochengi* miRNAs detected in host circulation. Mol Biochem Parasitol. 2014;198(1):14–7.
42. Shaw WR, Armisen J, Lehrbach NJ, Miska EA. The conserved miR-51 microRNA family is redundantly required for embryonic development and pharynx attachment in *Caenorhabditis elegans*. Genetics. 2010;185:897–905.
43. Brenner JL, Kemp BJ, Abbott AL. The mir-51 family of microRNAs functions in diverse regulatory pathways in *Caenorhabditis elegans*. PLoS One. 2012;7:e37185.
44. Van der Werf MJ, de Vlas SJ, Brooker S, Looman CW, Nagelkerke NJ, Habbema JDF, et al. Quantification of clinical morbidity associated with schistosome infection in sub-Saharan Africa. Acta Trop. 2003;86:125–39.

7.5 Small RNAs and extracellular vesicles in filarial nematodes: From nematode development to diagnostic applications

Juan F. Quintana, Simon A. Babayan, Amy H. Buck
Parasite Immunology, (2017) 39(2): e12395. DOI: 10.1111/pim.12395
Available at: http://onlinelibrary.wiley.com/doi/10.1111/pim.12395/abstract

Received: 23 August 2016 | Accepted: 12 October 2016
DOI: 10.1111/pim.12395

COMMISSIONED REVIEW ARTICLE

WILEY Parasite Immunology

Small RNAs and extracellular vesicles in filarial nematodes: From nematode development to diagnostics

J. F. Quintana[1] | S. A. Babayan[2] | A. H. Buck[1]

[1]Institute of Immunology and Infection Research and Centre for Immunity, Infection & Evolution, School of Biological Sciences, University of Edinburgh, Edinburgh, UK
[2]Institute of Biodiversity Animal Health and Comparative Medicine, University of Glasgow, Glasgow, UK

Correspondence
Amy H. Buck, Ashworth Laboratories, Edinburgh, UK.
Email: a.buck@ed.ac.uk

Funding information
WT Pathfinder Award, Grant/Award Number: 201083/Z/16/Z; Institute for Medical Microbiology, Immunology and Parasitology, University Hospital of Bonn, Germany; Bill and Melinda Gates Foundation

Summary

Parasitic nematodes have evolved sophisticated mechanisms to communicate with their hosts in order to survive and successfully establish an infection. The transfer of RNA within extracellular vesicles (EVs) has recently been described as a mechanism that could contribute to this communication in filarial nematodes. It has been shown that these EVs are loaded with several types of RNAs, including microRNAs, leading to the hypothesis that parasites could actively use these molecules to manipulate host gene expression and to the exciting prospect that these pathways could result in new diagnostic and therapeutic strategies. Here, we review the literature on the diverse RNAi pathways that operate in nematodes and more specifically our current knowledge of extracellular RNA (exRNA) and EVs derived from filarial nematodes in vitro and within their hosts. We further detail some of the issues and questions related to the capacity of RNA-mediated communication to function in parasite–host interactions and the ability of exRNA to enable us to distinguish and detect different nematode parasites in their hosts.

KEYWORDS
diagnostics, exosomes, extracellular vesicles, filarial nematodes, host–pathogen, microRNAs

1 | INTRODUCTION

Filarial nematodes, the causative agents of some of the most prevalent poverty-related diseases, are tissue-dwelling nematodes that are transmitted by blood-feeding arthropods to terrestrial vertebrate hosts, from amphibians to mammals. For those nematodes infecting humans, their distribution is confined to tropical and subtropical regions, therefore representing a matter of public health in developing countries.[1] Latest estimations of the World Health Organization suggest that over 120 million people are infected by filarial parasites, causing considerable morbidity despite long-term chemotherapy-based control programmes.[1,2] The clinical manifestations (e.g. lymphoedema, hypertrophy of the skin and blindness) are rarely associated with high mortality rates, but their chronicity and morbidity impose a tremendous socio-economic burden on these countries.

From a host–pathogen standpoint, filarial nematodes are fascinating organisms for their ability to persist in their hosts for long periods, surviving and reproducing for over a decade in some cases.[3] This can be attributed to a repertoire of adaptations and strategies that the parasites employ, including secretion of factors with immunomodulatory properties.[4,5] Furthermore, the complex life cycles and ecological interactions of parasitic nematodes make them an interesting object of study with regard to moulting, growth and survival in challenging environments, such as those encountered upon infection of the definitive host. However, many mechanistic and molecular aspects associated with the biology of these parasitic nematodes have not been fully elucidated. RNA interference (RNAi) pathways have been shown to play important roles in the free-living nematode *Caenorhabditis elegans*, including regulation of developmental timing, genome defence and adaptation to the environment.[6–8] Here, we describe the current understanding of how different RNAi pathways operate in filarial

nematodes, making use of comparisons with studies in *C. elegans* in which many mechanistic aspects of RNAi were discovered.[9,10]

In the last 8 years, it has been shown that the small RNAs involved in RNAi within cells are also found extracellularly. Their association with extracellular vesicles (EVs) in parasite infections may implicate them as novel players in the transmission of information between the parasites and their hosts.[11] We will describe recent evidence of extracellular RNAs derived from filarial nematodes, their potential use for diagnostics and current challenges and outstanding questions in the field.

2 | RNAI PATHWAYS IN FILARIAL NEMATODES

Three primary RNAi pathways have been characterized in animals: the microRNA (miRNA) pathway, the endo/exo-small interfering RNA (endo/exo-siRNA) pathway and the P-element-induced wimpy testis (PIWI)-interacting RNA (piRNA) pathway.[9,12] These pathways are distinguished by the origin and identity of the small RNA guide and target, as well as the properties of the Argonaute (AGO) protein to which they bind. In general, AGOs have two main functions: (1) recognizing and binding small RNA and (2) mediating the interaction with other proteins required for small RNA loading, association with targeted RNAs, gene silencing activity and/or subcellular localization.[8,13] From a structural standpoint, they are generally ~90- 100-kDa monomeric proteins containing several domains a PAZ domain involved in 3′-end recognition and binding of the small RNA, a MID domain that binds the 5′ end of the small RNA and a PIWI domain, that in some cases includes an RNaseH-like activity that can carry out endonucleolytic cleavage ("slicing") of the targets.[13,14] The ancestral AGOs that bind to miRNAs are called ALG1 and ALG2 (AGO-like gene). The piRNA pathway is thought primarily to operate in genome defence through targeting transposable elements, mediated by the PIWI clade of AGOs. Homologs to these proteins are not present in clade III nematodes; the phylogenetic classification proposed by Blaxter et al.[15] is used throughout this manuscript. Rather, it is thought instead that other AGOs and small RNA classes could be involved in genome defence in this clade.[16] Indeed, a remarkable feature of nematodes is their extended AGOs (27 identified in *C. elegans* [8,16,17]), reflecting the diversity of RNAi pathways that can operate in these animals. The majority of the AGOs in *C. elegans* belong to the WAGO (worm-specific AGO) clade, and many members of this clade are expected to be found in filarial nematodes.[8,18] From studies in *C. elegans*, the WAGOs are thought to bind to a class of secondary siRNAs that can act through a range of mechanisms including chromosome segregation and epigenetic modifications [18-20] and can mediate transgenerational inheritance.[21] A more extensive description of different structural, functional and mechanistic aspects of AGO proteins is provided in recent reviews.[8,13,22]

3 | BIOGENESIS OF MIRNAS

The microRNA pathway is one of the best characterized RNAi pathways in nematodes.[23] These molecules, first described in *C. elegans* over two decades ago, are encoded within the genome as stem-loop structures that undergo a series of maturation events to produce the short RNA guide. In nematodes, as in other animals, miRNAs can either derive from within intragenic sequences (generally within the introns) or from independent, intergenic transcriptional units.[24] These transcripts, termed the primary miRNAs (pri-miRNAs), are mostly derived from the activity of RNA polymerase II (Figure 1). Some miRNAs are clustered together in discrete genomic regions suggesting coordinated expression.[10]

Once transcribed, miRNA biogenesis involves a series of maturation events starting with cleavage by the microprocessor complex in the nucleus.[10,25] The microprocessor is composed of the RNase III endonuclease DROSHA and DCRG8, among other scaffold proteins, and cleaves the pri-miRNA to produce a shorter hairpin (pre-miRNA) with a 5′ monophosphate and a −2-nt overhang at the 3′ end (Figure 1). The pre-miRNA is then actively transported to the cytoplasm by Ran-GTP protein and members of the exportin family (predominantly EXP-5). Once in the cytoplasm, the pre-miRNA is recognized by a second RNase III endonuclease called DICER that catalyses cleavage of the hairpin to produce a double-stranded duplex approximately 22 nt in length, where both 3′ ends display a −2-nt overhang.[10,25] One strand of this miRNA duplex is then incorporated into the RNA-induced silencing complex (RISC) through association with the AGO protein (Figure 1). The miRNA then guides RISC to target messenger RNAs to elicit inhibition of translation, accelerated mRNA de-adenylation and/or endonucleolytic cleavage of the mRNA, depending on the degree of complementarity between the miRNA and its target.[10,25] In animals, miRNAs generally are not perfectly complementary to their targets and recognition is dominated by the "seed" site defined as nucleotides 2-7 in the 5′ end of the miRNA.

4 | MIRNA DISCOVERY AND EVOLUTION IN FILARIAL NEMATODES

A number of studies have now documented miRNAs in filarial nematodes as well as the related clade III nematodes *Ascaris suum* and *Ascaris lumbricoides* [26-28] (Table 1). Poole et al.[29] first reported miRNAs in the filarial nematode *Brugia malayi* (Table 1) using bioinformatic predications as well as classical cloning from mixed life stages: adult males, gravid adult females and microfilariae (Mf). The authors identified 32 miRNAs including families well conserved in nematodes. A subsequent report by Winter et al.[30]identified miRNAs in the genome of *B. pahangi*, reporting a total of 132 miRNA loci that encode 104 unique mature sequences, including 29 of the 32 miRNAs previously discovered in *B. malayi*. Winter et al. carried out a side-by-side comparison of miRNAs sequenced from the clade V gastrointestinal parasite *Haemonchus contortus* and the clade III filarial parasite *B. pahangi* and were able to show that most of the miRNAs in each organism were not conserved in the other. Some of the newly evolved miRNAs were highly abundant and/or showed stage-specific expression.

Beyond the studies with *Brugia spp.*, miRNAs have also been identified in the dog heartworm parasite *Dirofilaria immitis*.[31] Here, a total

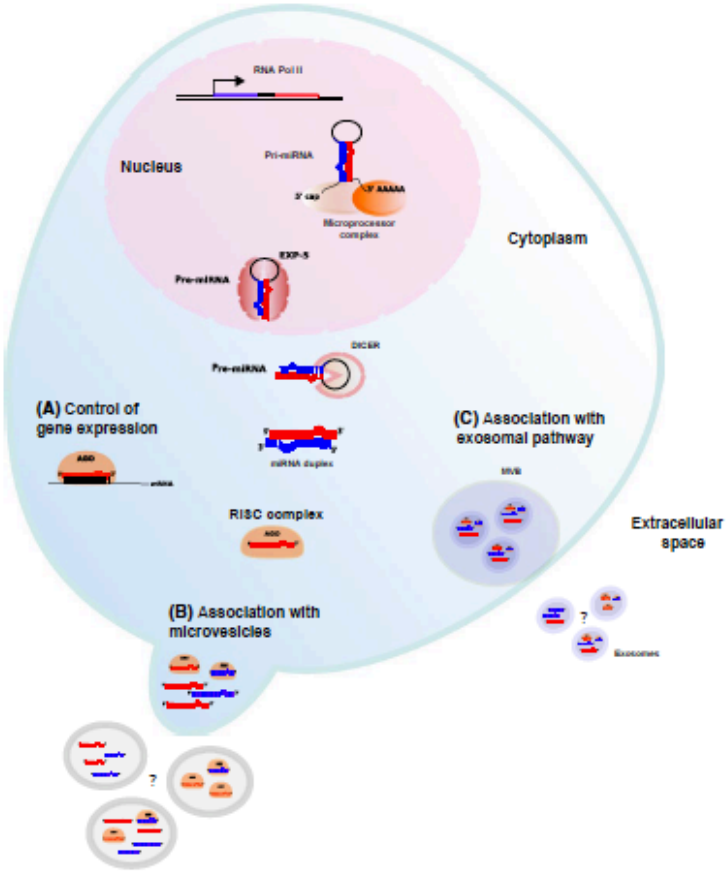

FIGURE 1 Simplified schematic of biogenesis and potential export pathways of microRNAs. miRNAs are generally produced from primary miRNA transcripts that are processed by the microprocessor in the nucleus and exported to the cytoplasm where they are further processed by Dicer to produce a 22-nt duplex RNA. One strand of the duplex (the mature miRNA) is loaded onto an Argonaute (AGO) protein and guides the RISC complex to mediate control of gene expression by translational repression or accelerated miRNA decay (A). The microRNA can also be exported out of the cell, either in association with AGO or in another form (the uncertainty is depicted with a question mark), through directly fusing with components of the plasma membrane into extracellular vesicles (EVs) termed microvesicles (B), or through incorporation into the exosomal biogenesis pathway into multivesicular bodies (MVBs) (C)

of 1063 miRNA candidates were identified by sequence alignment of mixed adult libraries against the miRBase repository,[52] corresponding to 808 miRNA families.[51] While the large number of miRNAs reported here could reflect an expanded miRNA repertoire in this parasite, it also highlights the fact that different studies use different criteria for assigning a small RNA sequence as a miRNA. In the study by Winter et al.[50], for example, the authors used both miReap and miRDeep prediction programs, but then further filtered the results manually with the requirement that both arms of the hairpin must be present in their data sets. All of these factors, along with the depth of sequencing that is carried out, will affect the number and identity of miRNAs identified in different nematode species, in addition to the quality of the genomes available. This becomes an issue when trying to examine acquisitions and losses, as well as species specificity of miRNAs for use in diagnostic applications (detailed further below).

While it is tempting to speculate that the evolution of miRNAs in filarial nematodes relates to parasitism, it should also be noted that a study comparing miRNAs in the free-living nematode *Pristionchus pacificus* to the *Caenorhabditis* spp. (clade V nematodes) also showed that the majority of miRNAs were not conserved.[55] Likewise, another study examining miRNAs in nematodes spanning clades I-V showed that at least 20% of *C. elegans* miRNAs were conserved. This work also demonstrated that homology inversely correlated with phylogenetic distance for both free-living and parasitic nematodes.[16] Consequently, it seems likely that different miRNAs follow diverse evolutionary trajectories linked to various aspects of nematode biology in both free-living and parasitic organisms. It is still challenging to pinpoint correlations between specific behavioural and physiological adaptations and the fluidity at which miRNA families are lost or gained. Gene duplication and "arm switching" (a process that leads to a switch in the arm from which the functional mature miRNA is derived) have been proposed as common mechanisms for the evolution of miRNAs and expansion of some miRNA family members.[50,54]

5 | FUNCTIONAL IMPLICATIONS OF STAGE-SPECIFIC EXPRESSION OF MIRNAS

A number of observations suggest that discrete miRNA subsets might be important regulators of processes in a particular life stage of filarial

TABLE 1 miRNA identification in clade III nematodes

Clade III nematode	Life stage(s)	Method	Depth of coverage	miRNA diversity	Reference
Filarial nematodes					
Brugia malayi	Mixed AM, gAF & Mf	RNA 5′ ligation independent protocol + RT-PCR/Capillary Sequencing	503 inserts cloned	32 miRNAs	[29]
Brugia pahangi	iL3s & mixed AM & gAF	Small RNA library prep kit/ Illumina sequencing platform	13 million reads for *B. pahangi* iL3s/~13 million reads for *B. pahangi* mixed adults	125 precursor sequences that produce 99 mature miRNAs and 81 unique star sequences	[30]
Brugia malayi	AM, gAF & Mf	RNA 5′ ligation-dependent protocol + RT-PCR/Illumina sequencing platform	3.5-3.7 million reads in adult stages and Mf (8.9-10.5 million reads in Mf libraries with alternative treatments)	129 precursor sequences that produce 145 mature miRNAs	[36]
Dirofilaria immitis	Mixed AM & gAF	RNA di-tagging + RT-PCR/ Solexa sequencing platform	9.8 million reads	1063 miRNA candidates	[31]
Ascaris genus					
Ascaris suum	Embryonic stages & early development	RNA di-tagging approach+ RT-PCR/Illumina sequencing platform	6-46 million reads	97 miRNAs grouped into 59 *Ascaris* seed families	[28]
Ascaris suum	AM & gAF	RNA di-tagged approach/ Solexa sequencing platform	11.7 million reads for each life stage	494 and 505 miRNA candidates in gAF and AM, respectively	[26]
Ascaris suum, *Ascaris lumbricoides*	gAF	Illumina small RNA library prep kit/Solexa sequencing platform	14.7 and 9.8 million reads in *A. lumbricoides* and *A. suum* libraries, respectively	494 miRNA candidates in *A. suum*; 171 miRNA candidates in *A. lumbricoides*	[27]

iL3s = infective L3s, AM = adult male, gAF = gravid adult female, Mf = microfilariae.

nematodes. For example, many of the miRNAs identified in *B. malayi* showed stage-specific expression, including miR-2b and let-7 which are abundant in adult stages.[50] Interestingly, in a further study, Winter et al.[55] demonstrated that one particular member of the let-7 family, miR-5364, is the most upregulated miRNA in the infective L3s (iL3s) during the vector-to-host transition (~12X compared to vector-derived L3s), as soon as 24 hours post-infection. Analysis of the pre-miRNA sequence suggests that this let-7 family member is present in all clade III nematodes for which there is sequence information but is absent in other nematodes, including the clade V nematodes *C. elegans*, *Heligmosomoides polygyrus* and *H. contortus*.

It has also been reported that miR-71 was one of the most abundant miRNAs in small RNA libraries prepared from total RNA from mixed adult worms in *D. immitis*.[51] A later study in *B. malayi* showed that miR-71 represents ~27% of the total miRNA reads identified in Mf data sets and is 3-5X more enriched in Mf than adult worms.[56] It is possible that some of miR-71 detected in the study with *D. immitis* could potentially originate from Mf found in gravid female worms and not from adult worms per se, although this is still unclear. A recent report demonstrated the functional activity of miR-71 in developmentally competent *B. malayi* embryos using a luciferase reporter assay, concluding that miR-71 can act as a post-transcriptional repressor of mRNA targets in this life stage.[57] In *C. elegans*, miR-71 regulates longevity and life span,[58] where it is upregulated in L1 diapause and dauer larvae but not particularly in other life stages.[59]

It has been shown that filarial nematodes adjust their developmental schedule and fecundity in response to host-derived immunological factors.[40] This is indicative of different developmental trajectories depending upon environmental signals, a phenomenon referred to as phenotypic plasticity.[41–44] miRNAs, as well as other RNAi pathways, have been shown to control developmental choices and life-history traits in post-dauer *C. elegans*, which shares behavioural and physiological traits with infective L3 larvae in parasitic nematodes.[41,45,45–47] Therefore, it is likely that the same mechanisms operate in filarial nematodes to control development and fertility in response to immunological cues from the host. A comparative analysis evaluating the RNAi landscape throughout filarial development in different environmental contexts will help to clarify whether such molecular "switches" (discrete small RNA populations) could be the drivers or modulators of such morphological and developmental choices.

6 | ENDOGENOUS SMALL INTERFERING RNA (ENDO-SIRNA) PATHWAYS IN FILARIAL NEMATODES

Most commonly, RNAi pathways in parasitic nematodes are discussed in relation to the ability to trigger an RNAi-mediated gene silencing response upon stimulation with exogenous (or environmental) double-stranded RNAs (exo-dsRNAs). This requires uptake of

TABLE 2 Extracellular filarial-derived miRNAs reported in vitro and in vivo

Clade III nematode	Host	Sample type	Depth of coverage (Total parasite- specific RNA reads)	miRNA diversity	Reference
In vitro					
Brugia malayi (iL3s + adult males and females)	iL3s derived from mosquito/Adult worms obtained from NIAID-NIH/FR3	Excretion/ Secretion (ES) products	11 139 *B. malayi* reads in extracellular vesicles (EV's) (2% of total reads)/1 519 403 *B. malayi* reads in iL3s (50% of total reads)	52 miRNAs detected in iL3s-derived EVs	[69]
In vivo					
L. sigmodontis	BALB/c mice	Serum (d60p.i.— Patent infection)	1188 *L. sigmodontis* reads (1.5% of total reads)	16 *L. sigmodontis* miRNAs in mouse serum	[68]
Dirofilaria immitis	Dog	Plasma	>338,694 *D. immitis* reads	245 *D. immitis* miRNAs in dog plasma	[78]
Onchocerca volvulus	Human	Serum	>46 *O. volvulus* reads	21 *O. volvulus* miRNAs in Human serum	
Loa loa	Baboon	Plasma	Unknown	22 *L. loa* miRNAs in baboon plasma	[79]
Onchocerca ochengi	Cattle	Plasma	Unknown	10 *O. ochengi* miRNAs in bovine serum	
Onchocerca ochengi	Cattle	Nodular fluid	157 633 *O. ochengi* reads (1.1% of total reads)	62 *Onchocerca* miRNAs in onchocercoma fluids	[80]
Onchocerca volvulus	Humans	Serum/plasma	108 323 and 355 397 *O. volvulus* reads in two separate libraries (1.1 and 1.5% of total reads)	6 *Onchocerca* miRNAs in human serum/ plasma	

double-stranded RNA (dsRNA), processing this into primary siRNAs, amplification involving an RNA-dependent RNA polymerase to produce the secondary siRNAs and ability to spread the signal, (reviewed in [48-51]). In many nematodes, the absence of the dsRNA import protein SID-1 is thought to explain the lack of efficient RNAi carried out experimentally.[52] However, endogenous pathways are expected to exist in these organisms where siRNAs are generated by a variety of mechanisms and these can have a variety of functions.[50,53] In *C. elegans*, two major categories of endo-siRNAs have been identified 22G-RNAs and 26G-RNAs, both displaying a strong bias for guanine at the 5′ end. The endogenous 26G-RNAs are normally produced from mature mRNA transcripts by the action of the RNA-dependent RNA polymerase (RdRP) RRF-3.[54] These 26G-RNA precursors act as triggers for the production of a second class of 22G-RNAs that are synthesized de novo by RdRPs.[54] Other triggers such as piRNAs can also induce the de novo synthesis of 22G-siRNAs.[55,54] The function of the secondary siRNAs is dictated by the association with different types of AGO proteins. These have been shown to have multiple roles in *C.elegans* including chromosome segregation,[18] genome defence, surveillance and integrity,[15] as well as transgenerational epigenetic inheritance.[21]

In *Ascaris*, it was shown that 26G-RNAs as well as 22G-RNAs were predominantly detected in the germline through to 128-cell embryos.[28] The majority of these endo-siRNAs mapped to a broad spectrum of coding genes in an antisense fashion.[28] On the other hand, a total of 40 repeat-associated siRNAs were identified in adult stages of *B. malayi*.[29] Similarly, several sense and antisense siRNAs were detected in the small RNA data from iL3s and mixed adult stages in *B. pahangi*, with at least eight sequences derived from repetitive elements.[50] A closer examination revealed that these sequences were mainly associated with retrotransposons and mapped to nonannotated repeats. Interestingly, a phylumwide survey suggested that in clade III nematodes, the 22G-RNAs preferentially target antisense to predicted repetitive elements and have been proposed as a mechanism to control transposon activity in the absence of piRNAs.[16] Beyond genome defence, it is possible that endo-siRNAs might be involved in a wide range of biological processes in nematodes, including sophisticated (and potentially novel) gene silencing mechanisms as well as epigenetic regulation. Our understanding of these phenomena will be greatly enhanced with further studies of the post-transcriptional regulatory networks of different life stages across this clade.

7 | EXTRACELLULAR VESICLES AND EXTRACELLULAR RNA IN FILARIAL NEMATODES

It is now recognized that RNA molecules can also operate beyond the limits of the cell. One key feature of extracellular RNA (exRNA) is its remarkable stability in hostile environments such as human biofluids. Several studies have demonstrated that the stabilization of exRNA can occur through direct association with protein and lipid partners such as AGO complexes or LDH particles or encapsulation within EVs,

reviewed in.[55-57] EVs and exRNAs have been found in excretion/secretion (ES) products from a diverse range of parasites, from microbes to nematodes (reviewed in [11]). This has been suggested as an active exchange of genetic material that can mediate communication between organisms of the same species, or even between evolutionarily distant organisms.[58,59]

Most of the literature detailing exRNA in helminths focuses on their encapsulation within EVs although the origins of these are not all well documented (Figure 1). EVs that pellet upon ultracentrifugation can derive from the endocytic pathway (termed exosomes) or from budding off the plasma membrane (often termed microvesicles), and these can be difficult to distinguish by their sizes: exosomes are generally 40-100 nm and microvesicles can range from 100 to 1000 nm. These can also be difficult to distinguish based on their protein content; for example, recent research with mammalian EVs has demonstrated that proteins previously referred to as "canonical exosomal markers" (MHC I and II, flotillins, actin or heat-shock proteins 70, among others [56,57]) can be detected in other classes of EV. The authors further showed that even within small EVs of the same density and size, there were multiple categories that could be distinguished by displaying different combinations of protein markers.[60] It seems likely that such heterogeneity exists in parasite EVs, an area that remains largely unexplored, which could be key to understanding the diversity of their functions.[11]

Initial reports in the trematodes *Echinostoma caproni* and *Fasciola hepatica* suggested that EVs (30-100 nm) could derive from tegumental structures and could be a mechanism for transferring material to host cells.[61,62] EVs with similar sizes have also been characterized in the human pathogenic trematodes *Schistosoma mansoni* [63] and *Schistosoma japonicum*,[64] the carcinogenic liver fluke *Opisthorchis viverrini*,[65] the clade V gastrointestinal nematode *Teladorsagia circumcincta* [66] and the clade I whipworm *Trichuris suis*.[67] In our own work, we showed that the clade V gastrointestinal parasitic nematode *H. polygyrus* secretes EVs that are enriched in proteins known to be abundant in the intestinal tissue of the parasite as well proteins associated with exosome biogenesis (e.g. Alix).[68] In the context of filarial infections, a recent report focusing on *B. malayi* showed that both iL3s and gravid adult females secreted EVs in vitro.[69] The EVs detected in excretion/secretion (ES) products from iL3s were described as homogeneous, based on size, ranging between 50 and 120 nm. Proteomic analysis of the iL3s revealed an enrichment for several proteins previously termed exosome markers, including HSP70 and Rab-1.[69]

Nematode-derived miRNAs were identified in both *H. polygyrus* and *B. malayi* EVs with some overlap in those that were found including miR-71 and members of the let-7 and miR-100 families. Both studies in *H. polygyrus* [68] and *B. malayi* [69] showed that the secreted RNA population is distinct from the RNA isolated from the total worm. Similar observations were made when comparing the RNA from EVs and worms in *F. hepatica*.[70] While this suggests distinct miRNAs are secreted, it does not inform on whether this subset is selectively exported from the cell from which it derives. Some mechanisms for selective sorting of miRNAs into EVs have been described in mammalian systems, involving RNA-binding proteins.[71,72] The presence of ribosomal proteins in the EV's secreted by *B. malayi* iL3s was also noted,[69] although it is not known whether these were associated with rRNA fragments that were also found. It is unclear whether or how different RNA processing pathways converge with EV biogenesis and secretion. In some systems, components of the RISC complex have been detected in EVs or shown to comigrate with endosomal MVB fractions in density gradients.[73] Interestingly, one AGO protein was also identified in both vesicle and vesicle-depleted fractions from *H. polygyrus* in vitro,[68] although the mechanistic aspects associated with secretion of AGO proteins in nematodes or others parasites are unknown.

8 | REGULATION AND PLASTICITY OF EV SECRETION?

The population of EVs detected in ES products seems to be variable between life stages, with reduced content observed in *B. malayi* gravid adult females compared to iL3s.[69] Interestingly, the EV release rate from iL3s was reduced by ~two fold between 24 and 72 hours (estimated as the amount of particles released by parasite over time), and this is thought to be associated with worm viability in the culture conditions tested. Indeed, one outstanding question in the field is whether exRNA and EVs could derive from dead or moribund worms. It is intriguing to think of vesicle secretion as a regulated mechanism involving specialized tissues and/or organs in the nematode, whereby release could occur in response to environmental conditions, vector-to-host transition, activation of specific receptors stimulated by host hormones, etc. However, there is very little evidence at present to support this, in part because of the youth of this field. It was proposed by Zamanian et al.[69] that the release of EVs could be a phenotype restricted to larval stages and might be involved in invasion during the onset of infection by modulating immune responses in the host. Given the precedent for immune modulation by parasite EVs,[11,68,74] it does seem likely that their release would be subject to control, possibly by both parasite and host. It is also possible that properties of the EVs and their cargo can change throughout filarial development and in response to particular environmental challenges and/or cues. In the context of filarial parasites, for example, iL3s could release exRNA-loaded EVs aiming to ensure successful migration through an active interaction with cells at the site of the infection and/or evasion of early innate immune cells. Similarly, gravid adult females could release exRNAs involved in downregulation of immune response against Mf, thus ensuring their survival. Although exciting, the hypothesis of "plasticity" in the exRNA signals and EVs secreted by different life stages in filarial nematodes remains unstudied.

9 | EXTRACELLULAR SMALL RNAS AS BIOMARKERS FOR FILARIASIS—TOWARDS DIAGNOSTIC APPLICATIONS

One potential application of these parasite-derived exRNAs is in the area of biomarkers for helminthiases. This is based on a key observation that parasite-derived exRNAs can be detected in biofluids from

their hosts as demonstrated by small RNA sequencing and qRT-PCR. This was first documented in schistosomiasis,[75-77] but has also been examined by multiple groups in the context of filarial infections[78-80] (Table 2). In an initial report, Tritten et al.[78] documented a total of 245 miRNA candidates of potential nematode origin in the plasma of dogs infected with the heartworm *D. immitis* based on sequencing. In a subsequent report, they documented a total of 22 unique sequences derived from *L. loa* in human serum and 10 sequences derived from *Onchocerca ochengi* in infected cattle serum.[79] We have also identified 62 *O. ochengi*-derived miRNAs in onchocercomata fluid [80] and found a total of 16 Litomosoides *sigmodontis* -derived miRNAs in the serum of mice during the patent stage of the infection.[68] Common to all of these studies was the presence of extracellular miR-71 and miR-100 family members. Further comparisons are challenging due to differences in the technical methods and analysis reported from the studies, which use different cut-offs for defining a candidate miRNA and are carried out at different depths of coverage. Identification of nematode-derived small RNAs in host fluids is also challenging given the dominance of host-derived sequences in these samples, and it may be appropriate to remove all sequences that could derive from the host prior to assignment of these as parasitic in origin.

While it might be expected that all nematode parasites can or do release exRNA and EVs, there are a number of factors that will influence the ability to detect these molecules in different host fluids. It is logical that the localization of the parasite within the host dictates the presence of parasite-derived exRNAs in different biofluids. In line with this, nematode miRNAs could be identified in the serum of mice infected with *L. sigmodontis*, but not in serum from mice infected with *H. polygyrus* (which resides in the small intestine) in a side-by-side comparison.[68] The close contact between some filarial nematodes and the lymphatic system (*Wuchereria bancrofti*, *Loa loa*, *Brugia spp.*) could account for a widespread distribution of secreted parasite products into the bloodstream, such that they are readily detectable in serum and plasma (and perhaps urine) (Figure 2). On the other hand,

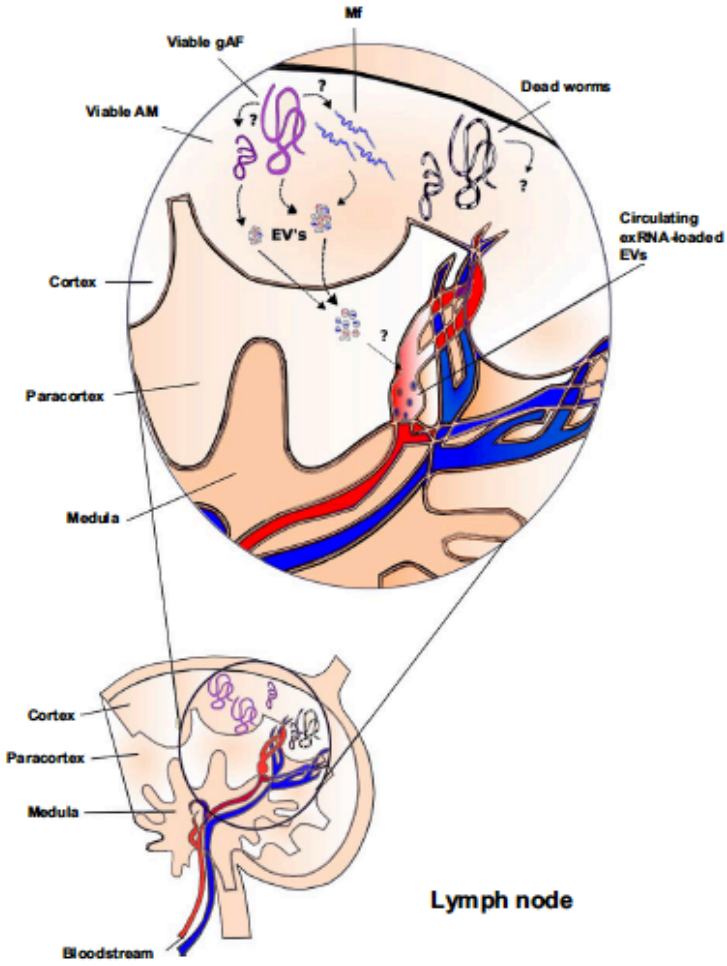

FIGURE 2 Proposed routes of extracellular vesicles (EV) secretion in vivo in lymphatic filariasis. Depiction of filarial nematodes (for example *Brugia* spp.) residing within a lymph node. A hypothesis is that the lack of a nodular structure (as observed in infection from *Onchocerca spp*) might facilitate the accessibility of EVs into the circulation. It is also unclear whether the detection of EVs and small RNAs is exclusively associated with viable worms or can be also derived from moribund or dead worms

the presence of a nodular structure in onchocerciasis may impose a physical barrier for the trafficking of locally secreted parasite products to the bloodstream. However, the presence of a vascularized system surrounding the onchocercomata nodule may be seen as a "window" for dissemination of such products [81] (Figure 3). The mechanisms by which parasite EVs and exRNAs can bypass physical barriers (e.g. those imposed by the nodular structure in *Onchocerca spp.*) and reach the bloodstream are not well understood yet but could help inform to what extent these molecules can be effectively used as biomarkers for different filarial infections.

The potential species specificity of some miRNAs makes them attractive candidates as diagnostics where co-infection is an issue, for example in distinguishing *Onchocerca volvulus* and *L. loa* in co-endemic communities. A pan-filarial small RNA-based biomarker could also be useful as a point-of-care diagnostic test aiming to monitor populations subjected to mass drug administration (MDA) or for elimination programs. Studies conducted in biofluids from several filarial infections suggest that, for instance, miR-71 can be used as a biomarker for filarial infection.[78–80] However, it is expected that several technological approaches will be considered to improve not only the platforms currently available for exRNA detection (reviewed in [82,85]) but also the way in which these technologies can be transferred in a field-friendly manner. Advancing inexpensive technologies and streamlined purification protocols will certainly increase the likelihood of adopting small RNA-based biomarkers in the field.

10 | FINAL CONSIDERATIONS & OUTSTANDING QUESTIONS

The field of EVs and small RNAs in parasitic nematodes is in its infancy and rapidly growing alongside efforts to exploit these in therapeutic and diagnostic applications. From a biological perspective, several outstanding questions should be addressed to drive this field forward. It is still unknown whether the secretion of exRNA-loaded EVs is developmentally regulated in parasitic nematodes, whether there are mechanisms to sort and package different small RNAs into EVs and whether all the different types of exRNAs reported so far in ES products play a role in parasite-to-host communication. If there are mechanisms in place in the parasitic nematodes

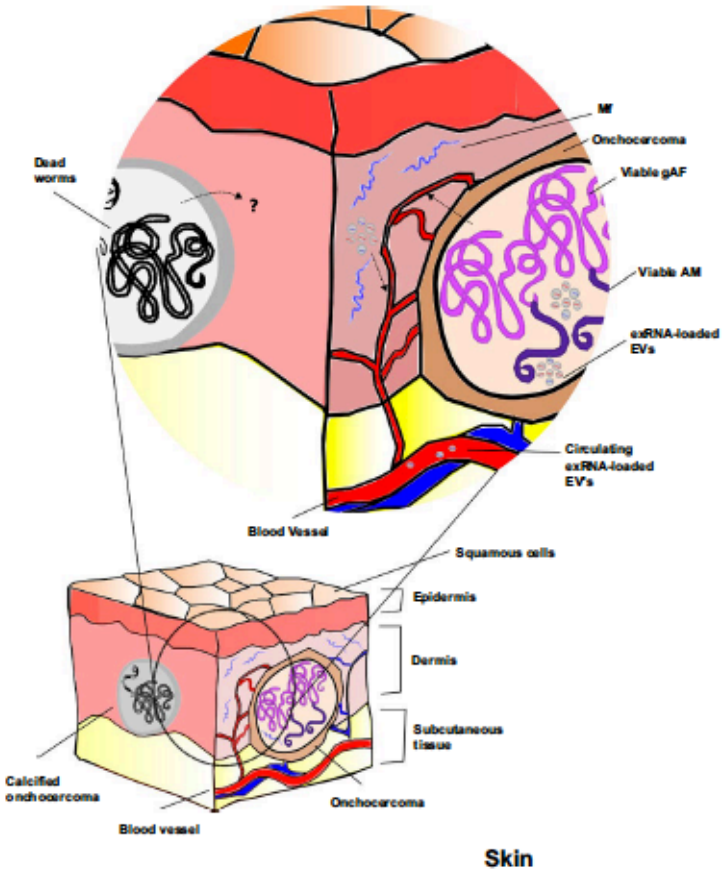

FIGURE 3 Proposed routes of extracellular vesicles (EV) secretion in vivo in Onchocerciasis. Depiction of a nodule-forming species member of the *Onchocerca* genus (e.g. *Onchocerca volvulus* or *Onchocerca ochengi*) residing within a nodular structure termed an onchocercoma. It is not yet clear whether or how the nodular structure imposes a physical barrier for dissemination of small RNA-loaded EVs into the bloodstream. As in Figure 2, it is unclear whether the detection of EVs and small RNAs is exclusively associated with viable worms or can be also derived from moribund or dead worms

to control EV secretion and dictate the cargo that is exported, then it is plausible that these mechanisms might have evolved as an additional axis of adaptation of the parasites to regulate their hosts' immune system.[84]

If this is the case, several aspects need to be considered. First, if the parasites effectively use EVs and small RNAs as a mechanism for invasion, colonization and immune evasion, then one possibility is that these functions are specifically compartmentalized within the parasites. We therefore should expect that certain tissues or organs be directly involved in their production and secretion/excretion, for example those with glandular functions such as the pharynx or cells producing ES products. Building from this idea, we could also propose that the profile and exRNA content of EVs, as well as the diversity of exRNAs, will be different between life stages, as a result of their development. For example, gravid adult females could actively secrete a plethora of exRNAs and EVs, which, together with other soluble proteins in the ES products, aim to maintain a downregulated immune status in the host in order to aid in survival not only of the adults but of the Mf as well, a life stage that is particularly less complex. This interplay with the host could begin early in the infection and would be maintained throughout. The idea of "maternally mediated" Mf survival is exciting as it offers a new possibility for treatment and intervention. However, the ideas proposed so far remain speculative and will require further analysis.

Although less explored in helminth infection, exRNAs and EVs could also have functions as mediators of parasite-to-parasite cross-talk. Studies in the protozoan Plasmodium *falciparum* showed that EVs can be involved in communication between parasite populations as well as with the host.[85] Other organisms such as fungi and bacteria, which are typically found in the normal microbiota in the host, also secrete EVs. EVs may not only be involved in communication with the vertebrate host but also could be relevant for the establishment of relevant ecological interactions between pathogens that might co-exist in natural conditions, for example in situations where multiple infections occur at the same time.[86] For example, it remains possible that exRNAs and EVs could be involved in *a*) intraspecies communication, for example chemoattractant derived from female worms to increase adult male motility or fertility, maternally derived prosurvival signals to increase Mf survival or *b*) interspecies communication, for example *Wolbachia*-derived EVs that confer nutritional advantages to the filarial host,[87–89] modulation of the host's immune response by filarial-derived EVs.[89]

Although still far off, further work in this area could contribute to the development of novel technological applications to diagnose and control filarial infections (reviewed in [90]). Basic research in this area also offers new scenarios to understand the real complexity that exists in the interaction between organisms at a molecular level. This is useful for understanding how parasitic nematodes can manipulate the gene expression machinery in their host for their own benefit, or the molecular basis of the mutualistic interactions between endosymbionts, for example *Wolbachia* and their nematode hosts. An exciting and intriguing avenue is the possibility of merging genome editing and functional genomic tools (reviewed in [91,92]) to engineer specific EVs cargos. These "tailored" EVs could be used as vehicles to further our understanding on how multiple organisms use these extracellular systems to transfer information and to maintain a dialogue with their surroundings. Towards this goal, further work will be required to improve the genetic manipulation toolkit currently available for filarial nematodes and to advance the basic research on EV and exRNA secretion and function in these parasites.

ACKNOWLEDGEMENTS

We thank our collaborators on filarial nematode projects for many helpful discussions and in particular Ken Pfarr, Achim Hoeruf, Ben Makepeace, Mark Blaxter, David Taylor and Coralie Martin. We also thank Ben Makepeace, Ken Pfarr and Paul Dickinson for comments on the manuscript. The studies on filarial nematode diagnostics are supported by a WT Pathfinder Award (201083/Z/16/Z) as well as previous funding from the Institute for Medical Microbiology, Immunology and Parasitology, University Hospital of Bonn, Germany, as part of a consortium grant funded by the Bill and Melinda Gates Foundation. Basic research in AB's laboratory on EVs and exRNA is supported by a WTRCDF (097394/Z/11/Z) and HFSP Young Investigator Award (RGY0069).

DISCLOSURES

None.

REFERENCES

1. Taylor MJ, Hoerauf A, Bockarie M. Lymphatic filariasis and onchocerciasis. *Lancet*. 2010;376:1175–1185.
2. Crump A, Morel CM, Omura S. The onchocerciasis chronicle: from the beginning to the end? *Trends Parasitol*. 2012;28:280–288.
3. Gems D. Longevity and ageing in parasitic and free-living nematodes. *Biogerontology*. 2000;1:289–307.
4. Maizels RM, McSorley HJ. Regulation of the host immune system by helminth parasites. *J Allergy Clin Immunol*. 2016;138:666–675.
5. Robinson MW, Donnelly S, Dalton JP. Helminth defence molecules-immunomodulators designed by parasites!. *Front Microbiol*. 2013;4:1–4.
6. Decottignies A. Endogenous RNAi and adaptation to environment in *C. elegans*. *Worm*. 2012;1:129–133.
7. Ghildiyal M, Zamore PD. Small silencing RNAs: an expanding universe. *Nat Rev Genet*. 2009;10:94–108.
8. Youngman EM, Claycomb JM. From early lessons to new frontiers: the worm as a treasure trove of small RNA biology. *Front Genet*. 2014;5:1–13.
9. Hoogstrate SW, Volkers RJ, Sterken MG, Kammenga JE, Snoek LB. Nematode endogenous small RNA pathways. *Worm*. 2014;3:e28234.
10. Kim VN, Han J, Siomi MC. Biogenesis of small RNAs in animals. *Nat Rev Mol Cell Biol*. 2009;10:126–139.
11. Coakley G, Maizels RM, Buck AH. Exosomes and other extracellular vesicles: the new communicators in parasite infections. *Trends Parasitol*. 2015;31:477–489.
12. Weick E-M, Miska E. piRNAs: from biogenesis to function. *Development*. 2014;141:3458–3471.
13. Buck AH, Blaxter M. Functional diversification of Argonautes in nematodes: an expanding universe. *Biochem Soc Trans*. 2013;41:881–886.

14. Hutvagner G, Simard MJ. Argonaute proteins: key players in RNA silencing. *Nat Rev Mol Cell Biol*. 2008;9:22–32.
15. Blaxter ML, De Ley P, Garey JR, et al. A molecular evolutionary framework for the phylum Nematoda. *Nature*. 1998;392:71–75.
16. Sarkies P, Selkirk ME, Jones JT, Blok V, et al. Ancient and novel small RNA pathways compensate for the loss of piRNAs in multiple independent nematode lineages. *PLoS Biol*. 2015;13:1–20.
17. Yigit E, Batista PJ, Bei Y, et al. Analysis of the *C. elegans* Argonaute family reveals that distinct Argonautes act sequentially during RNAi. *Cell*. 2006;127:747–757.
18. Wedeles CJ, Wu MZ, Claycomb JM. A multitasking Argonaute: exploring the many facets of *C. elegans* CSR-1. *Chromosome Res*. 2013;21:573–586.
19. Tu S, Wu MZ, Wang J, Cutter AD, Weng Z, Claycomb JM. Comparative functional characterization of the CSR-1 22G-RNA pathway in Caenorhabditis nematodes. *Nucleic Acids Res*. 2015;43:208–224.
20. Gu W, Shirayama M, Conte D, et al. Distinct Argonaute-mediated 22G-RNA pathways direct genome surveillance in the *C. elegans* germline. *Mol Cell*. 2009;36:231–244.
21. Klosin A, Lehner B. Mechanisms, timescales and principles of transgenerational epigenetic inheritance in animals. *Curr Opin Genet Dev*. 2016;36:41–49.
22. Meister G. Argonaute proteins: functional insights and emerging roles. *Nat Rev Genet*. 2013;14:447–459.
23. Bartel DP. MicroRNAs: target recognition and regulatory functions. *Cell*. 2009;136:215–233.
24. Grishok A. RNAi mechanisms in *Caenorhabditis elegans*. *FEBS Lett*. 2005;579:5932–5939.
25. Winter J, Jung S, Keller S, Gregory RI, Diederichs S. Many roads to maturity: microRNA biogenesis pathways and their regulation. *Nat Cell Biol*. 2009;11:228–234.
26. Xu MJ, Fu JH, Nisbet AJ, et al. Comparative profiling of microRNAs in male and female adults of *Ascaris suum*. *Parasitol Res*. 2013;112:1189–1195.
27. Shao C-C, Xu M-J, Alasaad S, et al. Comparative analysis of microRNA profiles between adult *Ascaris lumbricoides* and *Ascaris suum*. *BMC Vet Res*. 2014;10:99.
28. Wang J, Czech B, Crunk A, et al. Deep small RNA sequencing from the nematode Ascaris reveals conservation, functional diversification, and novel developmental profiles. *Genome Res*. 2011;21:1462–1477.
29. Poole CB, Davis PJ, Jin J, McReynolds LA. Cloning and bioinformatic identification of small RNAs in the filarial nematode, *Brugia malayi*. *Mol Biochem Parasitol*. 2010;169:87–94.
30. Winter A, Weir W, Hunt M, et al. Diversity in parasitic nematode genomes: the microRNAs of *Brugia pahangi* and *Haemonchus contortus* are largely novel. *BMC Genom*. 2012;13:4.
31. Fu Y, Lan J, Wu X, et al. Identification of *Dirofilaria immitis* miRNA using illumina deep sequencing. *Vet Res*. 2013;44:1–11.
32. Kozomara A, Griffiths-Jones S. MiRBase: annotating high confidence microRNAs using deep sequencing data. *Nucleic Acids Res*. 2014;42:68–73.
33. De Wit E, Linsen SEV, Cuppen E, Berezikov E. Repertoire and evolution of miRNA genes in four divergent nematode species. *Genome Res*. 2009;19:2064–2074.
34. Griffiths-Jones S, Hui JHL, Marco A, Ronshaugen M. MicroRNA evolution by arm switching. *EMBO Rep*. 2011;12:172–177.
35. Winter AD, Gillan V, Maitland K, et al. A novel member of the let-7 microRNA family is associated with developmental transitions in filarial nematode parasites. *BMC Genom*. 2015;16:331.
36. Poole CB, Gu W, Kumar S, et al. Diversity and expression of microRNAs in the filarial parasite, *Brugia malayi*. *PLoS ONE*. 2014;9:5.
37. Liu C, Voronin D, Poole CB, et al. Functional analysis of microRNA activity in *Brugia malayi*. *Int J Parasitol*. 2015;45:579–583.
38. Boulias K, Horvitz HR. The *C. elegans* microRNA mir-71 acts in neurons to promote germline-mediated longevity through regulation of DAF-16/FOXO. *Cell Metab*. 2012;15:439–450.
39. Karp X, Hammell M, Ow MC, et al. Effect of life history on microRNA expression during *C. elegans* development Effect of life history on microRNA expression during *C. elegans* development. *RNA*. 2011;17:639–651.
40. Babayan SA, Read AF, Lawrence RA, Bain O, Allen JE. Filarial parasites develop faster and reproduce earlier in response to host immune effectors that determine filarial life expectancy. *PLoS Biol*. 2010;8:e1000525.
41. Kochin BF, Bull JJ, Antia R. Parasite evolution and life history theory. *PLoS Biol*. 2010;8:10–13.
42. Schlichting CD. Origins of differentiation via phenotypic plasticity. *Evol Dev*. 2003;5:98–105.
43. Schlichting CD, Smith H. Phenotypic plasticity: linking molecular mechanisms with evolutionary outcomes. *Evol Ecol*. 2002;16:189–211.
44. Viney M, Cable J. Macroparasite life histories. *Curr Biol*. 2011;21:R767–R774.
45. Fielenbach N, Antebi A. *C. elegans* dauer formation and the molecular basis of plasticity. *Genes Dev*. 2008;22:2149–2165.
46. Davies SJ, McKerrow JH. Developmental plasticity in schistosomes and other helminths. *Int J Parasitol*. 2003;33:1277–1284.
47. Hall SE, Chirn G-W, Lau NC, Sengupta P. RNAi pathways contribute to developmental history-dependent phenotypic plasticity in *C. elegans*. *RNA*. 2013;19:306–319.
48. Maule AG, McVeigh P, Dalzell JJ, Atkinson L, Mousley A, Marks NJ. An eye on RNAi in nematode parasites. *Trends Parasitol*. 2011;27:505–513.
49. Piatek MJ, Werner A. Endogenous siRNAs: regulators of internal affairs. *Biochem Soc Trans*. 2014;42:1174–1179.
50. Hoogstrate S, Volkers R. Nematode endogenous small RNA pathways. *Worm*. 2014;3:e28234.
51. Britton C, Winter AD, Marks ND, et al. Application of small RNA technology for improved control of parasitic helminths. *Vet Parasitol*. 2015;212:47–53.
52. Dalzell JJ, McVeigh P, Warnock ND, et al. RNAi effector diversity in nematodes. *PLoS Negl Trop Dis*. 2011;5:e1176.
53. Sarkies P, Miska E. Small RNAs break out: the molecular cell biology of mobile small RNAs. *Nat Rev Mol Cell Biol*. 2014;15:525–535.
54. Billi AC. Endogenous RNAi pathways in *C. elegans*. *WormBook* (10) WormBook 2014;7:1–49.
55. Hoy AM, Buck AH. Extracellular small RNAs: what, where, why? *Biochem Soc Trans*. 2012;40:886–890.
56. Mittelbrunn M, Sánchez-Madrid F. Intercellular communication: diverse structures for exchange of genetic information. *Nat Rev Mol Cell Biol*. 2012;13:328–335.
57. Turchinovich A, Samatov TR, Tonevitsky AG, Burwinkel B. Circulating miRNAs: cell-cell communication function? *Front Genet*. 2013;4:1–10.
58. Sarkies P, Miska E. Is there social RNA? *Science*. 2013;341:467–468.
59. Knip M, Constantin ME, Thordal-Christensen H. Trans-kingdom cross-talk: small RNAs on the move. *PLoS Genet*. 2014;10:e1004602.
60. Kowal J, Arras G, Colombo M, et al. Proteomic comparison defines novel markers to characterize heterogeneous populations of extracellular vesicle subtypes. *Proc Natl Acad Sci USA*. 2016;113:E968–E977.
61. Marcilla A, Trelis M, Cortes A, et al. Extracellular vesicles from parasitic helminths contain specific excretory/secretory proteins and are internalized in intestinal host cells. *PLoS ONE*. 2012;7:e45974.
62. Cwiklinski K, de la Torre-Escudero E, Trelis M, et al. The extracellular vesicles of the helminth pathogen, Fasciola hepatica: biogenesis pathways and cargo molecules involved in parasite pathogenesis. *Mol Cell Proteomics*. 2015;14:3258–3273.
63. Nowacki FC, Swain MT, Klychnikov OI, et al. Protein and small non-coding RNA-enriched extracellular vesicles are released by the pathogenic blood fluke *Schistosoma mansoni*. *J Extracell Vesicles*. 2015;4:28665.

64. Wang L, Li Z, Shen J, et al. Exosome-like vesicles derived by *Schistosoma japonicum* adult worms mediates M1 type immune- activity of macrophage. *Parasitol Res*. 2015;114:1865–1873.
65. Chaiyadet S, Sotillo J, Smout M, et al. Carcinogenic liver fluke secretes extracellular vesicles that promote cholangiocytes to adopt a tumorigenic phenotype. *J Infect Dis*. 2015;212:1636–1645.
66. Tzelos T, Matthews JB, Buck AH, et al. A preliminary proteomic characterisation of extracellular vesicles released by the ovine parasitic nematode, *Teladorsagia circumcincta*. *Vet Parasitol*. 2016;221:84–92.
67. Hansen EP, Kringel H, Williams AR, Nejsum P. Secretion of RNA-containing extracellular vesicles by the porcine whipworm, *Trichuris suis*. *J Parasitol*. 2015;101:336–340.
68. Buck AH, Coakley G, Simbari F, et al. Exosomes secreted by a nematode parasite transfer small RNAs to mammalian cells and regulate genes of the innate immune system. *Nat Commun*. 2014;5:1–11.
69. Zamanian M, Fraser LM, Agbedanu PN, et al. Release of small RNA-containing exosome-like vesicles from the human filarial parasite *Brugia malayi*. *PLoS Negl Trop Dis*. 2015;9:1–23.
70. Fromm B, Trelis M, Hackenberg M, Cantalapiedra F, Bernal D, Marcilla A. The revised microRNA complement of *Fasciola hepatica* reveals a plethora of overlooked microRNAs and evidence for enrichment of immuno-regulatory microRNAs in extracellular vesicles. *Int J Parasitol*. 2015;45:697–702.
71. Villarroya-Beltri C, Gutiérrez-Vázquez C, Sánchez-Cabo F, et al. Sumoylated hnRNPA2B1 controls the sorting of miRNAs into exosomes through binding to specific motifs. *Nat Commun*. 2013;4:2980.
72. Mukherjee K, Ghoshal B, Ghosh S, et al. Reversible HuR-microRNA binding controls extracellular export of miR-122 and augments stress response. *EMBO Rep*. 2016;17:11841203.
73. Gibbings DJ, Ciaudo C, Erhardt M, Voinnet O. Multivesicular bodies associate with components of miRNA effector complexes and modulate miRNA activity. *Nat Cell Biol*. 2009;11:1143–1149.
74. Montaner S, Galiano A, Trelis M, et al. The role of extracellular vesicles in modulating the host immune response during parasitic infections. *Front Immunol*. 2014;5:1–8.
75. Hoy AM, Lundie RJ, Ivens A, et al. Parasite-derived microRNAs in host serum as novel biomarkers of helminth infection. *PLoS Negl Trop Dis*. 2014;8:e2701.
76. Cai P, Gobert GN, You H, Duke M, McManus DP. Circulating miRNAs: potential novel biomarkers for hepatopathology progression and diagnosis of Schistosomiasis japonica in two murine models. *PLoS Negl Trop Dis*. 2015;9:1–18.
77. Cheng G, Luo R, Hu C, Cao J, Jin Y. Deep sequencing-based identification of pathogen-specific microRNAs in the plasma of rabbits infected with *Schistosoma japonicum*. *Parasitology*. 2013;140:1751–1761.
78. Tritten L, Burkman E, Moorhead A, et al. Detection of circulating parasite-derived MicroRNAs in filarial infections. *PLoS Negl Trop Dis*. 2014;8:e2971.
79. Tritten L, O'Neill M, Nutting C, et al. *Loa loa* and *Onchocerca ochengi* miRNAs detected in host circulation. *Mol Biochem Parasitol*. 2014;198:14–17.
80. Quintana JF, Makepeace BL, Babayan SA, et al. Extracellular Onchocerca-derived small RNAs in host nodules and blood. *Parasit Vectors*. 2015;8:58.
81. Attout T, Hoerauf A, Dénécé G, et al. Lymphatic vascularisation and involvement of Lyve-1 + macrophages in the human Onchocerca nodule. *PLoS ONE*. 2009;4:e8234.
82. Pritchard CC, Cheng HH, Tewari M. MicroRNA profiling: approaches and considerations. *Nat Rev Genet*. 2012;13:358–369.
83. Alhassan A, Li Z, Poole CB, Carlow CKS. Expanding the MDx toolbox for filarial diagnosis and surveillance. *Trends Parasitol*. 2015;31:391–400.
84. Twu O, Johnson PJ. Parasite extracellular vesicles: mediators of intercellular communication. *PLoS Pathog*. 2014;10:8–10.
85. Mantel PY, Hoang AN, Goldowitz I, et al. Malaria-infected erythrocyte-derived microvesicles mediate cellular communication within the parasite population and with the host immune system. *Cell Host Microbe*. 2013;13:521–534.
86. Barteneva NS, Maltsev N, Vorobjev IA. Microvesicles and intercellular communication in the context of parasitism. *Front Cell Infect Microbiol*. 2013;3:49.
87. Fischer K, Beatty WL, Jiang D, Weil GJ, Fischer PU. Tissue and stage-specific distribution of Wolbachia in *Brugia malayi*. *PLoS Negl Trop Dis*. 2011;5:e1174.
88. McNulty SN, Fischer K, Curtis KC, Weil GJ, Brattig NW, Fischer PU. Localization of Wolbachia-like gene transcripts and peptides in adult *Onchocerca flexuosa* worms indicates tissue specific expression. *Parasit Vectors*. 2013;6:2.
89. Voronin D, Bachu S, Shlossman M, Unnasch TR, Ghedin E, Lustigman S. Glucose and glycogen metabolism in *Brugia malayi* is associated with wolbachia symbiont fitness. *PLoS ONE*. 2016;11:1–18.
90. Tritten L, Geary TG. MicroRNAs of filarial nematodes: a new frontier in host-pathogen interactions. In: Ana LL, Francisco JE, eds. *Non-coding RNAs Inter-kingdom Communication*. Switzerland: Springer International Publishing; 2016: 207–223.
91. Zamanian M, Andersen EC. Prospects and challenges of CRISPR/Cas genome editing for the study and control of neglected vector-borne nematode diseases. *FEBS J*. 2016;283:3204–3221.
92. Ward JD. Rendering the intractable more tractable: tools from *Caenorhabditis elegans* ripe for import into parasitic nematodes. *Genetics*. 2015;201:1279–1294.

How to cite this article: Quintana JF, Babayan SA, Buck AH. Small RNAs and extracellular vesicles in filarial nematodes: From nematode development to diagnostics. *Parasite Immunology*. 2017;39:e12395. https://doi.org/10.1111/pim.12395

Chapter 8: **References**

Al-Qaoud, K. M., Pearlman, E., Hartung, T., Klukowski, J., et al. (2000). A new mechanism for IL-5-dependent helminth control: neutrophil accumulation and neutrophil-mediated worm encapsulation in murine filariasis are abolished in the absence of IL-5. *International Immunology*, *12*(6), 899–908. https://doi.org/10.1093/intimm/12.6.899

Al-Qaoud, K., Taubert, A., Zahner, H., Fleischer, B., et al. (1997). Infection of BALB / c mice with the filarial nematode Litomosoides sigmodontis : role of CD4 + T cells in controlling larval development . Infection of BALB / c Mice with the Filarial Nematode Litomosoides sigmodontis : Role of CD4 ♀ T Cells in Controllin. *Infection and Immunity*, *65*(6), 2457–2461.

Alhassan, A., Li, Z., Poole, C. B., & Carlow, C. K. S. (2015). Expanding the MDx toolbox for filarial diagnosis and surveillance. *Trends in Parasitology*, *31*(8), 391–400. https://doi.org/10.1016/j.pt.2015.04.006

Alhassan, A., Makepeace, B. L., Lacourse, E. J., Osei-Atweneboana, M. Y., et al. (2014). A simple isothermal DNA amplification method to screen black flies for Onchocerca volvulus infection. *PLoS ONE*, *9*(10). https://doi.org/10.1371/journal.pone.0108927

Alhassan, A., Makepeace, B. L., LaCourse, E. J., Osei-Atweneboana, M. Y., et al. (2014). A simple isothermal DNA amplification method to screen black flies for Onchocerca volvulus infection. *PloS One*, *9*(10), e108927. https://doi.org/10.1371/journal.pone.0108927

Allen, J. E., Adjei, O., Bain, O., Hoerauf, A., et al. (2008). Of mice, cattle, and humans: the immunology and treatment of river blindness. *PLoS Neglected Tropical Diseases*, *2*(4), e217. https://doi.org/10.1371/journal.pntd.0000217

Allen, J. E., & Macdonald, A. S. (1998). Profound suppression of cellular proliferation mediated by the secretions of nematodes. *Parasite Immunology*, *20*(5), 241–247. https://doi.org/10.1046/j.1365-3024.1998.00151.x

Altschul, S. F., Gish, W., Miller, W., Myers, E. W., et al. (1990). Basic Local Alignment Search Tool.pdf. *J Mol Biol*, *215*. https://doi.org/10.1016/S0022-

2836(05)80360-2

Ameres, S. L., & Zamore, P. D. (2013). Diversifying microRNA sequence and function. *Nature Reviews Molecular Cell Biology*, *14*(8), 475–488. https://doi.org/10.1038/nrm3611

Armstrong, S. D., Babayan, S. a, Lhermitte-Vallarino, N., Gray, N., et al. (2014). Comparative Analysis of the Secretome from a Model Filarial Nematode (Litomosoides sigmodontis) reveals Maximal Diversity in Gravid Female Parasites. *Molecular & Cellular Proteomics : MCP*, *13*(10), 2527–2544. https://doi.org/10.1074/mcp.M114.038539

Armstrong, S. D., Xia, D., Bah, G. S., Krishna, R., et al. (2016). Stage-specific proteomes from Onchocerca ochengi , sister species of the human river blindness parasite , uncover adaptations to a nodular lifestyle. *Molecular & Cellular Proteomics*, *15*(8), 2554–75.

Arndts, K., Specht, S., Debrah, A. Y., Tamarozzi, F., et al. (2014). Immunoepidemiological profiling of onchocerciasis patients reveals associations with microfilaria loads and ivermectin intake on both individual and community levels. *PLoS Neglected Tropical Diseases*, *8*(2), e2679. https://doi.org/10.1371/journal.pntd.0002679

Attout, T., Babayan, S., Hoerauf, a, Taylor, D. W., et al. (2005). Blood-feeding in the young adult filarial worms Litomosoides sigmodontis. *Parasitology*, *130*(Pt 4), 421–428. https://doi.org/10.1017/S0031182005008176

Attout, T., Hoerauf, A., Dénécé, G., Debrah, A. Y., et al. (2009). Lymphatic vascularisation and involvement of Lyve-1+ macrophages in the human Onchocerca nodule. *PLoS ONE*, *4*(12), e8234. https://doi.org/10.1371/journal.pone.0008234

Attout, T., Martin, C., Babayan, S. a., Kozek, W. J., et al. (2000). Litomosoides sigmodontis in mice: reappraisal of an old model for filarial research. *Parasitology Today (Personal Ed.)*, *16*(2), 387–9. https://doi.org/10.1006/expr.1999.4475

Attout, T., Martin, C., Babayan, S. a., Kozek, W. J., et al. (2008). Pleural cellular reaction to the filarial infection Litomosoides sigmodontis is determined by the moulting process, the worm alteration, and the host strain. *Parasitology International*, *57*(2), 201–211. https://doi.org/10.1016/j.parint.2008.01.001

Avery, L., & Shtonda, B. B. (2003). Food transport in the C. elegans pharynx. *The*

Journal of Experimental Biology, *206*, 2441–2457. https://doi.org/10.1242/jeb.00433

Babalola, O. E. (2011). Ocular onchocerciasis: current management and future prospects. *Clinical Ophthalmology (Auckland, N.Z.)*, *5*, 1479–91. https://doi.org/10.2147/OPTH.S8372

Babayan, S. A., Allen, J. E., & Taylor, D. W. (2012). Future prospects and challenges of vaccines against filariasis. *Parasite Immunology*, *34*(5), 243–253. https://doi.org/10.1111/j.1365-3024.2011.01350.x

Babayan, S. A., Read, A. F., Lawrence, R. A., Bain, O., et al. (2010). Filarial parasites develop faster and reproduce earlier in response to host immune effectors that determine filarial life expectancy. *PLoS Biology*, *8*(10), e1000525. https://doi.org/10.1371/journal.pbio.1000525

Babayan, S., Ungeheuer, M. N., Martin, C., Attout, T., et al. (2003). Resistance and Susceptibility to Filarial Infection with Litomosoides sigmodontis Are Associated with Early Differences in Parasite Development and in Localized Immune Reactions. *Infection and Immunity*, *71*(12), 6820–6829. https://doi.org/10.1128/IAI.71.12.6820-6829.2003

Babu, S., Anuradha, R., Kumar, N. P., George, P. J., et al. (2011). Filarial lymphatic pathology reflects augmented Toll-Like receptor-mediated, mitogen-activated protein kinase-mediated proinflammatory cytokine production. *Infection and Immunity*, *79*(11), 4600–4608. https://doi.org/10.1128/IAI.05419-11

Bain, O., & Babayan, S. (2013). Behaviour of filariae: morphological and anatomical signatures of their life style within the arthropod and vertebrate hosts. *Filaria Journal*, *2*(16).

Ballesteros, C., Tritten, L., O'Neill, M., Burkman, E., et al. (2016). The Effect of In Vitro Cultivation on the Transcriptome of Adult Brugia malayi. *PLoS Neglected Tropical Diseases*, *10*(1), 1–20. https://doi.org/10.1371/journal.pntd.0004311

Ballesteros, C., Tritten, L., ONeill, M., Burkman, E., et al. (2016). The Effects of Ivermectin on Brugia malayi Females In Vitro: A Transcriptomic Approach. *PLoS Neglected Tropical Diseases*, *10*(8), 1–19. https://doi.org/10.1371/journal.pntd.0004929

Baraka, O., Mahmoud, B., Marschke, C., Geary, T., et al. (1996). Ivermectin distribution in the plasma and tissues of patients infected with Onchocerca volvulus. *European Journal of Clinical Pharmacology*, *50*(5), 407–410.

Bartel, D. P. (2009). MicroRNAs: Target Recognition and Regulatory Functions. *Cell*, *136*(2), 215–233. https://doi.org/10.1016/j.cell.2009.01.002

Beatty, M., Guduric-fuchs, J., Brown, E., Bridgett, S., et al. (2014). Small RNAs from plants , bacteria and fungi within the order Hypocreales are ubiquitous in human plasma. *BMC Genomics*, *15*(1), 933. https://doi.org/10.1186/1471-2164-15-933

Bennuru, S., Semnani, R., Meng, Z., Ribeiro, J. M. C., et al. (2009). Brugia malayi excreted/secreted proteins at the host/parasite interface: Stage- and gender-specific proteomic profiling. *PLoS Neglected Tropical Diseases*, *3*(4). https://doi.org/10.1371/journal.pntd.0000410

Blaxter, M., & Koutsovoulos, G. (2014). The evolution of parasitism in Nematoda. *Parasitology*, *142*, 1–14. https://doi.org/10.1017/S0031182014000791

Blaxter, M. L., De Ley, P., Garey, J. R., Liu, L. X., et al. (1998). A molecular evolutionary framework for the phylum Nematoda. *Nature*, *392*(6671), 71–75. https://doi.org/10.1038/32160

Boatin, B. A., Basáñez, M. G., Prichard, R. K., Awadzi, K., et al. (2012). A research agenda for helminth diseases of humans: Towards control and elimination. *PLoS Neglected Tropical Diseases*, *6*(4). https://doi.org/10.1371/journal.pntd.0001547

Boatin, B. a, Toé, L., Alley, E. S., Nagelkerke, N. J. D., et al. (2002). Detection of Onchocerca volvulus infection in low prevalence areas: a comparison of three diagnostic methods. *Parasitology*, *125*, 545–52. https://doi.org/10.1017/S0031182002002494

Boon, R. a, & Vickers, K. C. (2013). Intercellular transport of microRNAs. *Arteriosclerosis, Thrombosis, and Vascular Biology*, *33*(2), 186–92. https://doi.org/10.1161/ATVBAHA.112.300139

Bottomley, C., Isham, V., Vivas-Martínez, S., Kuesel, A. C., et al. (2016). Modelling Neglected Tropical Diseases diagnostics: the sensitivity of skin snips for Onchocerca volvulus in near elimination and surveillance settings. *Parasites & Vectors*, *9*(1), 343. https://doi.org/10.1186/s13071-016-1605-3

Bouchery, T., Lefoulon, E., Karadjian, G., Nieguitsila, A., et al. (2013). The symbiotic role of Wolbachia in Onchocercidae and its impact on filariasis. *Clinical Microbiology and Infection*, *19*(2), 131–40. https://doi.org/10.1111/1469-0691.12069

Branicky, R., & Hekimi, S. (2006). What keeps C. elegans regular: the genetics of defecation. *Trends in Genetics*, *22*(10), 571–579.

https://doi.org/10.1016/j.tig.2006.08.006

Brattig, N. W. (2004). Pathogenesis and host responses in human onchocerciasis: Impact of Onchocerca filariae and Wolbachia endobacteria. *Microbes and Infection*, *6*(1), 113–128. https://doi.org/10.1016/j.micinf.2003.11.003

Brattig, N. W., Bazzocchi, C., Kirschning, C. J., Reiling, N., et al. (2016). The Major Surface Protein of Wolbachia Endosymbionts in Filarial Nematodes Elicits Immune Responses through TLR2 and TLR4. https://doi.org/10.4049/jimmunol.173.1.437

Brenner, J. L., Kemp, B. J., & Abbott, A. L. (2012). The mir-51 family of microRNAs functions in diverse regulatory pathways in Caenorhabditis elegans. *PloS One*, *7*(5), e37185. https://doi.org/10.1371/journal.pone.0037185

Britton, C., Winter, A. D., Gillan, V., & Devaney, E. (2014). MicroRNAs of parasitic helminths - Identification, characterization and potential as drug targets. *International Journal for Parasitology: Drugs and Drug Resistance*, *4*(2), 85–94. https://doi.org/10.1016/j.ijpddr.2014.03.001

Bronsvoort, B. M. deC C., Renz, A., Tchakoute, V., Tanya, V. N., et al. (2005). Repeated high doses of avermectins cause prolonged sterilisation, but do not kill, Onchoceca ochengi adult worms in African cattle. *Filaria Journal*, *4*, 8. https://doi.org/10.1186/1475-2883-4-8

Buck, A. H., & Blaxter, M. (2013). Functional diversification of Argonautes in nematodes: an expanding universe. *Biochemical Society Transactions*, *41*(4), 881–6. https://doi.org/10.1042/BST20130086

Buck, A. H., Coakley, G., Simbari, F., Mcsorley, H. J., et al. (2014). Exosomes secreted by a nematode parasite transfer small RNAs to mammalian cells and regulate genes of the innate immune system. *Nature Communications*, *5*, 1–11. https://doi.org/10.1038/ncomms6488

Buck, A. H., Coakley, G., Simbari, F., McSorley, H. J., et al. (2014). Exosomes secreted by nematode parasites transfer small RNAs to mammalian cells and modulate innate immunity. *Nature Communications*, *5*, 5488. https://doi.org/10.1038/ncomms6488

Buechner, M. (2002). Tubes and the single C. elegans excretory cell. *Trends in Cell Biology*, *12*(10), 479–484. https://doi.org/10.1016/S0962-8924(02)02364-4

Burge, S. W., Daub, J., Eberhardt, R., Tate, J., et al. (2013). Rfam 11.0: 10 years of RNA families. *Nucleic Acids Research*, *41*(Database issue), D226-32.

https://doi.org/10.1093/nar/gks1005

Burgos, K. L., Javaherian, A., Bomprezzi, R., Ghaffari, L., et al. (2013). Identification of extracellular miRNA in human cerebrospinal fluid by next-generation sequencing. *RNA (New York, N.Y.)*, *19*(5), 712–22. https://doi.org/10.1261/rna.036863.112

Cai, P., Gobert, G. N., & McManus, D. P. (2016). MicroRNAs in Parasitic Helminthiases: Current Status and Future Perspectives. *Trends in Parasitology*, *32*(1), 71–86. https://doi.org/10.1016/j.pt.2015.09.003

Canga, A. G., Prieto, A. M. S., Liébana, M. J. D., Martínez, N. F., et al. (2008). Mini-Review The Pharmacokinetics and Interactions of Ivermectin in Humans — A Mini-review. *The AAPS Journal*, *10*(1), 42–46. https://doi.org/10.1208/s12248-007-9000-9

Carithers, D. S. (2017). Examining the role of macrolides and host immunity in combatting filarial parasites. *Parasites & Vectors*, *10*(1), 182. https://doi.org/10.1186/s13071-017-2116-6

Chaiyadet, S., Sotillo, J., Smout, M., Cantacessi, C., et al. (2015). Carcinogenic Liver Fluke Secretes Extracellular Vesicles That Promote Cholangiocytes to Adopt a Tumorigenic Phenotype. *The Journal of Infectious Diseases*, *212*(10), 1636–45. https://doi.org/10.1093/infdis/jiv291

Chehayeb, J. F., Robertson, A. P., Martin, R. J., & Geary, T. G. (2014). Proteomic Analysis of Adult Ascaris suum Fluid Compartments and Secretory Products. *PLoS Neglected Tropical Diseases*, *8*(6). https://doi.org/10.1371/journal.pntd.0002939

Choi, Y.-J., Tyagi, R., McNulty, S. N., Rosa, B. A., et al. (2016). Genomic diversity in Onchocerca volvulus and its Wolbachia endosymbiont. *Nature Microbiology*, *2*(November), 16207. https://doi.org/10.1038/nmicrobiol.2016.207

Coakley, G., Maizels, R. M., & Buck, A. H. (2015). Exosomes and Other Extracellular Vesicles : The New Communicators in Parasite Infections. *Trends in Parasitology*, *31*(10), 477–489. https://doi.org/10.1016/j.pt.2015.06.009

Coakley, G., McCaskill, J. L., Borger, J. G., Simbari, F., et al. (2017). Extracellular Vesicles from a Helminth Parasite Suppress Macrophage Activation and Constitute an Effective Vaccine for Protective Immunity. *Cell Reports*, *19*(8), 1545–1557. https://doi.org/10.1016/j.celrep.2017.05.001

Coffeng, L. E., Stolk, W. a, Zouré, H. G. M., Veerman, J. L., et al. (2013). African

Programme For Onchocerciasis Control 1995-2015: model-estimated health impact and cost. *PLoS Neglected Tropical Diseases*, *7*(1), e2032. https://doi.org/10.1371/journal.pntd.0002032

Cook, R. (1977). Influential Observations and Outliers in Regression. *Technometrics*, *19*(1), 15–18.

Cotton, J. A., Bennuru, S., Grote, A., Harsha, B., et al. (2016). The genome of Onchocerca volvulus, agent of river blindness. *Nature Microbiology*, *2*(November 2016), 16216. https://doi.org/10.1038/nmicrobiol.2016.216

Coumans, F. A. W., Pol, E. Van Der, Bo, A. N., & Hajji, N. (2014). Reproducible extracellular vesicle size and concentration determination with tunable resistive pulse sensing. *Journal of Extracellular Vesicles*, *3*(10), 1–8.

Crump, A., Morel, C. M., & Omura, S. (2012). The onchocerciasis chronicle: from the beginning to the end? *Trends in Parasitology*, *28*(7), 280–8. https://doi.org/10.1016/j.pt.2012.04.005

Cwiklinski, K., de la Torre-Escudero, E., Trelis, M., Bernal, D., et al. (2015). The Extracellular Vesicles of the Helminth Pathogen, *Fasciola hepatica* : Biogenesis Pathways and Cargo Molecules Involved in Parasite Pathogenesis. *Molecular & Cellular Proteomics*, *14*(12), 3258–3273. https://doi.org/10.1074/mcp.M115.053934

Darby, A. C., Armstrong, S. D., Bah, G. S., Kaur, G., et al. (2012). Analysis of gene expression from the Wolbachia genome of a filarial nematode supports both metabolic and defensive roles within the symbiosis. *Genome Research*, *22*(12), 2467–77. https://doi.org/10.1101/gr.138420.112

de la Torre-Escudero, E., Bennett, A. P. S., Clarke, A., Brennan, G. P., et al. (2016). Extracellular Vesicle Biogenesis in Helminths: More than One Route to the Surface? *Trends in Parasitology*, *32*(12), 921–929. https://doi.org/10.1016/j.pt.2016.09.001

De Ley, P. (2006). A quick tour of nematode diversity and the backbone of nematode phylogeny. *WormBook : The Online Review of C. Elegans Biology*, 1–8. https://doi.org/10.1895/wormbook.1.41.1

Debrah, A. Y., Specht, S., Klarmann-Schulz, U., Batsa, L., et al. (2015). Doxycycline Leads to Sterility and Enhanced Killing of Female *Onchocerca volvulus* Worms in an Area With Persistent Microfilaridermia After Repeated Ivermectin Treatment: A Randomized, Placebo-Controlled, Double-Blind Trial. *Clinical*

Infectious Diseases, *61*(4), 517–526. https://doi.org/10.1093/cid/civ363

Debrah, L. B., Nausch, N., Opoku, V. S., Owusu, W., et al. (2017). Epidemiology of Mansonella perstans in the middle belt of Ghana, 4–11. https://doi.org/10.1186/s13071-016-1960-0

Dhahbi, J. M., Spindler, S. R., Atamna, H., Yamakawa, A., et al. (2013). 5' tRNA halves are present as abundant complexes in serum, concentrated in blood cells, and modulated by aging and calorie restriction. *BMC Genomics*, *14*, 298. https://doi.org/10.1186/1471-2164-14-298

Ditgen, D., Anandarajah, E. M., Meissner, K. A., Brattig, N., et al. (2014). Harnessing the Helminth Secretome for Therapeutic Immunomodulators. *BioMed Research International*, *2014*. https://doi.org/10.1155/2014/964350

Drame, P. M., Fink, D. L., Kamgno, J., Herrick, J. a, et al. (2014). Loop-mediated isothermal amplification for rapid and semiquantitative detection of Loa loa infection. *Journal of Clinical Microbiology*, *52*(6), 2071–7. https://doi.org/10.1128/JCM.00525-14

Eason, R. J., Bell, K. S., Marshall, F. A., Rodgers, D. T., et al. (2016). The helminth product, ES-62 modulates dendritic cell responses by inducing the selective autophagolysosomal degradation of TLR-transducers, as exemplified by PKCδ. *Scientific Reports*, *6*(1), 37276. https://doi.org/10.1038/srep37276

Eberhard, M. L., Cupp, E. W., Katholi, C. R., Richards, F. O., et al. (2017). Skin snips have no role in programmatic evaluations for onchocerciasis elimination: a reply to Bottomley et al. *Parasit Vectors*, *10*(1), 154. https://doi.org/10.1186/s13071-017-2090-z

Ebhardt, H. A., Tsang, H. H., Dai, D. C., Liu, Y., et al. (2009). Meta-analysis of small RNA-sequencing errors reveals ubiquitous post-transcriptional RNA modifications. *Nucleic Acids Research*, *37*(8), 2461–2470. https://doi.org/10.1093/nar/gkp093

Edgar, R. C. (2004). MUSCLE: Multiple sequence alignment with high accuracy and high throughput. *Nucleic Acids Research*, *32*(5), 1792–1797. https://doi.org/10.1093/nar/gkh340

Elson, L., Guderian, R., Araujo, E., Bradley, J., et al. (1994). Immunity to onchocerciasis: identification of a putatively immune population in a hyperendemic area of Ecuador. *J Infect Dis*, *169*(3), 588–594.

Erickson, S. M., Thomsen, E. K., Keven, J. B., Vincent, N., et al. (2013). Mosquito-

parasite interactions can shape filariasis transmission dynamics and impact elimination programs. *PLoS Neglected Tropical Diseases*, *7*(9), e2433. https://doi.org/10.1371/journal.pntd.0002433

Fabian, M. R., & Sonenberg, N. (2012). The mechanics of miRNA-mediated gene silencing: a look under the hood of miRISC. *Nature Structural & Molecular Biology*, *19*(6), 586–93. https://doi.org/10.1038/nsmb.2296

Favia, G., Cancrini, G., Ricci, I., Bazzocchi, C., et al. (2000). 5 S ribosomal spacer sequences of some filarial parasites: comparative analysis and diagnostic applications. *Molecular and Cellular Probes*, *14*(5), 285–90. https://doi.org/10.1006/mcpr.2000.0317

Fenn, K., & Blaxter, M. (2006). Wolbachia genomes: Revealing the biology of parasitism and mutualism. *Trends in Parasitology*, *22*(2), 60–65. https://doi.org/10.1016/j.pt.2005.12.012

Fenn, K., Conlon, C., Jones, M., Quail, M. a, et al. (2006). Phylogenetic relationships of the Wolbachia of nematodes and arthropods. *PLoS Pathogens*, *2*(10), e94. https://doi.org/10.1371/journal.ppat.0020094

Fink, D. L., Fahle, G. a, Fischer, S., Fedorko, D. F., et al. (2011). Toward molecular parasitologic diagnosis: enhanced diagnostic sensitivity for filarial infections in mobile populations. *Journal of Clinical Microbiology*, *49*(1), 42–7. https://doi.org/10.1128/JCM.01697-10

Fischer, K., Beatty, W. L., Jiang, D., Weil, G. J., et al. (2011). Tissue and stage-specific distribution of Wolbachia in Brugia malayi. *PLoS Neglected Tropical Diseases*, *5*(5). https://doi.org/10.1371/journal.pntd.0001174

Fischer, P., Bamuhiiga, J., & Büttner, D. W. (1997). Treatment of human Mansonella streptocerca infection with ivermectin. *Tropical Medicine & International Health : TM & IH*, *2*(2), 191–9. Retrieved from http://www.ncbi.nlm.nih.gov/pubmed/9472305

Fischer, P., Bonow, I., Supali, T., Ruckert, P., et al. (2005). Detection of filaria-specific IgG4 antibodies and filarial DNA, for the screening of blood spots for Brugia timori. *Annals of Tropical Medicine & Parasitology*, *99*(1), 53–60. https://doi.org/10.1179/136485905X13339

Fischer, P. U., King, C. L., Jacobson, J. A., & Weil, G. J. (2017). Potential Value of Triple Drug Therapy with Ivermectin , Diethylcarbamazine , and Albendazole (IDA) to Accelerate Elimination of Lymphatic Filariasis and Onchocerciasis in

Africa. *PLoS Neglected Tropical Diseases*, *11*(1), 1–10. https://doi.org/10.1371/journal.pntd.0005163

Florkowski, C. M. (2008). Sensitivity, specificity, receiver-operating characteristic (ROC) curves and likelihood ratios: communicating the performance of diagnostic tests. *The Clinical Biochemist. Reviews / Australian Association of Clinical Biochemists*, *29 Suppl 1*(August), S83–S87.

Fonslow, B. R., Stein, B. D., Webb, K. J., Xu, T., et al. (2013). Filarial and Wolbachia genomics. *Parasite Immunol*, *34*(2–3), 121–129. https://doi.org/10.1038/nmeth.2250.Digestion

Friedländer, M. R., Mackowiak, S. D., Li, N., Chen, W., et al. (2012). miRDeep2 accurately identifies known and hundreds of novel microRNA genes in seven animal clades. *Nucleic Acids Research*, *40*(1), 37–52. https://doi.org/10.1093/nar/gkr688

Fromm, B., Trelis, M., Hackenberg, M., Cantalapiedra, F., et al. (2015). The revised microRNA complement of Fasciola hepatica reveals a plethora of overlooked microRNAs and evidence for enrichment of immuno-regulatory microRNAs in extracellular vesicles. *International Journal for Parasitology*, *45*(11), 697–702. https://doi.org/10.1016/j.ijpara.2015.06.002

Gallart-Palau, X., Serra, A., Wong, A. S. W., Sandin, S., et al. (2015). Extracellular vesicles are rapidly purified from human plasma by PRotein Organic Solvent PRecipitation (PROSPR). *Scientific Reports*, *5*(March), 14664. https://doi.org/10.1038/srep14664

Gardon, J., Gardon-Wendel, N., Demanga-Ngangue, Kamgno, J., et al. (1997). Serious reactions after mass treatment of onchocerciasis with ivermectin in an area endemic for Loa loa infection. *Lancet*, *350*(9070), 18–22. https://doi.org/10.1016/S0140-6736(96)11094-1

Geary, J., Satti, M., Moreno, Y., Madrill, N., et al. (2012). First analysis of the secretome of the canine heartworm , Dirofilaria immitis. *Parasites & Vectors*, *5*(1), 1. https://doi.org/10.1186/1756-3305-5-140

George, G. H., Palmieri, J. R., & Connor, D. H. (1985). The onchocercal nodule: interrelationship of adult worms and blood vessels. *The American Journal of Tropical Medicine and Hygiene*, *34*(6), 1144–8. Retrieved from http://www.ncbi.nlm.nih.gov/pubmed/3834800

Gibbings, D. J., Ciaudo, C., Erhardt, M., & Voinnet, O. (2009). Multivesicular bodies

associate with components of miRNA effector complexes and modulate miRNA activity. *Nature Cell Biology*, *11*(9), 1143–1149. https://doi.org/10.1038/ncb1929

Globisch, D., Moreno, A. Y., Hixon, M. S., Nunes, A. a K., et al. (2013). Onchocerca volvulus-neurotransmitter tyramine is a biomarker for river blindness. *Proceedings of the National Academy of Sciences of the United States of America*, *110*(11), 4218–23. https://doi.org/10.1073/pnas.1221969110

González Canga, A., Sahagún Prieto, A. M., Diez Liébana, M. J., Fernández Martínez, N., et al. (2008). The Pharmacokinetics and Interactions of Ivermectin in Humans—A Mini-review. *The AAPS Journal*, *10*(1), 42–46. https://doi.org/10.1208/s12248-007-9000-9

Goodridge, H. S., Wilson, E. H., Harnett, W., Campbell, C. C., et al. (2001). Modulation of Macrophage Cytokine Production by ES-62, a Secreted Product of the Filarial Nematode Acanthocheilonema viteae. *The Journal of Immunology*, *167*(2), 940–945. https://doi.org/10.4049/jimmunol.167.2.940

Grainger, J. R., Smith, K. A., Hewitson, J. P., McSorley, H. J., et al. (2010). Helminth secretions induce de novo T cell Foxp3 expression and regulatory function through the TGF-β pathway. *The Journal of Experimental Medicine*, *207*(11), 2331–2341. https://doi.org/10.1084/jem.20101074

Gregory, W. F., & Selkirk, M. E. (1989). Secreted antigens of filarial nematodes : a survey and characterization of in vitro excreted / secreted products of adult Brugia malayi, 629–654.

Grieve, R. B. (1990). Immunologic relevance of the cuticle and epicuticle of larval Dirofilaria immitis and Toxocara canis. *Acta Tropica*, *47*(5–6), 399–402. https://doi.org/10.1016/0001-706X(90)90041-W

Griffiths-Jones, S. (2003). Rfam: an RNA family database. *Nucleic Acids Research*, *31*(1), 439–441. https://doi.org/10.1093/nar/gkg006

Grishok, A. (2005). RNAi mechanisms in Caenorhabditis elegans. *FEBS Letters*, *579*(26), 5932–5939. https://doi.org/10.1016/j.febslet.2005.08.001

Gruber, A. R., Lorenz, R., Bernhart, S. H., Neuböck, R., et al. (2008). The Vienna RNA websuite. *Nucleic Acids Research*, *36*, 70–74. https://doi.org/10.1093/nar/gkn188

Guiliano, D. B., Hong, X., McKerrow, J. H., Blaxter, M. L., et al. (2004). A gene family of cathepsin L-like proteases of filarial nematodes are associated with

larval molting and cuticle and eggshell remodeling. *Molecular and Biochemical Parasitology*, *136*(2), 227–242. https://doi.org/10.1016/j.molbiopara.2004.03.015

Guzmán, G. E., Awadzi, K., Opoku, N., Narayanan, R. B., et al. (2002). Comparison between the skin snip test and simple dot blot assay as potential rapid assessment tools for Onchocerciasis in the postcontrol era in Ghana. *Clinical and Diagnostic Laboratory Immunology*, *9*(5), 1014–1020. https://doi.org/10.1128/CDLI.9.5.1014

Han, E. (2013). Loop-mediated isothermal amplification test for the molecular diagnosis of malaria. *Expert Review of Molecular Diagnostics*, *13*(2), 205–218.

Hansen, E. P., Kringel, H., Williams, A. R., & Nejsum, P. (2015). Secretion of RNA-Containing Extracellular Vesicles by the Porcine Whipworm, Trichuris suis. *Journal of Parasitology*, *101*(3), 336–340. https://doi.org/10.1645/14-714.1

Hansen, R. D. E., Trees, A. J., Bah, G. S., Hetzel, U., et al. (2011). A worm's best friend: recruitment of neutrophils by Wolbachia confounds eosinophil degranulation against the filarial nematode Onchocerca ochengi. *Proceedings. Biological Sciences / The Royal Society*, *278*(1716), 2293–302. https://doi.org/10.1098/rspb.2010.2367

Harnett, M. M., Melendez, A. J., & Harnett, W. (2010). The therapeutic potential of the filarial nematode-derived immunodulator, ES-62 in inflammatory disease. *Clinical and Experimental Immunology*, *159*(3), 256–267. https://doi.org/10.1111/j.1365-2249.2009.04064.x

Harnett, W., & Harnett, M. M. (2006). Filarial nematode secreted product ES-62 is an anti-inflammatory agent: Therapeutic potential of small molecule derivatives and ES-62 peptide mimetics. *Clinical and Experimental Pharmacology and Physiology*, *33*(5–6), 511–518. https://doi.org/10.1111/j.1440-1681.2006.04400.x

Harnett, W., McInnes, I. B., & Harnett, M. M. (2004). ES-62, a filarial nematode-derived immunomodulator with anti-inflammatory potential. *Immunology Letters*, *94*(1–2), 27–33. https://doi.org/10.1016/j.imlet.2004.04.008

Helgason, C., & Miller, C. (2005). *Methods in Molecular Biology - Basic cell Culture* (3rd ed.). Totowa, NJ: Humana Press.

Hewitson, J. P., Grainger, J. R., & Maizels, R. M. (2009). Helminth immunoregulation: The role of parasite secreted proteins in modulating host

immunity. *Molecular and Biochemical Parasitology*, *167*(1), 1–11. https://doi.org/10.1016/j.molbiopara.2009.04.008

Hewitson, J. P., Harcus, Y. M., Curwen, R. S., Dowle, A. a., et al. (2008). The secretome of the filarial parasite, Brugia malayi: Proteomic profile of adult excretory-secretory products. *Molecular and Biochemical Parasitology*, *160*, 8–21. https://doi.org/10.1016/j.molbiopara.2008.02.007

Hildebrandt, J. C., Eisenbarth, A., Renz, A., & Streit, A. (2014). Reproductive biology of Onchocerca ochengi, a nodule forming filarial nematode in zebu cattle. *Veterinary Parasitology*, *205*(1–2), 318–29. https://doi.org/10.1016/j.vetpar.2014.06.006

Hise, A. G., & Pearlman, E. (2004). Microreview The role of endosymbiotic Wolbachia bacteria in filarial disease. *Cellular Microbiology*, *6*(2), 97–104. https://doi.org/10.1046/j.1462-5822.2003.00350.x

Hoerauf, A., Satoguina, J., Saeftel, M., & Specht, S. (2005). Immunomodulation by filarial nematodes. *Parasite Immunology*, *27*, 417–429.

Hoffmann, W. H., Petit, G., Schulz-Key, H., Taylor, D. W., et al. (2000). Litomosoides sigmodontis in Mice: Reappraisal of an old model for filarial research. *Parasitology Today*, *16*(9), 387–389. https://doi.org/10.1016/S0169-4758(00)01738-5

Holden-Dye, L., Joyner, M., O'Connor, V., & Walker, R. J. (2013). Nicotinic acetylcholine receptors: A comparison of the nAChRs of Caenorhabditis elegans and parasitic nematodes. *Parasitology International*, *62*(6), 606–615. https://doi.org/10.1016/j.parint.2013.03.004

Hoogstrate, S. W., Volkers, R. J., Sterken, M. G., Kammenga, J. E., et al. (2014). Nematode endogenous small RNA pathways. *Worm*, *3*(March), e28234. https://doi.org/10.4161/worm.28234

Hotez, P. J., Alvarado, M., Basáñez, M.-G., Bolliger, I., et al. (2014). The global burden of disease study 2010: interpretation and implications for the neglected tropical diseases. *PLoS Neglected Tropical Diseases*, *8*(7), e2865. https://doi.org/10.1371/journal.pntd.0002865

Hotez, P. J., Bottazzi, M. E., Franco-Paredes, C., Ault, S. K., et al. (2008). The neglected tropical diseases of Latin America and the Caribbean: A review of disease burden and distribution and a roadmap for control and elimination. *PLoS Neglected Tropical Diseases*, *2*(9). https://doi.org/10.1371/journal.pntd.0000300

Hotez, P. J., Strych, U., Lustigman, S., & Bottazzi, M. E. (2016). Human anthelminthic vaccines: Rationale and challenges. *Vaccine*, *34*(30), 3549–3555. https://doi.org/10.1016/j.vaccine.2016.03.112

Houston, K., & Harnett, W. (2004). Structure and synthesis of nematode phosphorylcholine-containing glycoconjugates. *Parasitology*, *129*, 655–661.

Howe, K. L., Bolt, B. J., Shafie, M., Kersey, P., et al. (2016). WormBase ParaSite - a comprehensive resource for helminth genomics. *Molecular and Biochemical Parasitology*, *In press*. https://doi.org/10.1016/j.molbiopara.2016.11.005

Hoy, A. M., & Buck, A. H. (2012). Extracellular small RNAs: what, where, why? *Biochemical Society Transactions*, *40*(4), 886–890. https://doi.org/10.1042/BST20120019

Hoy, A. M., Lundie, R. J., Ivens, A., Quintana, J. F., et al. (2014). Parasite-derived microRNAs in host serum as novel biomarkers of helminth infection. *PLoS Neglected Tropical Diseases*, *8*(2), e2701. https://doi.org/10.1371/journal.pntd.0002701

Hutvagner, G., & Simard, M. J. (2008). Argonaute proteins: key players in RNA silencing. *Nature Reviews. Molecular Cell Biology*, *9*(1), 22–32. https://doi.org/10.1038/nrm2321

Katawa, G., Layland, L. E., Debrah, A. Y., von Horn, C., et al. (2015). Hyperreactive Onchocerciasis is Characterized by a Combination of Th17-Th2 Immune Responses and Reduced Regulatory T Cells. *PLoS Neglected Tropical Diseases*, *9*(1). https://doi.org/10.1371/journal.pntd.0003414

Kim, V. N., Han, J., & Siomi, M. C. (2009). Biogenesis of small RNAs in animals. *Nature Reviews. Molecular Cell Biology*, *10*(2), 126–39. https://doi.org/10.1038/nrm2632

Knopp, S., Steinmann, P., Hatz, C., Keiser, J., et al. (2012). Nematode Infections: Filariases. *Infectious Disease Clinics of North America*. https://doi.org/10.1016/j.idc.2012.02.005

Kochin, B. F., Bull, J. J., & Antia, R. (2010). Parasite evolution and life history theory. *PLoS Biology*, *8*(10), 10–13. https://doi.org/10.1371/journal.pbio.1000524

Kon, S. P., Pattison, J., Hicks, J., Labastide, W., et al. (1998). Depletion of wolbachia endobacteria in Onchocerca volvulus by doxycycline and microfilaridermia after ivermectin treatment For personal use . Only reproduce with permission from The Lancet Publishing Group . *The Lancet*, *357*, 1415–1416.

Korten, S., Hoerauf, a, Kaifi, J. T., & Büttner, D. W. (2011). Low levels of transforming growth factor-beta (TGF-beta) and reduced suppression of Th2-mediated inflammation in hyperreactive human onchocerciasis. *Parasitology*, *138*(1), 35–45. https://doi.org/10.1017/S0031182010000922

Kozomara, A., & Griffiths-Jones, S. (2014). miRBase: annotating high confidence microRNAs using deep sequencing data. *Nucleic Acids Research*, *42*(Database issue), D68-73. https://doi.org/10.1093/nar/gkt1181

Kreider, T., Anthony, R. M., Urban, J. F., & Gause, W. C. (2007). Alternatively activated macrophages in helminth infections. *Current Opinion in Immunology*, *19*(4), 448–453. https://doi.org/10.1016/j.coi.2007.07.002

Kurniawan, A., Yazdanbakhsh, M., van Ree, R., Aalberse, R., et al. (1993). Differential expression of IgE and IgG4 specific antibody responses in asymptomatic and chronic human filariasis. *Journal of Immunology (Baltimore, Md. : 1950)*, *150*(9), 3941–50. Retrieved from http://www.ncbi.nlm.nih.gov/pubmed/8473742

Kwan-Lim, G. E., Gregory, W. F., Selkirk, M. E., Partono, F., et al. (1989). Secreted antigens of filarial nematodes: a survey and characterization of in vitro excreted/secreted products of adult Brugia malayi. *Parasite Immunol*, *11*(6), 629–654. Retrieved from http://www.ncbi.nlm.nih.gov/pubmed/2616192

Lagatie, O., Batsa Debrah, L., Debrah, A., & Stuyver, L. J. (2017). Plasma-derived parasitic microRNAs have insufficient concentrations to be used as diagnostic biomarker for detection of Onchocerca volvulus infection or treatment monitoring using LNA-based RT-qPCR. *Parasitology Research*, *116*(3), 1013–1022. https://doi.org/10.1007/s00436-017-5382-5

Lagatie, O., Debrah, L. B., Debrah, A., & Stuyver, L. J. (2017). Plasma-derived parasitic microRNAs have insufficient concentrations to be used as diagnostic biomarker for detection of Onchocerca volvulus infection or treatment monitoring using LNA-based RT-qPCR. *Parasitology Research*, *116*, 1013–1022. https://doi.org/10.1007/s00436-017-5382-5

Lagatie, O., Ediage, E. N., Debrah, L. B., Diels, L., et al. (2016). Evaluation of the diagnostic potential of urinary N -Acetyltyramine- O , β -glucuronide (NATOG) as diagnostic biomarker for Onchocerca volvulus infection. *Parasites & Vectors*, (May), 1–10. https://doi.org/10.1186/s13071-016-1582-6

Laing, R., Gillan, V., & Devaney, E. (2017). Ivermectin - Old Drug, New Tricks?

Trends in Parasitology, *33*(6), 463–472. https://doi.org/10.1016/j.pt.2017.02.004

Lakshmi, V., Joseph, S. K., Srivastava, S., Verma, S. K., et al. (2010). Antifilarial activity in vitro and in vivo of some flavonoids tested against Brugia malayi. *Acta Tropica*, *116*(2), 127–133. https://doi.org/10.1016/j.actatropica.2010.06.006

Landgraf, P., Rusu, M., Sheridan, R., Sewer, A., et al. (2007). A mammlian microRNA Expression Atlas Based on Small RNA Library Sequencing. *Cell*, *129*(7), 1401–1414. https://doi.org/10.1016/j.cell.2007.04.040.A

Landmann, F., Bain, O., Martin, C., Uni, S., et al. (2012). Both asymmetric mitotic segregation and cell-to-cell invasion are required for stable germline transmission of Wolbachia in filarial nematodes. *Biology Open*, *1*(6), 536–547. https://doi.org/10.1242/bio.2012737

Landmann, F., Foster, J. M., Slatko, B., & Sullivan, W. (2010). Asymmetric wolbachia segregation during Early Brugia malayi embryogenesis determines its distribution in adult host tissues. *PLoS Neglected Tropical Diseases*, *4*(7). https://doi.org/10.1371/journal.pntd.0000758

Laney, S. J., Buttaro, C. J., Visconti, S., Pilotte, N., et al. (2008). A reverse transcriptase-PCR assay for detecting filarial infective larvae in mosquitoes. *PLoS Neglected Tropical Diseases*, *2*(6), 1–9. https://doi.org/10.1371/journal.pntd.0000251

Langmead, B., Trapnell, C., Pop, M., & Salzberg, S. L. (2009). Ultrafast and memory-efficient alignment of short DNA sequences to the human genome. *Genome Biology*, *10*(3), R25. https://doi.org/10.1186/gb-2009-10-3-r25

Laurence, M., Hatzis, C., & Brash, D. E. (2014). Common contaminants in next-generation sequencing that hinder discovery of low-abundance microbes. *PLoS ONE*, *9*(5), 1–8. https://doi.org/10.1371/journal.pone.0097876

Lawrence, R. A., & Devaney, E. (2001). Lymphatic filariasis : parallels between the immunology of infection in humans and mice. *Parasite Immunology*, *23*, 353–361.

Le Goff, L., Lamb, T. J., Graham, A. L., Harcus, Y., et al. (2002). IL-4 is required to prevent filarial nematode development in resistant but not susceptible strains of mice. *International Journal for Parasitology*, *32*(10), 1277–1284. https://doi.org/10.1016/S0020-7519(02)00125-X

Lefoulon, E., Bain, O., Bourret, J., Junker, K., et al. (2015). Shaking the Tree: Multi-locus Sequence Typing Usurps Current Onchocercid (Filarial Nematode)

Phylogeny. *PLoS Neglected Tropical Diseases*, *9*(11), 1–19. https://doi.org/10.1371/journal.pntd.0004233

Lefoulon, E., Bain, O., Makepeace, B. L., d'Haese, C., et al. (2016). Breakdown of coevolution between symbiotic bacteria *Wolbachia* and their filarial hosts. *PeerJ*, *4*, e1840. https://doi.org/10.7717/peerj.1840

Li, B.-W., Rush, A. C., & Weil, G. J. (2015). Expression of five acetylcholine receptor subunit genes in Brugia malayi adult worms. *International Journal for Parasitology. Drugs and Drug Resistance*, *5*(3), 100–9. https://doi.org/10.1016/j.ijpddr.2015.04.003

Li, B. W., Rush, A. C., & Weil, G. J. (2014a). High level expression of a glutamate-gated chloride channel gene in reproductive tissues of Brugia malayi may explain the sterilizing effect of ivermectin on filarial worms. *International Journal for Parasitology: Drugs and Drug Resistance*, *4*(2), 71–76. https://doi.org/10.1016/j.ijpddr.2014.01.002

Li, B. W., Rush, A. C., & Weil, G. J. (2014b). High level expression of a glutamate-gated chloride channel gene in reproductive tissues of Brugia malayi may explain the sterilizing effect of ivermectin on filarial worms q. *International Journal for Parasitology*, *4*, 71–76.

Love, M. I., Huber, W., & Anders, S. (2014). Moderated estimation of fold change and dispersion for RNA-seq data with DESeq2. *Genome Biology*, *15*(12), 550. https://doi.org/10.1186/s13059-014-0550-8

Luck, A. N., Anderson, K. G., McClung, C. M., VerBerkmoes, N. C., et al. (2015). Tissue-specific transcriptomics and proteomics of a filarial nematode and its Wolbachia endosymbiont. *BMC Genomics*, *16*(1), 920. https://doi.org/10.1186/s12864-015-2083-2

Luck, A. N., Evans, C. C., Riggs, M. D., Foster, J. M., et al. (2014). Concurrent transcriptional profiling of Dirofilaria immitis and its Wolbachia endosymbiont throughout the nematode life cycle reveals coordinated gene expression. *BMC Genomics*, *15*(1), 1041. https://doi.org/10.1186/1471-2164-15-1041

Mackenzie, C. D., & Geary, T. G. (2011). Flubendazole: a candidate macrofilaricide for lymphatic filariasis and onchocerciasis field programs. *Expert Review of Anti-Infective Therapy*, *9*(5), 497–501. https://doi.org/10.1586/eri.11.30

Mackenzie, C. D., Homeida, M. M., Hopkins, A. D., & Lawrence, J. C. (2012). Elimination of onchocerciasis from Africa: possible? *Trends in Parasitology*,

28(1), 16–22. https://doi.org/10.1016/j.pt.2011.10.003

Madathiparambil, M. G., Kaleysa, K. N., & Raghavan, K. (2009). A diagnostically useful 200-kDa protein is secreted through the surface pores of the filarial parasite Setaria digitata. *Parasitology Research*, *105*(4), 1099–1104. https://doi.org/10.1007/s00436-009-1525-7

Maizels, R. M., & McSorley, H. J. (2016). Regulation of the host immune system by helminth parasites. *Journal of Allergy and Clinical Immunology*, *138*(3), 666–75. https://doi.org/10.1016/j.jaci.2016.07.007

Maizels, R. M., & Yazdanbakhsh, M. (2003). Immune regulation by helminth parasites: cellular and molecular mechanisms. *Nature Reviews. Immunology*, *3*(9), 733–744. https://doi.org/10.1038/nri1183

Manzano-Román, R., & Siles-Lucas, M. (2012). MicroRNAs in parasitic diseases: potential for diagnosis and targeting. *Molecular and Biochemical Parasitology*, *186*(2), 81–6. https://doi.org/10.1016/j.molbiopara.2012.10.001

Marcilla, A., Martin-jaular, L., Trelis, M., Menezes-neto, A. De, et al. (2014). Extracellular vesicles in parasitic diseases, *1*.

Marcilla, A., Trelis, M., Cortes, A., Sotillo, J., et al. (2012). Extracellular Vesicles from Parasitic Helminths Contain Specific Excretory/Secretory Proteins and Are Internalized in Intestinal Host Cells. *PLoS ONE*, *7*(9). https://doi.org/10.1371/journal.pone.0045974

Maréchal, P., Le Goff, L., Hoffman, W., Rapp, J., et al. (1997). Immune response to the filaria Litomosoides sigmodontis in susceptible and resistant mice. *Parasite Immunology*, *19*(6), 273–279.

Marshall, F. A., Grierson, A. M., Garside, P., Harnett, W., et al. (2005). ES-62, an immunomodulator secreted by filarial nematodes, suppresses clonal expansion and modifies effector function of heterologous antigen-specific T cells in vivo. *Journal of Immunology (Baltimore, Md. : 1950)*, *175*(9), 5817–26. https://doi.org/10.4049/JIMMUNOL.175.9.5817

Martin, R. J. (1997). Modes of action of anthelmintic drugs. *Veterinary Journal*, *154*(1), 11–34. https://doi.org/10.1016/S1090-0233(05)80005-X

Martin, R. J., Robertson, A. P., Buxton, S. K., Beech, R. N., et al. (2012). Levamisole receptors : a second awakening. *Trends in Parasitology*, *28*(7), 289–296.

McGhee, J. (2007). The C. elegans intestine. *WormBook*, 1–36. https://doi.org/10.1895/wormbook.1.133.1

McInnes, I. B., Leung, B. P., Harnett, M., Gracie, J. A., et al. (2003). A Novel Therapeutic Approach Targeting Articular Inflammation Using the Filarial Nematode-Derived Phosphorylcholine-Containing Glycoprotein ES-62. *The Journal of Immunology*, *171*(4), 2127–2133. https://doi.org/10.4049/jimmunol.171.4.2127

McSorley, H. J., Hewitson, J. P., & Maizels, R. M. (2013). Immunomodulation by helminth parasites: defining mechanisms and mediators. *International Journal for Parasitology*, *43*(3–4), 301–10. https://doi.org/10.1016/j.ijpara.2012.11.011

Metenou, S., & Nutman, T. B. (2013). Regulatory T cell subsets in filarial infection and their function. *Frontiers in Immunology*, *4*(SEP), 1–8. https://doi.org/10.3389/fimmu.2013.00305

Mittelbrunn, M., & Sánchez-Madrid, F. (2012). Intercellular communication: diverse structures for exchange of genetic information. *Nature Reviews Molecular Cell Biology*, *13*(5), 328–335. https://doi.org/10.1038/nrm3335

Morales-Hojas, R., Cheke, R. a, & Post, R. J. (2006). Molecular systematics of five Onchocerca species (Nematoda: Filarioidea) including the human parasite, O. volvulus, suggest sympatric speciation. *Journal of Helminthology*, *80*(3), 281–90. https://doi.org/10.1079/JOH2005331

Moreno, Y., & Geary, T. G. (2008). Stage- and gender-specific proteomic analysis of Brugia malayi excretory-secretory products. *PLoS Neglected Tropical Diseases*, *2*(10), e326. https://doi.org/10.1371/journal.pntd.0000326

Moreno, Y., Nabhan, J. F., Solomon, J., Mackenzie, C. D., et al. (2010). Ivermectin disrupts the function of the excretory-secretory apparatus in microfilariae of Brugia malayi. *Proceedings of the National Academy of Sciences of the United States of America*, *107*(46), 20120–20125. https://doi.org/10.1073/pnas.1011983107

Morris, C. P., Bennuru, S., Kropp, L. E., Zweben, J. A., et al. (2015). A Proteomic Analysis of the Body Wall, Digestive Tract, and Reproductive Tract of Brugia malayi. *PLoS Neglected Tropical Diseases*, *9*(9), 1–21. https://doi.org/10.1371/journal.pntd.0004054

Mukherjee, K., Ghoshal, B., Ghosh, S., Chakrabarty, Y., et al. (2016). Reversible HuRmicroRNA binding controls extracellular export of miR122 and augments stress response. *EMBO Reports*, *17*(8), 11841203. https://doi.org/10.15252/embr

Murdoch, M. E., Asuzu, M. C., Hagan, M., Makunde, W. H., et al. (2002).

Onchocerciasis: the clinical and epidemiological burden of skin disease in Africa. *Annals of Tropical Medicine and Parasitology*, *96*(3), 283–96. https://doi.org/10.1179/000349802125000826

N, T., & Martin, M. (2011). Cutadapt removes adapter sequences from high-throughput sequencing reads. *EMBnet.journal*, *17*(1), 10–12. https://doi.org/http://dx.doi.org/10.14806/ej.17.1.200

Nfon, C. K., Makepeace, B. L., Njongmeta, L. M., Tanya, V. N., et al. (2006). Eosinophils contribute to killing of adult Onchocerca ochengi within onchocercomata following elimination of Wolbachia. *Microbes and Infection / Institut Pasteur*, *8*(12–13), 2698–705. https://doi.org/10.1016/j.micinf.2006.07.017

Notomi, T., Mori, Y., Tomita, N., & Kanda, H. (2015). Loop-mediated isothermal amplification (LAMP): principle, features, and future prospects. *Journal of Microbiology*, *53*(1), 1–5.

Nowacki, F. C., Martin T. Swain, Klychnikov, O. I., Niazi, U., et al. (2015). Protein and small non-coding RNA-enriched extracellular vesicles are released by the pathogenic blood fluke Schistosoma mansoni. *Journal of Extracellular Vesicles*, *4*, 28665. https://doi.org/10.3402/jev.v4.28665

Nowacki, F. C., Swain, M. T., Klychnikov, O. I., Niazi, U., et al. (2015). Protein and small non-coding RNA-enriched estracelullar vesicles are realesed by the pathogenic blood fluke Schistosoma mansoni. *Journal of Extracellular Vesicles*, *1*(October), 1–16. https://doi.org/10.3402/jev.v4.28665

Nutman, T. B., Miller, K. D., Mulligan, M., & Ottesen, E. a. (1986). Loa loa infection in temporary residents of endemic regions: recognition of a hyperresponsive syndrome with characteristic clinical manifestations. *The Journal of Infectious Diseases*, *154*(1), 10–18.

O'Connell, R. M., Rao, D. S., Chaudhuri, A. a., & Baltimore, D. (2010). Physiological and pathological roles for microRNAs in the immune system. *Nature Reviews Immunology*, *10*(2), 111–122. https://doi.org/10.1038/nri2708

Oguttu, D., Byamukama, E., Katholi, C. R., Habomugisha, P., et al. (2014). Serosurveillance to monitor onchocerciasis elimination: The Ugandan experience. *American Journal of Tropical Medicine and Hygiene*, *90*(2), 339–345. https://doi.org/10.4269/ajtmh.13-0546

Olmos-Ortiz, L. M., Barajas-Mendiola, M. A., Barrios-Rodiles, M., Castellano, L. E.,

et al. (2017). *Trichomonas vaginalis* exosome-like vesicles modify the cytokine profile and reduce inflammation in parasite-infected mice. *Parasite Immunology*, *39*(6), e12426. https://doi.org/10.1111/pim.12426

Osei-Atweneboana, M. Y., Eng, J. K. L., Boakye, D. a, Gyapong, J. O., et al. (2007). Prevalence and intensity of Onchocerca volvulus infection and efficacy of ivermectin in endemic communities in Ghana: a two-phase epidemiological study. *Lancet*, *369*(9578), 2021–9. https://doi.org/10.1016/S0140-6736(07)60942-8

Padmasiri, E. A., Montresor, A., Biswas, G., & de Silva, N. R. (2006). Controlling lymphatic filariasis and soil-transmitted helminthiasis together in South Asia: opportunities and challenges. *Transactions of the Royal Society of Tropical Medicine and Hygiene*, *100*(9), 807–810. https://doi.org/10.1016/j.trstmh.2005.12.001

Page, A. P., Hamilton, A. J., & Maizels, R. M. (1992). Toxocara canis: Monoclonal Antibodies to Carbohydrate Epitopes of Secreted (TES) Antigens Localize to Different Secretion-Related Structures in Infective Larvae. *Experimental Parasitology*, *75*(1), 56–71. https://doi.org/10.1016/0014-4894(92)90122-Q

Panic, G., Duthaler, U., Speich, B., & Keiser, J. (2014). Repurposing drugs for the treatment and control of helminth infections. *International Journal for Parasitology: Drugs and Drug Resistance*, *4*(3), 185–200. Retrieved from http://www.journals.elsevier.com/international-journal-for-parasitology-drugs-and-drug-resistance/%5Cnhttp://ovidsp.ovid.com/ovidweb.cgi?T=JS&PAGE=reference&D=emed16&NEWS=N&AN=600215894

Park, J., Dickerson, T. J., & Janda, K. D. (2008). Major sperm protein as a diagnostic antigen for onchocerciasis. *Bioorganic & Medicinal Chemistry*, *16*(15), 7206–9. https://doi.org/10.1016/j.bmc.2008.06.038

Pfarr, K. M., Debrah, A. Y., Specht, S., & Hoerauf, A. (2009). Filariasis and lymphoedema. *Parasite Immunology*, *31*(11), 664–672. https://doi.org/10.1111/j.1365-3024.2009.01133.x

Pionnier, N., Brotin, E., Karadjian, G., Hemon, P., et al. (2016). Neutropenic Mice Provide Insight into the Role of Skin-Infiltrating Neutrophils in the Host Protective Immunity against Filarial Infective Larvae. *PLoS Neglected Tropical Diseases*, *10*(4). https://doi.org/10.1371/journal.pntd.0004605

Poole, C. B., Gu, W., Kumar, S., Jin, J., et al. (2014). Diversity and expression of microRNAs in the filarial parasite, Brugia malayi. *PLoS ONE*, *9*(5). https://doi.org/10.1371/journal.pone.0096498

Poole, C. B., Tanner, N. a, Zhang, Y., Evans, T. C., et al. (2012). Diagnosis of brugian filariasis by loop-mediated isothermal amplification. *PLoS Neglected Tropical Diseases*, *6*(12), e1948. https://doi.org/10.1371/journal.pntd.0001948

Portillo, V., Jagannathan, S., & Wolstenholme, A. J. (2003). Distribution of glutamate-gated chloride channel subunits in the parasitic nematode Haemonchus contortus. *Journal of Comparative Neurology*, *462*(2), 213–222. https://doi.org/10.1002/cne.10735

Pritchard, C. C., Cheng, H. H., & Tewari, M. (2012). MicroRNA profiling: approaches and considerations. *Nature Reviews Genetics*, *13*(5), 358–369. https://doi.org/10.1038/nrg3198

Quintana, J. F., Babayan, S. A., & Buck, A. H. (2016). Small RNAs and extracellular vesicles in filarial nematodes: from nematode development to diagnostics. *Parasite Immunology*. https://doi.org/10.1111/pim.12395

Quintana, J. F., Makepeace, B. L., Babayan, S. a, Ivens, A., et al. (2015). Extracellular Onchocerca-derived small RNAs in host nodules and blood. *Parasites & Vectors*, *8*(1), 1–11. https://doi.org/10.1186/s13071-015-0656-1

Rahmah, N., Taniawati, S., Shenoy, R., Lim, B., et al. (2001). Specificity and sensitivity of a rapid dipstick test (Brugia Rapid) in the detection of Brugia malayi infection. *Transactions of the Royal Society of Tropical Medicine and Hygiene*, *95*(6), 601–604.

Rao, U. R., Mehta, K., Subrahmanyam, D., & Vickery, A. C. (1991). Brugia malayi and Acanthocheilonema viteae : Antifilarial Activity of Transglutaminase Inhibitors In Vitro, *35*(11), 2219–2224.

Raposo, G., & Stoorvogel, W. (2013). Extracellular vesicles: Exosomes, microvesicles, and friends. *Journal of Cell Biology*, *200*(4), 373–383. https://doi.org/10.1083/jcb.201211138

Rebollo, M. P., & Bockarie, M. J. (2017). Can Lymphatic Filariasis Be Eliminated by 2020? *Trends in Parasitology*, *33*(2), 83–92. https://doi.org/10.1016/j.pt.2016.09.009

Resnick, T. D., McCulloch, K. a., & Rougvie, A. E. (2010). miRNAs give worms the time of their lives: Small RNAs and temporal control in Caenorhabditis elegans.

Developmental Dynamics, *239*(5), 1477–1489. https://doi.org/10.1002/dvdy.22260

Sartono, E., Kruize, Y. C., Partono, F., Kurniawan, A., et al. (1995). Specific T cell unresponsiveness in human filariasis: diversity in underlying mechanisms. *Parasite Immunol*, *17*(11), 587–594. https://doi.org/10.1111/j.1365-3024.1995.tb01002.x

Scot, A. L., GHEDING, E., NUTMAN, T. B., McREYNOLDS, L. A., et al. (2012). Filarial and Wolbachia genomics. *Parasite Immunology*, *34*(2–3), 121–129. https://doi.org/10.1111/j.1365-3024.2011.01344.x.Filarial

Segura, M., Su, Z., Piccirillo, C., & Stevenson, M. M. (2007). Impairment of dendritic cell function by excretory-secretory products: A potential mechanism for nematode-induced immunosuppression. *European Journal of Immunology*, *37*(7), 1887–1904. https://doi.org/10.1002/eji.200636553

Shaw, W. R., Armisen, J., Lehrbach, N. J., & Miska, E. a. (2010). The conserved miR-51 microRNA family is redundantly required for embryonic development and pharynx attachment in Caenorhabditis elegans. *Genetics*, *185*(3), 897–905. https://doi.org/10.1534/genetics.110.117515

Simbari, F., Mccaskill, J., Coakley, G., Millar, M., et al. (2016). Plasmalogen enrichment in exosomes secreted by a nematode parasite versus those derived from its mouse host: implications for exosome stability and biology. *J Extracell Vesicles*, *5*, 30741.

Simonsen, P. E., Onapa, A. W., & Maria, S. (2011). Acta Tropica Mansonella perstans filariasis in Africa. https://doi.org/10.1016/j.actatropica.2010.01.014

Sotillo, J., Sanchez-Flores, A., Cantacessi, C., Harcus, Y., et al. (2014). Secreted proteomes of different developmental stages of the gastrointestinal nematode Nippostrongylus brasiliensis. *Molecular & Cellular Proteomics : MCP*, 1–16. https://doi.org/10.1074/mcp.M114.038950

Srivastava, P., Mehrotra, S., Tiwary, P., Chakravarty, J., et al. (2011). Diagnosis of Indian Visceral Leishmaniasis by Nucleic Acid Detection Using PCR, *6*(4), 4–8. https://doi.org/10.1371/journal.pone.0019304

Storey, B., Marcellino, C., Miller, M., Maclean, M., et al. (2014). Utilization of computer processed high definition video imaging for measuring motility of microscopic nematode stages on a quantitative scale: "The Worminator." *International Journal for Parasitology: Drugs and Drug Resistance*, *4*(3), 233–

243. https://doi.org/10.1016/j.ijpddr.2014.08.003

Strong, M. J., Xu, G., Morici, L., Splinter Bon-Durant, S., et al. (2014). Microbial Contamination in Next Generation Sequencing: Implications for Sequence-Based Analysis of Clinical Samples. *PLoS Pathogens*, *10*(11), 1–6. https://doi.org/10.1371/journal.ppat.1004437

Tamarozzi, F., Halliday, A., Gentil, K., Hoerauf, A., et al. (2011). Onchocerciasis: The role of Wolbachia bacterial endosymbionts in parasite biology, disease pathogenesis, and treatment. *Clinical Microbiology Reviews*, *24*(3), 459–468. https://doi.org/10.1128/CMR.00057-10

Taniuchi, M., Verweij, J. J., Noor, Z., Sobuz, S. U., et al. (2011). High Throughput Multiplex PCR and Probe-based Detection with Luminex Beads for Seven Intestinal Parasites, *84*(2), 332–337. https://doi.org/10.4269/ajtmh.2011.10-0461

Taylor, H., Keyvan-Larijani, E., Newland, H., White, A., et al. (1987). Sensitivity of skin snips in the diagnosis of onchocerciasis. *Tropical Medicine Parasitology*, *38*(2), 145–147.

Taylor, M. D., van der Werf, N., Harris, A., Graham, A. L., et al. (2009). Early recruitment of natural CD4+Foxp3+ Treg cells by infective larvae determines the outcome of filarial infection. *European Journal of Immunology*, *39*(1), 192–206. https://doi.org/10.1002/eji.200838727

Taylor, M. J. (2003). Wolbachia in the Inflammatory Pathogenesis of Human Filariasis. *Annals New York Academy of Sciences*, *990*, 444–449.

Taylor, M. J., Hoerauf, A., & Bockarie, M. (2010). Lymphatic filariasis and onchocerciasis. *The Lancet*, *376*(9747), 1175–1185. https://doi.org/10.1016/S0140-6736(10)60586-7

Taylor, M. J., Voronin, D., Johnston, K. L., & Ford, L. (2012). Wolbachia filarial interactions. *Cellular Microbiology*, *15*(December 2012), 520–526. https://doi.org/10.1111/cmi.12084

Tehler, D., Høyland-Kroghsbo, N. M., & Lund, A. H. (2011). The miR-10 microRNA precursor family. *RNA Biology*, *8*(5), 728–734. https://doi.org/10.4161/rna.8.5.16324

Thiele, E. A., Cama, V. A., Lakwo, T., Mekasha, S., et al. (2016). Detection of onchocerca volvulus in skin snips by microscopy and real-time polymerase chain reaction: Implications for monitoring and evaluation activities. *American Journal of Tropical Medicine and Hygiene*, *94*(4), 906–911.

https://doi.org/10.4269/ajtmh.15-0695

Tompkins, J. B., Stitt, L. E., & Ardelli, B. F. (2010). Brugia malayi: In vitro effects of ivermectin and moxidectin on adults and microfilariae. *Experimental Parasitology*, *124*(4), 394–402. https://doi.org/10.1016/j.exppara.2009.12.003

Trees, a J. (1992). Onchocerca ochengi: Mimic, model or modulator of O. volvulus? *Parasitology Today*, *8*(10), 337–339. https://doi.org/10.1016/0169-4758(92)90068-D

Tritten, L., Burkman, E., Moorhead, A., Satti, M., et al. (2014). Detection of Circulating Parasite-Derived MicroRNAs in Filarial Infections. *PLoS Neglected Tropical Diseases*, *8*(7). https://doi.org/10.1371/journal.pntd.0002971

Tritten, L., Clarke, D., Timmins, S., Mctier, T., et al. (2016). Dirofilaria immitis exhibits sex- and stage-specific differences in excretory / secretory miRNA and protein profiles. *Vet Parasitol.*, *232*, 1–7.

Tritten, L., & Geary, T. G. (2016). MicroRNAs of Filarial Nematodes: A New Frontier in Host-Pathogen Interactions. In *Non-coding RNAs and Inter-kingdom Communication* (pp. 207–223). Springer International Publishing. https://doi.org/10.1007/978-3-319-39496-1_13

Tritten, L., Neill, M. O., Wanji, S., Njouendoui, A., et al. (2014). Loa loa and Onchocerca ochengi miRNAs detected in host circulation. *Molecular & Biochemical Parasitology*, 1–4. https://doi.org/10.1016/j.molbiopara.2014.11.001

Turaga, P. S. D., Tierney, T. J., Bennett, K. E., McCarthy, M. C., et al. (2000). Immunity to onchocerciasis: Cells from putatively immune individuals produce enhanced levels of interleukin-5, gamma interferon, and granulocyte-macrophage colony-stimulating factor in response to Onchocerca volvulus larval and male worm antigens. *Infection and Immunity*, *68*(4), 1905–1911. https://doi.org/10.1128/IAI.68.4.1905-1911.2000

Turchinovich, a, Samatov, T. R., Tonevitsky, a G., & Burwinkel, B. (2013). Circulating miRNAs: cell-cell communication function? *Frontiers in Genetics*, *4*(June), 119. https://doi.org/10.3389/fgene.2013.00119

Turner, H. C., Osei-Atweneboana, M. Y., Walker, M., Tettevi, E. J., et al. (2013). The cost of annual versus biannual community-directed treatment of onchocerciasis with ivermectin: Ghana as a case study. *PLoS Neglected Tropical Diseases*, *7*(9), e2452. https://doi.org/10.1371/journal.pntd.0002452

Tzelos, T., Matthews, J. B., Buck, A. H., Simbari, F., et al. (2016). A preliminary proteomic characterisation of extracellular vesicles released by the ovine parasitic nematode, Teladorsagia circumcincta. *Veterinary Parasitology*, *221*, 84–92. https://doi.org/10.1016/j.vetpar.2016.03.008

Utzinger, J., Becker, S. L., Knopp, S., Blum, J., et al. (2012). Neglected tropical diseases: diagnosis, clinical management, treatment and control. *Swiss Medical Weekly*, *142*(November), w13727. https://doi.org/10.4414/smw.2012.13727

van der Werf, M. J., de Vlas, S. J., Brooker, S., Looman, C. W. ., et al. (2003). Quantification of clinical morbidity associated with schistosome infection in sub-Saharan Africa. *Acta Tropica*, *86*(2–3), 125–139. https://doi.org/10.1016/S0001-706X(03)00029-9

Vatta, A. F., Dzimianski, M., Storey, B. E., Camus, M. S., et al. (2014). Ivermectin-dependent attachment of neutrophils and peripheral blood mononuclear cells to Dirofilaria immitis microfilariae in vitro. *Veterinary Parasitology*, *206*(1–2), 38–42. https://doi.org/10.1016/j.vetpar.2014.02.004

Villarroya-Beltri, C., Gutiérrez-Vázquez, C., Sánchez-Cabo, F., Pérez-Hernández, D., et al. (2013). Sumoylated hnRNPA2B1 controls the sorting of miRNAs into exosomes through binding to specific motifs. *Nature Communications*, *4*, 2980. https://doi.org/10.1038/ncomms3980

Volkmann, L., Bain, O., Saeftel, M., Specht, S., et al. (2003). Murine filariasis: interleukin 4 and interleukin 5 lead to containment of different worm developmental stages. *Medical Microbiology and Immunology*, *192*(1), 23–31. https://doi.org/10.1007/s00430-002-0155-9

Volkmann, L., Saeftel, M., Bain, O., Fischer, K., et al. (2001). Interleukin-4 is essential for the control of microfilariae in murine infection with the filaria litomosoides sigmodontis. *Infection and Immunity*, *69*(5), 2950–2956. https://doi.org/10.1128/IAI.69.5.2950-2956.2001

Voronin, D., Bachu, S., Shlossman, M., Unnasch, T. R., et al. (2016). Glucose and glycogen metabolism in brugia malayi is associated with wolbachia symbiont fitness. *PLoS ONE*, *11*(4), 1–18. https://doi.org/10.1371/journal.pone.0153812

Wahl, G, Achu-Kwi, MD, Mbah, D, Dawa, O, Renz, A. (1994). Bovine onchocerciasis in North Cameroon. *Vet Parasitol.*, *52*(3–4), 297–311.

Wang, K., Li, H., Yuan, Y., Etheridge, A., et al. (2012). The complex exogenous RNA spectra in human plasma: an interface with human gut biota? *PloS One*,

7(12), e51009. https://doi.org/10.1371/journal.pone.0051009

Wang, L., Li, Z., Shen, J., Liu, Z., et al. (2015). Exosome-like vesicles derived by Schistosoma japonicum adult worms mediates M1 type immune- activity of macrophage. *Parasitology Research*, *114*, 1865–1873. https://doi.org/10.1007/s00436-015-4373-7

Wang, T., Van Steendam, K., Dhaenens, M., Vlaminck, J., et al. (2013). Proteomic analysis of the excretory-secretory products from larval stages of Ascaris suum reveals high abundance of glycosyl hydrolases. *PLoS Neglected Tropical Diseases*, *7*(10), e2467. https://doi.org/10.1371/journal.pntd.0002467

Wanji, S., Amazigo, U. V., Peter, J., Tekle, A. H., et al. (2011). The Geographic Distribution of Loa loa in Africa : Results of Large-Scale Implementation of the Rapid Assessment Procedure for Loiasis (RAPLOA), *5*(6). https://doi.org/10.1371/journal.pntd.0001210

Ward, J., Nutman, T. B., Zea-Flores, G., Portocarrero, C., et al. (1988). Onchocerciasis and Immunity in Humans: Enhanced T Cell Responsiveness to Parasite Antigen in Putatively Immune Individuals. *Journal of Infectious Diseases*, *157*(3), 536–543.

Weick, E.-M., & Miska, E. (2014). piRNAs: from biogenesis to function. *Development*, *141*(18), 3458–3471. https://doi.org/10.1242/dev.094037

Weil, G. J., & Ramzy, R. M. R. (2007). Diagnostic tools for filariasis elimination programs. *Trends in Parasitology*, *23*(2), 78–82. https://doi.org/10.1016/j.pt.2006.12.001

Weil, G. J., Steel, C., Liftis, F., Li, B., et al. (2000). A Rapid-Format Antibody Card Test for Diagnosis of Onchocerciasis. *J Infect Dis*, *186*(6), 1796–1799.

White, R. R., & Artavanis-Tsakonas, K. (2012). How helminths use excretory secretory fractions to modulate dendritic cells. *Virulence*, *3*(7), 668–677. https://doi.org/10.4161/viru.22832

Williamson, S. M., Walsh, T. K., & Wolstenholme, A. J. (2007). The cys-loop ligand-gated ion channel gene family of Brugia malayi and Trichinella spiralis: a comparison with Caenorhabditis elegans. *Invertebrate Neuroscience : IN*, *7*(4), 219–26. https://doi.org/10.1007/s10158-007-0056-0

Wilson, E. H., Deehan, M. R., Katz, E., Brown, K. S., et al. (2003). Hyporesponsiveness of murine B lymphocytes exposed to the filarial nematode secreted product ES-62 in vivo. *Immunology*, *109*(2), 238–245.

https://doi.org/10.1046/j.1365-2567.2003.01661.x

Winter, A. D., Gillan, V., Maitland, K., Emes, R. D., et al. (2015). A novel member of the let-7 microRNA family is associated with developmental transitions in filarial nematode parasites. *BMC Genomics*, *16*(1), 331. https://doi.org/10.1186/s12864-015-1536-y

Winter, J., Jung, S., Keller, S., Gregory, R. I., et al. (2009). Many roads to maturity: microRNA biogenesis pathways and their regulation. *Nature Cell Biology*, *11*(3), 228–234. https://doi.org/10.1038/ncb0309-228

Wolstenholme, A. J. (2012). Glutamate-gated chloride channels. *Journal of Biological Chemistry*, *287*(48), 40232–40238. https://doi.org/10.1074/jbc.R112.406280

Wolstenholme, A. J., Maclean, M. J., Coates, R., McCoy, C. J., et al. (2016). How do the macrocyclic lactones kill filarial nematode larvae? *Invertebrate Neuroscience*, *16*(3). https://doi.org/10.1007/s10158-016-0190-7

Wolstenholme, a J., & Rogers, a T. (2005). Glutamate-gated chloride channels and the mode of action of the avermectin/milbemycin anthelmintics. *Parasitology*, *131 Suppl*, S85–S95. https://doi.org/10.1017/S0031182005008218

Xu, M. J., Fu, J. H., Nisbet, A. J., Huang, S. Y., et al. (2013). Comparative profiling of microRNAs in male and female adults of Ascaris suum. *Parasitology Research*, *112*(3), 1189–1195. https://doi.org/10.1007/s00436-012-3250-x

Yeri, A., Courtright, A., Reiman, R., Carlson, E., et al. (2017). Total Extracellular Small RNA Profiles from Plasma, Saliva, and Urine of Healthy Subjects. *Scientific Reports*, *7*(February), 44061. https://doi.org/10.1038/srep44061

Youngman, E. M., & Claycomb, J. M. (2014). From early lessons to new frontiers: the worm as a treasure trove of small RNA biology. *Frontiers in Genetics*, *5*(November), 416. https://doi.org/10.3389/fgene.2014.00416

Zamanian, M., Fraser, L. M., Agbedanu, P. N., Harischandra, H., et al. (2015). Release of Small RNA-containing Exosome-like Vesicles from the Human Filarial Parasite Brugia malayi. *PLOS Neglected Tropical Diseases*, *9*(9), e0004069. https://doi.org/10.1371/journal.pntd.0004069

Zamanian, M., Fraser, L. M., Agbedanu, P. N., & Harischandra, H. (2015). Release of Small RNA-containing Exosome-like Vesicles from the Human Filarial Parasite Brugia malayi. *PLoS Negl Trop Dis*, *9*(9), 1–23. https://doi.org/10.1371/journal.pntd.0004069

Zang, X., Atmadja, A. K., Gray, P., Allen, J. E., et al. (2016). The Serpin Secreted by

Brugia malayi Microfilariae, Bm-SPN-2, Elicits Strong, but Short-Lived, Immune Responses in Mice and Humans. https://doi.org/10.4049/jimmunol.165.9.5161

Zhu, S., Wang, S., Lin, Y., Jiang, P., et al. (2016). Release of extracellular vesicles containing small RNAs from the eggs of Schistosoma japonicum. *Parasites & Vectors*, *9*(1), 574. https://doi.org/10.1186/s13071-016-1845-2

Ziewer, S., Hübner, M. P., Dubben, B., Hoffmann, W. H., et al. (2012). Immunization with L. sigmodontis microfilariae reduces peripheral microfilaraemia after challenge infection by inhibition of filarial embryogenesis. *PLoS Neglected Tropical Diseases*, *6*(3). https://doi.org/10.1371/journal.pntd.0001558

Ziewer, S., Hübner, M. P., Dubben, B., Hoffmann, W. H., et al. (2012). Immunization with L. sigmodontis microfilariae reduces peripheral microfilaraemia after challenge infection by inhibition of filarial embryogenesis. *PLoS Negl Trop Dis*, *6*(3), e1558. https://doi.org/10.1371/journal.pntd.0001558

Zimmerman, P. a, Guderian, R. H., Aruajo, E., Elson, L., et al. (1994). Polymerase chain reaction-based diagnosis of Onchocerca volvulus infection: improved detection of patients with onchocerciasis. *The Journal of Infectious Diseases*, *169*(3), 686–689. https://doi.org/30113804

Zouré, H. G. M., Noma, M., Tekle, A. H., Amazigo, U. V, et al. (2014). The geographic distribution of onchocerciasis in the 20 participating countries of the African Programme for Onchocerciasis Control: (2) pre-control endemicity levels and estimated number infected. *Parasites & Vectors*, *7*, 326. https://doi.org/10.1186/1756-3305-7-326